



ALTERNATIVES TO ANTIBIOTICS

The potential of silencing
bacterial chat

Wouter A.G. Beenker

Alternatives to antibiotics

The potential of silencing bacterial chat

Wouter A.G. Beenker

Colofon

Cover art: *Pseudomonas aeruginosa* bacteria. Work by: Christoph Burgstedt. Design by: Cloë Hendriks

Layout by: Wouter Beenker

Printing: Ridderprint | The Netherlands

ISBN: 978-94-6483-137-5

DOI: <https://doi.org/10.33540/1808>

The work described in this thesis was performed at the Hubrecht Institute for Developmental Biology and Stem Cell Research (Royal Netherlands Academy of Arts and Sciences, KNAW), which is part of the research school Cancer Stem Cells & Developmental Biology, which is part of the Utrecht Graduate School of Life Sciences (Utrecht University).

Copyright ©2023 by Wouter Beenker. All rights reserved. No part of this book may be reproduced, stored in a retrieval system or transmitted in any form or by any means, without prior permission of the author.

Alternatives to antibiotics

The potential of silencing bacterial chat

Alternatieven voor antibiotica

Het potentieel om bacteriële communicatie te verstoren

(met een samenvatting in het Nederlands)

Proefschrift

ter verkrijging van de graad van doctor aan de
Universiteit Utrecht
op gezag van de
rector magnificus, prof.dr. H.R.B.M. Kummeling,
ingevolge het besluit van het college voor promoties
in het openbaar te verdedigen op

maandag 26 juni 2023 des middags te 12.15 uur

door

Wouter Antonius Gerardus Beenker

geboren op 22 juni 1993
te Best

Promotoren:

Prof. dr. A. van Oudenaarden

Prof. dr. J. den Hertog

Beoordelingscommissie:

Dr. J. Collemare

Prof. dr. S.H.M. Rooijackers

Prof. dr. J.A.G. van Strijp

Prof. dr. G.P. van Wezel

Prof. dr. H.A.B. Wösten

Table of contents

Chapter 1	7
Introduction	
Chapter 2	17
Gregatins, a group of related fungal secondary metabolites, inhibit aspects of quorum sensing in Gram-negative bacteria	
Chapter 3	41
Paecilomycone inhibits quorum sensing in Gram-negative bacteria	
Chapter 4	75
Establishment and characterization of a new <i>Pseudomonas aeruginosa</i> infection model using 2D airway organoids and dual RNA sequencing	
Chapter 5	101
<i>Pseudomonas aeruginosa</i> quorum sensing related molecules affect the airway epithelial immune response	
Chapter 6	117
General Discussion	
References	127
Addendum	143
Dutch summary Nederlandse Samenvatting	
Curriculum vitae	
List of publications	
Acknowledgements Dankwoord	



Chapter 1

Introduction

In 1928, Alexander Fleming found that bacteria would not grow close to a fungal contamination on an agar plate. Serendipitously, he did not discard the plate immediately because of the contamination, but instead realized that the fungus might produce a substance that inhibits growth of the bacteria or even kill them¹. This discovery is known by many people. However, Fleming was not the first one to notice the potential of fungi to treat bacterial infections. Already thousands of years, it was known that molds, beer yeast, and mushrooms have healing effects in the treatment of infected wounds. John Parkinson was the first to describe this healing effect of molds in his *Theatrum Botanicum*. However, it took until the second half of the 19th century before scientists became interested again in the activity of molds. In 1884, Joseph Lister cured an abscess of a nurse with tissues soaked with *Penicillium glaucum*. While Lister did not publish his results, Ernest Duchesne described in his thesis that *P. glaucum* destroys pathogenic bacteria in guinea pigs. Unfortunately, his thesis was not accepted and it took until 1940 that his work was confirmed². Therefore, the discovery of Fleming in 1928 is often called the “birth of the antibiotic era”. It took another 10 years before Howard Walter Florey and Ernst Boris Chain elucidated the structure of penicillin and by 1943 penicillin became available for military use³⁻⁵.

After the discovery of penicillin, many more classes of antibiotics were discovered with a peak in the 1950s⁶. While penicillin inhibits the synthesis of the cell wall, other classes show different mechanisms of action. For example, aminoglycosides inhibit protein synthesis via the 30S subunit, while chloramphenicol and macrolides inhibit protein synthesis via the 50S subunit instead. Other targets are: RNA synthesis by rifampicin, DNA gyrase by quinolones, LPS by polymyxins^{7,8}. Despite this wide variety of targets, resistance has occurred against every class of antibiotics⁸.

Antimicrobial resistance

Samples from permafrost⁹ or isolated caves¹⁰ show that antimicrobial resistance (AMR) occurs even in the absence of human activity. However, overuse of antibiotics, both for treatment in humans as well as in animals and agriculture accelerates this problem due to Darwinian selection. When treated with antibiotics, bacteria that have developed mutations that lead to resistance against that antibiotic, will survive and start to proliferate again^{11,12}. So, while antibiotics have cured large groups of people and proven to be very effective, they become more ineffective the more they are used¹³. This is a major threat to human health, because bacterial infections can become deadly again when antibiotics are not effective. Moreover, surgical operations rely heavily on antibiotics. Already, bacteria are found that are resistant to multiple or even all known classes of clinical antibiotics, which is resulting in deadly infections¹⁴. In 2019, approximately 1.27 million people worldwide died as a result of antimicrobial resistance¹⁵.

The main concern of antimicrobial resistance encompasses a group of bacteria, collectively called the ESKAPE bacteria, which include: *Enterococcus faecium*, *Staphylococcus*

aureus, *Klebsiella pneumoniae*, *Acinetobacter baumannii*, *Pseudomonas aeruginosa* and *Enterobacter species*¹⁶. These organisms are responsible for many infections in hospitals, they often become resistant to antibiotics, and are associated with the highest mortality rates^{17,18}. These bacteria were also listed in 2017 in the World Health Organization list of 12 bacteria “that pose the greatest threat to human health”. The most critical among these 12 listed bacteria were *Acinetobacter*, *Pseudomonas* and various *Enterobacteriaceae* for their potential to cause deadly infections¹⁹. This thesis will mostly focus on one of these bacteria: *Pseudomonas aeruginosa*.

***Pseudomonas aeruginosa* infections**

P. aeruginosa is one of the most-studied Gram-negative bacteria. *P. aeruginosa* contains a relatively large genome with a size of 6.4 million base pairs and around 5,500 genes (the exact number varies per strain)^{20–22}. A large number of these genes is involved in metabolism and regulatory genes, making *P. aeruginosa* strains ultimate generalists that can survive in a wide variety of circumstances²². Therefore, *P. aeruginosa* is found all over the planet, from water to soil, in animals and humans^{23–25}.

In case of human infections, *P. aeruginosa* causes nosocomial infections in immunocompromised patients and causes a major healthcare concern. It is responsible for a variety of life-threatening acute and chronic infections including burn or wound infection, urinary tract infection, and respiratory diseases like cystic fibrosis (CF)^{25,26}. In case of the latter, *P. aeruginosa* establishes itself in the lung where the infection often becomes chronic^{27–30}. This infection state with *P. aeruginosa* causes increased morbidity and eventually mortality due to respiratory failure in CF patients³⁰.

Treatment of *P. aeruginosa* infections is difficult due to the high intrinsic resistance via a variety of mechanisms^{26,31} (Figure 1). The unique outer membrane of Gram-negative bacteria impedes the passive diffusion of molecules into the bacterial cells. Even though the outer membrane is comparable among Gram-negative bacteria, the permeability of the outer membrane of *P. aeruginosa* is estimated to be 12-100 x smaller than *E. coli*³². This might be due to the expression of specific porins on the outer membrane of *P. aeruginosa*. Due to the low permeability of the outer membrane, compounds often pass through the water-filled channels of the porins to enter the cell. The porins in the outer membrane of *P. aeruginosa* are mostly restricted for a selective group of compounds^{33,34}. In addition, upon exposure to antibiotics, bacteria can downregulate or modify these porins to make it even harder to enter the cell^{35,36}. If a compound does make it into the cell, it is often subject to efflux pumps. *P. aeruginosa* contains a high number of efflux pumps that transport the antimicrobial out of the cell again^{37,38}. These permeability factors make it hard for antibiotics to accumulate in the cell and kill the bacteria. Another type of high antibiotic tolerance by *P. aeruginosa* is conferred by the notorious formation of biofilms. Biofilms are aggregates of bacteria, which make the bacteria tolerant for high doses of antimicrobials³⁹. In addition,

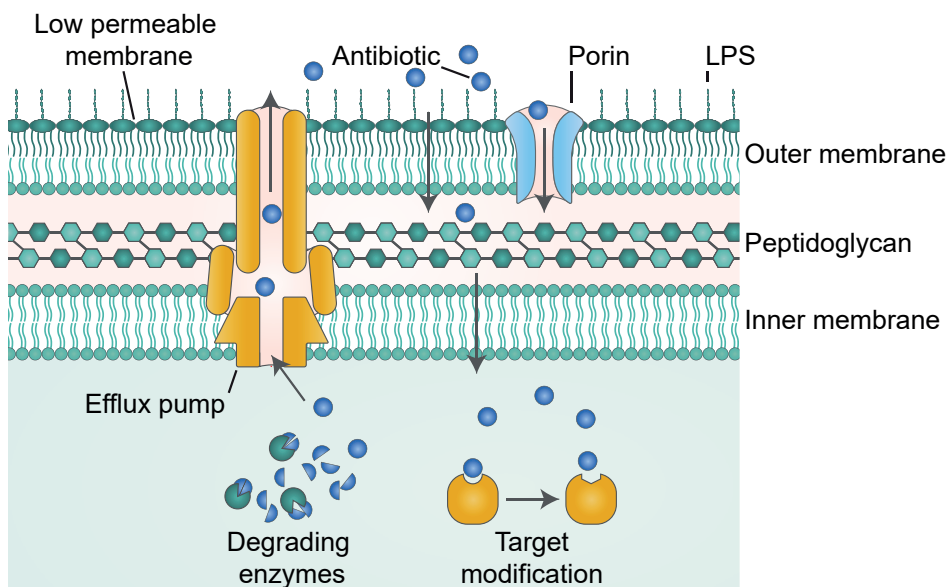


Figure 1: Various factors involved in intrinsic resistance in *P. aeruginosa*. *P. aeruginosa* has a high tolerance against antibiotics via various mechanisms. First, the low permeable outer membrane makes it hard for antibiotics to enter the cell. The antibiotics have to cross via selective water-filled porins. When entered in the cell, the antibiotics are often subject for efflux pumps making it hard to accumulate. In addition, *P. aeruginosa* can express enzymes that degrade the antibiotic or modify the target making it impossible for the antibiotic to bind to the target.

mutations in target genes or the acquisition of genes encoding enzymes that degrade antimicrobials make the repertoire of antibiotic resistance mechanisms in *P. aeruginosa* extensive^{26,40}. Therefore, *P. aeruginosa* infections are difficult to treat, and more research and treatments are needed for future treatments.

Search for new antibiotics

Finding new antimicrobials has been a major challenge for decades, especially against Gram-negative bacteria. In the golden age of antibiotics, a large number of microorganisms were screened leading to more than 23,000 active natural products^{41,42}. However, due to the large screening efforts a problem arose: dereplication, in which most of the active compounds are repeatedly discovered. At the time the first genomes of bacteria were fully sequenced, hopes were up again to find novel targets. However, a large number of high-throughput screens against novel potential targets, containing millions of natural and synthetic compounds, were without success^{43–45}.

One of the problems in the discovery of novel antibiotics is that traditional screening methods are being used. The concept of the traditional screens is to grow the target bacteria in nutrient-rich medium, add the compound of interest and check the viability of the bacteria the next day. This approach has two main flaws. First, the rich-medium does not represent

the growth of the bacteria in the harsh environment of the human body. Therefore, a different set of genes is essential under the conditions that are found *in vivo*, leading to different targets. Second, the traditional screens base the success of the compounds on the minimum inhibitory concentration (MIC). This is the lowest concentration of a compound at which the bacteria do not grow. For this reason, compounds that weaken the bacteria but do not disturb their growth will be missed⁴⁶. Other, non-conventional approaches are needed to find new antimicrobials.

One of the ways to find new antimicrobials is searching at unexplored places like deep seas, high mountains, or microbiomes. This way, darobactin was recently discovered in bacteria inhabiting the microbiome of Nematodes⁴⁷. In addition, only a small percentage of the bacteria can be cultured under laboratory circumstances. New methods in culturing techniques led to the discovery of teixobactin in 2015⁴⁸. Furthermore, genome mining of uncultivated soil bacteria or activating “silent gene clusters” in fungi, might lead to finding novel active secondary metabolites^{49–52}.

Another approach to find new antibiotics is to find new ways to attack the bacteria. An interesting example is the synthetic modification of antibiotics by adding a siderophore. Since iron is needed for all living organisms, and the iron concentration at the site of infection is often low, bacteria secrete siderophores that bind iron. This principle makes it possible to overcome the permeation barrier in Gram-negative bacteria by adding a siderophore to the antimicrobial⁵³. This approach has led to the successful approval of cefiderocol, active against Gram-negative bacteria, by the US Food and Drug Administration⁵⁴. Another new way to attack the bacteria is by targeting structures in the outer membrane. This way, antimicrobials avoid the permeability problem. A successful example is the aforementioned darobactin, which effectively targets the BAM complex, which is an important chaperone and translocator in the outer membrane of Gram-negative bacteria⁴⁷.

Altogether, these are some examples of innovative research in the search for novel antimicrobials. Until today, the majority of antimicrobials are natural products or derivatives of these products, and natural products will likely continue to play an important role in the development of novel antimicrobials^{55–57}. Although new approaches to find or use these compounds will be needed. An interesting approach includes targets that do not necessarily kill the bacteria but weaken them, making it possible for the immune system or other antibiotics to get rid of them.

Quorum sensing as alternative target to treat bacterial infections

An interesting target to weaken the bacteria is quorum sensing (QS). Bacterial QS is the regulation of gene expression that relies upon cell-population density. QS consists of synthesis, release, and detection of signaling molecules. These signal molecules are called autoinducers, since they also influence their own biosynthesis⁵⁸. The autoinducers can cross the membrane and bind to receptors that regulate gene expression in a bacterial

cell. Therefore, when the number of bacteria is high, the concentration of autoinducers will be high, and a different set of genes will be activated compared to when the number of bacteria is low. This way, bacteria can collaborate and can produce compounds that are costly for a single bacterium, but will be advantageous when the biomass is sufficient⁵⁹.

QS regulates a plethora of signaling pathways in different bacteria. Downstream genes include genes for the production of virulence factors and genes involved in the formation of biofilms. Virulence factors are involved in motility, adhesion, and include lytic enzymes that cause damage to host tissues^{59,60}. The formation of biofilms causes a lower susceptibility against antibiotics^{61–64}. Therefore, inhibition of QS would lead to less damage to host tissues and higher susceptibility to antibiotics, making it an interesting target to fight bacterial infections.

The process of QS was first discovered in *Vibrio fischeri*, which emits a bioluminescent signal upon activation of QS. In this species, the *luxI* gene encodes a synthase producing the autoinducer, an acyl homoserine lactone (AHL) (Figure 2). The *luxR* gene encodes a receptor that detects its cognate AHL and subsequently binds to the promoter of downstream genes. This affects gene expression, involving activation of *luxA-E* operon responsible for the production of the bioluminescent signal^{65,66}. Other Gram-negative bacteria have similar QS systems using homologues of the *luxI/luxR* genes that produce and detect species-specific AHLs⁶⁷.

QS is a complex system in *P. aeruginosa*, consisting of various interregulated pathways (Figure 3). Two of these pathways are similar to the LuxI/LuxR QS system in *V. fischeri*, namely LasI/LasR and RhII/RhIR. LasI produces the AHL N-3-oxo-dodecanoyl-homoserine lactone (3-oxo-C12-HSL), while RhII produces N-butyrylhomoserine lactone (C4-HSL)⁶⁸. In addition, *P. aeruginosa* contains a unique third QS system that involves 3,4-dihydroxy-2-heptylquinoline (also named *Pseudomonas* quinolones signal; PQS) and its precursor 4-hydroxy-2-heptylquinoline (HHQ) that bind to the PqsR receptor. PQS is

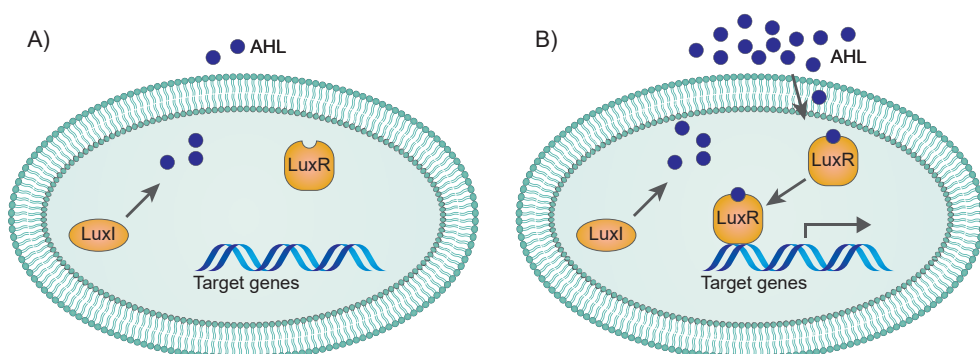


Figure 2: Overview of quorum sensing in Gram-negative bacteria. The concept of quorum sensing (QS) is similar among Gram-negative bacteria. LuxI-type synthases produce small acyl homoserine lactones (AHLs) that diffuse out of the cell. **A)** When the number of bacteria is low, the concentration of AHLs will be low. **B)** When the number of bacteria increases, the concentration of AHL increases. AHL will diffuse into the bacterial cells, bind to their cognate LuxR-type receptors. These LuxR-type receptors will then bind to the DNA and alter gene expression.

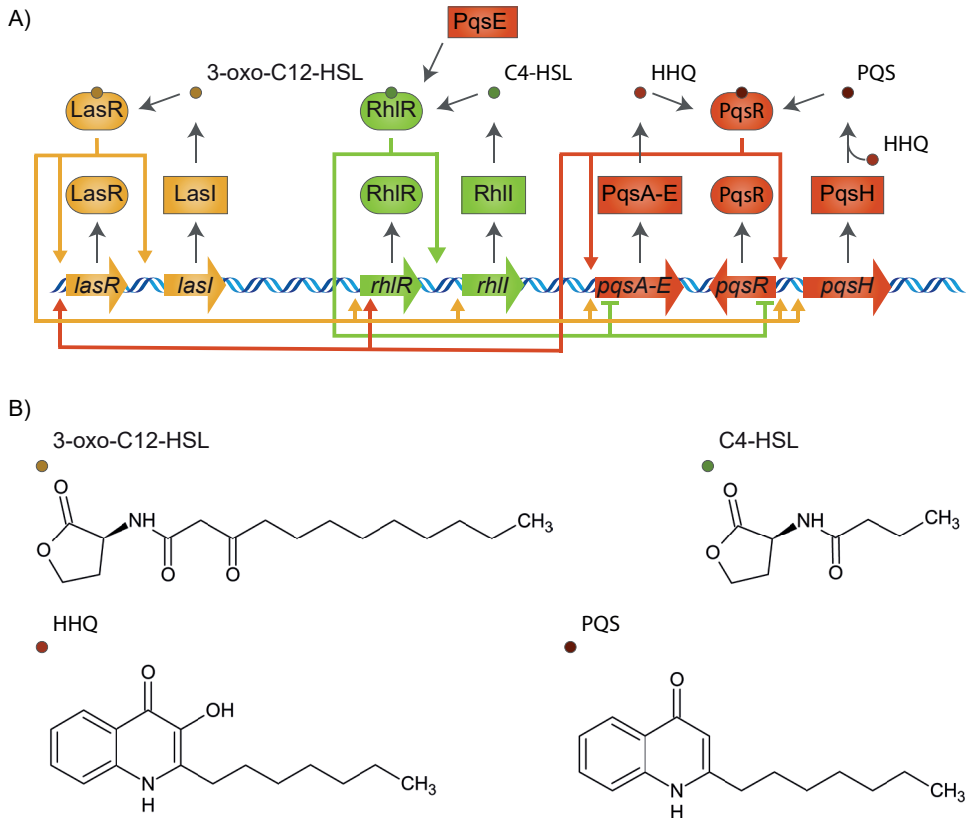


Figure 3: Overview of the complex QS system in *P. aeruginosa*. A) *P. aeruginosa* expresses three QS systems that are highly interconnected. The Las system involves the LasI synthase, which produces 3-oxo-C12-HSL, which binds to the LasR receptor. The LasR receptor positively regulates the expression of the QS genes of all three pathways. The Rhl system involves the RhlI synthase, which produces C4-HSL, which binds to the RhlR receptor. Next to C4-HSL, PqsE can also bind to RhlR. RhlR positively regulates the expression of *rhlI*, while it negatively regulates the expression of the *pqsABCDE* operon and *pqsR*. The enzymes of the *pqsABCDE* operon produce HHQ, which is hydroxylated by PqsH to form PQS. Both HHQ and PQS can bind to PqsR, which positively regulates various other QS genes. B) The chemical structure of the signal molecules involved in QS in *P. aeruginosa*.

synthesized by the enzymes of the *pqsABCDE* operon and *pqsH*⁶⁹. These pathways are highly interconnected by positive and negative regulation⁶⁸.

Transcriptomic studies reveal that QS in *P. aeruginosa* regulates hundreds of genes. Most of these genes include extracellular products such as toxins and extracellular enzymes⁷⁰. A couple of examples are: proteases and elastases that are involved in damaging and degrading host tissues and components of the immune system⁷¹⁻⁷⁴; factors involved in biofilm formation^{75,76}; and exotoxins and hydrogen cyanide that cause cell death^{72,74,77,78}. Therefore, inhibition of QS blocks the virulence of *P. aeruginosa* and the capacity to form biofilms⁷⁹.

The potential of QS inhibitors was first shown by Hentzer and colleagues^{77,80}. They chemically modified the natural halogenated furanones (produced by marine micro-alga

Delisea pulchra) into furanone C-30. Biofilms treated with furanone C-30 made *P. aeruginosa* susceptible again for tobramycin. Moreover, furanone C-30 treatment showed efficient clearing of *P. aeruginosa* in a pulmonary mouse model⁷⁷. Since then, a large number of compounds with QSI activity have been identified from various sources, including ajoene from garlic⁸¹, quercetin from oak⁸², penicillic acid and patulin from fungi⁸³, and synthetically produced flavones⁸⁴.

Quorum sensing during infection

Most of the research studying QS is conducted *in vitro*. This is an easy approach to study QS and to find novel QS inhibitors. However, to get a more relevant understanding of QS, the effect of QS is studied in *in vivo* models. Various studies in mice have shown that *P. aeruginosa* strains with mutations in QS genes are less virulent and lead to lower mortality rates compared to WT strains^{85–87}. In line with these results, a variety of QS inhibitors have beneficial effects in rodents after *P. aeruginosa* infection leading to a reduced virulence of the bacteria, a prolonged survival of the rodents and more efficient clearing^{77,88,89}. Although studies in rodents are promising, no QS inhibitors have reached the clinic yet and the role of QS during human infection is still underexplored⁹⁰.

A classic example in the debate of the role of QS during human infection is the frequent mutation of *lasR* in *P. aeruginosa* isolates derived from the lungs of CF patients⁹¹. LasR is often seen on top of the QS hierarchy since it activates both the Rhl and PQS system (Figure 3)⁶⁸. However, *P. aeruginosa lasR* mutants can activate their QS system independently of LasR^{74,92}. Therefore, making it possible for *P. aeruginosa* to communicate via the Rhl and PQS system, without activation of LasR. The fact that QS in *P. aeruginosa* is indeed still active (with or without an active LasR receptor) in CF infections is evident from the presence of autoinducers involved in QS in *P. aeruginosa* in sputum samples from patients^{93–96}. Taken together, during human infections, the QS regulation is altered by LasR mutations compared to *in vitro* conditions, but nevertheless, remains active.

There have been several studies that compared gene expression *in vivo* (e.g. *P. aeruginosa* from the sputum of CF patients) to gene expression of *P. aeruginosa* when grown *in vitro* (in bacterial medium in the lab). The *P. aeruginosa* transcriptome from human infection differs greatly from *in vitro* samples. Altered gene expression was measured among various gene classes involved in metabolism and antimicrobial resistance⁹⁷. When focusing on QS, various studies have found that the QS regulon is downregulated in human infection compared to *in vitro*^{97–99}. This shows that indeed *in vitro* settings do not mimic the complexities of *P. aeruginosa* infections of human patients and might overestimate the impact of QS in human infections.

Although more information on the role of *P. aeruginosa* QS in human infections is needed, studying this is difficult. Taking human samples has limitations. A couple of limitations include the difficulty to obtain human samples, the impossibility to study early

infections and to microscopically track these infections, and the challenge to use proper control settings. Therefore, to overcome these challenges, model systems are needed that recapitulate human infections as good as possible.

Aim and outline of this thesis

The aim of this thesis is to shine more light on the potential of QS inhibition as alternative treatment against bacterial infections. In **Chapter 2**, we will discuss the search for novel QS inhibitors using a high-throughput screening method to screen a library of more than 10,000 fungal filtrates. This led to the identification of several novel QS inhibitors. In **Chapter 3**, we will describe the effect of paecilomycone (a fungal secondary metabolite) on QS in detail. We show its effect on biofilm formation and virulence factor production. In addition, we try to elucidate the mechanism of action of this compound. Subsequently, in **Chapter 4**, we describe a novel method to study *P. aeruginosa* infections using 2D airway organoids, both from a healthy and CF donor. We describe the potential of this model to study early airway infections and to study the role of QS during these infections. Next, in **Chapter 5**, we investigate the effect of various QS-induced molecules on the airway epithelium using bacterial supernatant extracts and 2D airway organoids. Finally, in **Chapter 6**, I will summarize and discuss the data presented in this thesis. Furthermore, I will share my thoughts about the future of antimicrobials in the clinic.



Chapter 2

Gregatins, a group of related fungal secondary metabolites, inhibit aspects of quorum sensing in Gram-negative bacteria

Wouter A. G. Beenker, Jelmer Hoeksma, and Jeroen den Hertog

Frontiers of Microbiology (2022)

Abstract

Quorum sensing (QS) is a process that regulates gene expression based on cell density. In bacteria, QS facilitates collaboration and it controls a large number of pathways including biofilm formation and virulence factor production, which leads to lower sensitivity to antibiotics and higher toxicity in the host, respectively. Inhibition of QS is a promising strategy to combat bacterial infections. In this study, we tested the potential of secondary metabolites from fungi to inhibit bacterial QS using a library derived from more than ten thousand different fungal strains. We used the reporter bacterium, *Chromobacterium violaceum*, and identified 39 fungal strains that produced QS inhibitor activity. These strains expressed two QS inhibitors that had been described before, as well as eight QS inhibitors that had not been described before. Further testing for QS inhibitor activity against the opportunistic pathogen *Pseudomonas aeruginosa* led to the identification of gregatins as an interesting family of compounds with QS inhibitor activity. Whereas various gregatins inhibited QS in *P. aeruginosa*, these gregatins did not inhibit virulence factor production and biofilm formation. We conclude that gregatins inhibit some, but not all aspects of QS.

Keywords: Quorum sensing, Gregatins, *Chromobacterium violaceum*, *Pseudomonas aeruginosa*, Antimicrobial activity, Fungi

Introduction

Antibiotic resistance is a growing problem leading to ineffective antibiotic treatments, causing bacterial infections to be lethal again^{14,100–102}. Especially the treatment of Gram-negative bacteria is challenging due to the composition of their outer membrane, which makes it hard for antibiotics to enter the cells^{31,103,104}. While new antibiotics are still being introduced into the clinic, these often represent synthetically optimized antibiotics from existing classes leading to a quick rise of resistance¹⁰⁵. Therefore, it is important to look for alternative approaches to fight bacterial infection. Targeting bacterial quorum sensing (QS) is one of these promising approaches.

QS is effectively a bacterial communication system triggered by changes in cell density. Bacteria secrete signal compounds, termed autoinducers. In the case of Gram-negative bacteria these autoinducers are acyl-homoserine lactones (AHLs) produced by LuxI-type autoinducer synthases. The AHLs cross the membrane and bind to LuxR-type receptors. If the cell population density increases, the signal increases, eventually leading to altered gene expression¹⁰⁶. QS regulates various pathways involved in the production of virulence factors and strengthening of the biofilm^{59,71,75}. The opportunistic pathogen *Pseudomonas aeruginosa* has three different QS pathways, two N-Acyl Homoserine Lactone (AHL)-based pathways (*las*-encoded system and *rhl*-encoded system) and a unique *Pseudomonas* Quinolone Signal (*pqs*)-based pathway. These three pathways are interconnected through feedback and feed-forward mechanisms^{68,107}. Some studies refer to IQS as the fourth QS system in *P. aeruginosa*, but because this is controversial¹⁰⁸, we have not addressed IQS here. The QS system in *P. aeruginosa* plays a role in the production of virulence factors, including elastase⁷¹, protease⁷² and pyocyanin¹⁰⁹, and strengthens biofilm formation by the production of rhamnolipids¹¹⁰ and extracellular DNA^{75,111}. In general, inhibition of QS decreases the production of toxic virulence factors and weakens biofilm formation^{63,81}. Therefore, inhibition of QS may have beneficial effects, including less tissue damage, due to reduced levels of toxic virulence factors and higher susceptible to antibiotics, because of the weakened biofilm. QS inhibitors have been isolated from various sources over the years, including ajoene from garlic⁸¹, quercetin from oak⁸², furanones from alga¹¹², and flavones from natural origin or synthetically generated flavones⁸⁴.

In general, fungi are an interesting source of natural compounds that have progressed into the clinic^{113,114}. For instance, the antibiotics penicillin and cephalosporin have a fungal origin and have been used to treat many patients¹¹³. Yet, fungi remain rather unexplored with respect to production of QS inhibitors¹¹⁵. Nevertheless, QS inhibitors have also been found to be produced by fungi, including patulin and penicillic acid⁸³, making them an interesting potential source for QS inhibitors. In collaboration with the Westerdijk Fungal Biodiversity Institute, our lab has developed a unique library that consists of filtrates of 10,207 fungal strains¹¹⁶, which facilitates the search for novel natural compounds produced by a large variety of fungal species.

The aim of this study was to identify novel QS inhibitors. To this end, we screened our library of fungal filtrates, which allowed us to assess the potential of QS inhibition among 10,207 strains of fungi. For the screening, we used the Gram-negative bacterium *Chromobacterium violaceum* as a reporter. *C. violaceum* produces violacein – a purple pigment – upon activation of QS, making it an excellent reporter for high-throughput screens^{84,117}. This approach led to the identification of eight compounds that had not been described before to have QS inhibitor activity. In addition, we tested selected compounds for inhibition of specific aspects of QS in the opportunistic pathogen *Pseudomonas aeruginosa*. We identified gregatins as a promising group of compounds to inhibit QS in various Gram-negative bacterial strains.

Materials and Methods

Bacterial strains and growth conditions

Bacterial strains used in this study are listed in Table 1. Bacteria were stored at -80 °C in a 20 % glycerol stock solution. *C. violaceum* was inoculated on tryptic soy agar (TSA) and single colonies were grown in tryptic soy broth (TSB) at 27 °C. PAO1 strains were inoculated on Luria agar (LA) at 37 °C and single colonies were grown in AB minimal medium supplemented with 0.5 % glucose and 0.5 % casamino acids¹¹⁸, unless stated otherwise.

Table 1 | Bacterial strains used in this study

Bacterial strain	Characteristic	Source
<i>Chromobacterium violaceum</i>	WT, ATCC 12472	Westerdijk Fungal Biodiversity Institute
<i>P. aeruginosa</i>	WT, PAO1	
PAO1-GFP	WT, PAO1 gfp-tagged	Yang <i>et al.</i> (2007) ¹⁹⁴
PAO1 <i>lasB</i> -GFP	WT, PAO1, gfp fusion to <i>lasB</i> gene	Hentzer <i>et al.</i> (2002) ¹⁹⁵
PAO1 <i>rhIA</i> -GFP	WT, PAO1, gfp fusion to <i>rhIA</i> gene	Fong <i>et al.</i> (2017) ¹⁹⁶
PAO1 <i>pqsA</i> -GFP	WT, PAO1, gfp fusion to <i>pqsA</i> gene	Fong <i>et al.</i> (2017) ¹⁹⁶
PAO1 $\Delta lasI$ - $\Delta rhII$	PAO1, QS mutant	Hentzer <i>et al.</i> (2003) ¹⁹³

High-throughput screen for quorum sensing inhibitors

The high-throughput screen for QS inhibitors using *C. violaceum* as a reporter was performed as previously described with minor modifications^{84,117}. Overnight grown *C. violaceum* was diluted and grown until an OD₆₀₀ of 0.5-0.7. Then, bacteria were diluted 1:1000 before addition to the 96-well plate containing the fungal supernatant to a total volume of 80 μ l (1:1, v:v). In addition to the wells with fungal supernatant, plates also included untreated bacteria and TSB only to check sterility of the medium. Quercetin (Sigma-Aldrich, Merck Life Science, Amsterdam, the Netherlands) was added at a concentration of 125 μ M as positive control of violacein inhibition and 130 μ M of meropenem (Sigma-Aldrich, Merck Life Science, Amsterdam, the Netherlands) was used as control in the viability assay. Plates

were incubated for 20 h at 27 °C with 200 rpm shaking.

To measure the violacein production, plates were centrifuged at 3000 rpm for 10 min to collect precipitated violacein. Supernatant was discarded and the pellet was resuspended in 200 μ l 96 % ethanol. Plates were centrifuged again at 3000 rpm for 10 min to separate the cells from the violacein to avoid interference of the signal. Half of the supernatant was transferred to a new 96-well plate and the violacein production was quantified by measuring the optical density at 562 nm on the ASYS expert plus microplate reader (Biochrom Ltd, Cambridge, UK).

Resazurin staining was used to measure the viability of the bacteria. Following incubation for 20 h as described above, plates were centrifuged at 3000 rpm for 10 min. Supernatant was removed and resazurin (25 μ g/mL in PBS) solution was added. Plates were incubated in darkness for 45 min at 27 °C before fluorescence was measured on a PHERAstar microplate reader (BMG Labtech, de Meern, the Netherlands) using 540 nm excitation and 590 nm emission wavelength. Viability was calculated using the following equation:

$$\% \text{ Viability} = \frac{\text{Fluorescence sample} - \text{Fluorescence background}}{\text{Fluorescence untreated} - \text{Fluorescence background}}$$

The same approach was used in follow-up experiments, measuring the effect of single molecules on violacein production. Dilution ranges of the compounds were tested in triplicates using a maximum concentration of 2.5 % DMSO to minimize the effect of DMSO on QS and bacterial viability.

QS inhibition in *Pseudomonas aeruginosa*

The experiments were performed as previously described¹¹⁸. In brief, overnight grown cultures were diluted in PBS to an OD₄₅₀ of 0.1-0.2 before addition to a 96-well plate with dilution ranges of compounds up to a volume of 200 μ l (1:1, v:v). The GFP fluorescence (excitation 485 nm, emission 535 nm) and absorbance (600 nm) were measured every 15 min for 15 h at 34 °C on a CLARIOstar microplate reader (BMG Labtech, de Meern, the Netherlands). IC₅₀ values were calculated using PRISM software, plotting the maximum slope of GFP/OD.

Biofilm assay

Overnight cultures were diluted 1:1000 to a final OD₆₀₀ of ~0.01. Diluted bacterial cells were added to a 96-well plate containing concentration ranges of compound in triplicates up to a volume of 200 μ L (1:1, v:v). Plates were sealed with BreatheEasy seal (Sigma-Aldrich, Merck Life Science, Amsterdam, the Netherlands) to prevent evaporation and incubated at 37 °C under static conditions. After 24 h, medium was discarded and the wells were rinsed once with PBS. The biomass was then stained with 0.1 % (w:v) crystal violet solution for 5 min. Crystal violet was discarded and excess crystal violet was removed by rinsing 3 times with water. Plates were dried overnight and bound crystal violet was

resuspended in 33% (v:v) acetic acid and quantified at a wavelength of 562 nm using a ASYS expert plus microplate reader (Biochrom Ltd, Cambridge, UK).

Pyocyanin extraction

Pyocyanin quantification was based on a previously described assay with minor modifications¹¹⁹. In brief, treated bacteria were grown in Kings' A medium (2 % (w:v) protease peptone, 1 % (w:v) potassium sulfate, 0.164 % (w:v) magnesium chloride, 1 % (v:v) glycerol in MQ) for 24 h at 37 °C in triplicates, before pelleting the cells. 900 µL of bacterial supernatant was added to chloroform (1:1) and tubes were shaken vigorously. Then, 800 µL of chloroform was added to 700 µL of 0.2 M HCl and vortexed. Samples were centrifuged for 2 min at 10,000 rpm and 600 µL of 0.2 M HCl was transferred to a cuvette. Absorbance was measured at 520 nm, using 0.2 M HCl as a blank.

Rhamnolipid extraction

Rhamnolipid concentrations were measured based on the standard orcinol-sulfuric acid assay¹²⁰. In brief, treated cultures were grown at 37 °C for 24 h before collecting 900 µL of supernatant. Diethyl ether was added (1:1) to the supernatant and mixed. Then, 800 µL of diethyl ether was taken to a fresh tube and dried via evaporation at RT. To each extract, 100 µL of MQ was added before addition of another 800 µL of 12.9 mM orcinol (Sigma-Aldrich, Merck Life Science, Amsterdam, the Netherlands) (in 70 % (v:v) H₂SO₄). Reaction was maintained at 80 °C for 30 minutes and absorbance was measured at a wavelength of 495 nm.

Purification of compounds

Fungal strains corresponding to the active filtrates were grown on a specific agar plate preferred by the strain and incubated at 25 °C. After 7 d, cubes of 5x5 mm were cut out and 2 cubes were used per 50 mL of medium in 100 mL bottles. Standard medium consisted of 3.5 % Czapek dox broth + 0.5 % yeast extract. To produce gregatins, potato dextrose broth (23 % (v:v) potato extract + 2 % glucose) was used. Fungi were incubated in liquid medium for 7 d at preferred conditions (15 °C static, 25 °C static or 25 °C + 100 rpm on an orbital shaker) before filter sterilizing the medium with a 0.22 µm Millipore filter (Werck, Amsterdam, the Netherlands). The sterile supernatant was extracted using 3x 1/3 volume of ethyl acetate using a separation funnel. The ethyl acetate layers were collected and evaporated to dryness using a rotary evaporator with a water bath at 40 °C. The dried pellet was dissolved in DMSO. The extracts were fractionated using a preparative high performance liquid chromatography (HPLC) system consisting of a Shimadzu CBM-20A controller, a Shimadzu LC-20AP pump and a Shimadzu FRC-10A fraction collector using a C18 reversed-phase Reprosil column (10 µm, 120 Å, 250 x 22 mm) and a Shimadzu SPD-20A UV-detector set at 214 nm and 254 nm (Shimadzu, 's Hertogenbosch, the Netherlands). The mobile phase consisted of 100 % MQ with 0.1 % trifluoroacetic acid (Buffer A) and 100 % acetonitrile with 0.1 % trifluoroacetic acid (Buffer B). Protocols consisted of: 5 % Buffer B for

5 min followed by a linear gradient to 95 % buffer B for 40 min, 5 min of 95 % buffer B before returning to 5 % buffer B for another 5 min with a constant flow rate of 12 mL/min. Fractions were collected every 63 s starting after the DMSO peak and ending at 95 % buffer B resulting in 40 fractions. 1.9 mL of the fraction was dried in a speed-vac overnight and dissolved in 50 μ L DMSO to test for QS inhibitory activity.

Identification of compounds

Active fractions were analyzed for their purity using an analytical Shimadzu LC-2030 system with PDA detection (190-800 nm) with a Shimadzu Shim-pack GIST C18-HP reversed-phase column (3 μ m, 4.6x100 mm) (Shimadzu, 's Hertogenbosch, the Netherlands). Besides determining the purity, also a UV-VIS spectrum of the fractions was obtained. Pure fractions were further analyzed by measuring the mass using a Shimadzu LC-2030C 3D plus system, sometimes followed by more accurate high resolution mass spectrometry (HRMS), measured on a LCT-instrument (MicroMass Ltd, Manchester UK). For HRMS the sample was mixed with sodium formate for detection of sodium adduct ions. In addition, this procedure gave an internal calibrant in each sample to facilitate a more accurate measurement of the mass of the sample. Obtained masses and UV spectra were compared with previously identified samples and literature. If needed, further chemical analysis using NMR measurements were performed. For the NMR measurements, the fractions were dried in a speed-vac overnight and dissolved in DMSO- d_6 before measurements on a Bruker 600 MHz.

Commercial compounds used:

Rubrofusarin (Sigma-Aldrich) was used to test for QS inhibitory activity. Penicillic acid (VWR) and Indole-3-acetic acid (Thermo-Fisher) were used to compare with identified fungal compounds.

Results

Screen for quorum sensing inhibitors

To search for novel QS inhibitors, we used a high-throughput method using a Gram-negative bacterium as reporter strain, *C. violaceum*, which produces a purple pigment, violacein, upon activation of QS^{84,117}. As a source of potential QS inhibitors, we used a library consisting of the secondary metabolites of 10,207 fungal strains, that was described by Hoeksma and colleagues¹¹⁶. All fungi were obtained from the Westerdijk Fungal Biodiversity Institute. The fungal supernatant was added (1:1, v:v) to the *C. violaceum* and after overnight incubation, the amount of violacein was determined.

Of the 10,207 fungal filtrates, 324 inhibited violacein production by more than 80% compared to untreated (Figure 1A). Since loss of violacein production might also be due to loss of viability of the bacteria, analysis of violacein production in response to the 324 hits was repeated and viability of the bacteria was determined in parallel using a resazurin

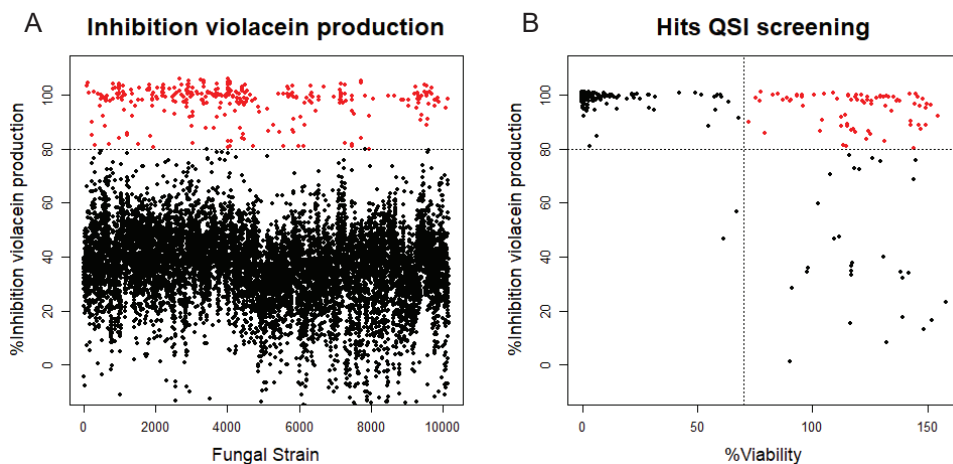


Figure 1: Screening of fungal secondary metabolites on *C. violaceum* reporter. **A)** Inhibition of violacein production after treatment with fungal supernatant. Every dot represents the supernatant of a single fungal strain. Fungal supernatants that show inhibition of more than 80 % are shown as red dots (N=324). **B)** The 324 strains that showed an inhibition of >80 % were screened again, measuring both inhibition of violacein production and the viability of the bacteria. The compounds that show an inhibition of >80 %, while not affecting the viability (>70 %) are shown as red dots (N=79).

staining assay^{121,122}. 79 strains were identified to inhibit violacein production without affecting viability. Viability is calculated as the ratio of fluorescence intensity in the sample and fluorescence intensity in the control. Violacein interferes somewhat with fluorescence. Therefore, it is not surprising that in samples with high QS inhibitor activity and hence low violacein production, the apparent fluorescence in the resazurin assay is higher than in the control and thus higher than 100%. 214 strains reduced violacein production and at the same time reduced viability of *C. violaceum*, which presumably caused the observed reduction in violacein production. 31 strains from the initial screen did not affect violacein production significantly and hence, turned out to be false positives (Figure 1B).

The 79 strains that inhibited violacein production without affecting viability in *C. violaceum* were selected for further analysis. The fungi were cultured again and the growth conditions were optimized (15 °C static, 25 °C static, and 25 °C with shaking) to maximize the inhibitory response. Of the 79 hits, 39 showed activity after reculturing: 7 preferred 15 °C cultivation, 20 preferred 25 °C cultivation, and 12 preferred 25 °C cultivation with shaking. Of the other strains that were cultured again, 29 did not show QS inhibitor activity in any of the growth conditions, and 11 turned out to be toxic for the bacteria. These 40 strains were disregarded. The 39 remaining fungal strains harbored QS inhibitor activity and were cultured in larger volumes at the optimized growth condition for activity-guided purification of the QS inhibitors and further chemical analysis.

Identification of bioactive compounds

To identify the compounds with QS inhibitor activity, an activity-guided purification

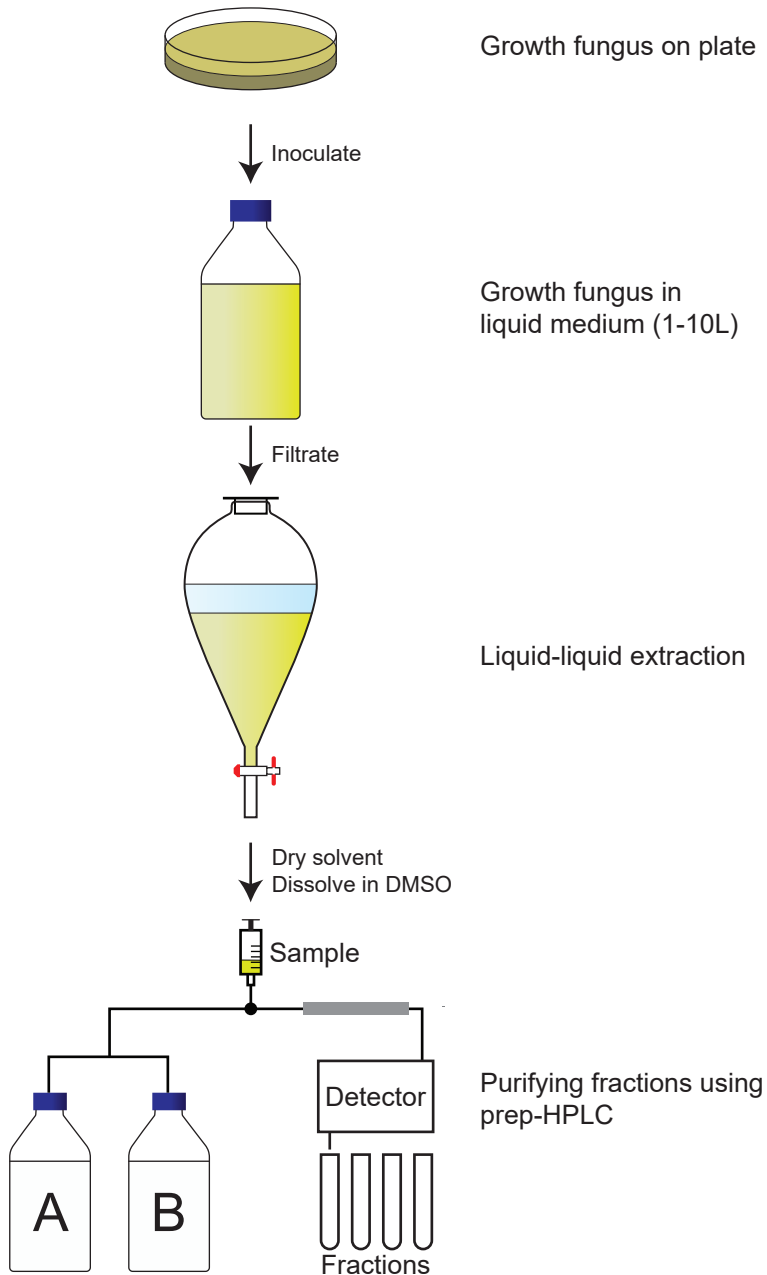


Figure 2: Activity-guided purification approach to identify QS inhibitors. A fungus of interest is grown on an agar plate for a week before inoculation in large volume (1-10 L) for another week at preferred conditions. The supernatant is then filtrated before liquid-liquid extraction with ethyl acetate. The ethyl acetate is dried and the pellet is dissolved in DMSO before fractionating the extract using a preparative HPLC. Fractions are dried and tested for QS inhibitory activity before identification of the fraction.

approach was used (Figure 2). Briefly, after 7 d of growth in liquid medium, the supernatant was separated from the fungus by filtration. The secondary metabolites were isolated by liquid-liquid extraction, evaporation of the solvent and dissolving in DMSO. The samples were tested for QS inhibitor activity using violacein production as read-out. Active samples were analyzed using analytical HPLC, which allowed us to avoid repeated re-identification of the same compounds with identical retention times and UV-VIS absorbance. In case the extract did not appear to contain known compounds with QS inhibitor activity, the extract was fractionated using preparative HPLC and single fractions were tested for QS inhibitor activity.

The purity of active fractions was examined using analytical HPLC. Pure fractions with QS inhibitor activity were further analyzed using various methods to identify the compound, including: LC-MS, high-resolution MS, and ^1H and ^{13}C Nuclear magnetic resonance (NMR). If necessary, subsequent 2D-NMR methods were used to identify the chemical structure of the compound, including Correlation Spectroscopy (COSY); Heteronuclear Single-Quantum Correlation (HSQC); and Heteronuclear Multiple-Bond Correlation spectroscopy (HMBC).

Proof of principle: Identification of penicillic acid as QS inhibitor

One of the active fungi identified in the screen is *Penicillium simplicissimum* (CBS 392.78A) with an inhibition of violacein production of 100% while viability was not significantly affected (85% compared to untreated). We inoculated this fungus in a large volume at 25 °C, extracted the supernatant with ethyl acetate, and dissolved the sample in DMSO. Purification and subsequent analysis of the fractions led us to fraction 15 as the active fraction (Figure 3A). Sub-lethal levels of this compound show a concentration-dependent violacein inhibition (Figure 3B). Viability levels appear to be upregulated when QS is inhibited. This is likely due to low violacein production at these concentrations, compared to the control, which leads to an enhanced ratio of fluorescence in this assay.

Measuring the bioactive fraction 15 on the analytical HPLC showed a single peak with a maximum UV-absorbance of 223 nm (Figure 3C). Further chemical analysis showed a m/z of 171.1 [M+H] (Figure 3D). Next, the fraction was dried and dissolved in DMSO- d_6 for ^1H -NMR spectrum analysis (Figure 3E). Analysis of these data suggested that fraction 15 from *Penicillium simplicissimum* contained penicillic acid.

To verify the identity of the active compound in fraction 15, commercially available penicillic acid was analyzed by analytical HPLC (Figure 3F) and tested on *C. violaceum* (Figure 3G). The results showed that the retention time, absorbance, and QS inhibitor activity of commercially available penicillic acid matched that of bioactive fraction 15. Penicillic acid was identified as a QS inhibitor before¹²³. Our results together with the published data of penicillic acid provide proof-of-principle for our approach to identify QS inhibitors.

Other QS inhibitors from fungi

Penicillic acid was identified as the bioactive compound in six more fungi, based

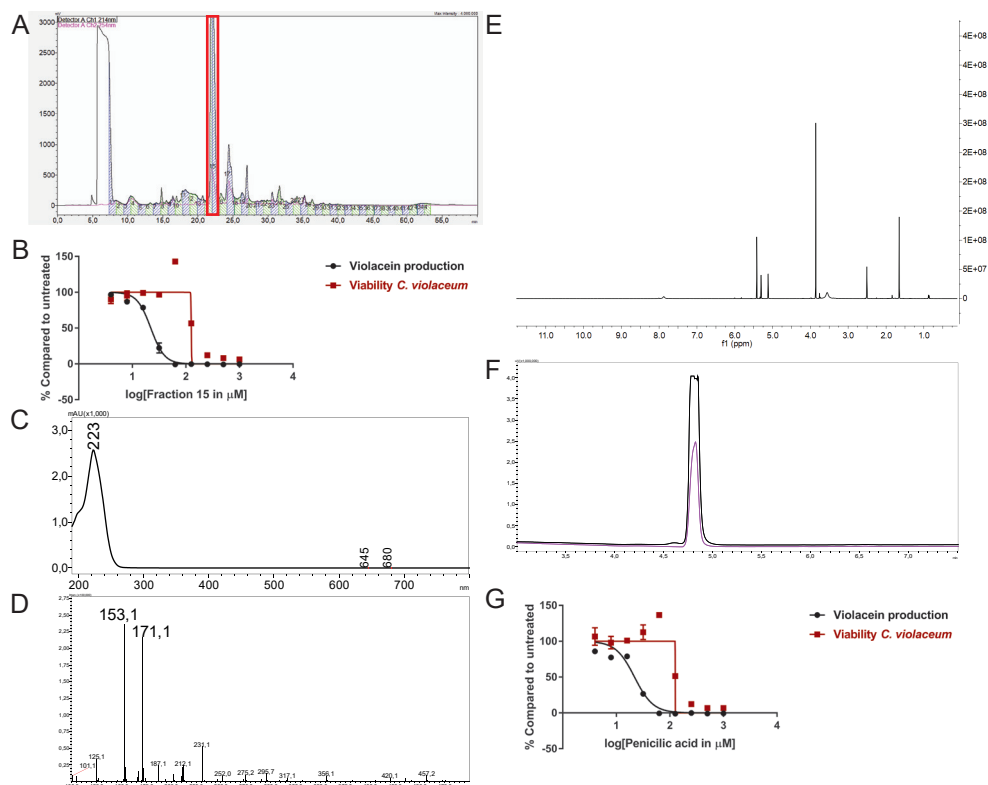


Figure 3: Identification of penicillic acid as QS inhibitor. **A)** After growing *Penicillium simplicissimum* in large volume, the extract was fractionated using prep-HPLC. Fraction 15 (red box) was the active fraction. **B)** QS inhibitory activity of fraction 15 using *C. violaceum* as reporter (black line and symbols) and cell viability in parallel (red line and symbols). A range of concentrations was tested. **C)** UV-VIS spectrum of fraction 15. **D)** LC/MS analysis of fraction 15. **E)** $^1\text{H-NMR}$ of fraction 15. **F)** Analytical HPLC chromatogram of fraction 15 (black line) compared to commercial penicillic acid (pink line), showing a similar retention time. **G)** QS inhibitor activity and viability of commercial penicillic acid. Experiments were done in triplicate. Error bars represent SEM.

on analytical HPLC retention time and UV-VIS spectrum (Table 2). Our approach led to the identification of a variety of other known QS inhibitors, including patulin¹²³ and derivatives or compounds closely related to known QS inhibitors, including 6-methylsalicylic acid and indole-3-acetic acid^{124–130}. Interestingly, our approach led to the identification of compounds that had not been described before as QS inhibitors, including citrinin, rubrofusarin and the family of gregatins (Table 2, Figure 4 and Supplementary figure 1).

Rubrofusarin was detected in the active fraction of *Aspergillus carbonarius* (CBS 101.14). However, the active fraction was not pure and also contained fonsecin (Supplementary figure 2). We were not able to separate rubrofusarin and fonsecin by preparative HPLC. We obtained commercially available rubrofusarin and established that it exhibited potent QS inhibitor activity without affecting viability (Table 2, Supplementary figure 1). Unfortunately, fonsecin is not commercially available and hence, it remains to be determined if fonsecin also has QS inhibitor activity.

The difference between concentrations that elicited bacterial toxicity and QS inhibitory activity in *C. violaceum* was two-fold for patulin and six-fold for penicillic acid, respectively (Figure 3G, Table 2, Supplementary Figure 1). Interestingly, this difference in concentrations was much bigger for the newly identified QS inhibitors. For instance, the IC_{50} of desmethyl-gregatin A, isolated from *Aspergillus allahabadii* (CBS164.63), for the viability of bacteria was 74 times higher than the IC_{50} for violacein inhibition (Table 2, Supplementary Figure 1). These results suggest that these newly discovered QS inhibitors were effective at concentrations that did not affect bacterial viability and therefore, these QS inhibitors were selected for further analysis using other bacterial species.

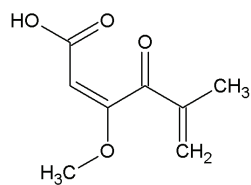
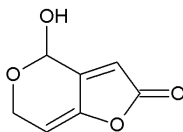
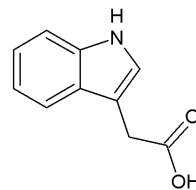
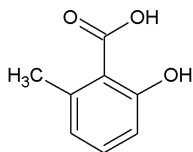
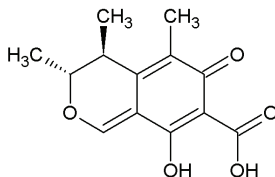
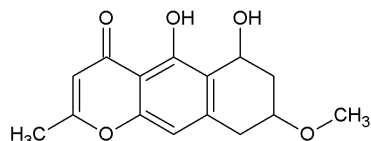
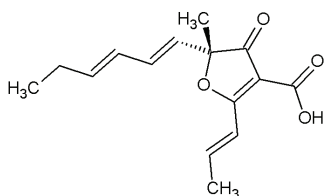
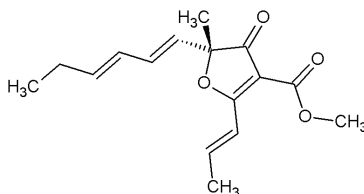
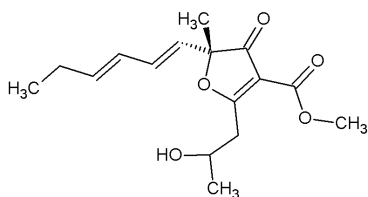
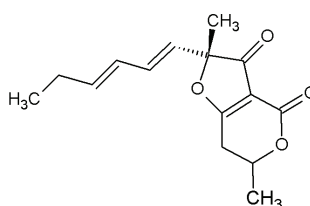
Table 2 | Compounds with QS inhibitor activity.

Compound	IC_{50} Violacein	IC_{50} viability	Fungus
Penicillic acid	22.13 μ M	126.2 μ M	<i>Aspergillus auricomus</i> (CBS639.78)
			<i>Aspergillus melleus</i> (CBS622.75)
			<i>Aspergillus ostianus</i> (CBS627.78)
			<i>Aspergillus sulphureus</i> (CBS117.26)
			<i>Eupenicillium baarnense</i> (CBS315.59)
			<i>Penicillium simplicissimum</i> (CBS392.78A)
			<i>Penicillium simplicissimum</i> (CBS391.78A)
Patulin	12 μ M	22 μ M	<i>Metarhizium brunneum</i> (CBS316.51)
			<i>Penicillium tardum</i> (CBS378.48)
Indole-3-acetic acid	481 μ M	6091 μ M	<i>Colletotrichum fragariae</i> (CBS142.31)
6-methyl salicylic acid	419 μ M	5789 μ M	<i>Penicillium tardum</i> (CBS378.48)
Citrinin	201 μ M	~1-2 mM	<i>Aspergillus allahabadii</i> (CBS164.63)
			<i>Penicillium citrinum</i> (CBS309.48)
			<i>Penicillium citrinum</i> (CBS252.55)
			<i>Penicillium citrinum</i> (CBS341.61)
			<i>Penicillium citrinum</i> (CBS139.45)
<i>Penicillium spinulosum</i> (CBS294.62)			
Rubrofusarin	92 μ M	>250 μ M	Commercial compound
desmethyl gregatin A	14 μ M	>1 mM	<i>Aspergillus allahabadii</i> (CBS164.63)
Gregatin A	344 μ M	>4 mM	<i>Aspergillus panamensis</i> (CBS120.45)
Gregatin D	210 μ M	>4 mM	<i>Aspergillus panamensis</i> (CBS120.45)
Cyclogregatin	26 μ M	>1 mM	<i>Aspergillus panamensis</i> (CBS120.45)

Compounds with QS inhibitor activity are listed. IC_{50} for QS inhibitor activity (violacein production) and IC_{50} for viability of *C. violaceum* bacteria is depicted as well as the name of the fungi that produce the respective compounds.

QS inhibitor activity on *P. aeruginosa*

To test if the active compounds also inhibited QS in other bacterial species, the newly discovered compounds with QS inhibitor activity were tested on *P. aeruginosa*. GFP-reporters for each of the effector protein pathways, Las, Rhl and Pqs, were used to test for QS inhibition in the *P. aeruginosa* strain PAO1. In addition, a PAO1-GFP strain was used

Penicillic acidPatulinIndole-3-acetic acid6-methyl salicylic acidCitrininRubrofusarinDesmethyl-gregatin AGregatin AGregatin DCyclogregatin**Figure 4: Chemical structures of the compounds identified as QS inhibitors in this study.**

as control to test if the compounds were specific QS inhibitors or merely affected GFP or bacterial growth. GFP values were normalized to the growth of the bacteria and the IC_{50} was determined based on the slope of the curves at different concentrations of compound (Figure 5). Various compounds showed a clear, concentration-dependent reduction of the slope in one or more PAO1 QS reporters (Figure 5, Supplementary Figure 3). However, not all

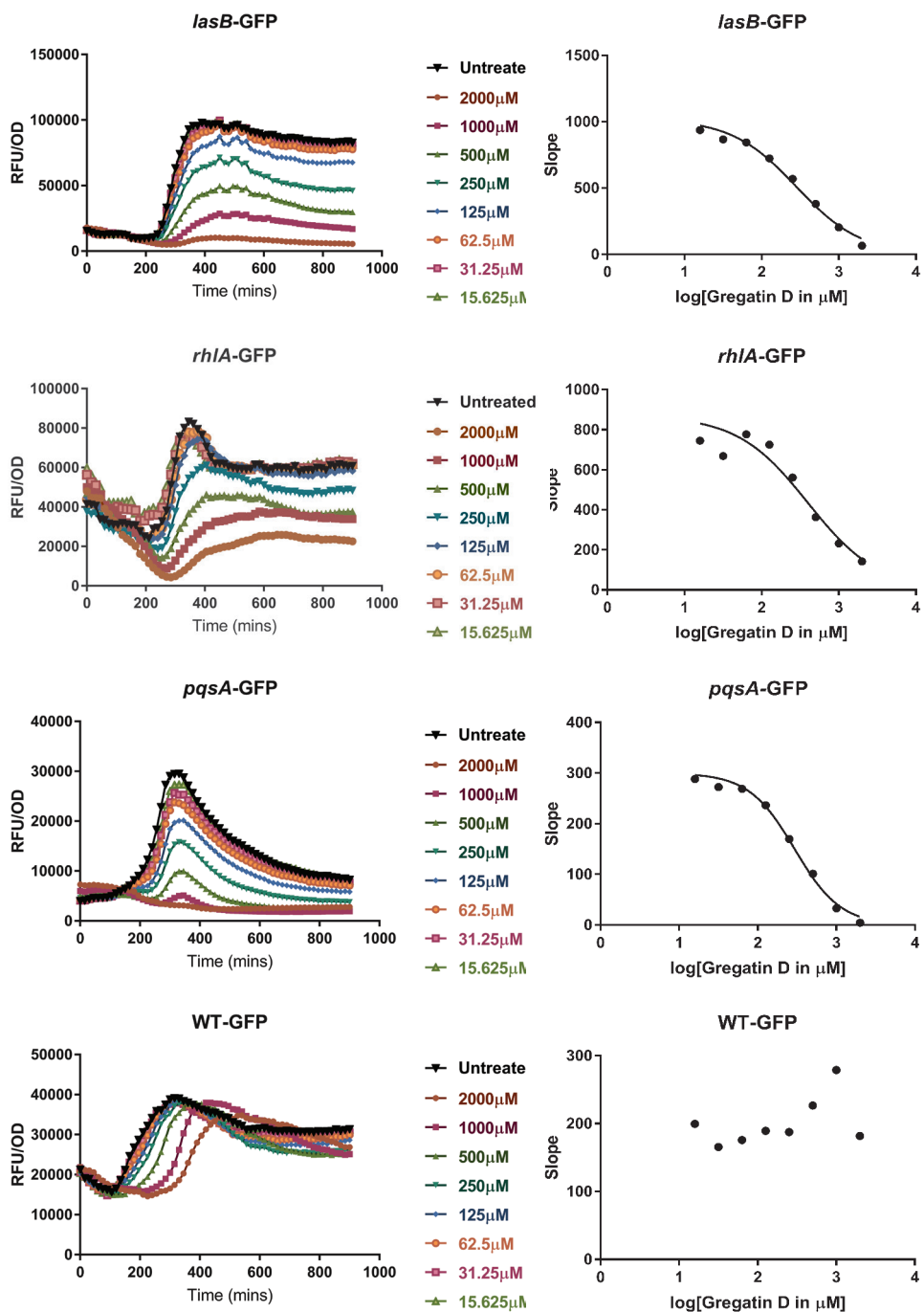


Figure 5: QS inhibitor activity of gregatin D on *Pseudomonas aeruginosa* strain PAO1. Gregatin D was tested on the three QS reporters of *P. aeruginosa* and a WT-GFP control. The GFP signal was normalized by dividing by the OD_{600} values giving RFU/OD plots (graphs on the left). The maximum slopes are plotted (graphs on the right) by which the IC_{50} was calculated. Experiments were done in triplicates, the mean of RFU/OD is plotted and used for the calculations of the maximum slope.

compounds with QS inhibitory activity in *C. violaceum* inhibited one or more QS pathways in PAO1. For most compounds, much higher concentrations were needed to inhibit QS in PAO1 than in *C. violaceum*. Overall, the compounds had the strongest effect on the *pqsA*-reporter and the least effect or no effect on the *rhIA*-GFP reporter.

An interesting difference between *C. violaceum* and PAO1 was also observed among the family of gregatins. The most promising compounds in *C. violaceum* were desmethyl-gregatin A and cyclogregatin. However, in PAO1, gregatin A and gregatin D seem to be the most potent QS inhibitors and they affected all three pathways (Table 3). Therefore, gregatin A and gregatin D were selected for further analysis.

Table 3 | QS inhibitor activity of selected compounds in *P. aeruginosa* (PAO1) reporters.

Compound	IC ₅₀ <i>lasB</i> -GFP	IC ₅₀ <i>rhIA</i> -GFP	IC ₅₀ <i>pqsA</i> -GFP	IC ₅₀ PAO1-GFP
Indole-3-acetic acid	Not active	Not active	>3125 μM	Not active
6-methyl salicylic acid	Not active	Not active	2809 μM	Not active
Rubrofusarin	Not active	>62,5 μM	17 μM	Not active
Citrinin	>2000 μM	Not active	1062 μM	Not active
Desmethyl Gregatin A	509 μM	Not active	130 μM	Not active
Gregatin A	228 μM	516 μM	203 μM	Not active
Gregatin D	282 μM	398 μM	294 μM	Not active
Cyclogregatin	>500 μM	Not active	>500 μM	Not active

IC₅₀s of the different the different reporters were determined. Compounds were scored as “non-active” when it was not possible to plot a nonlinear regression curve because of lack of inhibitory activity. In case there was inhibitory activity, but 50% inhibition was not reached, the IC₅₀ was estimated to be higher than the highest concentrations tested. Higher concentrations could not be tested due to excessively high DMSO concentrations or precipitation of the compound.

Gregatins increase biofilm formation in PAO1 QS mutants

Since QS is involved in the formation of biofilms, we hypothesized that inhibition of QS would inhibit biofilm formation. To test this, we measured the effect of gregatin A and gregatin D on the formation of biofilms in *P. aeruginosa* PAO1 using crystal violet staining. We tested the gregatins both on the formation of biofilm in WT bacteria and QS mutant (Δ *lasI*- Δ *rhII*). Gregatin A and gregatin D both did not show a significant decrease or increase in biofilm formation in WT PAO1 (Figure 6). Interestingly, biofilm formation was increased in QS mutants, after treatment with gregatin A and gregatin D. Gregatin A appeared to be more potent than gregatin D. Both compounds showed maximum effects at 1000 μM, at which concentration biofilm formation of the QS mutant exceeded that of WT (Figure 6). We conclude that gregatin A and gregatin D do not affect biofilm formation of PAO1 significantly, but may somehow affect biofilm formation in *P. aeruginosa* with impaired QS.

Gregatins alter the expression levels of virulence factors

QS also regulates the production of virulence factors in *P. aeruginosa*. Therefore, we expected that the QS inhibitor activity of gregatin A and gregatin D would inhibit production of virulence factors. To test this, we measured the relative levels of the virulence factors

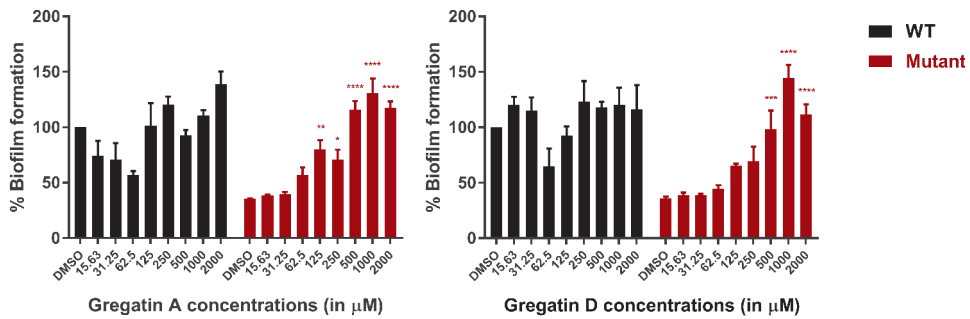


Figure 6: The effect of the gregatins on biofilm formation in *P. aeruginosa*. Biofilm formation was measured by crystal violet staining, after treatment with gregatin A and gregatin D and normalized to DMSO treated. The effect on biofilm formation in both WT and QS mutant ($\Delta las/\Delta rhl$) were measured. The mean of three experiments performed in triplicates was plotted. The error bars represent the SEM. A one-way ANOVA, corrected for multiple comparisons with Dunnett's test was performed to determine statistical significance. Values are compared to DMSO treated controls (*, $P < 0.05$; **, $P < 0.005$; ***, $P < 0.001$; ****, $P < 0.0001$).

pyocyanin and rhamnolipids. As a control, the QS mutant was included, which produced more than 10-fold less virulence factor than WT PAO1 (Fig. 7). Gregatin A treatment led to a dose-dependent increase in pyocyanin production in *P. aeruginosa* with an optimum at 500 µM ($p < 0.0001$) (Figure 7A). Gregatin D did not show an increase in pyocyanin expression, but a significant decrease ($p < 0.0001$) was observed at the highest concentration

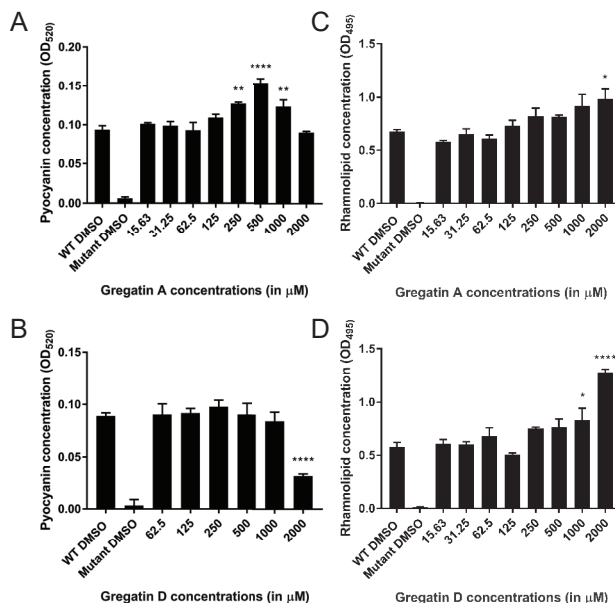


Figure 7: Distinct effects of gregatins on production of virulence factors. The effect of gregatin A and gregatin D was tested on the production of the virulence factors A-B) pyocyanin and C-D) rhamnolipid. The mean of the experiment performed in triplicates was plotted. A one-way ANOVA, corrected for multiple comparisons with Dunnett's test was performed to determine statistical significance. Values are compared to DMSO treated controls (*, $P < 0.05$; **, $P < 0.005$; ****, $P < 0.0001$)

we tested, 2000 μM (Fig. 7B). Gregatin A and gregatin D treatment increased rhamnolipid concentrations significantly only at high concentrations, 2000 μM and 1000 μM , respectively, in stark contrast to diminished rhamnolipid production of the QS mutant (Figure 7C, D). Taken together, our data show different effects of gregatins on virulence factor production.

Discussion

In this study, we found various active compounds in fungal filtrates that inhibited QS in *C. violaceum*. The identification of the known QS inhibitors (patulin and penicillic acid) showed that *C. violaceum* works well as reporter in high-throughput format. However, patulin and penicillic acid did not show a big difference between concentrations that affected QS inhibition and toxicity in bacteria, resulting in a small concentration range to evaluate QS inhibition without effects on viability. The newly identified QS inhibitors were more promising in this respect and the family of gregatins was the most promising. While desmethyl-gregatin A and cyclogregatin showed the strongest inhibitory effect in *C. violaceum*, gregatin A and gregatin D showed a stronger effect in the opportunistic pathogen *P. aeruginosa*. Interestingly, although QS was inhibited in *P. aeruginosa*, gregatin A and gregatin D did not show inhibition of biofilm formation. Only gregatin D showed inhibition of pyocyanin production, whereas treatment with gregatin A led to an increase in pyocyanin synthesis. Treatment with both gregatins also led to an increase in rhamnolipid production.

While gregatin A has been identified as anti-bacterial and anti-fungal¹³¹, the function of other gregatins is not well-studied. Gregatins are a group of molecules with an alkylated furanone core¹³², which could explain the potency of gregatins as QS inhibitors. Furanones have been well described as QS inhibitors, probably due to the high similarity of the ring structure to the lactone of the AHL autoinducers¹³³. Therefore, the effect of the gregatins might be due to binding to the QS receptors.

Interestingly, whereas gregatins share a highly similar structure (Figure 4), the effect of different gregatins on *C. violaceum* and *P. aeruginosa* is distinct. Cyclogregatin and desmethyl-gregatin A showed stronger effects on *C. violaceum* than on *P. aeruginosa*, whereas gregatin A and gregatin D showed stronger effects on *P. aeruginosa* than on *C. violaceum*. This might be due to differences in QS networks between these bacterial strains. Although the LuxIR type QS system in *C. violaceum* and *P. aeruginosa* shows resemblance, they do differ. The amino acid sequence of the LuxR type receptor of *C. violaceum* (CviR) shares 24 % and 22 % identity with LasR and RhlR from *P. aeruginosa* respectively^{134,135}. This might explain why the removal of a methyl group to get desmethyl-gregatin A alters the specificity of the compound. This also provides an opportunity for chemical alteration of the compound to develop an optimized structure that shows strong QS inhibitor activity in multiple species.

It is interesting to note that various molecules with QS inhibitor activity on *C. violaceum* failed to show an effect on the opportunistic pathogen *P. aeruginosa*. This

might be due to the robust, interconnected QS network in *P. aeruginosa*. *C. violaceum* has a single QS network (Cvii/R)¹³⁶, whereas *P. aeruginosa* uses three systems (LasI/R, RhII/R, and PQS)^{68,92}. These three systems regulate each other, but also have redundant effects. For example, in the absence of C4-HSL, RhIR is still activated via PqsE and regulates various downstream genes including *rhlA*¹⁰⁷. The robustness of the *P. aeruginosa* system might explain the high concentrations needed to inhibit QS compared to *C. violaceum*.

Another reason for the high concentrations needed or failure of QS inhibition in *P. aeruginosa* compared to *C. violaceum* might be the high intrinsic resistance of *P. aeruginosa*. All Gram-negative bacteria have a low permeability due to the structure of the outer membrane. However, *P. aeruginosa* shows a 12-100-fold lower permeability than *E. coli* due to the absence of general porins^{32,34}. This low permeability makes it hard for compounds to cross the membrane and enter the bacteria. In addition, compounds that were able to cross the membrane are often targets for the efflux pumps, making it even harder to accumulate within *P. aeruginosa*¹³⁷.

Given the difference in effects on *C. violaceum* and *P. aeruginosa*, the question arises if *C. violaceum* is the best reporter bacterium to screen for QS inhibitors that are active in *P. aeruginosa*. The QS systems of *C. violaceum* and *P. aeruginosa* overlap partially. The Cvii/R QS system of *C. violaceum* resembles the two AHL-dependent QS systems in *P. aeruginosa*, LasI/R and RhII/R. The PQS system of *P. aeruginosa* uses a distinct autoinducer¹³⁸. High-throughput screens using *P. aeruginosa* reporters have been conducted before¹³⁹⁻¹⁴¹. For instance, Starkey and colleagues fused the *pqsA* promoter to the *sacB* gene, resulting in a reporter bacterium that will only grow in sucrose-supplemented medium when the PQS pathway is inhibited¹⁴⁰. More specific screens for *P. aeruginosa* QS inhibitors using our fungal library or other sources of potential QS inhibitors may result in identification of additional fungi with QS inhibitor activity in *P. aeruginosa*. Nevertheless, screening *C. violaceum* led to the identification of a range of QS inhibitors that are active against *P. aeruginosa* and may be active in other Gram-negative strains as well. Given the differential activities of the QS inhibitors that we identified in our screen towards different bacterial strains, it is important to verify the QS inhibitor activity in the bacterial strain of choice.

It is often reported that inhibition of QS leads to inhibition of biofilm formation and the production of virulence factors⁷⁸. However, in this study we only find an inhibitory activity of gregatin D on pyocyanin production, while it activates rhamnolipid synthesis and biofilm formation in QS mutants. Gregatin A also shows activation of both pyocyanin and rhamnolipid production. This might be due to the highly interconnected QS pathways in *P. aeruginosa*. For example, Welsh and colleagues found that QS inhibition leads to a decrease of pyocyanin production but an increase of rhamnolipids by agonistic binding to the Rhl receptor¹⁴². In addition, molecules specific for a single QS receptor do not show big effects on virulence factor production, and the effect is strongly dependent on the nutrient composition of the medium¹⁴³. Smith and colleagues describe various QS inhibitors in *P. aeruginosa* that do not show an effect on biofilm formation nor on pyocyanin

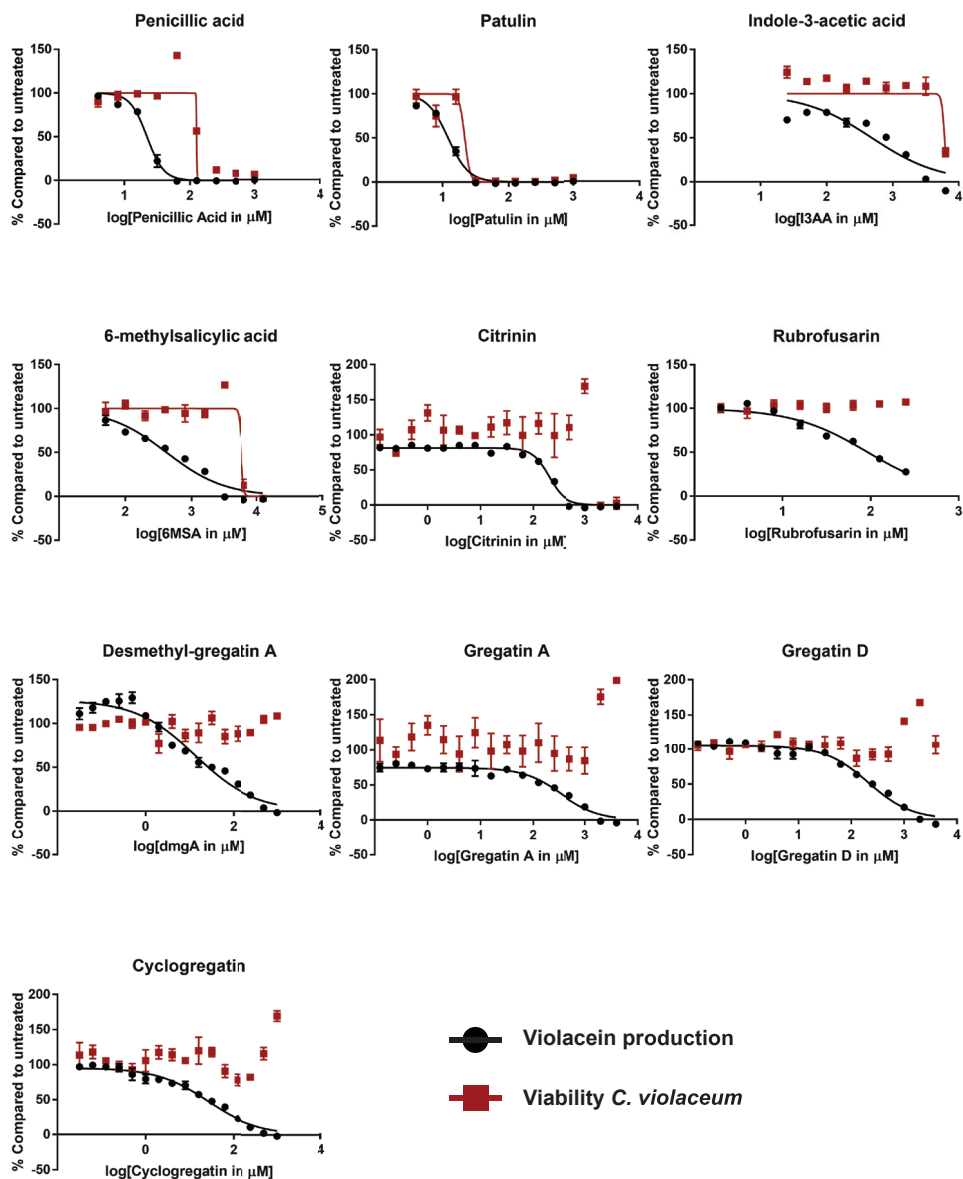
production^{144,145}. They describe strong inhibition with Rhl inhibitors, whereas inhibitors specific for the Las pathway do not have a downstream effect. The effect of the QS inhibitors is weak on the Rhl pathway, which may explain the lack of downstream effects. Moreover, both biofilm formation and virulence factor production are also controlled by various other pathways and molecules^{75,146–148}. Transcriptomic analysis of a variety of QS inhibitors shows a wide variation in number of genes affected by the QS inhibitors. This is probably due to the exact target of the inhibitor and its position in the hierarchy⁷⁶. Therefore, to explain the contradictory results, it is important to identify the exact target of the gregatins.

Although we identified many fungal secondary metabolites that play a role in QS, there are still many more to be found. To find QS inhibitors, bacteria need to be treated at a specific concentration range. Low concentrations show no QS inhibitory activity, whereas high concentrations might be toxic. The fungi in the library were grown in a standard growth condition. Altering the growth conditions may lead to higher production of the active compound, or synthesis of other metabolites¹⁴⁹. Hence, fungi that did not show activity in the current study might produce interesting compounds when grown under different conditions.

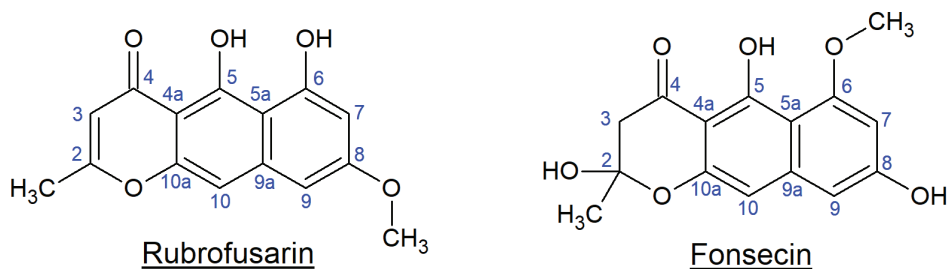
In conclusion, this study shows that fungi are a highly potent source of novel bioactive compounds. Through screening of 10,207 fungal filtrates, we found a diverse array of compounds that showed an inhibitory effect on QS, both in *C. violaceum* and in *P. aeruginosa*. Interestingly, we also found that QS inhibition in *P. aeruginosa* does not necessarily lead to a decrease in biofilm formation and production of virulence factors. It is important to find out more about the mechanism of action of gregatins, which may allow optimization of their structure to increase the potential of this family of compounds as QS inhibitors to ultimately combat antimicrobial resistance.

Acknowledgments

We would like to thank Tim Holm Jakobsen for sharing the *P. aeruginosa* strains with us and for making the time for some valuable discussions. In addition, we would like to thank Helen Buttstedt and Jesse de Ruijter for technical support.



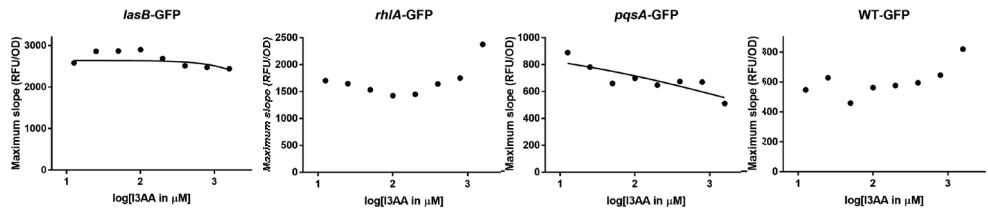
Supplementary Figure 1. Graphs of the compounds tested on the reporter *C. violaceum* of which the IC_{50} values were calculated (Table 2). Experiments were done in triplicate. Error bars represent SEM.



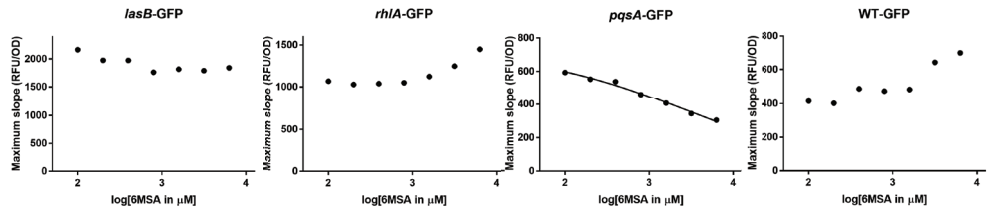
Position	Rubrofusarin		Fonsecin	
	¹ H	¹³ C	¹ H	¹³ C
2-CH ₃	2,37 (3H, s, <i>J</i> =0.5)	20.5	1,6 (3H, s)	28.07
2		168.9		100.5
3	6,15 (1H, d, <i>J</i> =0.7)	107.0	2,74 (1H, d) 3,18 (1H, d, <i>J</i> =16.8)	48,0
4		184.1		198.1
4a		103.3		104.0
5		160.5	14,2 (1H, s)	164.7
5a		102.9		105.6
6		161.0		161.2
6-CH ₃ O			3,84 (3H, s, <i>J</i> =6.9)	56.1
7	6,42 (1H, s, <i>J</i> =2.7)	97.9	6,30 (1H, d, <i>J</i> =2.1)	97.0
8		161.8		162.8
8-CH ₃ O	3,86 (3H, s, <i>J</i> =5.4)	56.2		
9	, <i>J</i> =2.0H	101.5	6,46 (1H, d, <i>J</i> =2.1)	102.0
9a		141.4		143.4
10	7,03 (1H, s)	100.3	6,42 (1H, s, <i>J</i> =2.7)	101.5
10a		153.0		153.9

Supplementary Figure 2. NMR data of the active fraction from *Aspergillus carbonarius* suggesting a combination of foncecin and rubrofusarin.

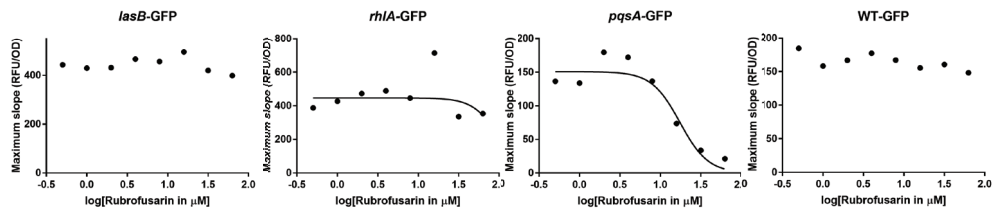
I3AA:



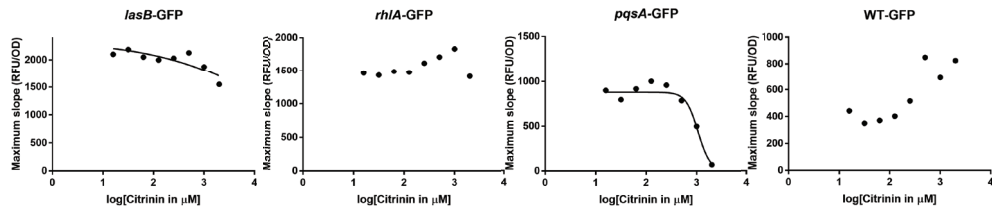
6MSA:



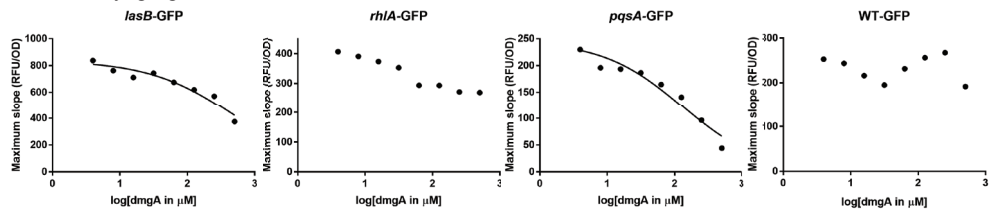
Rubrofusarin:



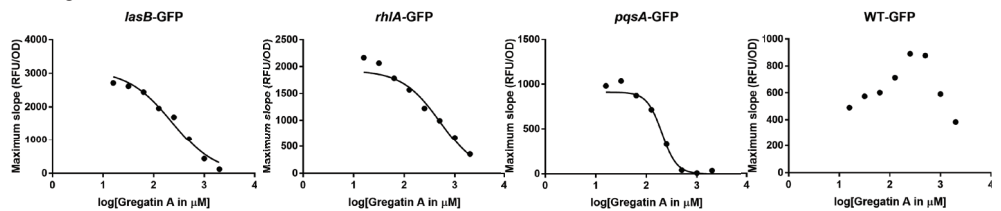
Citrinin:

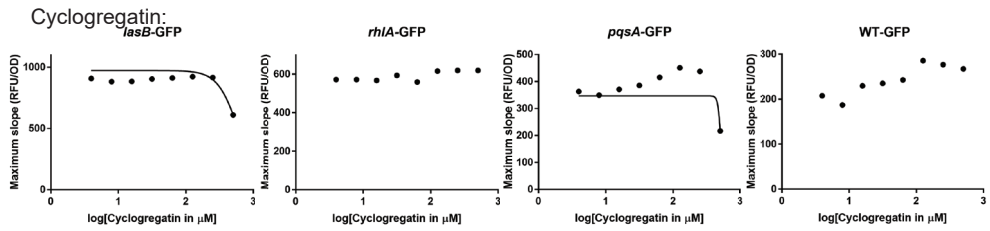


Desmethyl-gregatin A:

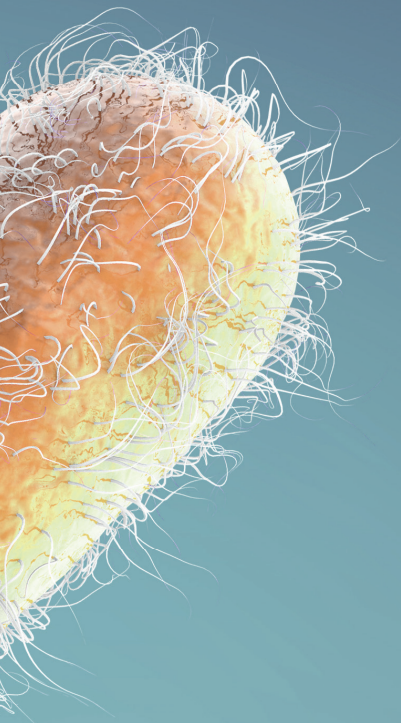


Gregatin A:





Supplementary Figure 3. QS inhibitory activity of the other compounds on *P. aeruginosa* strain PAO1. The plots represent the maximum slopes used to calculate the IC_{50} values. If no line is drawn, it was not possible to perform a non-linear regression analysis. Experiments were done in triplicate, the mean of RFU/OD is plotted and used for the calculations of the maximum slope.



Chapter 3

Paecilomycone inhibits quorum sensing in Gram-negative bacteria

Wouter A. G. Beenker, Jelmer Hoeksma, Marie Bannier-Hélaouët, Hans Clevers, Jeroen den Hertog

Microbiology Spectrum (2023)

Abstract

Pseudomonas aeruginosa is an opportunistic pathogen that causes major healthcare concerns due to its virulence and high intrinsic resistance to antimicrobial agents. Therefore, new treatments are highly needed. An interesting approach is to target quorum sensing (QS). QS regulates the production of a wide variety of virulence factors and biofilm formation in *P. aeruginosa*. This study describes the identification of paecilomycone as inhibitor of QS in both *Chromobacterium violaceum* and *P. aeruginosa*. Paecilomycone strongly inhibited the production of virulence factors in *P. aeruginosa*, including various phenazines, and biofilm formation. In search of the working mechanism, we found that paecilomycone inhibited the production of 4-hydroxy-2-heptylquinoline (HHQ) and 3,4-dihydroxy-2-heptylquinoline (PQS), but not 2'-aminoacetophenone (2-AA). Therefore, we suggest that paecilomycone affects parts of QS in *P. aeruginosa* by targeting the PqsBC complex and alternative targets, or alters processes that influence the enzymatic activity of the PqsBC complex. The toxicity of paecilomycone towards eukaryotic cells and organisms was low, making it an interesting lead for further clinical research.

Keywords: Paecilomycone, *P. aeruginosa*, Quorum Sensing, Phenazines, 4-hydroxy-2-alkylquinolines

Introduction

Pseudomonas aeruginosa is a Gram-negative pathogen that causes nosocomial infections in immunocompromised patients. It is involved in a variety of acute and chronic infections including urinary tract infections, burns or wound infections, and in respiratory diseases like cystic fibrosis (CF)^{25,26}. *P. aeruginosa* has a high intrinsic resistance due to the low permeability of its outer membrane, the high amount of efflux pumps and the capability to form biofilms. Therefore, *P. aeruginosa* infections are difficult to treat^{26,150}. Once established in the lung, *P. aeruginosa* infections often become chronic, contributing to morbidity and mortality of the patients^{30,151}. Therefore, new treatments against *P. aeruginosa* infections are highly needed, and quorum sensing (QS) as target might be an interesting approach.

QS in bacteria is a communication system that involves changes in gene expression in response to cell density. In Gram-negative bacteria, the QS systems are very similar with small modifications. These systems contain homologues of a LuxI-type synthase that produces acylated homoserine lactones (AHL) that are specific to that bacterial strain. When the number of bacteria increases, the concentration of AHL increases. The AHL will bind to its cognate LuxR-type receptor, which subsequently binds to the promoter of QS target genes and alters gene expression^{59,106,152}.

Chromobacterium violaceum contains a single LuxI/R-type QS network, with Cvil as synthase and CviR as receptor. In contrast, *P. aeruginosa* has three different QS systems. Two of these systems are typical Gram-negative bacterial LuxI/R-type QS systems, the *las*-encoded system and the *rhl*-encoded system. The third system in *P. aeruginosa* is a unique system based on 4-hydroxy-2-alkylquinolines (HAQs) that are synthesized by the enzymes of the *pqsABCDE* operon and PqsH. Among these HAQs are 3,4-dihydroxy-2-heptylquinoline (PQS) and its precursor 4-hydroxy-2-heptylquinoline (HHQ) that can bind to PqsR (also called MvfR)^{68,69,92}. Via positive and negative feedback mechanisms, these three QS systems are highly interconnected. The Las system is often placed on top of this hierarchy due to positive regulation of the Rhl and PQS system⁶⁸. However, this hierarchy is flexible and can shift under certain growth conditions¹⁵³. Some papers report IQS as a fourth QS system in *P. aeruginosa*. However, this is highly debatable and therefore IQS is excluded from this paper¹⁰⁸.

The three QS systems in *P. aeruginosa* play a major role in the production of virulence factors and biofilm formation. Therefore, inhibition of QS would lead to decreased production of virulence factors, including pyocyanin, rhamnolipids, and elastase and a concomitant decrease in biofilm formation^{154,155}. This way, QS inhibitors might reduce toxicity of the bacteria towards the host, due to lower production of toxic virulence factors, and at the same time higher susceptibility to conventional antibiotics, due to a weakened biofilm^{81,156}. Promising effects of QS inhibition have already been shown by a wide variety of QS inhibitors from various sources, including quercetin from oak⁸², ajoene from garlic⁸¹, and furanones from algae¹¹².

In a previous study from our lab, we reported the search for novel QS inhibitors

among secondary metabolites of 10,207 strains of fungi. One of the QS inhibitors we identified was desmethyl-gregatin A, produced by *Aspergillus allahabadii*¹⁵⁷. Here, we report identification of another active fraction from *Aspergillus allahabadii*, containing paecilomycone, which has QS inhibitor activity against *C. violaceum* and *P. aeruginosa*. Paecilomycone treatment showed a great reduction in biofilm formation, phenazine production and HAQ synthesis. In addition, toxic effects appeared to be low, especially in complex systems, making paecilomycone an interesting molecule for further development for clinical use.

Materials and methods

Bacterial strains and growth conditions

Bacterial strains used in this study (Table S1) were stored at -80 °C in 20 % glycerol stock solutions. *C. violaceum* was plated on tryptic soy agar (TSA) and grown in tryptic soy broth (TSB) at 27 °C. PAO1 strains were grown on Luria agar (LA) plates at 37 °C and grown in medium specific for the assay. *E. coli* RHO3 strains were used for conjugation and medium was supplemented with 400 µg/mL 2,6-Diaminopimelic acid (Sigma-Aldrich, Merck Life Science, Amsterdam, the Netherlands) to support growth.

Mutants were generated using allelic exchange following the method described before¹⁵⁸. For the generation of mutants we inserted upstream (UP.Fw and UP.Rv primers used) and downstream (DN.Fw and DN.Rv primers used) regions of the gene of interest in pEX18Gm vector (gift from Joe Harrison, University of Calgary) using Gibson assembly restriction cloning, using the restriction enzymes SmaI and SphI (Table S2 and S3). After Gibson assembly, the vector containing the regions flanking the gene of interest-was transformed into RHO3 *E. coli* donor strains before conjugation with WT PAO1 cells. Mutant cells were identified with colony PCR (seq.Fw and seq.Rv primers used) and confirmed by sequencing (performed by Macrogen Europe BV).

Chemical analysis

Purification of paecilomycone

Paecilomycone was purified using the same method as described before with minor changes¹⁵⁷. In brief, the fungal strain *Aspergillus allahabadii* was grown on a malt extract agar (MEA) plate at 25 °C. After 7 d, cubes of 5x5 mm were cut out and 2 cubes were inoculated per 100 mL bottle containing 50 mL of potato dextrose broth (PDB). The liquid culture was inoculated at 25 °C with 100 rpm orbital shaking. After 7 d, the liquid medium was filter sterilized using a 0.22 µm Millipore filter (Merck, Amsterdam, the Netherlands). The sterile supernatant was extracted using 3x 1/3 volume of ethyl acetate and evaporated to dryness using a rotary evaporator with a water bath at 40 °C. The dried pellet was dissolved in DMSO.

The extract was fractionated using a preparative high-performance liquid

chromatography (HPLC) system consisting of a Shimadzu CBM-20A controller, a Shimadzu LC-20AP pump and a Shimadzu FRC-10A fraction collector using a C18 reversed-phase Reprosil column (10 μm , 120 \AA , 250 x 22 mm) and a Shimadzu SPD-20A UV-detector set at 214 nm and 254 nm. The mobile phase consisted of 100 % Milli-Q (MQ) with 0.1 % trifluoroacetic acid (Buffer A) and 100 % acetonitrile with 0.1 % trifluoroacetic acid (Buffer B). Protocol consisted of 5 % Buffer B for 5 min, followed by a linear gradient to 95 % buffer B for 40 min, 5 min of 95 % buffer B before returning to 5 % buffer B for another 5 min with a constant flow rate of 12.5 mL/min. The active fraction with a retention time of 31 min was collected and dried overnight using a speedvac.

Next day, the dried pellet was dissolved in DMSO and fractionated again using the same preparative HPLC system but with different buffers. Buffer A consisted of 95:5 MQ:acetonitrile + 10 mM NH_4OAc . Buffer B consisted of 80:20 acetonitrile:MQ + 10 mM NH_4OAc . Protocol consisted of 0 % Buffer B for 5 min, followed by a linear gradient to 100 % buffer B for 40 min, 5 min of 100 % buffer B before returning to 0 % buffer B for another 5 min with a constant flow rate of 12.5 mL/min. Paecilomycone had a retention time of 23 min and was collected and dried using a speedvac.

Paecilomycone was dissolved in a stock concentration of 40 mM in DMSO and stored at $-20\text{ }^\circ\text{C}$. Purity was checked using a Shimadzu LC-2030C 3D Plus analytical HPLC system with PDA detection (190-800 nm) with a Dr. Maisch Reprosil-PUR 120 C18 AQ column (3 μm , 120 \AA , 4.6x100 mm). The mobile phase consisted of 100 % MQ with 0.1 % trifluoroacetic acid (Buffer A) and 100 % acetonitrile with 0.1 % trifluoroacetic acid (Buffer B). Protocol consisted of a linear gradient from 5 % to 95 % buffer B for 10 min, followed by 2.5 min of 95 % buffer B before returning to 5% buffer B with a constant flow rate of 1 mL/min.

Identification of paecilomycone

The UV-VIS spectrum of paecilomycone was obtained using analytical HPLC methods mentioned above. The compound was further analyzed by measuring the mass using the same LC system with a Shimadzu LCMS-2020 mass spectrometer. For LC-MS analysis, the mobile phase consisted of 100 % MQ with 0.05 % formic acid (Buffer A) and 100 % acetonitrile with 0.05 % formic acid (Buffer B). Protocol consisted of a linear gradient from 5 % to 95 % buffer B for 10 min, followed by 2.5 min of 95 % buffer B before returning to 5 % buffer B with a constant flow rate of 0.5 mL/min. Mass spectrometry settings were as follows: nebulizing gas flow: 1.5 L/min; drying gas flow: 15 L/min; desolvation line temperature: $250\text{ }^\circ\text{C}$; capillary voltage: 4500 V for positive mode, 3500 V for negative mode; mass range: 100 to 1000 m/z; scan speed: 5000 u/s. Paecilomycone A had a retention time of 12.7 min, paecilomycone B had a retention time of 9.8 min, and paecilomycone C had a retention time of 8.9 min.

This was followed by a more accurate high resolution mass spectrometry using an LCT instrument (Micromass Ltd. Manchester). The instrument was calibrated using sodium formate, followed by direct injection of the sample with the following settings: cone gas flow:

50 L/h; desolvation gas flow: 250 L/h; desolvation temperature: 120 °C; source temperature: 80 °C; capillary voltage 3000 V; microchannel plate (MCP) detector: 2450 V; reflectron: 1786 V; Time Of Flight (TOF) tube: 4567 V; mass range 150 to 750 m/z; scan speed: 600 u/s.

For Nuclear Magnetic Resonance (NMR) analysis, paecilomycone was dissolved in DMSO- d_6 . The NMR measurements (^1H , ^{13}C , Heteronuclear Single-Quantum Correlation (HSQC) and Heteronuclear Multiple-Bond Correlation spectroscopy (HMBC)) were performed on a Bruker 600 MHz.

Quorum sensing inhibition in *C. violaceum*

To measure the effect on QS inhibition in *C. violaceum*, we used a protocol based on previous work with minor changes⁸⁴. In brief, *C. violaceum* was plated on tryptic soy agar (TSA) and grown in TSB overnight at 27 °C. Next morning, bacteria were diluted and grown until $\text{OD}_{600} = 0.5\text{--}0.7$. Then, bacteria were diluted 1000 x and added to a 96-well plate containing paecilomycone in serial dilutions up to a volume of 100 μL (range 31 nM – 1 mM). High concentrations of DMSO are toxic to the bacteria, and therefore the maximum concentration of DMSO was limited to 2.5 %. Plates were incubated for 20 h at 27 °C while shaking at 180 rpm.

To measure violacein production, the plate was centrifuged for 10 min at 3000 rpm to pellet the violacein. Subsequently, the supernatant was discarded and the violacein pellet was dissolved in 200 μL of 96 % ethanol. The plate was centrifuged for 10 min at 3000 rpm to avoid interference of cell turbidity in absorbance measurements. Half of the supernatant was then transferred to a new 96-well plate and violacein was quantified by measured the OD at 562 nm on the ASYS expert plus microplate reader (Biochrom Ltd, Cambridge, UK).

To measure the effect of paecilomycone on viability of the bacteria, resazurin staining was used. In parallel with the measurements of violacein production, another plate with *C. violaceum* and paecilomycone dilutions was prepared and incubated overnight. Next morning, the plate was centrifuged for 10 min at 3000 rpm to pellet the bacterial cells. The supernatant was aspirated and 0.1 mM resazurin (in PBS) solution was added. Plates were incubated for another 45 min at 27 °C before fluorescence was measured on a PHERAstar microplate reader (BMG Labtech) using 540 nm excitation and 590 nm emission wavelength.

Quorum sensing inhibition in *P. aeruginosa*

The experiments were performed as previously described¹¹⁸. In brief, *P. aeruginosa* PAO1 reporter lines were grown overnight in AB minimal medium supplemented with 0.5 % glucose and 0.5 % casamino acids. Cultures were diluted until $\text{OD}_{450} = 0.1\text{--}0.2$ before adding to a 96-well plate containing serial dilutions of paecilomycone up to a volume of 200 μL (range 4 nM – 500 μM). The GFP fluorescence (excitation 485 nm, emission 535 nm) and absorbance (600 nm) were measured every 15 min for 15 h at 34 °C on a CLARIOstar microplate reader (BMG Labtech). IC_{50} values were calculated using PRISM software, plotting the maximum slope of $\text{GFP}/\text{OD}_{600}$.

Growth curves

P. aeruginosa was grown overnight in desired medium. Next day, bacteria were diluted in PBS until an $OD_{600}=0.1-0.2$. Diluted bacteria were added to a honeycomb microplate containing the desired medium with paecilomycone up to a volume of 300 μL (1:1, v:v). The absorbance (600 nm) was measured every 15 min for 24 h at 34 °C on a Bioscreen C (Growth Curves Ab Ltd).

Biofilm assay

Bacteria were grown overnight in AB minimal medium supplemented with 0.5 % glucose and 0.5 % casamino acids before diluting 1000 x. Diluted bacterial cells were added to a 96-well plate containing paecilomycone in serial dilutions (range 3.9 μM – 500 μM) in triplicates to a final volume of 200 μL . Plates were sealed with Breathe-Easy sealing membrane (Sigma-Aldrich, Merck Life Science, Amsterdam, the Netherlands) to prevent evaporation and incubated at 37 °C under static conditions for 24 h. Next day, the medium was removed and the wells were rinsed with PBS. Biomass was stained with 0.1 % (w:v) crystal violet solution for 5 min. Crystal violet was discarded and excess crystal violet was removed by rinsing with water. Plates were dried and bound crystal violet was dissolved in 33 % (v:v) acetic acid and quantified at 562 nm using an ASYS expert plus microplate reader (Biochrom Ltd, Cambridge, UK).

Virulence factor assays

Pyocyanin assay

The pyocyanin assay was performed as previously described with minor modifications¹¹⁹. Bacteria were grown overnight in King's A medium (2 % (w:v) protease peptone, 1 % (w:v) potassium sulfate, 0,164 % (w:v) magnesium chloride, 1 % (v:v) glycerol in MQ), before diluting them 100 x. The assay was performed in bacterial tubes containing 1 mL of diluted bacterial culture in combination with paecilomycone at desired concentrations (range 2 μM – 125 μM). A $\Delta lasI/\Delta rhII$ QS mutant strain was included as negative control. The tubes were incubated at 37 °C on an orbital shaker set at 180 rpm. After 24 h, bacterial cells were pelleted by centrifugation at 4000 rpm for 10 min and 900 μL supernatant was extracted with a similar volume of chloroform. 800 μL of chloroform was then added to 700 μL of 0.2 M HCl and samples were mixed well. The HCl phase was then measured at 520 nm to measure relative pyocyanin concentrations.

Rhamnolipid assay

The rhamnolipid assay was performed as previously described with minor modifications¹²⁰. Bacteria were grown overnight in AB minimal medium supplemented with 0.5 % glucose and 0.5 % casamino acids, before diluting 100 x. The assay was performed in bacterial tubes containing 1 mL of diluted bacterial culture in combination with paecilomycone at desired concentration (range 2 μM – 125 μM). A $\Delta lasI/\Delta rhII$ QS mutant strain was included as negative control. The tubes were incubated at 37 °C on an orbital shaker set at 180 rpm. After 24 h, bacterial cells were pelleted and 900 μL of supernatant

was added to diethyl ether (1:1, v:v) and tubes were shaken vigorously. The diethyl ether layer was then transferred to a fresh tube and dried at room temperature. 100 μL was added to dissolve the dried pellet before addition of 800 μL of 12.9 mM orcinol (Sigma Aldrich, Merck Life Science, Amsterdam, the Netherlands) in 70 % (v:v) H_2SO_4 . The reaction was maintained at 80 °C for 30 min before measuring the absorbance at 495 nm.

Phenazine and HAQ assay

The phenazines and HAQ assay was based on the pyocyanin assay with minor modifications. Bacteria were grown in King's A medium before 100 x dilution. The assay was performed in bacterial tubes containing 3 mL of diluted bacterial culture in combination with paecilomycone at desired concentrations (range 1 μM – 125 μM). A $\Delta\text{lasI}/\Delta\text{rhII}$ QS mutant strain was included as negative control. The tubes were incubated at 37 °C with 180 rpm orbital shaking. After 24 h, the bacterial cells were pelleted and the supernatant was extracted with 2 x 1 mL chloroform. Chloroform was dried overnight and the pellet was dissolved in DMSO. Extracts were run using previously described analytical HPLC methods, with a slightly altered gradient: buffer B gradient from 5 % to 95 % for 20 min, followed by 2.5 min of 95 % buffer B before returning to 5% buffer B with a constant flow rate of 1 mL/min. Compounds were quantified by using calibration curves made by serial dilutions of standard commercial phenazines and HAQs. If needed, extra verification of the compounds was performed using previously described LC-MS methods.

Toxicity assays

HepG2 toxicity assay

HepG2 cells were seeded in 96-well plates and grown in DMEM low glucose medium (ThermoFisher Scientific, 10567014) supplemented with 10 % FBS. Cells were grown until a confluence of approximately 70-80 % before addition of paecilomycone (range 244 nM – 500 μM) in triplicates, with a final DMSO concentration of 1 % DMSO. Treated cells were incubated at 37 °C with 5 % CO_2 for 24 h. To measure the viability of the cells, 0.1 mM resazurin (Sigma-Aldrich) solution was added and cells were incubated for another 3 h. Fluorescence intensity was measured on a PHERAstar microplate reader (BMG Labtech), using an excitation wavelength of 540 nm and emission wavelength of 590 nm.

Organoid toxicity assay

Human colon tissue was obtained from the UMC Utrecht with patient informed consent. The patient was a male diagnosed with small colon adenocarcinoma. After resection, a sample from non-transformed, normal mucosa was taken for this study. This study was approved by the UMC Utrecht (Utrecht, the Netherlands) ethical committee and was in accordance with the Declaration of Helsinki and according to Dutch law. This study is compliant with all relevant ethical regulations regarding research involving human participants. All organoids experiments were performed in the lab of Hans Clevers.

Human colon organoids were maintained in human colon expansion medium as previously described¹⁵⁹. The toxicity assay was largely performed as described elsewhere¹⁶⁰.

In brief, 2 d after the previous split, organoids were dissociated from the Cultrex Basement Membrane Extract (BME, R&D Biosystems, Bio-Techne, 3533-001-02) using dispase (ThermoFisher Scientific, 17105-041) for 30 min at 37 °C. Then, organoids were washed in advanced DMEM/F12 (ThermoFisher Scientific, 12634-010) supplemented with penicillin-streptomycin (ThermoFisher Scientific, 15140122), Hepes (ThermoFisher Scientific, 15630080) and GlutaMAX (ThermoFisher Scientific, 35050061) [hereafter called washing medium], filtered through a 70 µm cell strainer (Greiner) and pelleted at 500 g for 5 min. The pellet was resuspended in 1 mL of washing medium and organoids were counted. Organoids were resuspended at a concentration of 18,750 organoids/mL in 5 % cold BME/95 % cold human colon expansion medium. 40 µL of organoid suspension (750 organoids) was dispensed in each well of a 384 well-plate (Corning, 4588) using a multi-drop combi reagent dispenser (ThermoFisher Scientific, 5840300). Paecilomycone was added immediately after plating the organoids at concentrations ranging from 10 nM to 200 µM using the Tecan D300e Digital dispenser (Tecan). The stock concentration was 10 mM and hence, the highest concentration contained 2 % DMSO. Therefore, a 2 % DMSO only viability control was added. Organoids were incubated in a humidified incubator with 5 % CO₂ at 37 °C for 5 d. After 5 d, the ATP levels were measured by a Cell Titer GLO 3D assay (Promega, G9681) following the manufacturer's instructions. Luminescence was measured using a Spark multimode microplate reader (Tecan) with an integration time of 500 ms. Results were normalized to 1 % DMSO control (100 % viability) and 1 µM staurosporine (0 % viability). Concentrations were measured in triplicates.

Zebrafish toxicity assay

Zebrafish eggs were obtained from Tübingen long fin family crosses. The zebrafish embryos were allowed to develop normally for 48 h. At 48 hpf the embryos were divided over 24-well plates, 10 embryos per well in 1 mL of fresh E3-medium. Subsequently, paecilomycone was added in serial dilutions to the wells (range 3.9 nM – 250 µM). The effects were scored at 72 hpf.

All procedures involving experimental animals were approved by the local animal experiments committee (Koninklijke Nederlandse Akademie van Wetenschappen-Dierexperimentencommissie) and performed according to local guidelines and policies in compliance with national and European law. Adult zebrafish were maintained as previously described¹⁶¹.

Commercial compounds used

2'-aminoacetophenone (2-AA), 4-hydroxy-2-heptylquinoline (HHQ), 2-heptyl-3-hydroxy-4(1H)-quinolone (PQS) (Sigma Aldrich, Merck Life Science, Amsterdam, the Netherlands), 2-heptyl-4-quinolinol 1-oxide (HQNO), 1-phenazinecarboxylic acid (PCA), and phenazine-1-carboxamide (PCN) (Cayman Chemicals), used to make calibration curves to quantify molecules in bacterial extract. Funalenone (AdipoGen Life Sciences) to compare activity with paecilomycone.

Results

Identification of paecilomycone

For the purification of paecilomycone, we fractionated the growth medium containing *Aspergillus allahabadii* secondary metabolites by using a preparative HPLC system, using TFA as modifier (Fig. S1A). The fractions were tested for quorum sensing (QS) inhibitor activity using *C. violaceum* as reporter bacteria and violacein production as read-out. *C. violaceum* produces a purple pigment, named violacein, upon activation of this QS network, making it a good reporter to search for novel QS inhibitors¹³⁶. In a previous study, we reported desmethyl-gregatin A as active compound from this fungus¹⁵⁷. However, another fraction, fraction 20, also showed inhibition of violacein production.

In this study, we purified the active compound from fraction 20 by refractionating the active fraction by preparative HPLC using ammonium acetate as modifier (Fig. S1B). Again, the fractions were tested, and fraction 1 showed QS inhibitor activity. The yield of 3 L *Aspergillus allahabadii* supernatant was on average 3.5 mg of dried fraction 1.

When running fraction 1 on analytical HPLC, we found three peaks (Fig. 1A). Peak 1 was the largest and showed a characteristic UV-VIS spectrum (**213(100)**, 238sh, 277sh, 388(40)) and a m/z of 289.1 [M+H]⁺ and 287.0 [M-H]⁻ suggesting a nominal mass of 288 (Fig. 1B, E, H). In addition, high-resolution mass spectrometry measured a mass of 289.5937, giving a calculated mono-isotopic mass of 289.0692 [M+H]⁺, with a molecular formula prediction of C₁₅H₁₂O₆ (Fig. S2). This UV-VIS spectrum and mass showed similarities with paecilomycone A¹⁶². Therefore, the NMR data were compared to the published data of paecilomycone A (Table 1, Fig. S3).

Whereas not all carbons were detected, the NMR data, like the UV-VIS and LC-MS, showed high similarities with the data of Lu *et al.*¹⁶². For further validation, the HMBC data were compared (Fig. S4). The HMBC data showed the same correlations as described before by Lu *et al.*¹⁶², validating that this compound is indeed paecilomycone A (Fig. 1K).

However, next to paecilomycone A, two other small peaks were observed in the analytical HPLC chromatogram (Fig. 1). Peak 2 showed a UV-VIS spectrum (**218(90)**, **254(100)**, 331(50)) and a m/z of 287.1 [M+H]⁺ and 285.0 [MH]⁻ suggesting a nominal mass of 286, corresponding to paecilomycone B (Fig. 1C, F, I, L)¹⁶². Peak 3 showed a UV-VIS (**207(100)**, 256 (50), 378 (50)) and a m/z of 288.1 [M+H]⁺ and 286.1 [MH]⁻ suggesting a nominal mass of 287, corresponding to paecilomycone C (Fig. 1D, G, J, M)¹⁶². The ratio of the various paecilomycones was approximately 85:5:10 (paecilomycone A: B: C, respectively), when dissolved in acetonitrile/water with 0.1% TFA. Using this set-up, it was not possible to separate the various paecilomycones further. Therefore, the combination of the three paecilomycones will be referred to as paecilomycone, unless stated otherwise. In conclusion, the fraction of *Aspergillus allahabadii* with QS inhibitor activity contained paecilomycone.

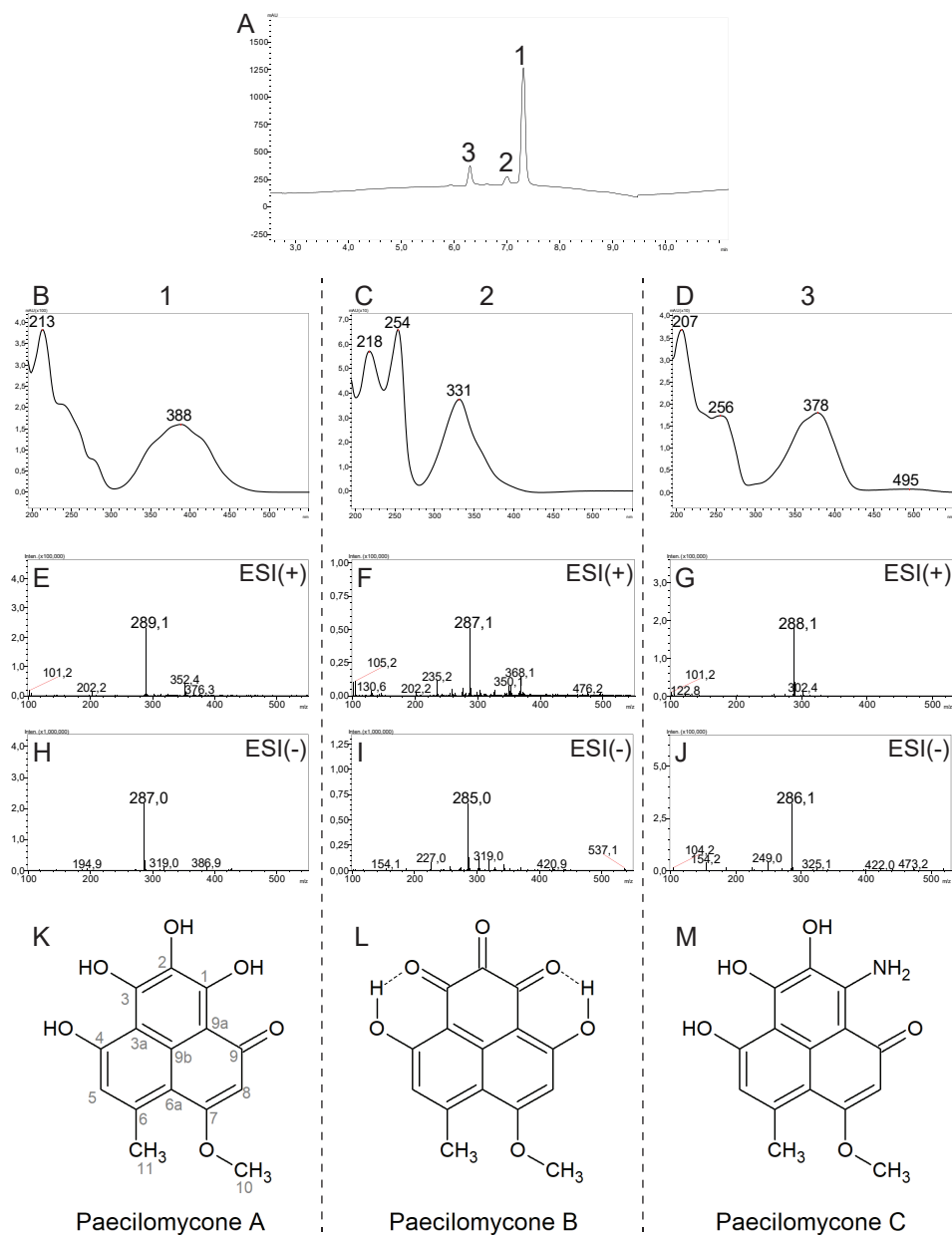


Figure 1: Identification of paecilomycone. A) aHPLC spectrogram of paecilomycone showing 3 peaks. UV-VIS chromatogram of B) peak 1, C) peak 2, D) peak 3. LC-MS ESI⁺ (positive mode) spectrogram of E) peak 1, F) peak 2, G) peak 3. LC-MS ESI⁻ (negative mode) spectrogram of H) peak 1, I) peak 2, J) peak 3. Chemical structures of paecilomycones belonging to K) peak 1, L) peak 2, M) peak 3.

Table 1 | ^{13}C and ^1H NMR spectral data of paecilomycone compared to Lu *et al* (2014)¹⁶² in DMSO- d_6

Position	Our data		Lu <i>et al</i> (2014) ¹⁶²	
	^{13}C	^1H	^{13}C	^1H
1	Not detected		166.8	
2	Not detected		131.7	
3	Not detected		172	
3a	105.96		105.4	
4	Not detected		162.2	
5	117.05	6.57 (s, 1H)	117.3	6.82 (s, 1H)
6	144.08		144.9	
6a	109.67		111.6	
7	165.97		166.8	
8	97.13	6.30 (s, 1H)	97.4	6.51 (s, 1H)
9	173.38		172.3	
9a	102.83		103.3	
9b	Not detected		127.8	
10	56.33	3.89 (s, 3H)	56.7	4.00 (s, 3H)
11	25.97	2.65 (s, 3H)	25.8	2.74 (s, 3H)

Paecilomycone shows QS inhibitor activity in *C. violaceum*

Paecilomycone strongly inhibited violacein production in *C. violaceum* with an IC_{50} of 72.5 μM (Fig. 2A). Viability was measured in parallel to distinguish between effects on QS and effects on bacterial growth that could affect violacein production. No toxic effects of paecilomycone were detected on bacteria at these concentrations. Therefore, paecilomycone was a potent QS inhibitor at concentrations that do not affect cell viability.

Whereas the three forms of paecilomycone could not be separated further with the two-step purification we used, we found that, by using TFA instead of ammonium acetate in the second purification step, the amine group was not incorporated in the compound and paecilomycone C was not present in the mixture (Fig. S5). The fraction lacking paecilomycone C still contained paecilomycone A, a small amount of paecilomycone B (ratio A:B of 91:9), and an unidentified peak. This fraction showed a concentration dependent effect on violacein production with a similar IC_{50} as paecilomycone ($\text{IC}_{50} = 96.5 \mu\text{M}$) (Fig. 2B). Toxic effects on the viability of *C. violaceum* were not detected. This suggests that the most abundant paecilomycone A was responsible for most of the QS inhibitor effect of paecilomycone.

Next, we tested the effect of funalenone on QS inhibition. Funalenone is structurally highly related to paecilomycone A with only the position of the methoxy group being different (cf. Fig. 2D and 1K). Interestingly, this small difference in structure resulted in a big difference in activity since we did not find inhibition in the production of violacein after funalenone treatment up to a concentration of 1 mM (Fig. 2C).

Taken together, paecilomycone A and potentially paecilomycone B, but not the highly related funalenone had QS inhibitor activity in *C. violaceum*.

Paecilomycone shows QS inhibitor activity in *P. aeruginosa*

To test the potential of paecilomycone as QS inhibitor in more clinically relevant bacteria, the effect on various *P. aeruginosa* QS reporters was tested. *P. aeruginosa* PAO1 reporter strains were used that express GFP when the QS pathway is activated, including *lasB*-GFP, *rhIA*-GFP, and *pqsA*-GFP. WT-GFP that constitutively expressed GFP was used as control. GFP expression was normalized to the growth of the bacteria and the IC_{50} was calculated by plotting the maximum slope of GFP expression/ bacterial growth (Fig. 3).

Paecilomycone inhibited GFP expression in the *lasB*-GFP reporter and *pqsA*-GFP reporter with an IC_{50} of 49.8 μ M and 31.5 μ M respectively (Fig. 3), which is 3- to 4.5-fold lower than in control WT-GFP bacteria (IC_{50} = 143.2 μ M), respectively. Concentrations of paecilomycone above 125 μ M affected growth of *P. aeruginosa* explaining the effect observed in WT-GFP bacteria (Fig. S6). The *rhIA*-GFP reporter was not sensitive to paecilomycone with an apparent IC_{50} of 233.8 μ M, which was actually higher than of WT-GFP. We also tested the effect of funalenone on QS inhibition in PAO1. Funalenone did not show an inhibitory

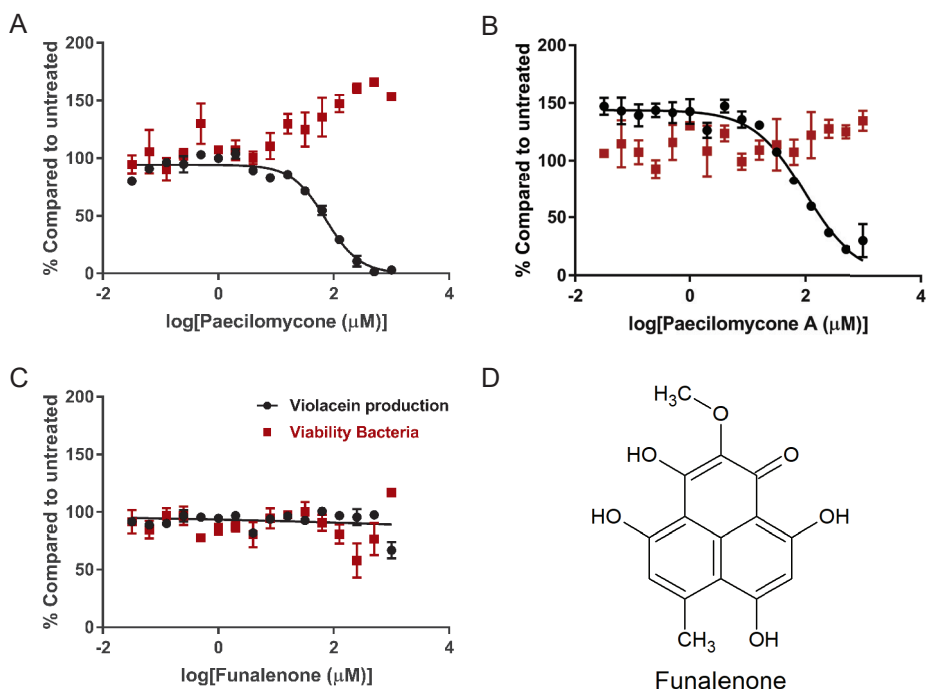


Figure 2: Quorum sensing inhibition by paecilomycone using *C. violaceum* as reporter bacterium. Violacein production and viability of *C. violaceum* after treatment with **A)** paecilomycone, **B)** a paecilomycone fraction lacking paecilomycone **C)** Funalenone. **D)** structure of funalenone. Experiments were done in triplicates and error bars represent standard error of the mean (SEM).

effect in any of the reporters (Fig. S7), indicating that funalenone did not inhibit QS in *P. aeruginosa*.

These results indicate that various, but not all, QS pathways were inhibited by paecilomycone -but not by the highly related funalenone- in clinically relevant *P. aeruginosa* (PAO1) bacteria, with paecilomycone showing the strongest effect on the *pqsA*-GFP reporter.

Paecilomycone inhibits biofilm formation in *P. aeruginosa*

QS regulates various downstream processes including biofilm formation⁷⁵. Therefore, we tested if paecilomycone inhibits biofilm formation by staining biomass using crystal violet after treatment with various concentrations of paecilomycone for 24 h. Concentrations of 62.5 μM and higher showed a significant concentration-dependent inhibition of biofilm formation in *P. aeruginosa* PAO1 strain (Fig. 4). The highest concentration tested (500 μM) showed an inhibition of 75 % compared to WT control. High concentrations

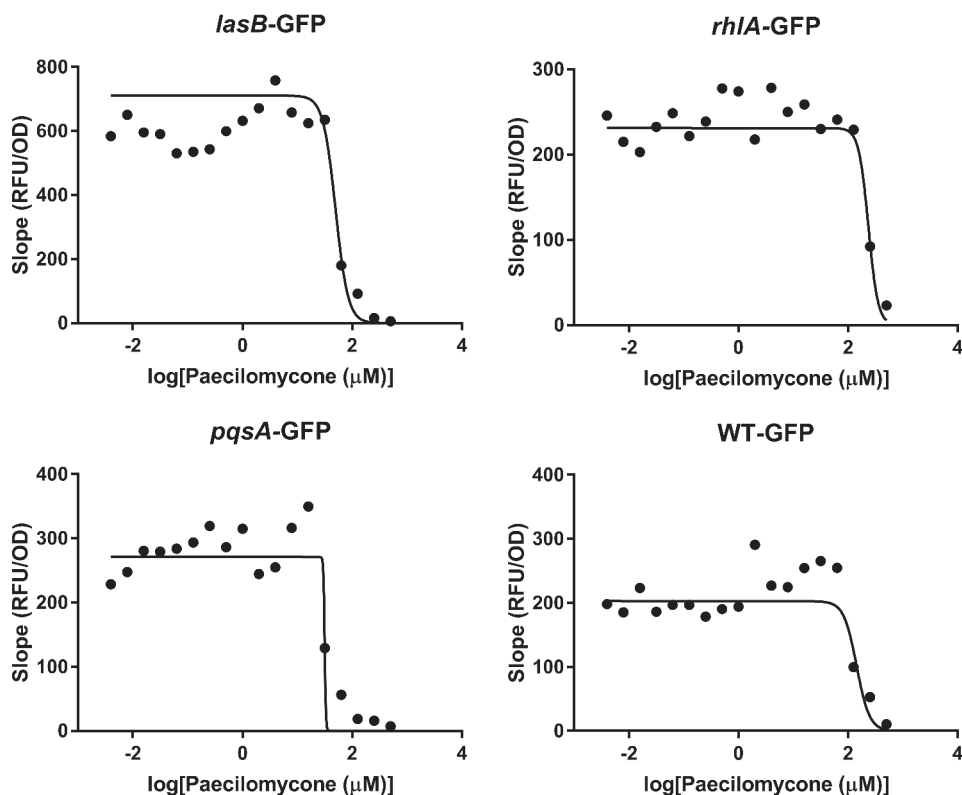


Figure 3: Quorum sensing inhibition in *P. aeruginosa* PAO1 reporter strains after paecilomycone treatment. The effect of paecilomycone was tested using *lasB*-GFP, *rhlA*-GFP, *pqsA*-GFP reporters and WT-GFP as control. The maximum slope of RFU, normalized by growth, was plotted and used to calculate the IC_{50} . Experiments were done three times in triplicates; the mean of RFU/OD of a representative experiment was plotted.

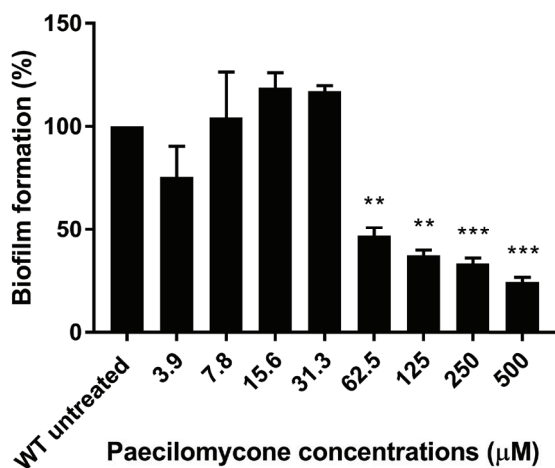


Figure 4: Inhibition of biofilm formation in *P. aeruginosa* PAO1 strain by paecilomycone treatment for 24 h. Biofilm formation was measured by crystal violet staining and normalized to untreated. The mean of three experiments in triplicates was plotted and error bars represent SEM. A one-way ANOVA, corrected for multiple comparisons using Dunnett's test was done to determine statistical significance. Treated samples were compared to untreated controls (**, $P < 0.005$; ***, $P < 0.001$)

affected growth of the bacteria (Fig. S6), which could contribute to decreased biofilm formation. However, the OD_{600} was similar at 24 hours after treatment with 62.5 µM, a concentration that inhibited biofilm formation of *P. aeruginosa* for 50 %. Therefore, we conclude that paecilomycone is able to inhibit biofilm formation via mechanisms that are unrelated to growth.

Paecilomycone alters the production of various virulence factors

Besides biofilm formation, QS regulates the synthesis of virulence factors in *P. aeruginosa*^{109,110,163}. Therefore, we tested the effect of paecilomycone treatment on the synthesis of various virulence factors. Paecilomycone induced a strong and significant inhibitory effect on the production of pyocyanin with a maximum inhibition of 88 % and an IC_{50} of 8.5 µM (Fig. 5A). The lowest concentration tested, 2.0 µM, still showed a significant decrease in pyocyanin production. To rule out inadvertent effects on PAO1 due to altered growth, growth kinetics were determined using planktonic cells in King's A medium, the medium used for analysis of pyocyanin. The initial slopes of the PAO1 bacterial density curves were similar in control and paecilomycone treated samples, indicating that bacterial growth was similar (Fig. S8). Yet, bacterial density did not reach the same level in samples treated with high paecilomycone concentrations (from 31.3 µM onwards). However, the difference in bacterial densities after 24 h treatment was relatively small and could not explain the large decrease in pyocyanin production in response to paecilomycone.

Interestingly, rhamnolipid production in PAO1 cells in response to paecilomycone was increased (Fig. 5B). A modest but significant increase, up to 33 %, was observed following treatment with 31 µM paecilomycone.

Because the synthesis of pyocyanin showed a strong inhibition, we also measured the effect of paecilomycone on other phenazines produced by *P. aeruginosa*:

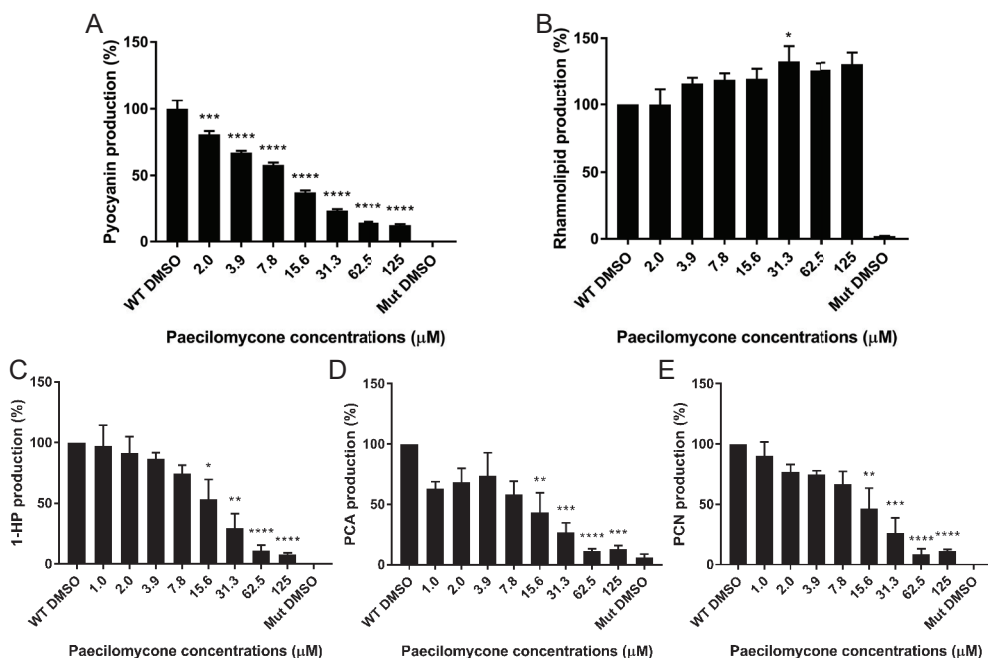


Figure 5: Production of virulence factors by *P. aeruginosa* PAO1 strain after paecilomycone treatment. Graphs show the production of **A)** pyocyanin, **B)** rhamnolipids, **C)** 1-hydroxyphenazine (1-HP), **D)** phenazine-1-carboxylic acid (PCA), **E)** phenazine-1-carboxamide (PCN), after treatment with paecilomycone for 24 h. A QS mutant ($\Delta lasI/\Delta rhII$) was included as negative control. Experiments were performed in biological triplicates containing technical triplicates (with exception of pyocyanin, which was performed once in this setting). Values were normalized to WT DMSO control and the mean was plotted, error bars represent SEM. A one-way ANOVA, corrected for multiple comparisons using Dunnett's test was done to determine statistical significance. Paecilomycone treated samples were compared to WT DMSO control (*, $P < 0.05$; **, $P < 0.005$; ***, $P < 0.001$; ****, $P < 0.0001$).

1-hydroxyphenazine (1-HP), phenazine-1-carboxylic acid (PCA), and phenazine-1-carboxamide (PCN)¹⁶³. The synthesis of these phenazines all showed a significant inhibition after paecilomycone treatment with a concentration of 15.6 μM or higher (Fig. 5C-E). Maximum inhibition was reached after treatment with 62.5-125 μM paecilomycone with inhibition up to 92 % (1-HP), 89 % (PCA), and 91 % (PCN) compared to untreated. This shows that paecilomycone inhibited the production of phenazines, but not rhamnolipids.

Paecilomycone inhibits production of PQS pathway metabolites

Since the strongest inhibition of QS was measured in the PQS pathway (Fig. 3) and a strong inhibition was observed in the synthesis of phenazines (Fig. 5), we tested the effect of paecilomycone treatment on the production of various metabolites in PQS synthesis (Fig. 6A). In short, PQS synthesis starts with PqsA, which converts anthranilic acid to anthraniloyl-CoA¹⁶⁴⁻¹⁶⁶. After condensation by PqsD, PqsE hydrolyses 2-aminobenzoylacyl-CoA (2-ABA-CoA) into 2-aminobenzoylacyl (2-ABA)¹⁶⁷⁻¹⁶⁹. This hydrolysis can be taken over by TesB thioesterase¹⁶⁹. 2-ABA is condensed to HHQ by the PqsBC complex which is hydroxylated by PqsH to form PQS^{167,170}. In addition, 2-ABA can spontaneously decarboxylate

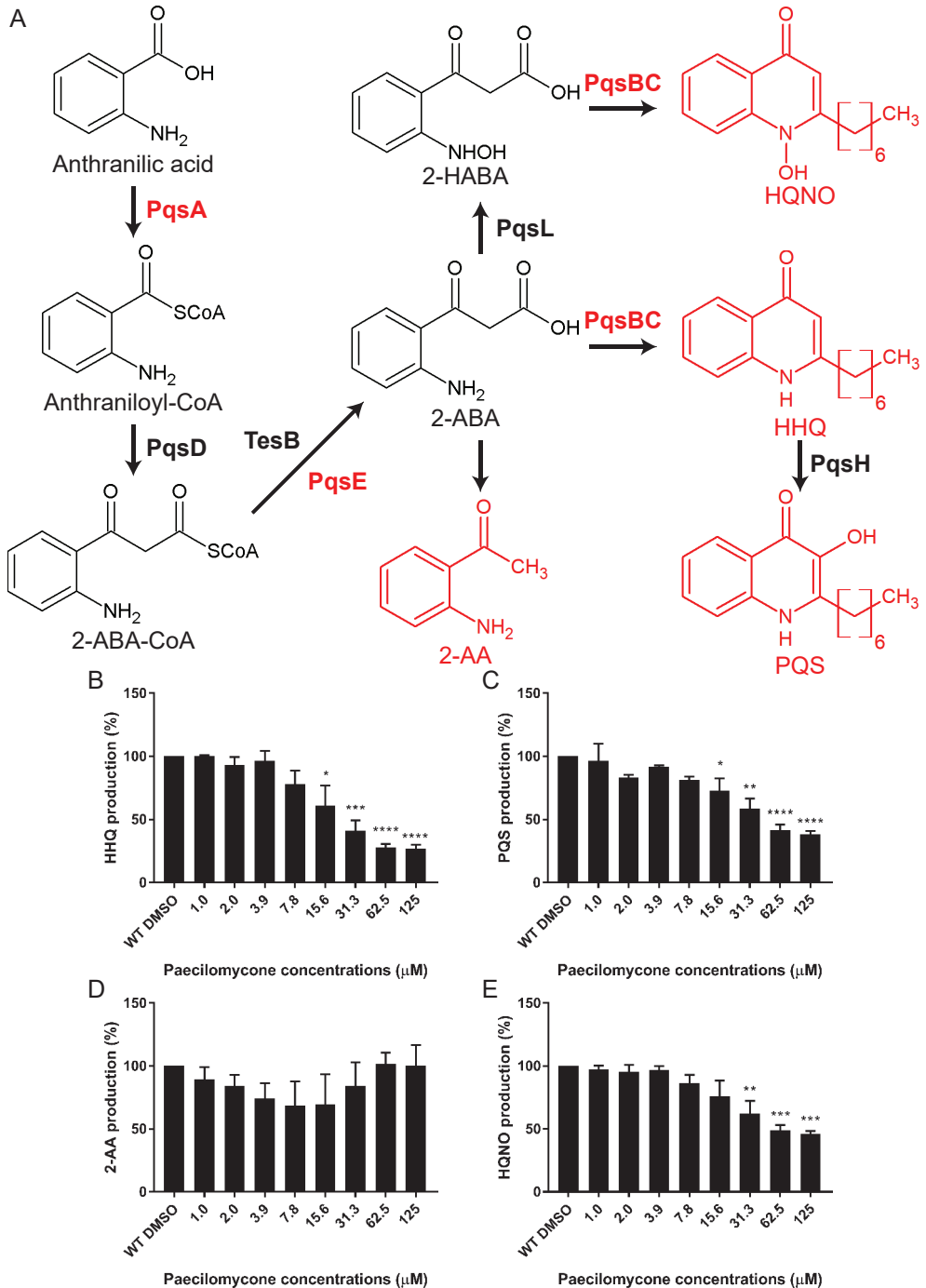


Figure 6: Inhibition of various metabolites in PQS synthesis after paecilomycone treatment. A) PQS synthesis pathway starts from anthranilic acid, which is converted by enzymes from the *pqsABCDE* operon to produce HHQ, which is then hydroxylated by PqsH to form PQS. 2-ABA can also spontaneously decarboxylate into 2-AA or be converted into HQNO by PqsL and subsequently the PqsBC complex. Enzymes in red indicate mutants used in

Figure 6 legend (continued)

figure 7. Graphs show the production of the metabolites indicated in red: **B)** HHQ, **C)** PQS, **D)** 2-AA, **E)** HQNO. Experiments were done three times in triplicates, values were normalized to DMSO treated control, and the mean of the experiments is plotted with error bars representing the SEM. A one-way ANOVA, corrected for multiple comparisons using Dunnett's test, was done to determine statistical significance. Treated samples were compared to DMSO control (*, $P < 0.05$; **, $P < 0.005$; ***, $P < 0.001$; ****, $P < 0.0001$).

to 2'-aminoacetophenone (2-AA), or form 2-heptyl-4-quinolinol 1-oxide (HQNO) by PqsL and the PqsBC complex^{69,167,171}. To test the effect of paecilomycone on PQS synthesis, we tested the production of 2-AA, HQNO, HHQ, and PQS.

After treatment for 24 h, we measured a significant concentration-dependent inhibition of HHQ and PQS using paecilomycone concentrations of 15.6 μM and higher (Fig. 6B-C). The strongest inhibition was measured after treatment with 125 μM paecilomycone with inhibition up to 73 % and 62 % for HHQ and PQS, respectively. Besides HHQ and PQS production, paecilomycone also significantly inhibited HQNO production up to 54 % compared to control (Fig. 6D). Interestingly, the production of 2-AA was not significantly affected after paecilomycone treatment (Fig. 6E). This suggests that paecilomycone treatment did not inhibit the complete PQS synthesis, but only specific enzymes like the PqsBC complex.

To exclude the possibility that paecilomycone C inhibited phenazine production and the PQS pathway, we compared the activity of paecilomycone with the fraction without paecilomycone C. We observed no differences, indicating that paecilomycone C is dispensable for inhibition of phenazine production (Fig. S9).

Paecilomycone is a potential inhibitor of the PqsBC complex

Since various metabolites of the PQS pathway were inhibited, except for 2-AA, we expected paecilomycone to target the PqsBC complex (Fig. 6A). PqsBC inhibitors have been reported before and show similar patterns as paecilomycone treatment^{140,172,173}. To test involvement of the *pqs* genes in the PQS synthesis pathway in our conditions (King's A medium), we analyzed metabolite expression in PAO1 mutants, which lack genes encoding PQS synthesis enzymes ($\Delta pqsA$, $\Delta pqsE$, $\Delta pqsBC$). We expected the *pqsBC* mutant to show a similar pattern as paecilomycone treatment, *i.e.* inhibition of HQNO, HHQ, PQS, pyocyanin and PCA production while not affecting 2-AA.

Indeed, we measured a strong inhibition of both HHQ and PQS in $\Delta pqsA$ and $\Delta pqsBC$ (Fig. 7A-B). $\Delta pqsE$ only showed a slight decrease in PQS and even an increase in HHQ (Fig. 7A-B), which may be due to TesB, which hydrolyses 2-ABA-CoA to 2-ABA in absence of PqsE¹⁶⁹ (Fig. 6A). HQNO production was significantly inhibited in all mutant strains, with complete inhibition in both *pqsA* and *pqsBC* mutants (Fig. 7C). In contrast to paecilomycone treatment, which did not affect 2-AA, the *pqsA* mutant showed almost a 100% decrease in 2-AA production, which was expected because PqsA mediates the first step in PQS synthesis (Fig. 7D). Surprisingly, the *pqsBC* mutant still showed a strong decrease in 2-AA production. This may be due to inhibition of the positive feedback of HHQ and PQS on the *pqsABCDE*

operon upon complete inhibition of HHQ and PQS production¹⁶⁵.

PqsE regulates the synthesis of pyocyanin. Consistent with this notion, production of pyocyanin and PCA was abolished in *pqsE* mutant. Production of PCA and pyocyanin was also abolished or reduced in *pqsA* and *pqsBC* mutants (Fig. 7E-F). This may be due to positive feedback, leading to reduced expression of PqsE in *pqsA* and *pqsBC* mutants. Together, these data suggest that paecilomycone treatment did not completely inhibit the PQS pathway (*cf.* $\Delta pqsA$), or specifically target phenazine synthesis (*cf.* $\Delta pqsE$), but rather that paecilomycone inhibited aspects of PQS synthesis (*cf.* $\Delta pqsBC$).

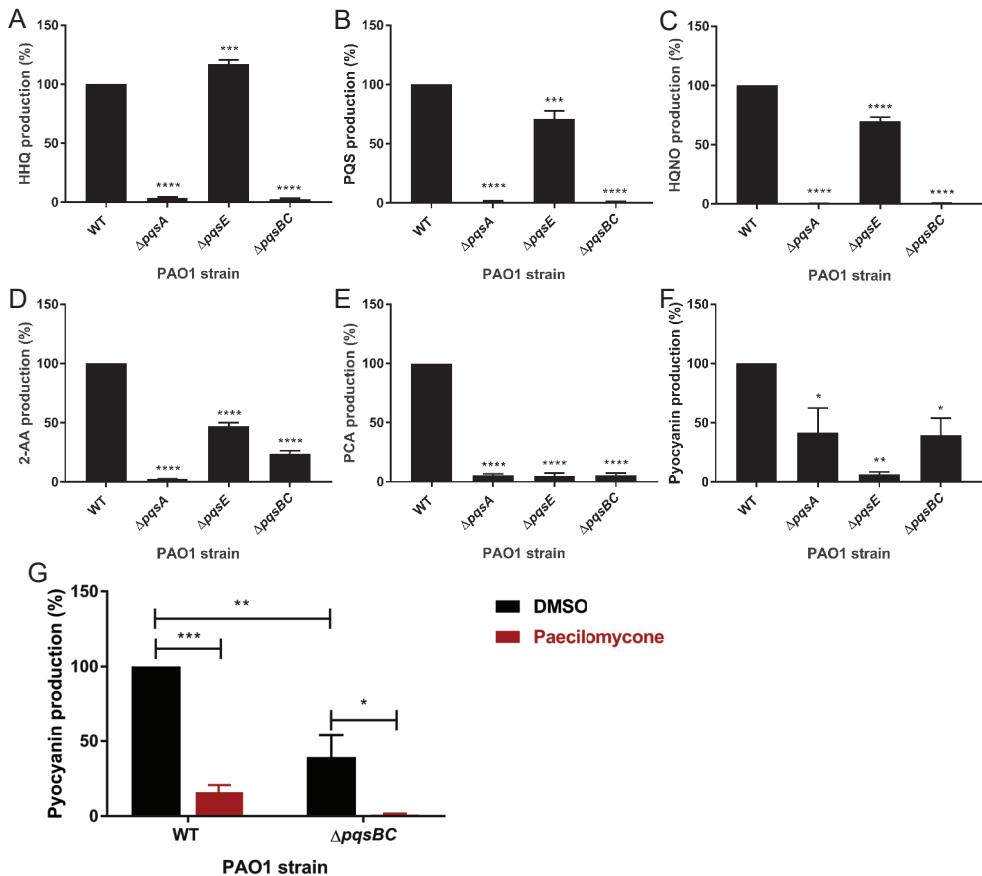


Figure 7: The effect of mutations in PQS synthesis enzymes on the production of various HAQs, phenazines and 2-AA in King's A medium. *P. aeruginosa* PAO1 strain and various mutant ($\Delta pqsA$ / $\Delta pqsE$ / $\Delta pqsBC$) were grown in King's A medium for 24 h and the production of **A)** HHQ, **B)** PQS, **C)** HQNO, **D)** 2-AA, **E)** PCA, **F)** pyocyanin was measured and normalized to WT control. **G)** WT and $\Delta pqsBC$ mutants were treated with paecilomycone and pyocyanin levels were measured. Experiments were done three times in triplicates, the mean of the normalized values is plotted with error bars representing the SEM. A one-way ANOVA, corrected for multiple comparisons using Dunnett's test, was done to determine statistical significance. Mutants were compared to WT control (*, $P < 0.05$; **, $P < 0.005$; ***, $P < 0.001$; ****, $P < 0.0001$).

Interestingly, while the *pqsBC* mutant already showed decreased levels of pyocyanin, treatment with paecilomycone strengthened this inhibition significantly to almost 100% (Fig. 7G). This suggests that paecilomycone might have alternative targets, or targeted a process related to the enzymatic activity of the PqsBC complex instead of directly targeting the PqsBC complex, which caused an even stronger inhibition of pyocyanin in the absence of the PqsBC complex.

Toxicity of paecilomycone

To test if paecilomycone has clinical potential, we determined the cytotoxicity of paecilomycone on various viability models. First, we used human liver-derived HepG2 cells. Viability of HepG2 cells was assessed after paecilomycone treatment for 24 h. Up to a concentration of 125 μM paecilomycone, there was no difference in the viability of HepG2 cells compared to untreated control cells (Fig. 8A). Paecilomycone was toxic to HepG2 cells only at high concentrations with an IC_{50} of 219 μM .

Second, we tested the cytotoxic effect of paecilomycone on more complex systems, human colon organoids. Viability of the organoids was measured after paecilomycone treatment for 5 days. High concentrations (200 μM and 120 μM) showed reduced

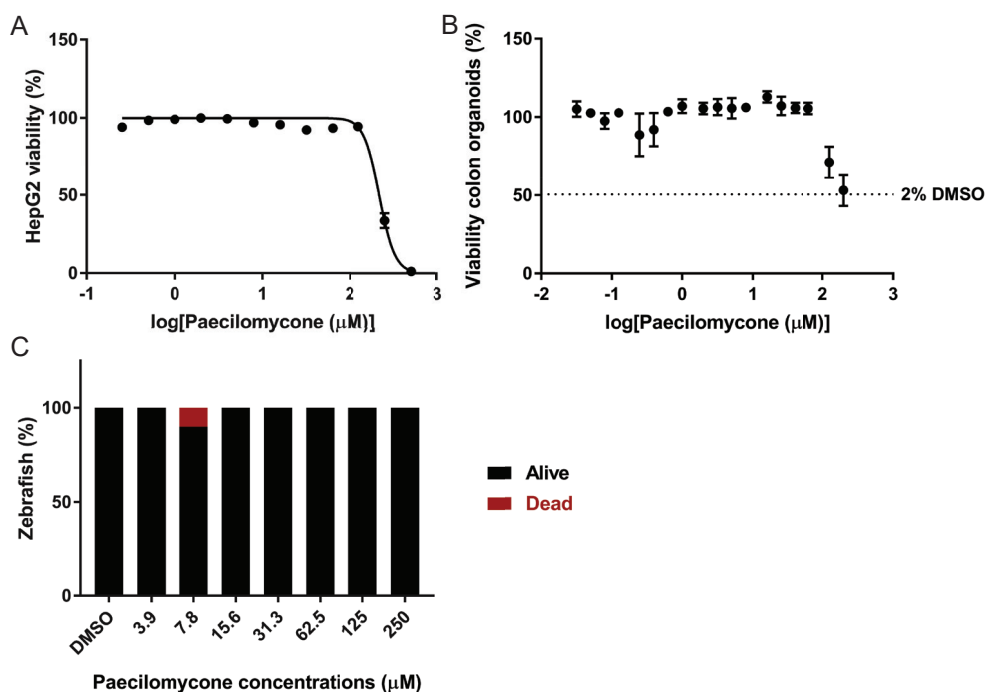


Figure 8: Toxicity of paecilomycone treatment using various toxicity models. A) Viability of HepG2 cells treated with paecilomycone for 24 h, viability was measured using resazurin assay. **B)** Viability of colon organoids treated with paecilomycone for 5 d, viability was measured by measuring ATP levels by a Cell Titer GLO 3D assay. **C)** Viability of zebrafish embryos that were treated after 48 h for 24 h.

viability compared to 1% DMSO (Fig. 8B). However, at these high concentrations, the final concentration of paecilomycone solvent was higher than 1%, up to 2% DMSO, which by itself already showed a 50% reduction in viability. It is therefore highly likely that the apparent effect of 120 μ M and 200 μ M paecilomycone on organoid viability was actually caused by high concentrations of DMSO.

Third, we tested the cytotoxic effect of paecilomycone on a whole organism *in vivo*, 2-day old zebrafish embryos. The viability of the embryos was measured after paecilomycone treatment for 24 h. Each concentration was tested on approximately 10 embryos. No toxic effect of paecilomycone was apparent (Fig. 8C).

In conclusion, paecilomycone did not affect eukaryotic cells at concentrations that inhibited QS in Gram-negative bacteria. Only at high paecilomycone concentrations, an effect was detected on HepG2 cells, whereas no effect was specifically attributable to paecilomycone treatment of more complex systems, like organoids and zebrafish embryos.

Discussion

In this study, we describe the identification of paecilomycone as a novel QS inhibitor. Paecilomycone showed inhibition of QS in Gram-negative bacterial strains, *C. violaceum* and *P. aeruginosa* PAO1. Paecilomycone showed the strongest inhibitory effect on the PQS pathway and it strongly inhibited the production of HHQ and PQS. In addition, paecilomycone inhibited biofilm formation and the production of phenazines, including pyocyanin. Paecilomycone might have promising clinical value because cytotoxicity was very low.

Paecilomycone treatment showed strong inhibition of QS in the *pqsA*-GFP reporter (Fig. 3), production of related virulence factors (Fig. 5), and production of HHQ and PQS (Fig. 6). Since paecilomycone did not interfere with the production of 2-AA (Fig. 6), we suggest that paecilomycone affected the activity of the PqsBC complex. Only a limited number of PqsBC inhibitors are identified so far. Previously described PqsBC inhibitors show similar profiles as paecilomycone: inhibition of HHQ and PQS while 2-AA is unaffected or even upregulated^{140,172,173}. Only dual PqsBC / PqsR inhibitors showed inhibition of 2-AA, something that is comparable with our $\Delta pqsBC$ mutant strain^{140,172,173}. Unfortunately, these studies do not describe the effect of the PqsBC inhibitors on expression of virulence traits in *P. aeruginosa* except for a small decrease in pyocyanin production, whereas we observed a strong inhibition after paecilomycone treatment¹⁴⁰. Based on our data, the PqsBC complex is the most likely target of paecilomycone treatment.

It was unexpected that paecilomycone targets the PQS system in *P. aeruginosa* after we identified its QS inhibitory effect in *C. violaceum*. Although both bacteria contain LuxI/R type QS, the PQS system is unique for *P. aeruginosa*^{68,69,92,136}. More specifically, the PqsBC complex is a FabH-like enzyme that catalyzes the condensation of an octanoyl-CoA with

2-ABA^{174,175}. This complex does not show similarity with the Cvil synthase in *C. violaceum*. Therefore, interaction of paecilomycone with a LuxI/R type system of *P. aeruginosa* would be expected. However, there are several reasons we believe paecilomycone has a different mechanism of action in *C. violaceum* than in *P. aeruginosa*.

In *P. aeruginosa*, paecilomycone induced *lasB*-GFP reporter inhibition, whereas *rhlA*-GFP was not affected. The Las regulatory system is believed to be on top of the QS hierarchy, positively regulating the Rhl and PQS system⁶⁸. Therefore, inhibition of Las might also lead to inhibition of PQS. However, this inhibition would lead to complete inhibition of the entire *pqsABCDE* operon and thus to inhibition of 2-AA, which we did not observe. Moreover, conditions with low phosphate concentrations (like King's A medium, used in this study for pyocyanin, phenazine and HAQ assays) might bypass Las, resulting in direct activation of Rhl and PQS. Note that because of this bypass, LasR inhibitors are not effective in low phosphate conditions¹⁴³. Therefore, inhibition of the *lasB*-GFP reporter might be due to positive regulation of *lasR* by PqsR¹⁷⁶, instead of direct inhibition by paecilomycone.

Inhibition of pyocyanin production was also detected after activation of the Rhl pathway, because RhlR inhibits the *pqsABCDE* operon¹⁴². Therefore, another explanation is that paecilomycone acts as RhlR agonist. However, similar to inhibition of the Las system, RhlR activation would also lead to inhibition of 2-AA. Therefore, unless the production of 2-AA can be bypassed somehow, we favor the explanation that paecilomycone affects the activity of the PqsBC complex.

PqsBC complex might be a direct target of paecilomycone. PqsE regulates the production of phenazines via RhlR^{107,177–182}. A mutant lacking PqsE did not produce PCA or pyocyanin, underlining the importance of PqsE for production of these phenazines. The observed inhibition of PCA and pyocyanin production in $\Delta pqsA$ and $\Delta pqsBC$ may be explained by inhibition of the *pqsABCDE* operon via inhibition of a feed-forward loop, which eventually results in reduced expression of PqsE. However, paecilomycone treatment did not inhibit 2-AA production; therefore, we do not expect a strong inhibition of the entire *pqsABCDE* operon by paecilomycone treatment. Moreover, paecilomycone still had a significant inhibitory effect on pyocyanin production in the $\Delta pqsBC$ strain (Fig. 7G), suggesting that the PqsBC complex cannot be the only target of paecilomycone. Because of the strong inhibition of phenazines, and inhibition of pyocyanin in the *pqsBC* mutant, we believe that paecilomycone did not only target the PqsBC complex. Instead, we suggest that paecilomycone affects QS by directly targeting the PqsBC complex and alternative targets, or paecilomycone alters processes that influence the enzymatic activity of the PqsBC complex. Further research will be needed to study if paecilomycone indeed targets the PqsBC complex and to elucidate the exact mechanism of action of paecilomycone.

Paecilomycone consisted of three different paecilomycones. Analytical HPLC analysis showed that the concentration of paecilomycone A is highest (Fig. 1). To validate that paecilomycone A is responsible for the measured activity, we tested the purified fraction without paecilomycone C (Fig. S5) in various assays. Both in *C. violaceum* (Fig. 2) and

in the inhibition of phenazines and HAQs (Fig. S9) we measured similar activities between paecilomycone and the fraction lacking paecilomycone C, suggesting that paecilomycone C was not required for the effect of paecilomycone in QS inhibition. Interestingly, although funalenone shows high resemblance to paecilomycone A, funalenone did not show inhibition of QS in *C. violaceum* (Fig. 2) or *P. aeruginosa* (Fig. S7). This suggests that the position of the methoxy group, which is the main difference between paecilomycone and funalenone, is important in the QS inhibitor activity.

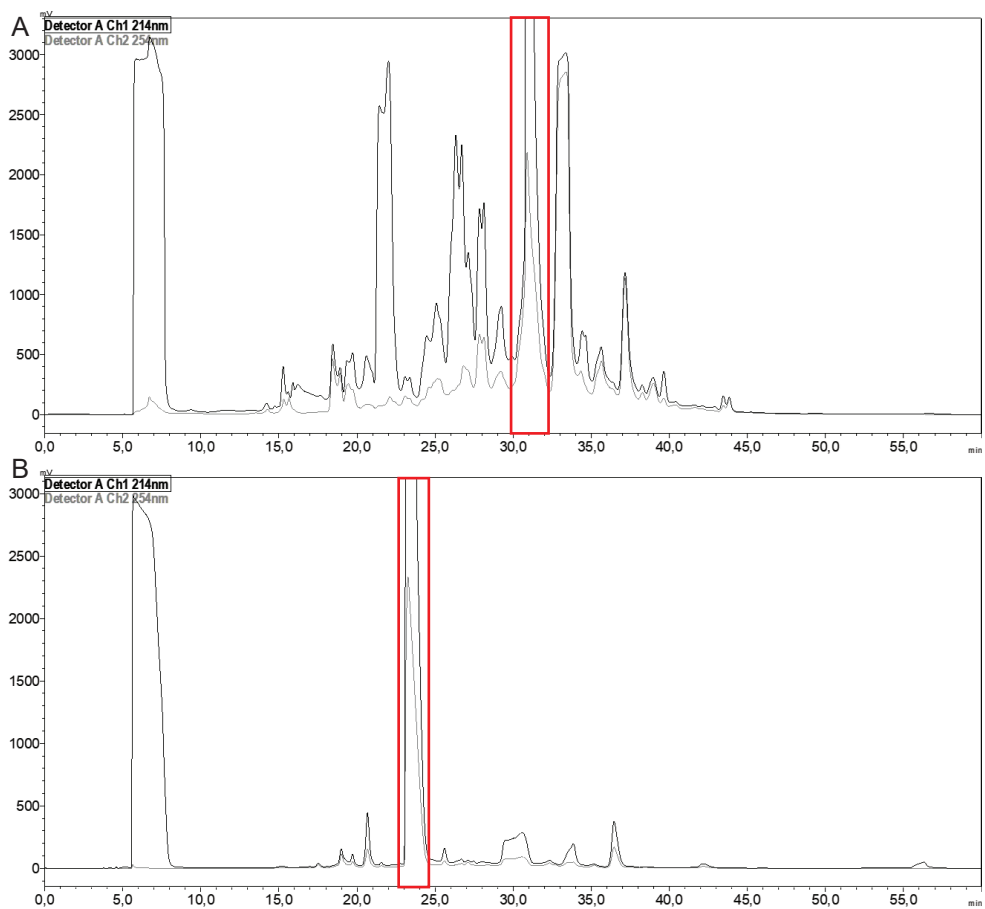
Inhibition of HAQ and phenazine production is interesting to fight the virulence of *P. aeruginosa*. Phenazines are among the major virulence factors produced by *P. aeruginosa*, and play an important role in the acute and chronic lung infections through various mechanisms^{60,183–186}. Phenazines have been shown to be toxic in various model organisms, including *Caenorhabditis elegans*¹⁸⁷, *Drosophila melanogaster*¹⁸⁸, mice¹⁸⁹ and epithelial lung cells^{185,186}. In addition, in humans, phenazine production has been measured in sputum samples in concentrations that are able to inhibit ciliary beating, which is important for the clearance of bacteria¹⁹⁰. Moreover, phenazines are also involved in biofilm formation¹⁹¹ and in the acquisition of iron¹⁹². In general, phenazines are important for the survival of bacteria and for damaging the host. Therefore, inhibition of phenazines by paecilomycone holds potential as an interesting therapeutic lead, by reducing toxicity and subsequently morbidity and mortality in patients.

Whereas the effect of paecilomycone on phenazine synthesis was strong with an IC_{50} of 8.5 μ M for pyocyanin synthesis, this inhibitory effect was less strong on biofilm formation. The inhibition of biofilm formation after treatment of paecilomycone with concentrations higher than 125 μ M might be explained by effects on growth. However, a concentration of 62.5 μ M still inhibited biofilm formation for 50 %, without affecting the growth. Next to QS, there are various pathways that control biofilm formation, including c-di-GMP signaling and the Gac/Rsm cascade⁷⁵. This might explain the difference in effective concentrations for inhibition of biofilm formation and phenazine production.

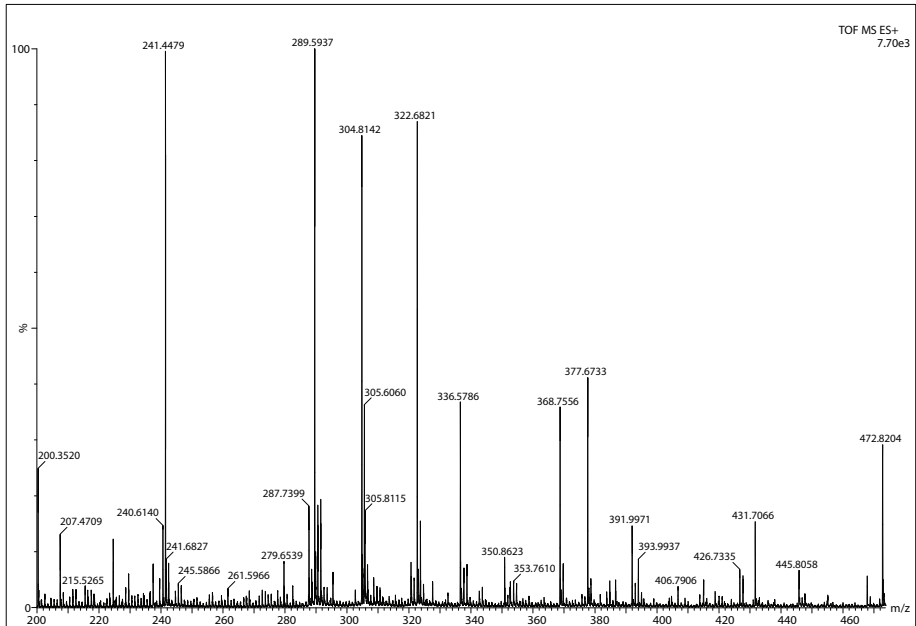
Because of its potential to inhibit QS and downstream targets like phenazine production and biofilm formation, we believe paecilomycone is an interesting lead for further clinical research. We showed that concentrations that inhibit virulence factor production and biofilm formation were not toxic to cell cultures. Moreover, we did not measure toxic effects in more complex systems up to the highest concentrations tested (200–250 μ M). The difference in toxicity between HepG2 cells on the one hand and organoids and zebrafish on the other might be attributed to the fact that complex systems have higher capacity to negotiate and/or abolish the homeostasis and toxic effects of drug compounds. Taken together, our results suggest that paecilomycone is an interesting lead for further research as potential agent to fight *P. aeruginosa* infections.

Acknowledgments

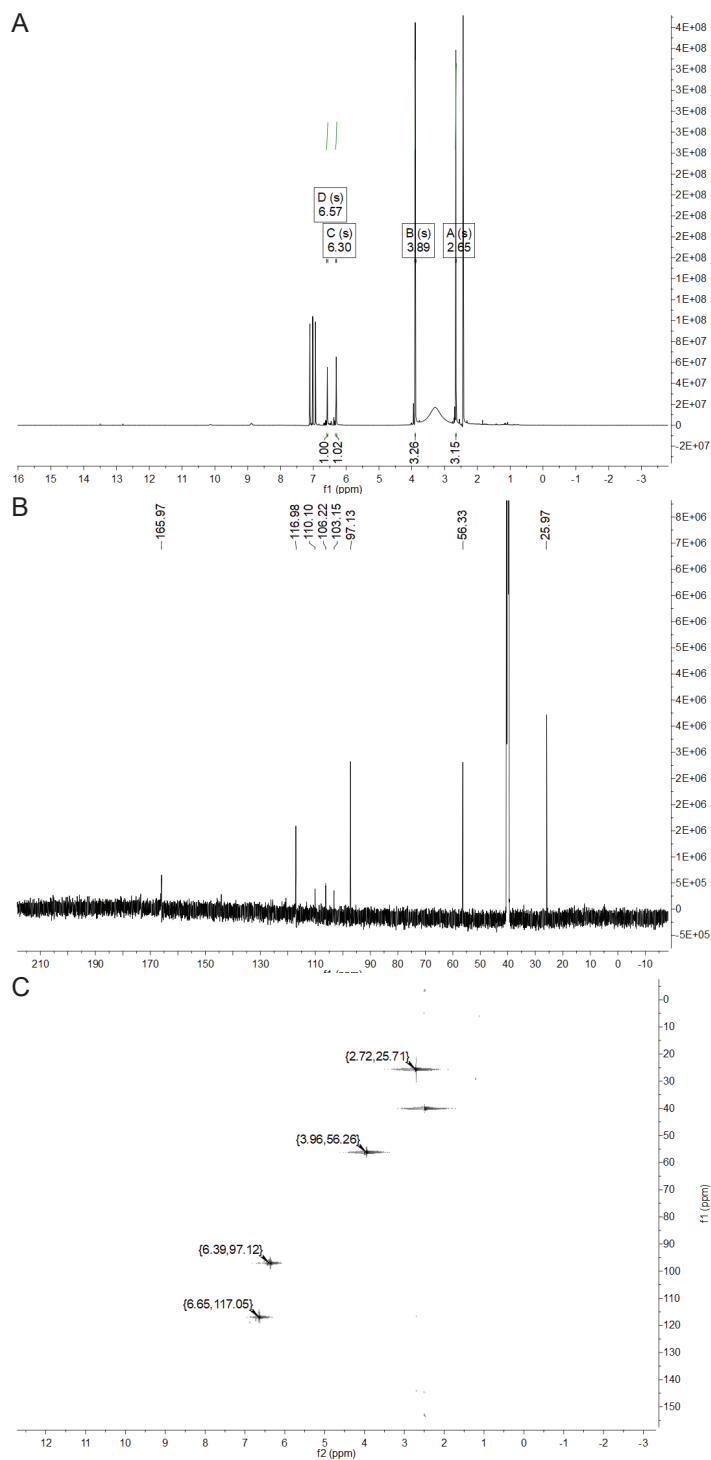
We would like to thank Tim Holm Jakobsen, and Bart W. Bardoel for sharing bacterial strains with us. We would like to thank Joe J. Harrison for sharing the pEX18Gm plasmid. We thank Justyna M. Dobruchowska and Geert-Jan Boons for help with NMR and Arjan Barendregt and Albert Heck for help with high-resolution mass spectrometry.



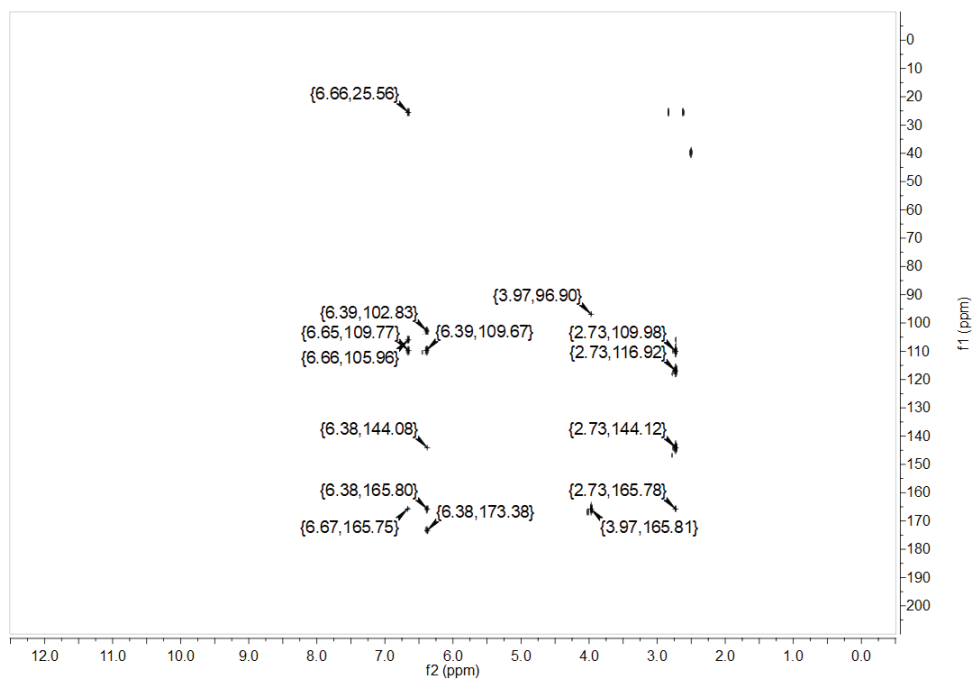
Supplementary Figure 1: Purification of paecilomycone. A) Preparative HPLC spectrogram of *A. allahabadii* supernatant extract using TFA as a modifier, red box outlines the active fraction. B) Subsequent preparative HPLC spectrogram of active fraction using NH_4OAc as a modifier, red box outlines the active fraction that contains paecilomycone.



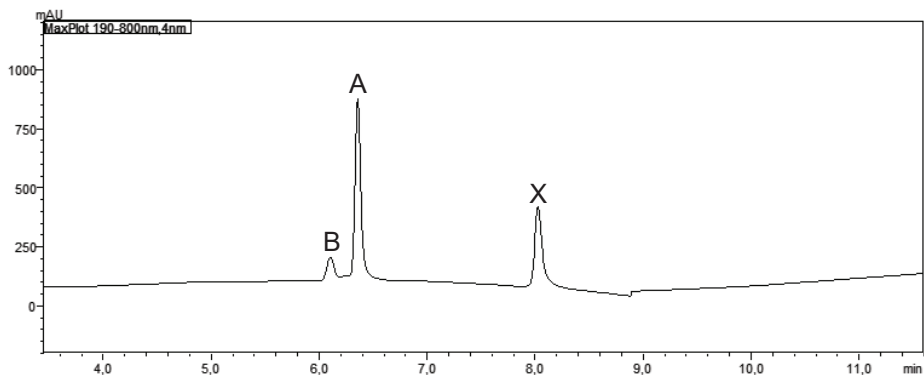
Supplementary Figure 2: High-resolution mass spectrometry chromatogram of paecilomycone A. Indicating a mass of 289.5937.



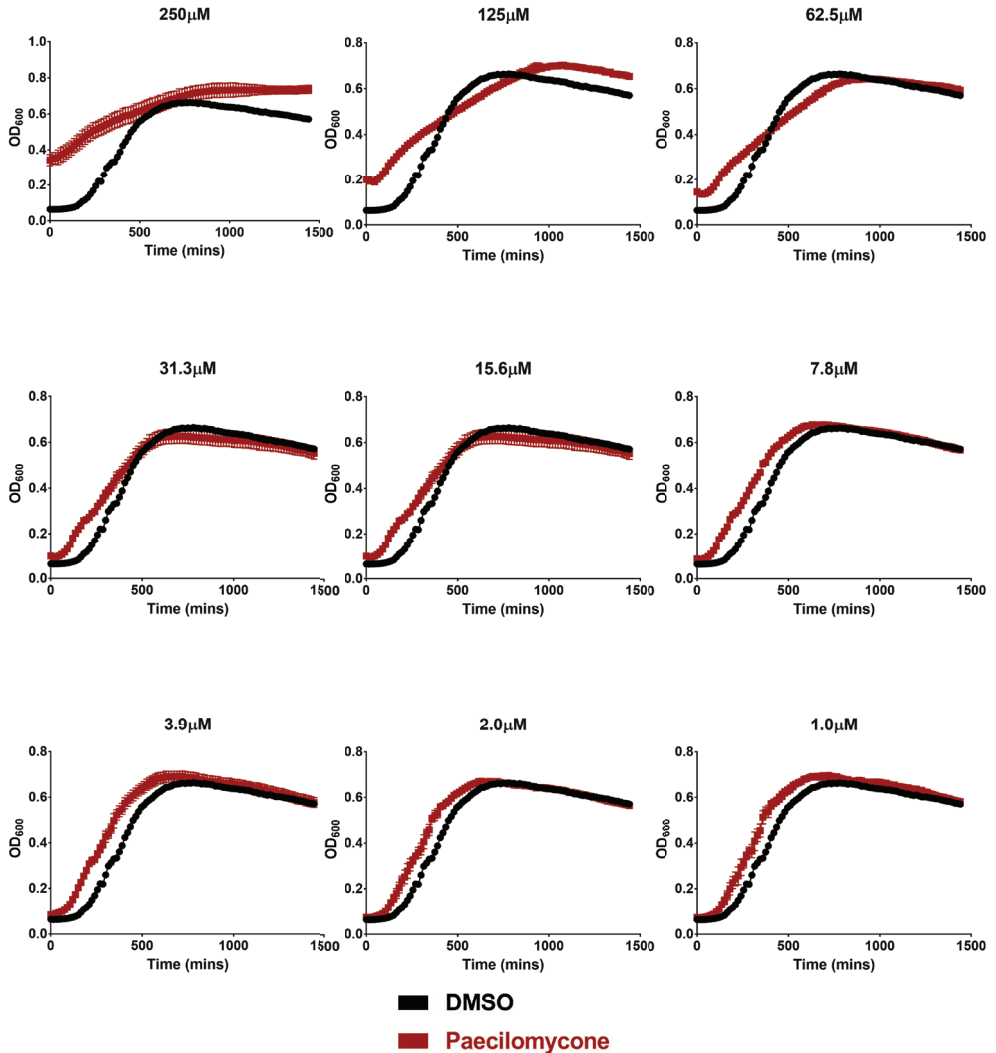
Supplementary Figure 3: NMR data of paecilomycone. A) ^1H -NMR of paecilomycone. **B)** ^{13}C -NMR of paecilomycone. **C)** 2D-NMR HSQC spectrum



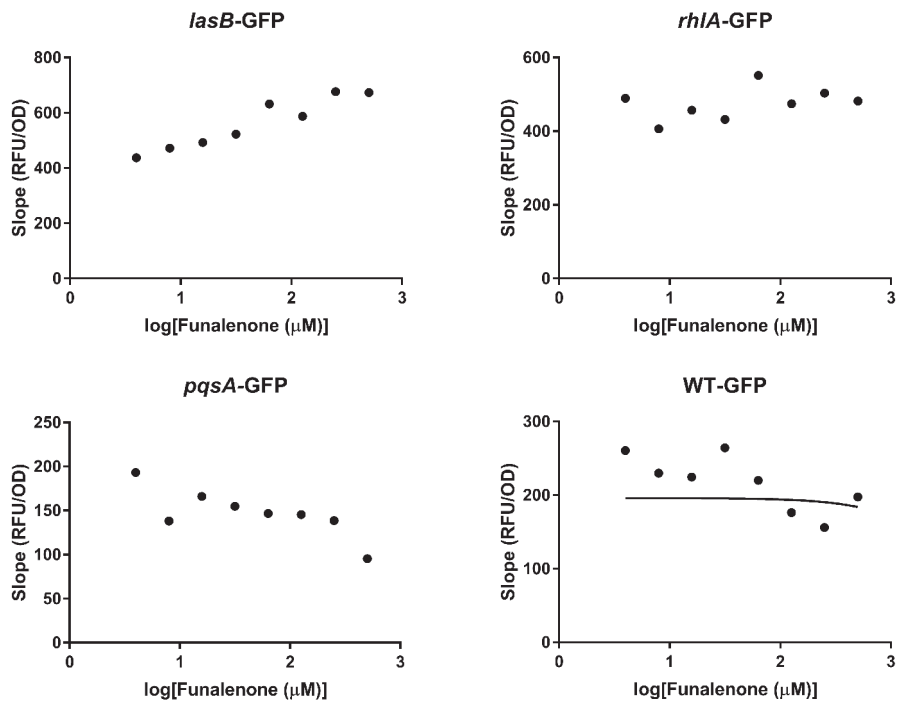
Supplementary Figure 4: 2D-NMR HMBC spectrum



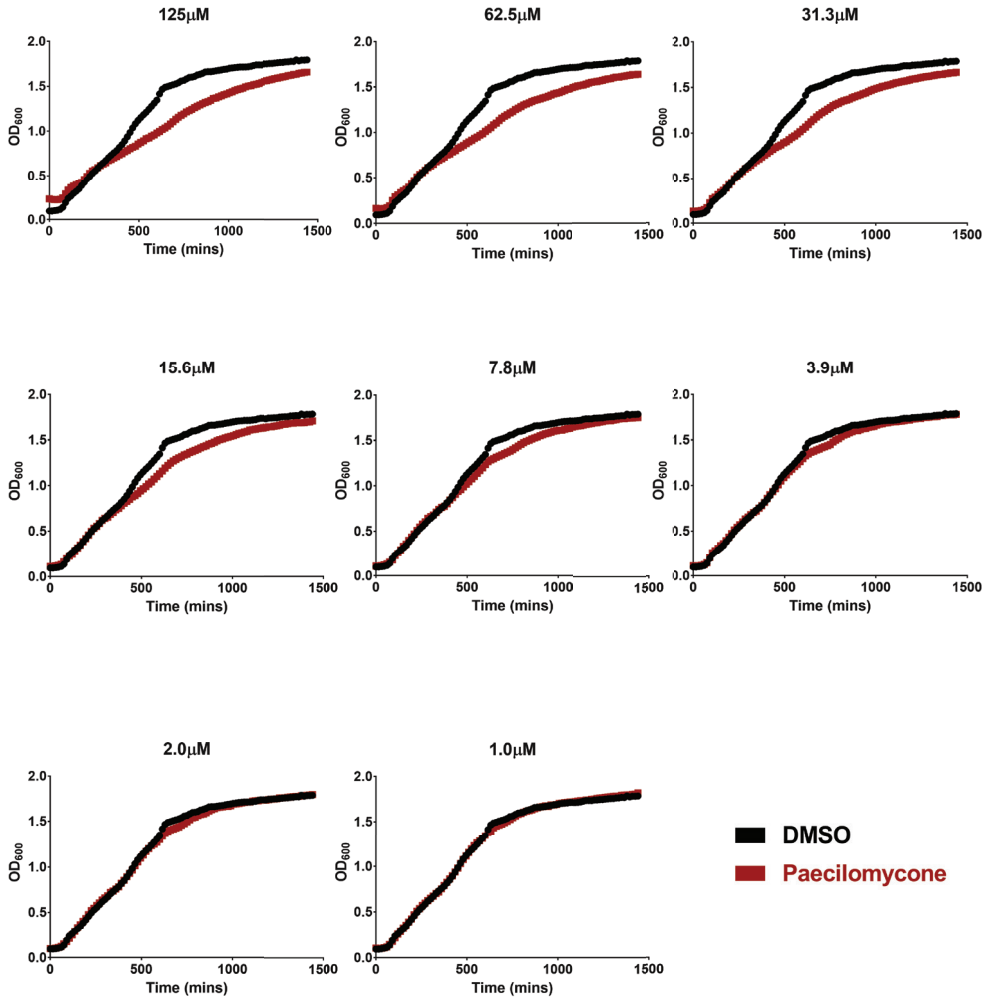
Supplementary Figure 5: aHPLC spectrogram of paecilomycone A without paecilomycone C. This purified fraction does still contain paecilomycone B and an uncharacterized peak



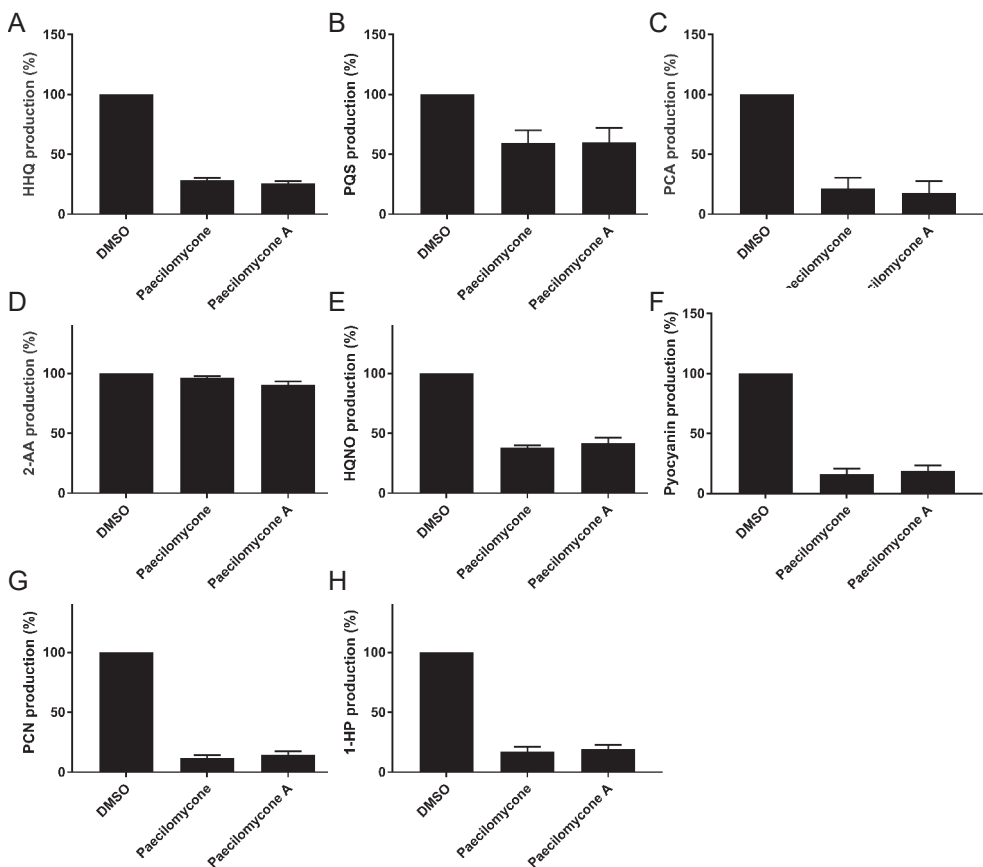
Supplementary Figure 6: Growth of *P. aeruginosa* PAO1 after treatment of paecilomycone in AB medium at 37 °C. Graphs show the growth of 1% DMSO treated (black) versus paecilomycone treated (red). Paecilomycone could interfere with OD₆₀₀ and therefore the start OD₆₀₀ is higher at high concentrations of paecilomycone. Concentrations of paecilomycone used are above the graphs. The experiment was done in triplicates, error bars represent SEM.



Supplementary Figure 7: Quorum sensing inhibition in *P. aeruginosa* PAO1 reporter strains after funalenone treatment. The effect of funalenone was tested using *lasB*-GFP, *rhlA*-GFP, *pqsA*-GFP reporters. In addition, the effect on WT-GFP as control was tested. The maximum slope of RFU, normalized by growth, was plotted and used to calculate the IC_{50} . Experiments were done three times in triplicates, the mean of RFU/OD of a representable experiment was plotted in this figure.



Supplementary Figure 8: Growth of *P. aeruginosa* PAO1 after treatment of paecilomycone in King's A medium at 37 °C. Graphs show the growth of 1% DMSO treated (black) versus paecilomycone treated (red). Paecilomycone could interfere with OD₆₀₀ and therefore the start OD₆₀₀ is higher at high concentrations of paecilomycone. Concentrations of paecilomycone used are above the graphs. The experiment was done in triplicates, error bars represent SEM.



Supplementary Figure 9: Comparison between the effect of paecilomycone and paecilomycone A in the production of various metabolites. Graphs show the production of **A)** HHQ, **B)** PQS, **C)** PCA, **D)** 2-AA, **E)** HQNO, **F)** pyocyanin, **G)** PCN, **H)** 1-HP. Experiments were done three times in triplicates, values were normalized to DMSO treated control, and the mean of the experiments is plotted with error bars representing the SEM. Unpaired t-tests were performed to determine if there is a statistical difference between paecilomycone and paecilomycone A treatment. No statistical difference was found.

Supplementary Table 1 | Bacterial strains used in this study

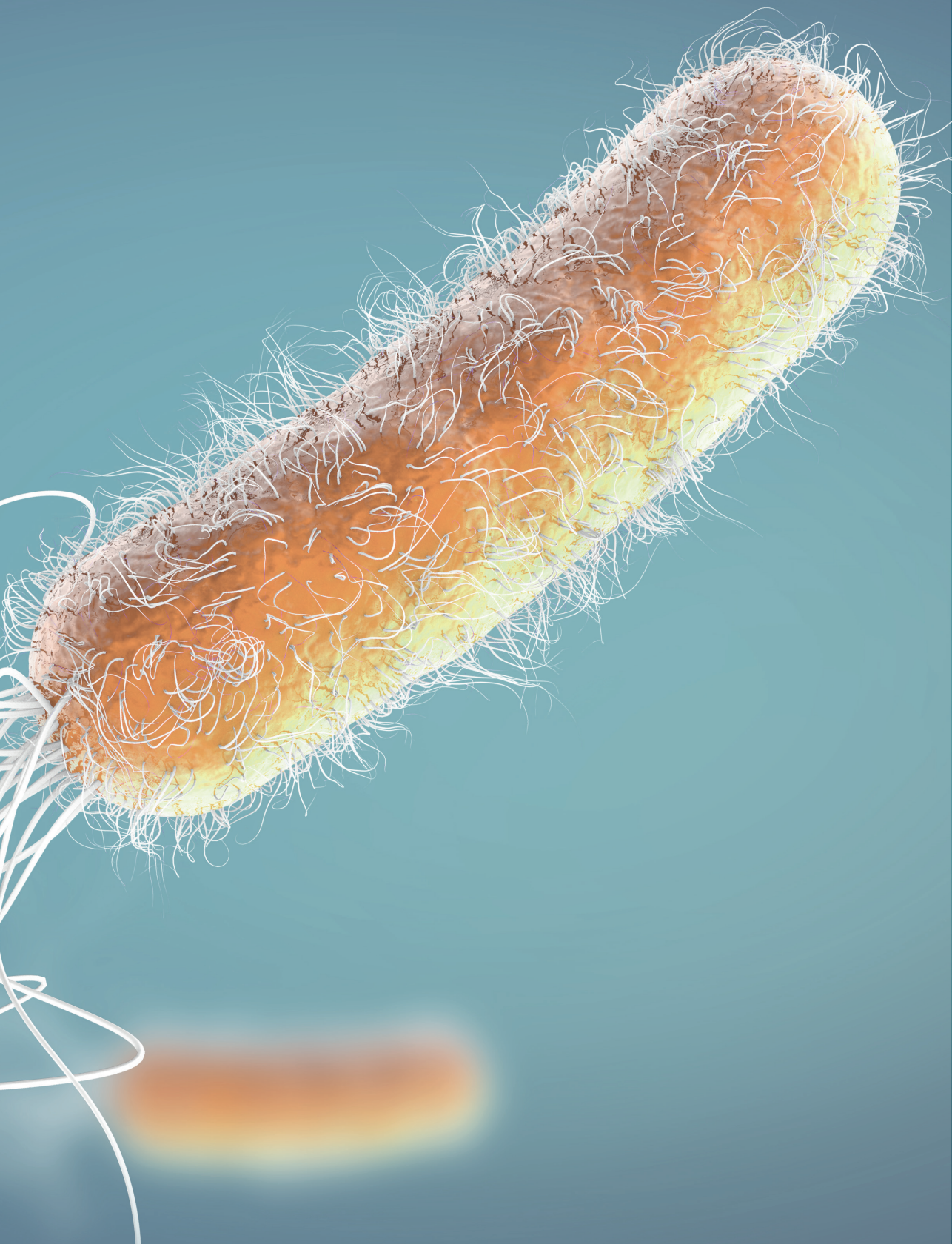
Bacterial strain	Characteristic	Source
<i>Chromobacterium violaceum</i>	WT, ATCC 12472	Westerdijk Fungal Biodiversity Institute
<i>P. aeruginosa</i>	WT, PAO1	
<i>P. aeruginosa</i> $\Delta lasI/\Delta rhII$	PAO1, QS mutant	Hentzer <i>et al.</i> (2003) ¹⁹³
PAO1-GFP	WT, PAO1 GFP-tagged	Yang <i>et al.</i> (2007) ¹⁹⁴
PAO1 <i>lasB</i> -GFP	WT, PAO1, GFP fusion to <i>lasB</i> gene	Hentzer <i>et al.</i> (2002) ¹⁹⁵
PAO1 <i>rhIA</i> -GFP	WT, PAO1, GFP fusion to <i>rhIA</i> gene	Fong <i>et al.</i> (2017) ¹⁹⁶
PAO1 <i>pqsA</i> -GFP	WT, PAO1, GFP fusion to <i>pqsA</i> gene	Fong <i>et al.</i> (2017) ¹⁹⁶
PAO1 $\Delta lasI-\Delta rhII$	PAO1, QS mutant	Hentzer <i>et al.</i> (2003) ¹⁷⁷
PAO1 $\Delta pqsA$	PAO1, <i>pqsA</i> mutant	This study
PAO1 $\Delta pqsE$	PAO1, <i>pqsE</i> mutant	This study
PAO1 $\Delta pqsBC$	PAO1, <i>pqsBC</i> mutant	This study
<i>E. coli</i> RHO3	Conjugation proficient <i>E. coli</i>	Gift from University Medical Center Utrecht

Supplementary Table 2 | Primers used in this study

Primer name	Sequence
<i>pqsA</i> .UP.Fw	GCCAGTGCCAAGCTTGCATGCATGTAGGTGCCTCTTC
<i>pqsA</i> .UP.Rv	GGTGTGCGCCAGGAACAGAACCTCGGTCAGG
<i>pqsA</i> .DN.Fw	GTTCTGTTCTCTGGCCGACACCCTTT
<i>pqsA</i> .DN.Rv	CATGATTACGAATTCGAGCTGCCTACCTGGCGAATATC
<i>pqsA</i> .seq.Fw	TCCCGTTCCTGACAAAGCAA
<i>pqsA</i> .seq.Rv	CACACATAGGATGGGGGCGAG
<i>pqsE</i> .UP.Fw	GCCAGTGCCAAGCTTGCATGTGTCCAAGCGCATGGACTG
<i>pqsE</i> .UP.Rv	GTCTCAGTCCAGCCTCAACATGGCCGG
<i>pqsE</i> .DN.Fw	CCATGTTGAGGCTGGACTGAGACGGGACAT
<i>pqsE</i> .DN.Rv	CATGATTACGAATTCGAGCTAGGTGGAAGCTGAACAGG
<i>pqsE</i> .seq.Fw	GGACGACATCGACCATGTGA
<i>pqsE</i> .seq.Rv	CGTGCGGTACTCCAGACTTT
<i>pqsBC</i> .UP.Fw	GCCAGTGCCAAGCTTGCATGAGGGCTGAGTCCGGGTTAC
<i>pqsBC</i> .UP.Rv	TCACCAATTGGTTACCCCCACAGCC
<i>pqsBC</i> .DN.Fw	GGGGGTGAACCAATTGGGTGAGGTGCTGGT
<i>pqsBC</i> .DN.Rv	CATGATTACGAATTCGAGCTGTCTCGAGACTCTCGCC
<i>pqsBC</i> .seq.Fw	CTGGCCGACACCCTTTATCA
<i>pqsBC</i> .seq.Rv	ATGATTGCTGACCTGGCGTT

Supplementary Table 3 | Plasmids used in this study

Plasmid	Use
pEX18Gm:: $\Delta pqsA$	Plasmid containing <i>pqsA</i> deletion construct for use in PAO1
pEX18Gm:: $\Delta pqsE$	Plasmid containing <i>pqsE</i> deletion construct for use in PAO1
pEX18Gm:: $\Delta pqsBC$	Plasmid containing <i>pqsBC</i> deletion construct for use in PAO1



Chapter 4

Establishment and characterization of a new *Pseudomonas aeruginosa* infection model using 2D airway organoids and dual RNA sequencing

Cayetano Pleguezuelos-Manzano[#], Wouter A. G. Beenker[#], Gijs J.F. van Son, Harry Begthel, Gimano D. Amatngalim, Jeffrey M. Beekman, Hans Clevers, Jeroen den Hertog

[#]Authors contributed equally

Manuscript under review

Abstract

Pseudomonas aeruginosa is a Gram-negative bacterium that is notorious for infections in the airway of cystic fibrosis (CF) subjects. Often, these infections become chronic, leading to higher morbidity and mortality rates. Bacterial quorum sensing (QS) coordinates the expression of virulence factors and the formation of biofilms at a population level. QS has become the focus of attention for development of alternatives to antimicrobials targeting *P. aeruginosa* infections. However, a better understanding of the bacteria-host interaction, and the role of QS in infection, is required. In this study, we set up a new *P. aeruginosa* infection model, using 2D airway organoids derived from healthy and CF individuals. Using dual RNA-sequencing, we dissected their interaction, focusing on the role of QS. As expected, *P. aeruginosa* induced epithelial inflammation. However, QS signaling did not affect the epithelial airway cells. The epithelium influenced several infection-related processes of *P. aeruginosa*, including metabolic changes, induction of type 3 and type 6 secretion systems (T3SS and T6SS), and increased expression of antibiotic resistance genes, including *mexXY* efflux pump and several porins. Interestingly, the epithelium influenced the regulation by QS of the type 2 (T2SS) and T6SS. Finally, we compared our model with *in vivo* *P. aeruginosa* transcriptomic datasets, from samples directly isolated from the airways of CF subjects. This shows that our model recapitulates important aspects of *in vivo* infection, like enhanced denitrification, betaine/choline metabolism, increased antibiotic resistance, as well as an overall decrease of motility-related genes. This relevant infection model is interesting for future investigations, helping to reduce the burden of *P. aeruginosa* infections in CF.

Keywords: Airway organoids, *Pseudomonas aeruginosa*, 2D co-culture, Infection model, Dual RNA-sequencing, Quorum sensing

Introduction

Pseudomonas aeruginosa is a Gram-negative opportunistic bacterium, which is known to chronically infect the airways of people with cystic fibrosis (CF). CF is a genetic disorder caused by mutations in the gene coding for the cystic fibrosis transmembrane conductance regulator (CFTR) protein. Mutated CFTR leads to an osmotic misbalance of the epithelial surface in multiple organs^{197–199}. However, the airways are most affected due to their obstruction by desiccated mucus, which can lead to pulmonary failure^{200,201}. This CF mucus presents a perfect condition for *P. aeruginosa* growth²⁰². Because *P. aeruginosa* has a high intrinsic resistance to antibiotics, infections often become chronic^{26–28,30,203}, contributing to the high morbidity and mortality observed in people with CF³⁰.

A growing field of research focuses on quorum sensing (QS) as an alternative target to treat *P. aeruginosa* infections. Via QS, bacteria regulate a broad range of cellular processes based on their local cell density. QS in Gram-negative bacteria is highly conserved: a LuxI-type synthase produces a signal molecule (an acyl-homoserine lactone (AHL)) that can diffuse across membranes and bind to its cognate LuxR-type receptor, altering the expression of target genes^{106,152}. Thus, when bacterial density is high, the concentration of AHLs increases, inducing downstream processes like biofilm formation and the production of virulence factors¹⁰⁶.

P. aeruginosa presents a relatively complex QS network, involving three different systems: two typical LuxI/R systems (*las*-encoded and *rhl*-encoded system) and a unique *Pseudomonas* Quinolone Signal (PQS)-based system. These systems are hierarchical and highly interconnected. The Las system is the QS master regulator that induces expression of the Rhl and PQS systems⁶⁸. Importantly, inhibition of QS reduces the toxicity of *P. aeruginosa* in animal models and leads to faster clearing and prolonged survival of the infected animal^{77,88,204}. However, the exact role of QS in human infection and CF is still underexplored⁹⁰.

To date, *P. aeruginosa* CF infection models vary from the study of *P. aeruginosa* isolates from CF subjects^{97,205,206} to growing *P. aeruginosa* *in vitro* in artificial CF sputum and other bacterial media^{207–211}, using various CF animal models^{212–214}, working with *ex vivo* CF lungs^{215,216}, or co-culture systems using cancer cell lines and primary cells^{217–222}. Each of these models present distinct advantages and disadvantages²²³.

Human airway organoids derived from adult stem cells faithfully resemble the cellular composition and physiology of the airway²²⁴. Additionally, airway organoids derived from CF subjects capture the molecular characteristics of the disorder and therefore are a useful tool to study CF phenotypes *in vitro*²²⁵. Furthermore, organoid co-cultures have recently been used to investigate the role of bacteria in colorectal cancer^{159,226}. In the current study, we describe a new co-culture method using upper airway organoids grown in 2D -derived from healthy individuals and CF subjects- to study *P. aeruginosa* infections. By performing dual RNA-seq²²⁷, this analysis captures the interaction between the host cells and the bacteria.

Materials and methods

Bacterial strains and growth conditions

For this study, we used *P. aeruginosa* PAO1 strains, which constitutively express GFP. Stocks were stored in -80 °C in 20 % glycerol solutions. PAO1 strains were plated on Luria agar (LA) at 37 °C and grown in medium specific for the assay. *E. coli* RHO3 strains were used for conjugation and medium was supplemented with 400 µg/mL 2,6-Diaminopimelic acid (Sigma-Aldrich, Merck Life Science, Amsterdam, The Netherlands) to support growth. The PAO1 $\Delta pqsA$ strain has been described before²²⁸. The PAO1 $\Delta lasI/\Delta rhII$ strain was generated using allelic exchange following the method described before¹⁵⁸. For the generation of the mutants we inserted upstream (using UP.Fw and UP.Rv primers) and downstream (using DN.Fw and DN.Rv primers) regions of the gene of interest in pEX18Gm plasmids using Gibson assembly restriction cloning, using the restriction enzymes ScaI and SphI (Primers and plasmids are listed in Supplementary table 1 and 2). After Gibson assembly, the plasmid was transformed into RHO3 *E. coli* donor strains before conjugation via puddle mating with PAO1 GFP strain. Mutant colonies were identified with colony PCR (using seq.FW and seq.Rv primers) and confirmed by sequencing (performed by MacroGen Europe BV).

Organoid cultures

Nasal brushing-derived epithelial stem cells were collected and stored with informed consent of all donor and was approved by a specific ethical board for the use of biobanked materials TcBIO (Toetsingscommissie Biobanks), an institutional Medical Research Ethics Committee of the University Medical Center Utrecht (protocol ID: 16/586). Nasal epithelial stem cells were isolated and expanded in 2D cell cultures as previously described²²⁹. After initial expansion, nasal cells were grown as organoids and cultured as previously described²²⁴. In brief, organoids were cultured in expansion medium containing Advanced DMEM F12, 1X GlutaMax (Life Technologies; 12634-034), 10mM HEPES (Life Technologies; 15630-056) (AdvDMEMF12++), supplemented with penicillin and streptomycin (10,000 IU/ml each; Life Technologies; 15140-122) 1× B27 supplement (Life Technologies; 17504-044), 1.25 mM N-acetyl-l-cysteine (Sigma-Aldrich; A9165), 10 mM nicotinamide (Sigma-Aldrich; N0636), 500 nM A83-01 (Tocris; 2939), 5 µM Y-27632 (Abmole; Y-27632), 1 µM SB202190 (Sigma-Aldrich; S7067), 100 ng/ml human FGF10 (PeproTech; 100-26), 25 ng/ml FGF7 (PeproTech; 100-19), 1% (vol/vol) RSPO3, and Noggin (produced via the r-PEX protein expression platform at U-Protein Express BV). For its passage, organoids were collected, washed and resuspended in TrypLE (Gibco) and incubated at 37 °C for 15 minutes. Then, organoids were mechanically disrupted into single cells and plated in droplets of Cultrex growth factor reduced BME type 2 (Biotechne | R&D systems 3533-010-02). For the 2D culture of airway organoids, 10⁵ cells were seeded into 24-well polystyrene membranes (Greiner Bio-One) and cultured for one week in expansion medium in both top and bottom compartments until confluency. After confluency, cells were differentiated in air liquid interface during 1 month using PneumaCult™-ALI Medium (Stem cell technologies) supplemented with

Hydrocortisone stock solution (5 μ l/ml; Stem cell technologies #07925) and Heparin solution (2 μ l/ml; Stem cell technologies #07980).

2D airway organoid - *Pseudomonas aeruginosa* co-culture

Bacterial colonies were picked and grown in DMEM medium (ThermoFisher Scientific, 31966-021), supplemented with 10 mM HEPES (ThermoFisher Scientific, 15630080) and 1X GlutaMAX (ThermoFisher Scientific, 35050061) until an $OD_{600} = 0.35 - 0.45$. 1 mL of early log-phase bacterial culture was taken and centrifuged for 3 min at 15,000 g, before washing once with PBS. Bacterial cells were pelleted again and resuspended in AdvDMEMF12++ (without antibiotics) to normalize to $OD_{600} = 0.4$. Bacteria were diluted 100 x in the same medium before adding 50 μ L to the organoids to reach a multiplicity of infection (MOI) of 0.1. Organoids in transwells were washed three times in AdvDMEMF12++ (without antibiotics) before addition of the bacteria. Co-cultures were incubated at 37 °C with 5 % CO_2 for 14 h. In parallel, 50 μ L of bacteria were grown in a 96-well plate and organoid transwells without bacteria were incubated as controls. The epithelial cells were checked for damage using the fluorescent EVOS FL Auto 2 microscope (ThermoFisher Scientific) at 14 h. Damaged co-cultures were excluded for analysis.

Imaging of organoid 2D cultures and PAO1-GFP co-culture

Organoid 2D culture and PAO1 co-cultures were fixed with 4% formaldehyde for 2 hours at room temperature. Then, 2D cultures were processed for immunohistochemistry following standard techniques and embedded in paraffin. After sectioning, hematoxylin/eosin staining was performed according to manufacturer instructions. After blocking, the used primary antibodies included anti-MUC5AC (Thermo, MA5-12175), anti-acetylated Tubulin (SantaCruz, sc-23950) and anti-P63 (Abcam, ab735). Co-cultures were processed for wholemount immunofluorescence imaging using standard techniques⁴⁵⁹. Then, co-culture was stained with Phalloidin Atto-647 (65906-10NMOL) and DAPI and imaged with SP8 confocal microscope (Leica).

Colony forming unit (CFU) test

For the CFU test, organoid infection protocol was followed as described before. For time point 0 h, plates were incubated for only 5 min. For time point 14 h, plates were incubated 14 h. After incubation, 50 μ L of 0.5 % saponin was added to the wells and incubated for 10 min at room temperature. Then, the volume was resuspended and transferred to Eppendorf tubes before centrifugation for 10 min at 15,000 g. Supernatant was aspirated and pellets were resuspended in PBS before making 10-fold dilutions. 5 μ L of the dilutions were plated on tryptic soy agar and plates were incubated overnight at 34 °C before the colonies were counted.

RNA isolation

RNA was isolated from the cultures using the MasterPure Complete DNA and RNA

Purification Kit (Immunosource, Belgium) following manufacturer instructions. To remove all the gDNA, two additional rounds of DNase treatment were performed using TURBO DNase (ThermoFisher Scientific) following manufacturer's protocol. RNA was subsequently isolated again using the MasterPure RNA isolation kit and the RNA was dissolved in MQ and stored at -80 °C until further use. For RNA-sequencing, RNA libraries were validated with Agilent 2100 bioanalyzer. Samples were sent for sequencing to the Utrecht Sequencing Facility (Useq). Library preparation was performed using Truseq RNA stranded ribo-zero kit. RNAseq was performed using the Illumina NextSeq2000 platform.

Mapping of raw-reads to the genome

To analyze the dataset, a variety of bioinformatics tools were used and we followed a similar protocol as described before, with minor modifications (Supplementary figure 1)²³⁰. First, the reads were mapped to the human genome (hg19) using STAR mapping software²³¹. Unmapped reads were written into a new FastQ-file. Gene counts were assigned to the mapped reads using FeatureCounts²³². Unmapped reads were then mapped against the PAO1 genome (NCBI: txid208964)^{22,231,233}. Gene counts were again assigned using FeatureCounts. The code for this pipeline is available on Github (https://github.com/GJFvanSon/Hubrecht_clevers.git).

Bioinformatic analysis

Human and PAO1 count tables were independently analyzed using DESeq2²³⁴. DEGs were calculated using the lfcShrink function with argument type set to "apglm". Volcano plots were generated using EnhancedVolcano package²³⁵. For the human dataset, GO enrichment analysis was performed using the function enrichGO() from the package clusterProfiler()²³⁶ with arguments OrgDb=org.Hs.eg.db, ont="BP", pAdjMethod="fdr", minGSSize="1", maxGSSize="2000", qvalueCutoff= "0.05" and readable="TRUE". For PAO1 dataset, GO enrichment analysis was performed using the online tool PANTHER 17.0, with the following settings: analysis type: PANTHER overrepresentation test (Released 20221013), annotation version and release date: GO ontology database DOI: 10.5281/zenodo.6799722 released 2022-07-01, reference list: *Pseudomonas aeruginosa* (all genes in database), annotation data set: GO biological process complete, test type: Fisher's exact, correction: calculate false discovery rate. KEGG pathway was generated using the Pathview R package. *Pseudomonas* category and GO gene lists were downloaded from *Pseudomonas* Genome DB version 21.1 (2022-11-20)²³⁷. Protein-protein association network analysis was performed using the STRING v11 online tool²³⁸. Common genes with a $\log_2\text{Foldchange} / \log\text{SE} > |4|$ were used as input. The input parameters were set as follow: Organism = "*Pseudomonas aeruginosa* PAO1", Network Type = "full string network", Required score = "high confidence (0.700)", and FDR stringency = "medium (5 percent)". MCL clustering was performed on the resulting network using the following parameters: inflation parameter = "3", and edges between clusters = "Don't show".

Results

Establishment of 2D airway organoid co-cultures with *P. aeruginosa*

We aimed to study the interaction between *P. aeruginosa* and the airway epithelium during early infection. For this, we established an epithelial co-culture system composed of upper airway (nasal) organoids cultured in 2D and the well-characterized *P. aeruginosa* PAO1 strain constitutively expressing GFP. Organoid cultures were differentiated for 1 month in 2D air liquid interface (ALI) (Figure 1A). This approach gave rise to a pseudostratified epithelium containing the main cell types of the mature airway epithelium: goblet cells marked by MUC5AC, ciliated cells marked by acetylated tubulin, and basal cells marked by TP63 (Figure 1B). 2D ALI cultures allow for easy apical exposure to bacteria. PAO1 bacteria were pipetted apically at a multiplicity of infection (MOI) of 0.1 (Figure 1C). After 14 hours, bacterial aggregates had formed on the epithelial cells implying that downstream pathways including biofilm formation are active in co-culture (Figure 1D, E). Longer co-culture time was not feasible due to elevated epithelial cell death caused by the bacteria. Wild type PAO1 cells and PAO1 strains Δ QS (*rhlI/lasI* KO) and Δ *pqsA* (*pqsA* knockout) that display impaired QS were alive and proliferated during this time span (Figure 1F).

Dual RNA-sequencing of the co-culture model

To study the interplay between upper airway epithelial organoids and *P. aeruginosa*, we subjected the 14 hours co-cultures to dual RNA-seq, in order to capture the transcriptomic response of both components. For this, we used organoid lines derived from a healthy donor or from a CF subject and either WT, Δ *pqsA* or Δ QS PAO1 cells (Figure 2A). Organoid cultures without bacteria and pure bacterial cultures were used as controls. As an initial step to validate the feasibility of our approach, we performed bacterial RNA sequencing of PAO1-WT strain, both in co-culture and by itself (Supplementary figure 1). We added these samples to the analysis of the dual RNA-seq cohort unless otherwise stated. After a two-step mapping approach (Supplementary Figure 1A), approximately half of the reads from co-culture samples were aligned to the bacterial or human genome, indicating that the dual RNA-seq approach efficiently captured the transcriptome of both components. As expected, the analysis of separately cultured 2D organoids and bacteria yielded almost 100% reads of the corresponding species (Figure 2B).

We first validated the differential expression of the bacterial KO genes in the bacterial strains. As expected, the PAO1 Δ *pqsA* strain showed inhibition of *pqsA*, while not affecting *lasI* and *rhlI*. PAO1 Δ QS showed inhibition of all three QS pathways, including inhibition of *pqsA* due to the hierarchical QS system in *P. aeruginosa* PAO1 (Figure 2C). These three strains allowed us to study and compare the effect of QS and of the PQS system in co-culture. Comparison of the PAO1 transcriptomes showed a major difference between PAO1 cells grown in mono-culture and in co-culture with organoids (Figure 2D). The effect of Δ QS was also evident in co-culture and in bacterial mono-culture (Figure 2D). However, Δ *pqsA* did not show a marked transcriptional change, other than *pqsA* expression itself, compared

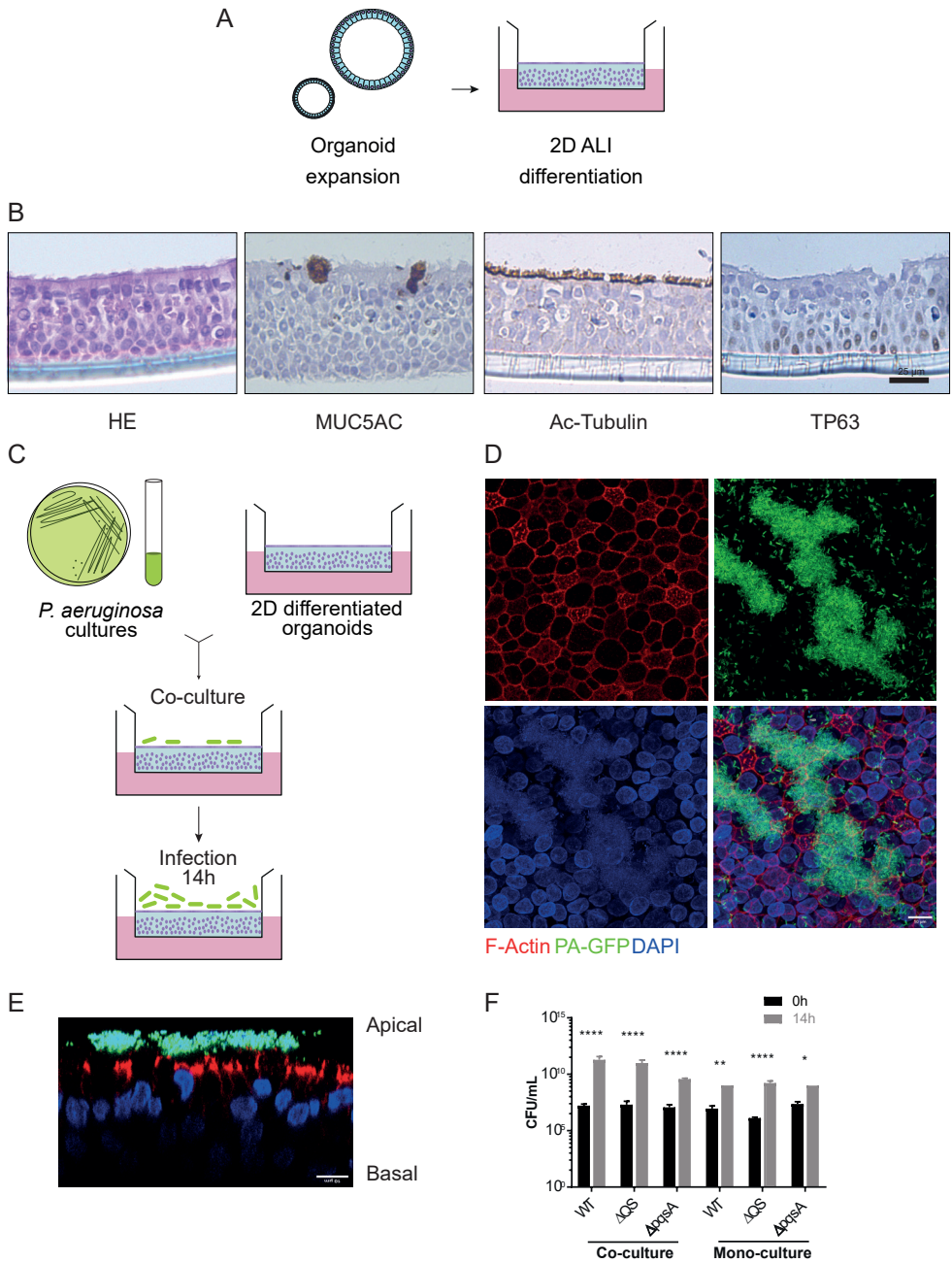


Figure 1. Co-culture establishment of 2D-airway organoids with *P. aeruginosa* PAO1. **A)** Schematic representation of organoid 2D culture establishment and ALI differentiation. **B)** HE and staining of the major cell types present in ALI differentiated airway organoids, goblet cells stained by MUC5AC, ciliated cells by acetylated (Ac) tubulin and basal cells by TP63. Scale bar indicates 25 μ m **C)** Schematic representation of co-culture establishment of PAO1-GFP and differentiated airway organoids. **D)** Z projections and **E)** cross-section of confocal imaging of the co-culture after 14 h. Red: F-Actin; green: PAO1-GFP; blue: DAPI. Scale bar indicates 10 μ m. **F)** CFU assay of WT PAO1 bacteria and PAO1 Δ QS and Δ pqsA strains following co-culture with organoids and in liquid medium at time points 0 h and

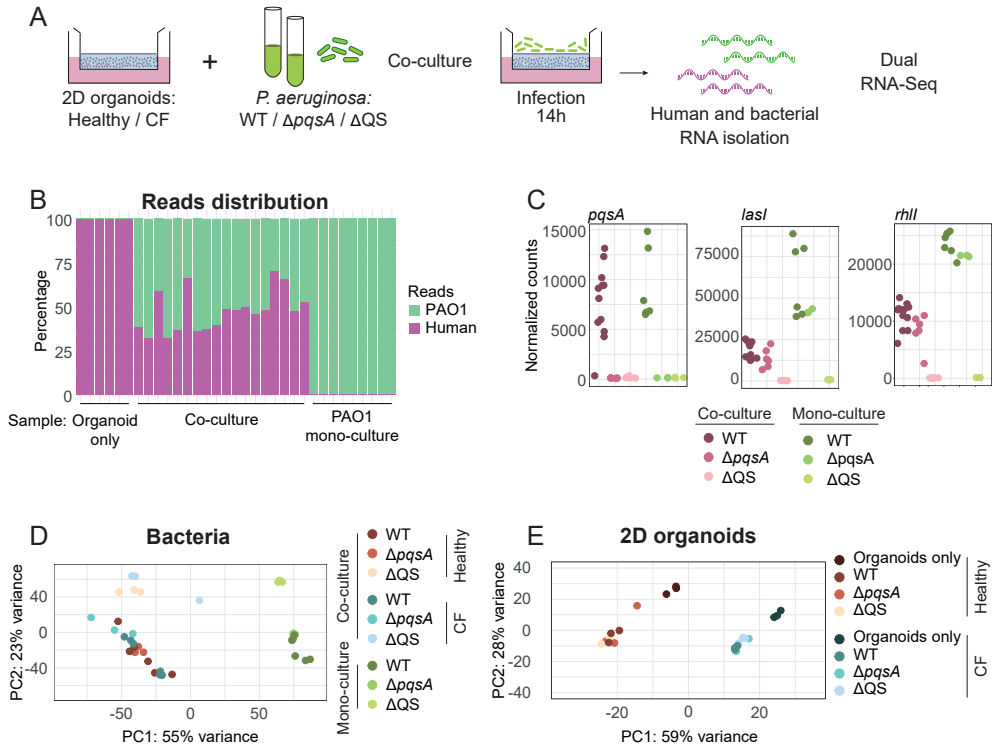


Figure 2. Co-culture characterization by Dual RNA-seq. **A)** Schematic representation of the dual RNA-seq experiment. **B)** Distribution of human and bacterial reads across the different samples included in the run after performing the mapping and count assignment (as in Supplementary figure 1). **C)** Knock-out validation by gene expression. Normalized counts of *pqsA*, *lasI* and *rhlI* across the different samples of the cohort. Color code indicates culture condition (Green: mono-culture; magenta: co-culture) and PAO1 genotype (Dark: WT; middle: $\Delta pqsA$; light: ΔQS). **D)** PCA plot of PAO1 samples. **E)** PCA plot of 2D organoid samples. Color code indicates PAO1 genotype, culture condition (co-culture or mono-culture) and organoid genotype (Healthy or CF).

to WT bacteria, irrespective of the culture method (Figure 2D). Since our analysis included only one healthy and CF organoid line, conclusions about CF-specific effects of PAO1 cannot be drawn. Nevertheless, both organoid lines showed a clear transcriptional response to the presence of PAO1 irrespective of the bacterial genotype (Figure 2E).

P. aeruginosa induces epithelial inflammation

Next, we focused on the effect induced by the different PAO1 strains on the 2D organoid cultures (Figure 3A). Coculture with PAO1 cells led to upregulation of 1610 genes in 2D organoids and downregulation of 638 genes. This occurred irrespective of the PAO1 genotype (Fig. 3B) For both healthy and CF 2D organoids, these changes reflected pathways involved in NF- κ B-mediated inflammation and response to lipopolysaccharides (LPS),

Figure 1 legend (continued)

14 h. The mean of the triplicates was plotted and error bars represent standard error of the mean (SEM). To determine statistical significance between the time points, log-transformed data was analyzed using two-way ANOVA, corrected for multiple comparisons using Sidak's test (*, $P < 0.05$; **, $P < 0.005$; ***, $P < 0.0001$).

including *IL1A/B*, *TNFA*, and various *CXCL* chemokines (Figure 3D and E). Whereas previous studies have shown that QS molecules affect epithelial cells^{239–241}, no clear QS-derived effect was observed when organoids were exposed to PAO1 WT compared to $\Delta pqsA$ and ΔQS strains (Figure 3B). Since the $\Delta pqsA$ and ΔQS strains lack expression of some or most QS signaling molecules, this observation contrasted with a previous report suggesting that the epithelium can sense and respond to QS molecules²³⁹.

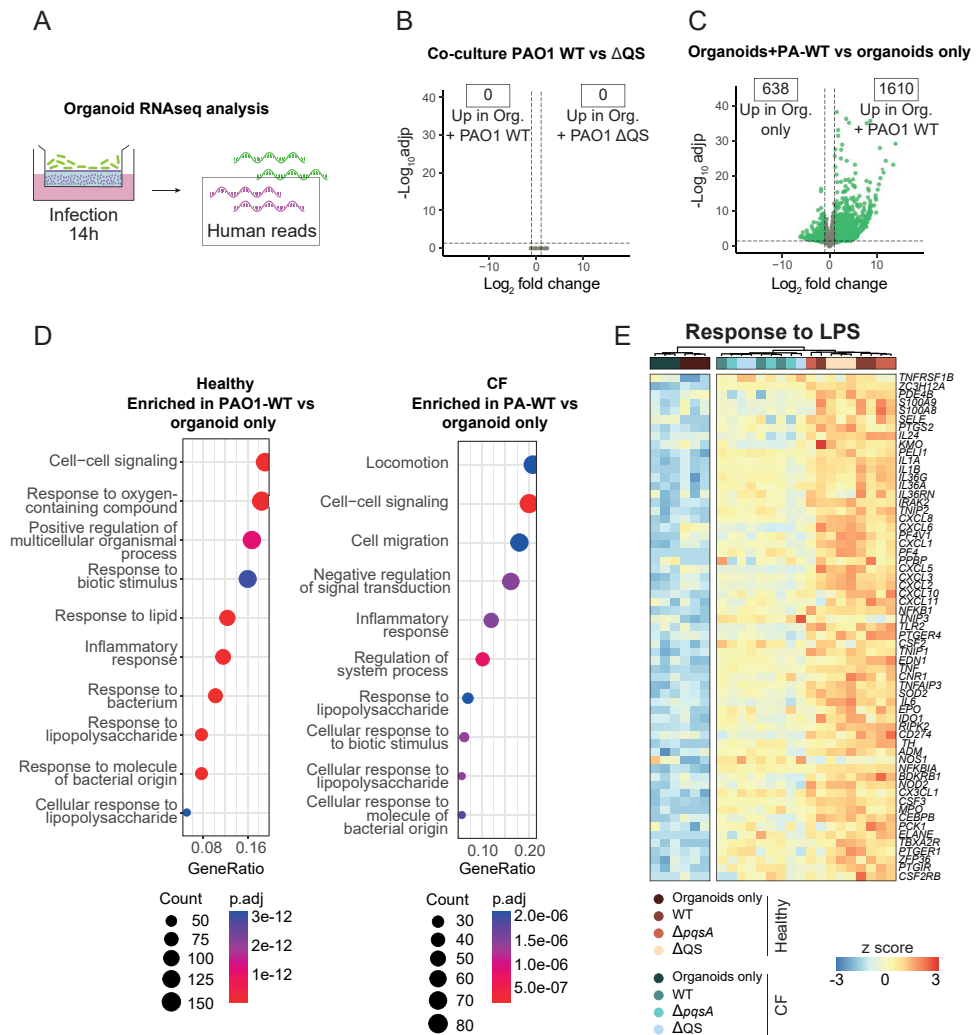


Figure 3. Transcriptional response of the epithelium to infection with the different PAO1 strains. **A)** Schematic representation of the analysis. **B)** Volcano plot showing the \log_2 fold change and $-\log_{10}$ adjusted p-value of all genes, when comparing the transcriptome of 2D organoids exposed to PAO1 WT or PAO1 ΔQS . **C)** Volcano plot showing the \log_2 fold change and $-\log_{10}$ adjusted p-value per gene comparing the transcriptome of 2D organoids exposed to PAO1 WT or unexposed controls. Green indicates differentially expressed genes (DEGs) (\log_2 fold change > 1 and adjusted p value < 0.05). **D)** Gene ontology enrichment analysis showing top 10 categories enriched in 2D organoids exposed to PAO1 WT. Left panel: Healthy organoid line. Right: CF organoid line. **E)** Gene expression heatmap of genes from “Response to lipopolysaccharide” GO term category (GO:0032496). Color code indicates culture condition (co-culture or mono-culture) and PAO1 genotype (WT, $\Delta pqsA$ or ΔQS).

The epithelium induces *P. aeruginosa* transcriptional changes associated with infection

We next focused on the effect of the organoids on *P. aeruginosa* PAO1 (Figure 4A). Comparing the gene expression profile of PAO1 grown in co-culture versus mono-culture revealed a total of 2215 differentially expressed genes (DEGs) (979 upregulated in co-culture; 1136 upregulated in mono-culture) (Figure 4B). Gene ontology enrichment analysis of these genes revealed broad metabolic differences between the two culture modes. Genes involved in iron acquisition (e.g., siderophore and pyoverdine processes) showed higher expression in pure bacterial cultures (Supplementary Figure 2A). This contrasted with what has been observed in human infections^{97,242}, but was in agreement with previous co-culture attempts²²⁰.

PAO1 cells co-cultured with airway cells increased their expression of genes related to peptide, glycolipid and amide biosynthetic pathways (Figure 4C), suggesting major metabolic rearrangements. Interestingly, co-cultured PAO1 cells presented increased *crc* and decreased *crcZ* levels (Figure 4D), two main regulators of the carbon catabolite repression (CCR) pathway^{243,244}. This pathway is central to the hierarchical utilization of preferred carbon sources by *P. aeruginosa*. This finding suggested that the epithelium provides a source of preferred nutrients compared to the medium alone. Interestingly, expression change was observed in only a subset of genes known to be regulated by the CCR pathway (Supplementary Figure 2B). This highlights the complexity of metabolic regulation.

Another important aspect of *P. aeruginosa* infection of individuals with CF is its ability to perform denitrification²⁴⁵. This mechanism enables the utilization of nitrogenous oxides (nitrate, nitrite, and nitrous oxide) as electron acceptor for respiratory growth in anoxic conditions, such as during the course of infection²⁴⁶. We found that co-cultured PAO1 expressed increased levels of many genes involved in nitrogen metabolism (Supplementary Figure 2C), and particularly those used in denitrification (Figure 4E). This suggests that there is local anoxia due to the oxygen consumption by the epithelium and high-density bacterial population, which is similar as observed in airway infections^{99,202}. Beyond metabolism, the bacteria also showed elevated levels of genes involved in resistance to antibiotics (Supplementary Figure 2D). Particularly striking was the effect of the epithelium on genes encoding the MexXY efflux pump, porins, and genes like *aph*, *PA5514*, *arnA* and *PA2528* encoding antibiotic degrading enzymes (Figure 4F and Supplementary Figure 2E). Of note, our co-culture system is performed in antibiotic-free conditions. Finally, the presence of epithelial cells induced the expression of type 3 (Supplementary Figure 2F) and type 6 (Figure 4G) secretion systems (T3SS and T6SS). These bacterial secretion systems are syringe-like structures used to inject toxins into the cytoplasm of target cells^{247–250}. The epithelium mainly induced the expression of the H2-T6SS, and to a lesser extent H1-T6SS, but it repressed those belonging to the H3-T6SS subtype. H1 and H2 subtypes are known to act against other prokaryotes and eukaryotes, respectively^{249,251}. Little is known about the role and regulation of H3-T6SS in infection.

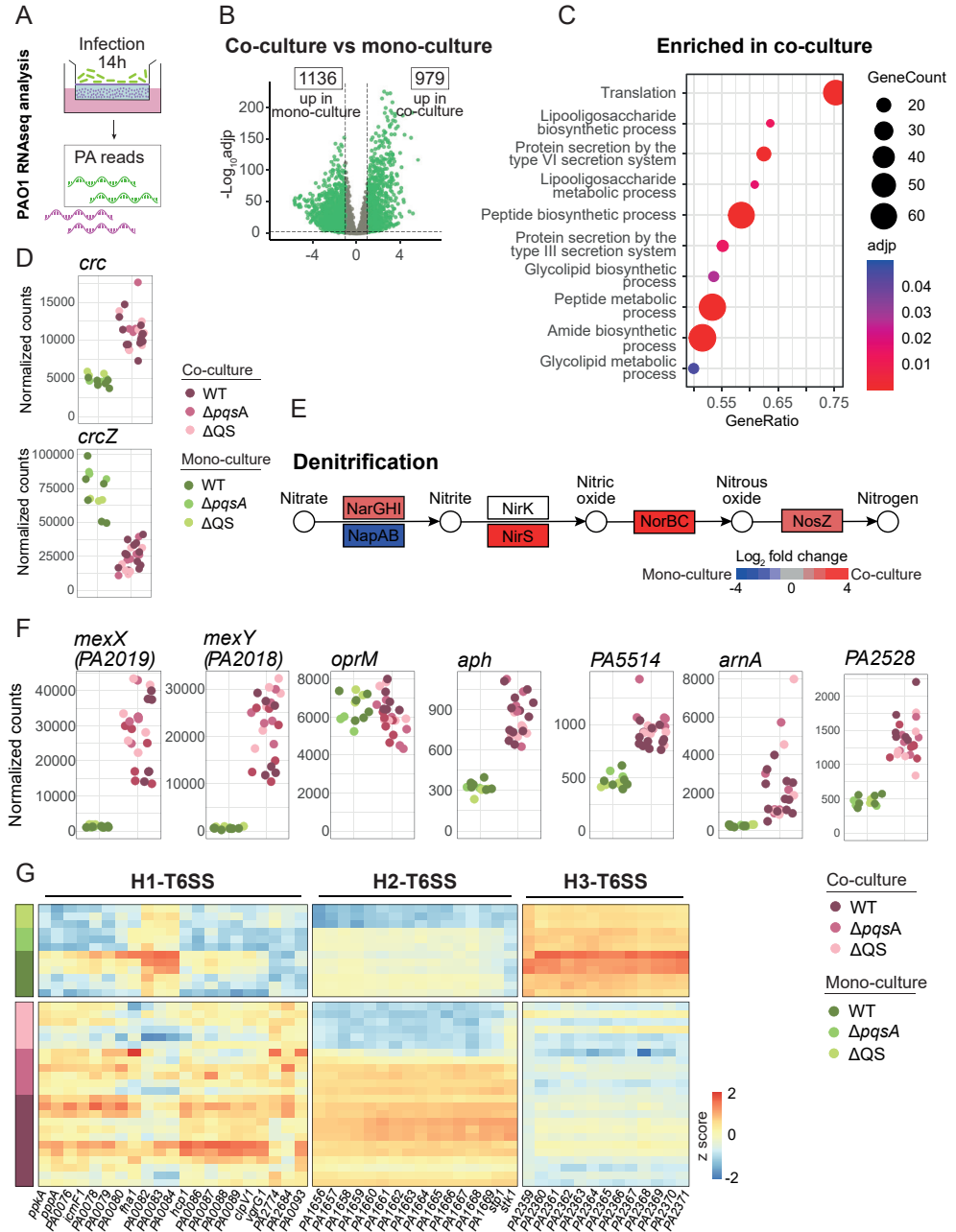


Figure 4. Transcriptional response of PAO1 to the presence of airway epithelium. **A)** Schematic representation of the analysis. **B)** Volcano plot displaying the \log_2 fold change and $-\log_{10}$ adjusted p-value of all genes, when comparing the PAO1 transcriptomes of co-culture and bacterial mono-culture samples. Green indicates differentially expressed genes (DEGs) (\log_2 fold change > 1 and adjusted p value < 0.05). The number of genes upregulated in co-culture and bacterial mono-culture is indicated. **C)** Gene ontology enrichment analysis showing top 10 categories enriched in PAO1 exposed to airway epithelium in co-culture. **D)** Normalized count plots of genes involved in CCR pathway, *crc* and *crcZ*. **E)** KEGG pathway pae00910 plot displaying the \log_2 fold change of genes involved in denitrification. DEGs from co-culture vs bacterial culture mono-culture comparison of PAO1 transcriptomes. **F)** Normalized count plots

The epithelium influences aspects of *P. aeruginosa* QS regulation

Next, we investigated how the presence of the epithelium affected QS-regulated processes in *P. aeruginosa* PAO1. Since only the dual RNA-seq run contained samples from all three bacterial conditions (WT, $\Delta pqsA$, and ΔQS), only samples from this run were included in the analysis to avoid batch-induced bias. In general, LasR- and RhIR-regulated genes and only some PQS-regulated genes were downregulated in PAO1 WT co-culture conditions compared to bacterial mono-cultures (Figure 5A). This correlates with previous descriptions of stronger QS-induced responses in pure bacterial cultures than in clinical infections⁹⁷⁻⁹⁹. Interestingly, the QS receptor levels (*mvfR*, *lasR* and *rhIR*) seemed to be more affected by ΔQS when the bacteria were co-cultured with the epithelium than in mono-culture. This could impact the QS regulatory network and therefore it is worth taking into consideration when interpreting results of QS regulation using *in vitro* models. Only 46 and 23 DEGs were found when comparing WT PAO1 with $\Delta pqsA$ in co-culture and in mono-culture respectively (Supplementary Figure 3A-B). From these, the *antABC* operon was affected only in mono-culture (Supplementary Figure 3C). This operon encodes the enzymes responsible for derivatizing the PqsA substrate anthranillic acid to catechol, before degradation to intermediates of the tricarboxylic acid (TCA) cycle²⁵². The loss of PqsA in the $\Delta pqsA$ strain could lead to an accumulation of anthranillic acid. Via upregulation of *antABC* in bacterial mono-cultures, anthranillic acid might be used as a nutrient.

In contrast, deletion of *rhII* and *lasI* in ΔQS led to 308 and 465 DEGs in co-culture and in mono-culture, respectively (Figure 5B). In order to dissect which QS-regulated processes were affected by the epithelium, we identified DEGs that occurred specifically in co-culture (52 up and 75 downregulated). Iron uptake pathways were downregulated only in ΔQS co-culture condition (Supplementary Figure 3D). This highlighted the differences of the two culture systems regarding iron utilization by the bacteria. On the other hand, genes involved in leucine and tyrosine catabolism were upregulated (Figure 5C-D). The amino acid utilization by *P. aeruginosa* is thought to be a key element of *P. aeruginosa* adaptation to the human airways, since amino acid auxotrophy is common in CF clinical isolates. This could explain why the QS effect is not observed in isolated bacterial cultures²⁵³. Furthermore, we found genes regulated by QS specifically in co-culture involved in bacterial adhesion and biofilm formation (*pprB*), and phosphatase and phosphodiesterase activities (*eddA*)^{146,254}. Additionally, a number of T2SS and T6SS related genes (Figure 5C-D) were specifically regulated by QS in co-culture. T2SS-related genes from WT PAO1 in co-culture showed slightly reduced levels compared to mono-culture. In contrast, QS mutants in co-culture showed a greatly reduced expression of T2SS-related genes. This suggested that the epithelium potentially inhibits T2SS, which can be counteracted by QS-regulated molecules in WT bacteria. The expression of T6SS-related genes was low in all PAO1 strains

Figure 4 legend (continued)

of genes involved in *P. aeruginosa* antibiotic resistance. **G**) Heat map displaying expression of genes involved in *P. aeruginosa* T6SS. Genes grouped by H1, H2 or H3 T6SS subtype^{249,250}. Samples grouped by culture condition. Color code indicates culture condition (Green: bacterial mono-culture; magenta: co-culture) and PAO1 genotype (Dark: WT; middle: $\Delta pqsA$; light: ΔQS).

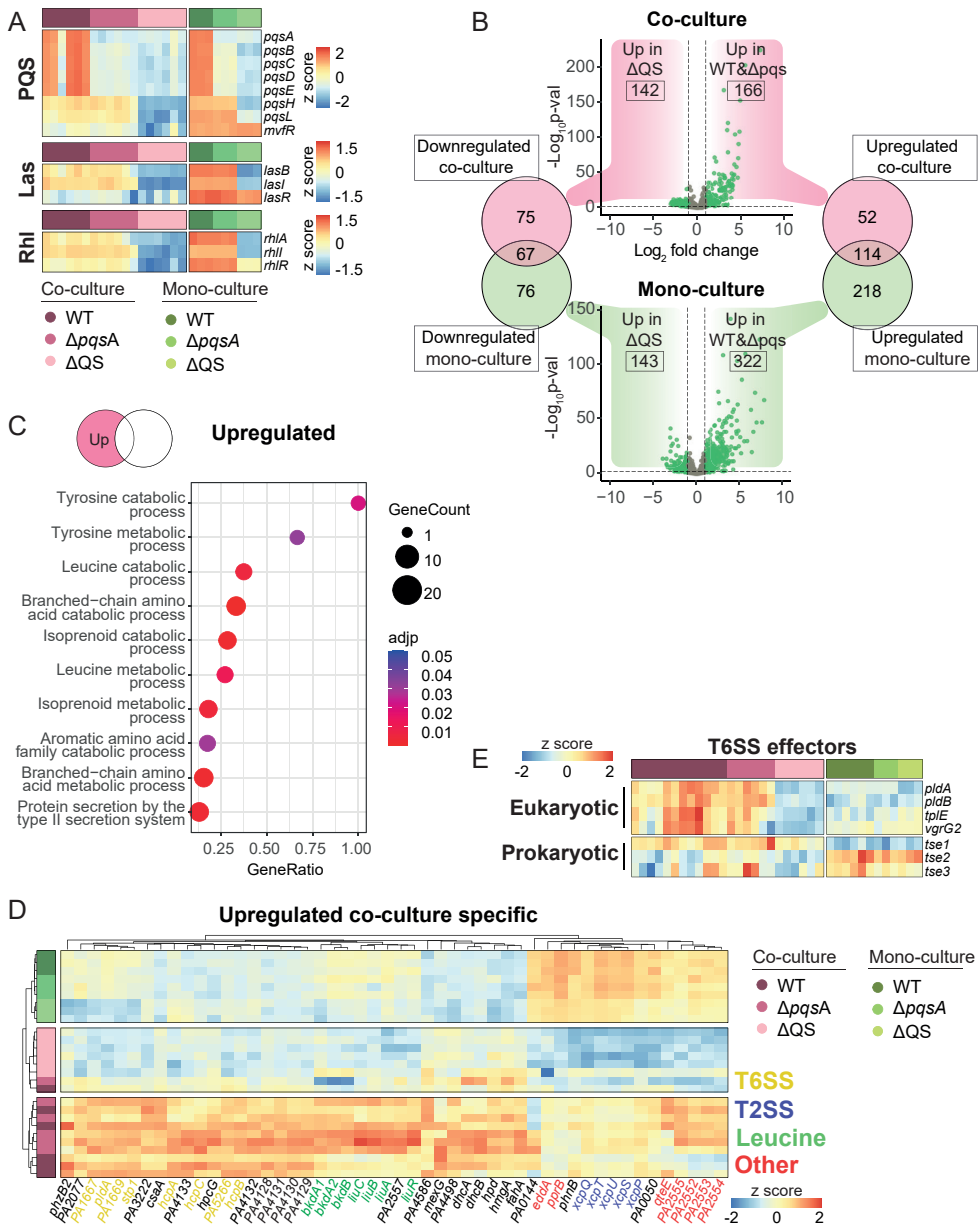


Figure 5. Epithelial effect on PAO1 QS regulation. **A)** Gene expression heat map of genes involved in Pqs, Las or Rhl QS pathways. **B)** Volcano plots displaying gene \log_2 fold change and $-\log_{10}$ adjusted p-value when comparing the transcriptomes of WT and $\Delta pqsA$ PAO1 to those of ΔQS in co-culture (top) and in pure bacterial cultures (bottom). Venn diagrams display the overlap between genes up (right) and downregulated (left) in the comparisons. **C)** Gene ontology enrichment analysis showing top 10 categories enriched in genes that are specifically upregulated in co-culture in WT and $\Delta pqsA$ PAO1 transcriptomes compared to ΔQS . **D)** Gene expression heat map showing top 50 co-culture-specific DEGs. Genes are color-coded according to the following categories (Yellow: T6SS; purple: T2SS; green: Leucine metabolism; red: other pathways). **E)** Gene expression heat map of T6SS eukaryotic and prokaryotic effectors. Sample color code indicates culture condition (Green: bacterial culture mono-culture; magenta: co-culture) and PAO1 genotype (Dark: WT; middle: $\Delta pqsA$; light: ΔQS).

in mono-culture. Co-culture conditions specifically showed a QS-regulatory effect on the expression of these genes. This suggested that a combination of epithelial and QS factors induce the expression of some T6SS genes. In addition, T6SS effectors that are involved in pathogenicity of eukaryotic cells were both induced by a combination of epithelial and QS signals (Figure 5E).

Benchmarking 2D co-culture model with chronic clinical samples

Next, we addressed which aspects from *in vivo* *P. aeruginosa* infections were recapitulated in our 2D co-culture model. We compared the transcriptional profiles of clinical *P. aeruginosa* strains directly isolated from airway biopsies from CF subjects to the PAO1 co-culture samples. Pure bacterial culture samples from this and other studies were included in the comparison^{97,99,255} (Supplementary Figure 4). After dataset integration, PCA analysis revealed that the origin of the bacterial samples (*in vivo*, co-culture, or mono-culture) explained the clustering of the samples best (Figure 6A). The comparison of the *in vivo* and co-culture transcriptomes to all mono-culture samples revealed a total of 1382 and 2045 DEGs, respectively (Figure 6B). Despite the fact that our co-culture represented an early stage of infection compared to the chronic state of the clinical samples, 269 genes were common between both comparisons (4.7% of all PAO1 genes) (Figure 6C-D). This core gene signature captured the aspects of an *in vivo* infection present in our co-culture model. In order to understand pathways enriched in this core gene signature, we performed protein-protein interaction network analysis (Figure 6E). This confirmed that denitrification is an important process for *P. aeruginosa* infection and that this was captured by our model (Figure 6E-F, Figure 4E and Supplementary Figure 5). Increased expression of *mexYX* antibiotic efflux pump (Figure 6E-F, Figure 4F, Supplementary Figure 5) was also confirmed *in vivo*. Additionally, the expression of some T2SS proteins (Figure 6E-F, Supplementary Figure 5) was reduced in the core signature compared to *in vitro* cultures, which is in line with our previous analysis (Figure 5D).

Beyond confirming the relevance of some of the pathways previously discovered by our cohort, the comparative analysis (Figure 6) uncovered other processes relevant for *in vivo* infection. This included elevated levels of choline/betaine metabolic genes (*betAB1*), responsible for the production of glycine-betaine (GB) (Figure 6E-F, Supplementary Figure 5). The accumulation of GB has been proposed as a bacterial osmo-protective mechanism⁹⁹, and to be important in *P. aeruginosa* infection in mice²⁵⁶. Additionally, our 2D co-culture model captured the reduced levels of motility- and chemotaxis-related genes that are observed *in vivo* compared to pure bacterial cultures (Figure 6E-F, Supplementary Figure 5), which is another important aspect for biofilm formation.

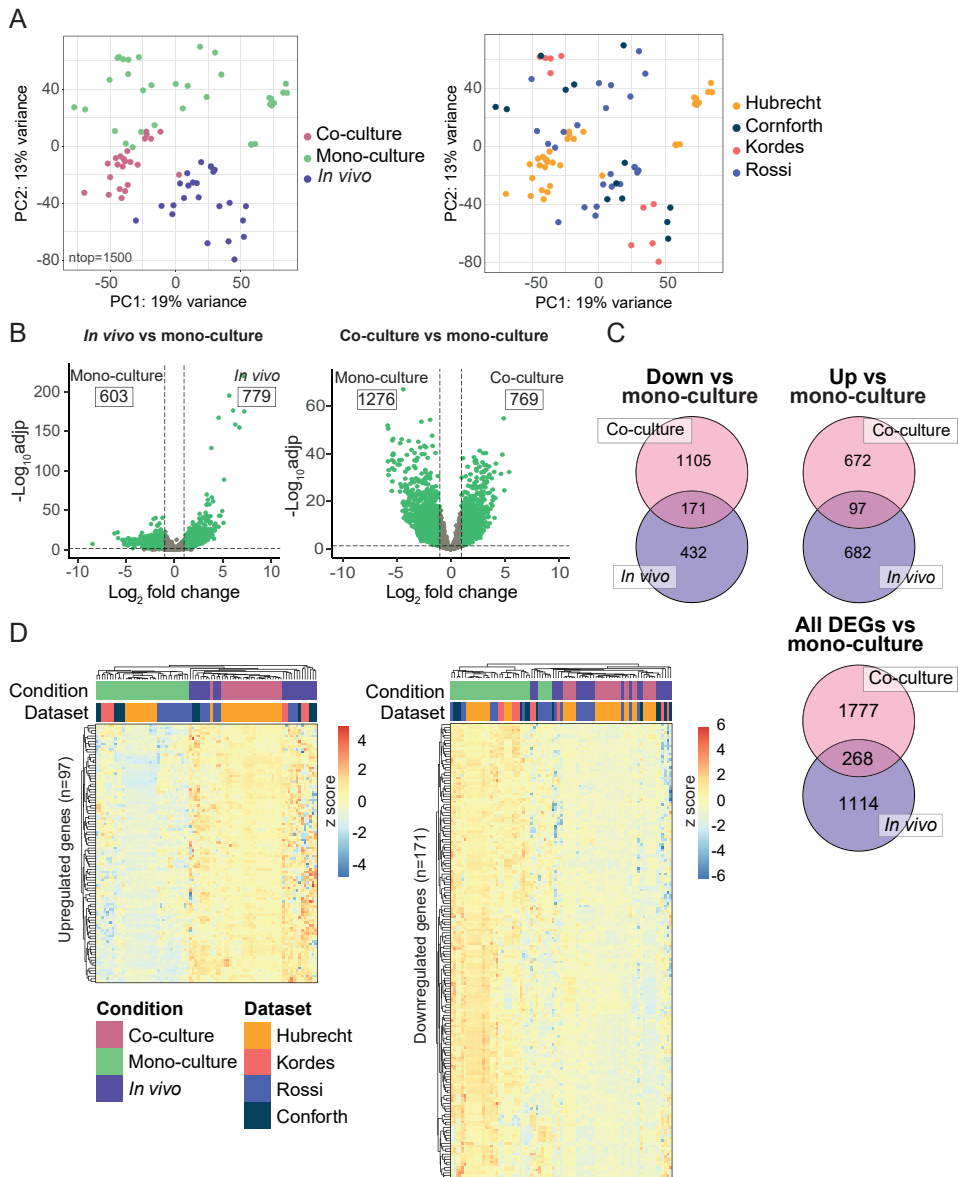


Figure 6. Benchmarking co-culture model with *in vivo* *P. aeruginosa* transcriptomic datasets directly isolated from the airways of CF subjects. **A)** PCA plots showing sample distribution by condition (Magenta: co-culture; green: bacterial culture in isolates; purple: *in vivo*) or by study of origin (Orange: this study; purple: Cornforth *et al.*, 2018⁹⁷; pink: Kordes *et al.*, 2019²⁵⁵; blue: Rossi *et al.*, 2018⁹⁹). **B)** Volcano plots displaying gene \log_2 fold change and $-\log_{10}$ adjusted p-value comparing transcriptomes of *in vivo* *P. aeruginosa* (left) or co-cultured PAO1 (right) to those of all pure bacterial culture samples. Green indicates differentially expressed genes (DEGs) (\log_2 fold change > 1 and adjusted p value < 0.05). Indicated in the boxes the number of up- or downregulated DEGs. **C)** Venn diagrams displaying the overlap between genes that are upregulated (left), downregulated (middle), or both (right) in the previous *in vivo* and co-culture comparison to *in vitro* and mono-culture samples (B). **D)** Expression heat map displaying the common up-(left) and downregulated (right) genes. Samples clustered based on the expression of all genes plotted per heat map. Color-code indicates condition (Magenta: co-culture; green: pure bacteria; purple: *in vivo*) and study of origin (Orange: this study; purple: Cornforth *et al.*, 2018; pink: Kordes *et al.*, 2019; blue: Rossi *et*

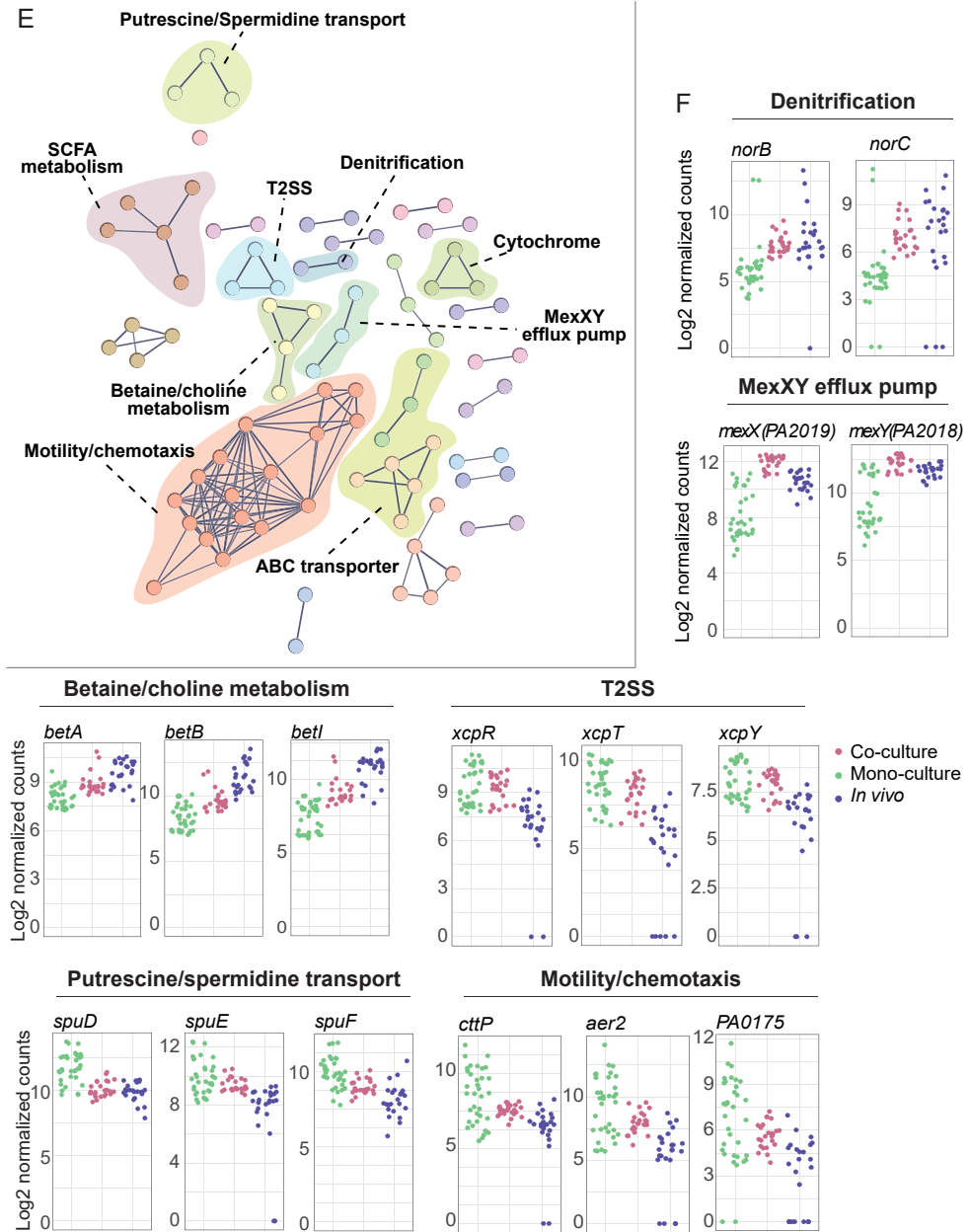


Figure 6 legend (continued)

al., 2018). **E**) Protein-protein interaction network of common DEGs (in vivo and co-culture. Each node represents a protein encoded by a DEG. Edges represent known protein-protein association (either physical or functional) with a confidence level higher than 0.7. Node color represent clusters generated MCL method. Highlighted pathway to which the cluster proteins belong. **F**) Log₂ normalized count plots of representative genes from pathways highlighted by the network analysis. Color-code indicates Magenta: co-culture, green: pure bacteria and purple: *in vivo*.

Discussion

In this study, we describe a novel *P. aeruginosa* co-culture system using 2D human airway organoids derived from healthy and CF individuals. Subjecting the co-culture to dual RNA-seq allowed us to gain insight into how both components interact with, and respond to each other, focusing on the role of QS molecules and downstream signaling. Finally, we benchmarked our findings with a cohort of publicly available RNA-seq datasets from clinical samples of *P. aeruginosa* infected airways. Our co-culture model recapitulates metabolic aspects, CCR and nitrogen usage, as well as the expression of several secretion systems, important for *P. aeruginosa* persistence and virulence. Furthermore, the upregulation of genes involved in *P. aeruginosa* antibiotic resistance could be of particular relevance for research of bacterial mechanisms of antibiotic resistance and discovery of novel antibacterial compounds. This is highly relevant in the case of *P. aeruginosa* due to its high intrinsic resistance²⁶. Since it is not possible to study early stages of infection using clinical isolates, our model offers a tool to understand the initial steps of the infectious process in near-physiological conditions.

Previous attempts to co-culture *P. aeruginosa* in 2D have been performed using cancer cell lines^{217–221,257,258} or primary human airway cultures^{219,222}. The latter offers clear advantages over the former, because of the non-cancerous nature of the primary cultures. Human airway organoids allow for the indefinite biomass expansion and thus for longitudinal experiments using a defined and constant organoid source. Additionally, the indefinite expansion of airway organoids will enable *P. aeruginosa* co-culture with genetically engineered organoid lines and isogenic WT controls, once genome editing of airway organoids becomes efficient enough to perform experiments at this scale²⁵⁹. This will open the door to understanding which epithelial factors shape the course of *P. aeruginosa* infection and how to harness them to fight the infection.

In this dataset, we do not observe a major organoid response specific to QS pathways. Using live co-cultures could lead to lower effective concentrations of QS-induced molecules, compared to what has been used in studies testing the effect of single QS compounds on epithelial cells^{260,261}. In addition, the strong LPS-induced inflammation, present in all conditions, might abrogate the effect of QS-derived molecules. Particularly, LPS is not accounted for in studies that solely focus on QS-derived molecules. Additionally, it is likely that only specific cell types respond to QS molecules, i.e. chemosensory tuft cells^{262,263}, and therefore bulk RNAseq would not allow the study of these cell-specific effects.

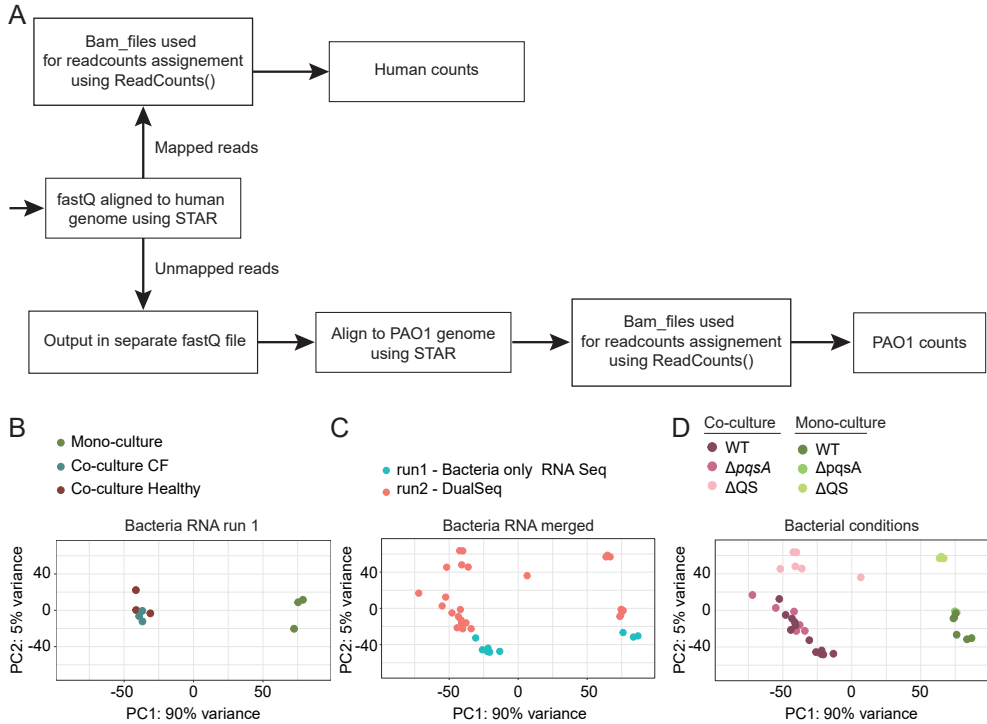
Future expansion of the co-culture infection models, with the addition of immune cells, will yield insight into how this important aspect affects the behavior of the *P. aeruginosa* infections. Importantly, co-culture models that recapitulate a more complex tissue architecture²⁶⁴ will also help to understand biofilm formation under more physiological conditions. Furthermore, QS pathways coordinate the population-scale behavior of individual bacteria, which leads to the functional and spatial heterogeneity found in bacterial biofilms.

The recent application of spatial transcriptomics to *P. aeruginosa* biofilms grown on solid surfaces have allowed detailed study of these two aspects^{265,266}. It will be very interesting to address this spatial and functional heterogeneity in the presence of the epithelial and immune cells using co-cultures. Furthermore, our 14-hour co-culture system represents an early stage of the infectious process. While this time span allows studying QS regulation, it is too short to focus on biofilm development and other aspects of chronic infections. Longer incubation using our method was technically challenging due epithelial damage caused by the bacterial cells. Developing co-culture strategies that enable sustained chronic infection of the mucosa will help to investigate these aspects of later infection stages.

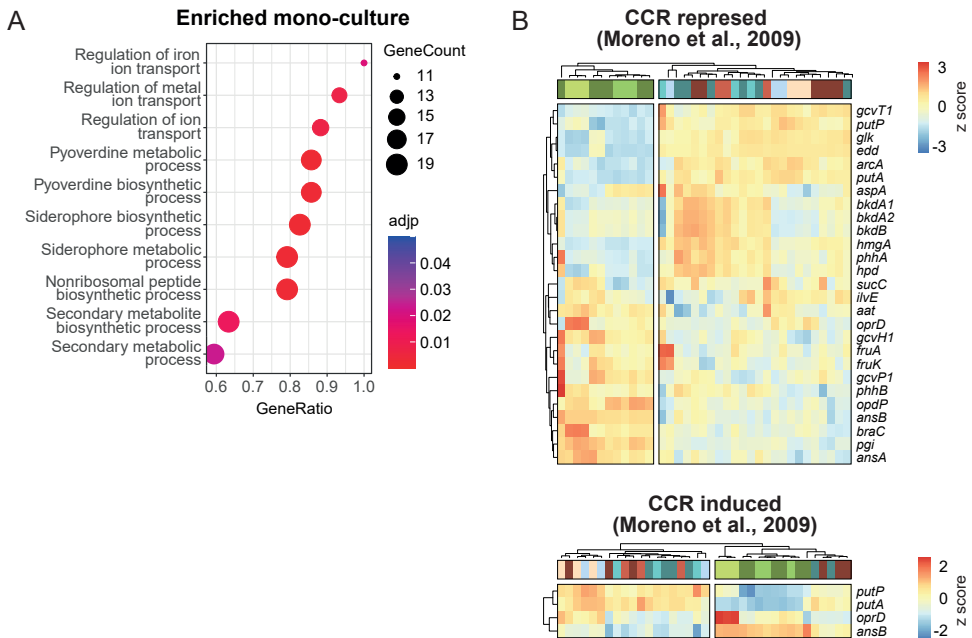
In conclusion, 2D organoid co-cultures with *P. aeruginosa* represent a new development of the current methods to study host-bacterium interplay. The system recapitulates major infection traits from both bacteria and epithelium, including bacterial metabolism, expression of virulence factors and the induction of an inflammatory response in the epithelium.

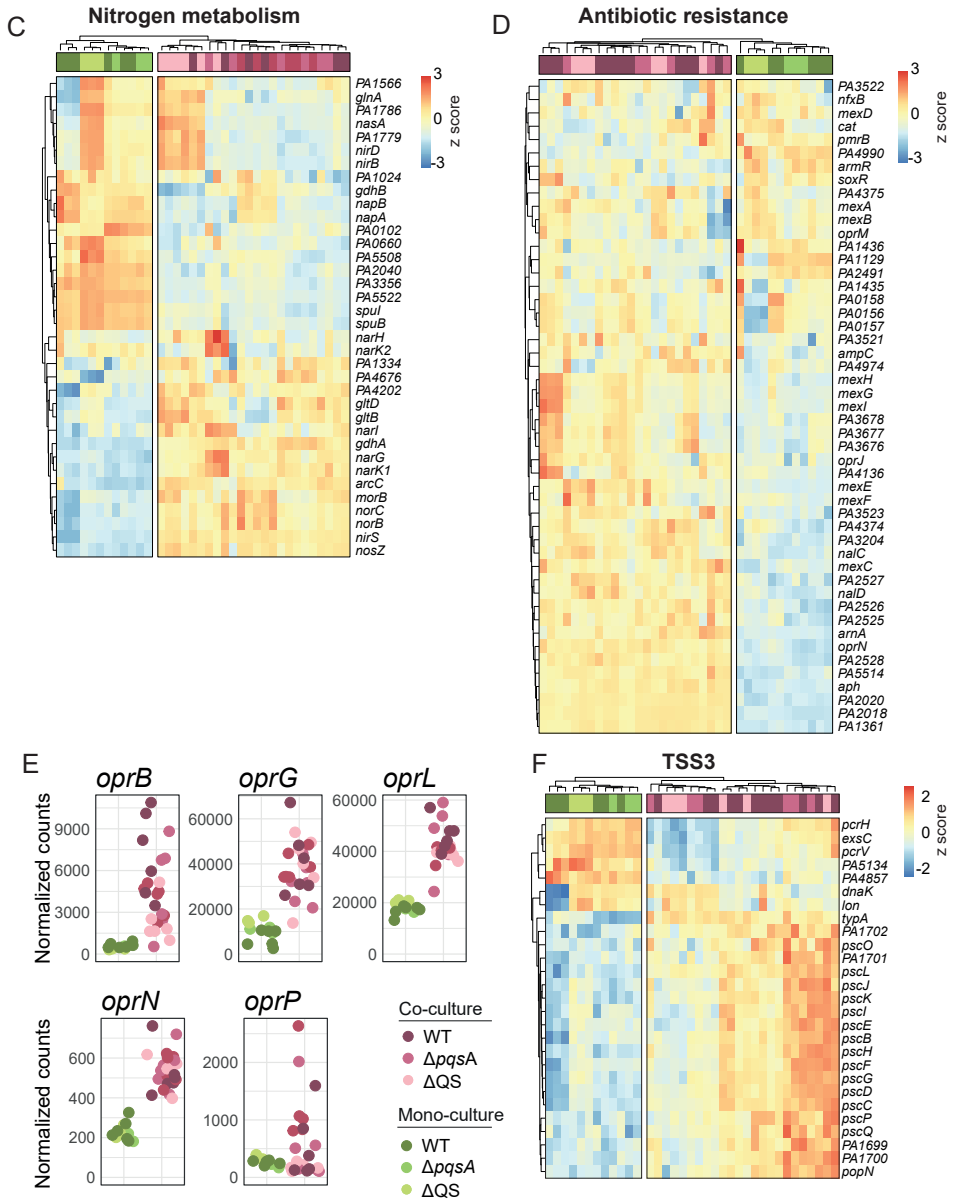
Acknowledgements

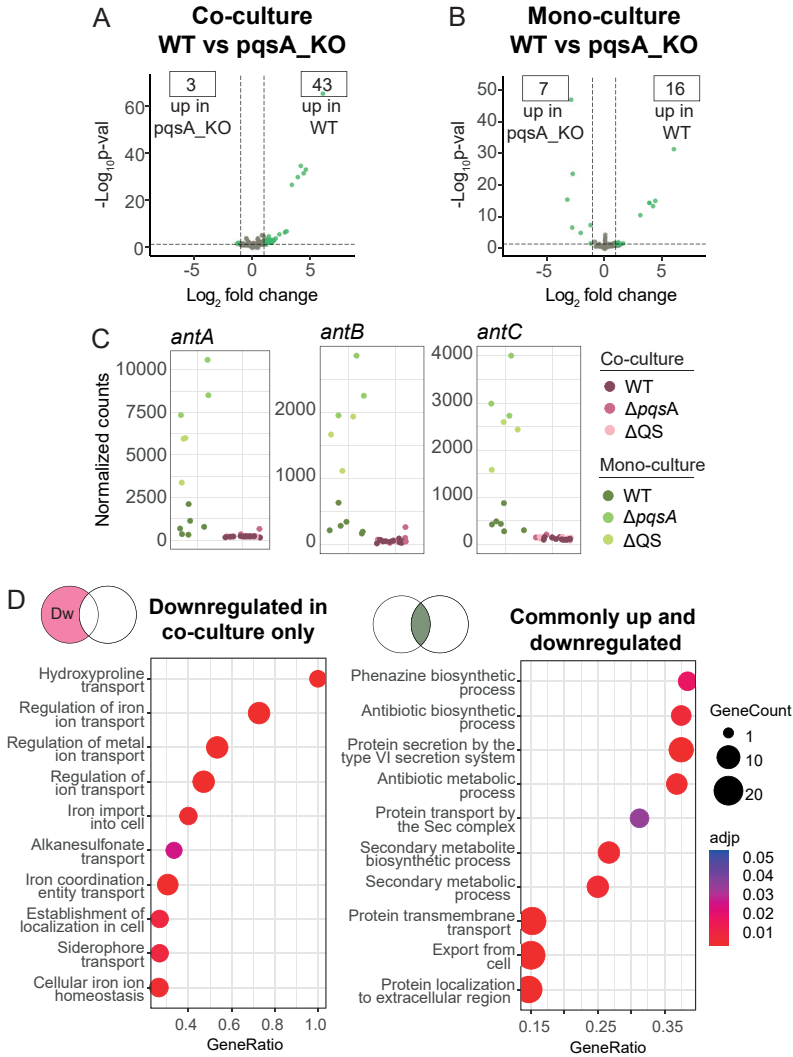
We acknowledge the Utrecht Sequencing Facility (USEQ) for providing sequencing service and data. USEQ is subsidized by the University Medical Center Utrecht and The Netherlands X-omics Initiative (NWO project 184.034.019). We would also like to thank Dr. Tim Holm Jakobsen for kindly providing PAO1-GFP strain, Dr. Bart Bardoel for kindly providing *E. coli* RHO3 strain, and Joe J. Harrison for kindly providing the pEX18Gm plasmid.



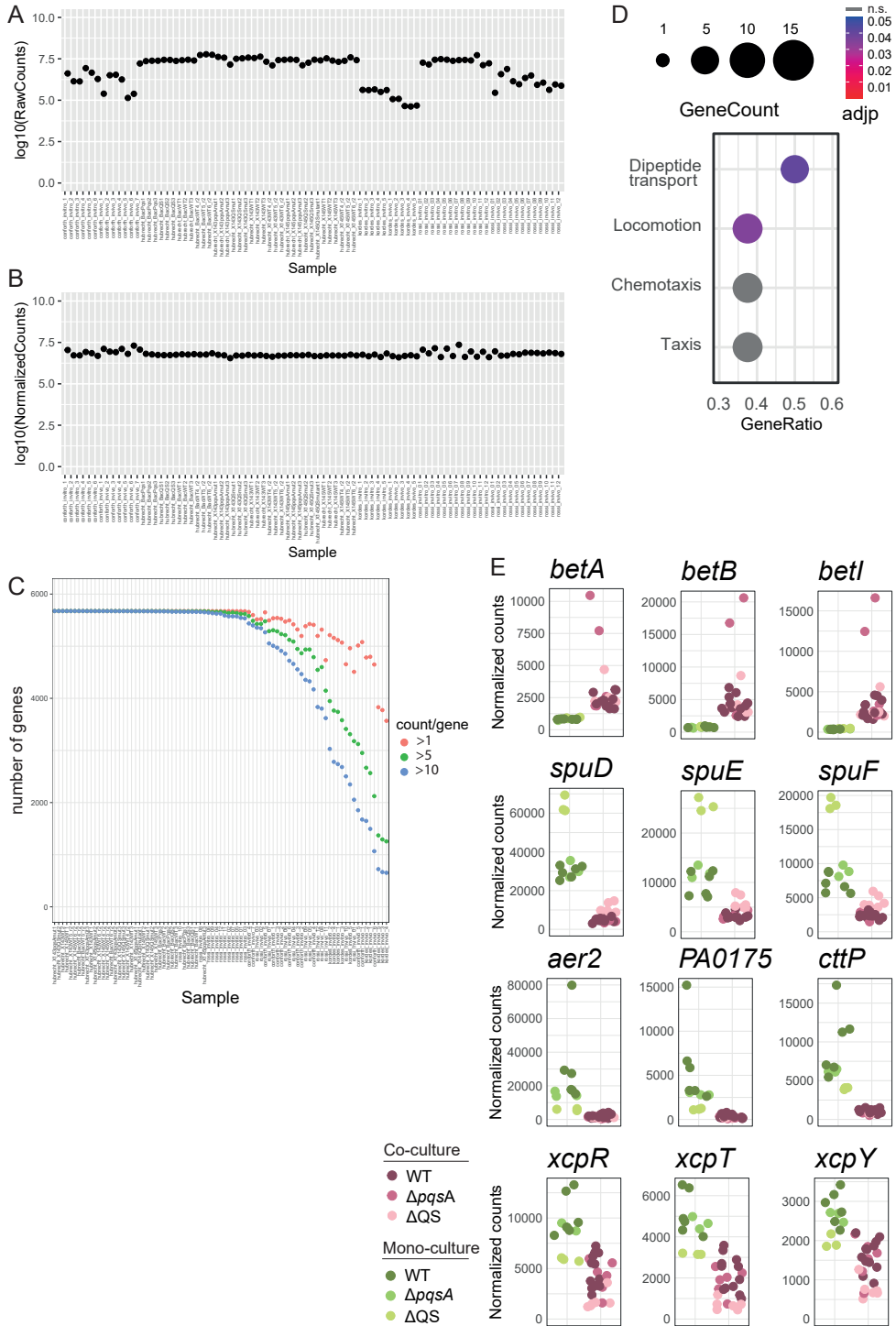
Supplementary figure 1. Mapping strategy and PAO1 bulk dataset integration. A) Mapping and count assignment strategy. **B)** PCA plot of PAO1-only bulk RNA samples from run 1. **C)** PCA plot showing samples by run (PAO1-only bulk RNA-seq or Dual RNA-seq). **D)** PCA plot of the integrated dataset color-coded by culture type and PAO1 genotype.







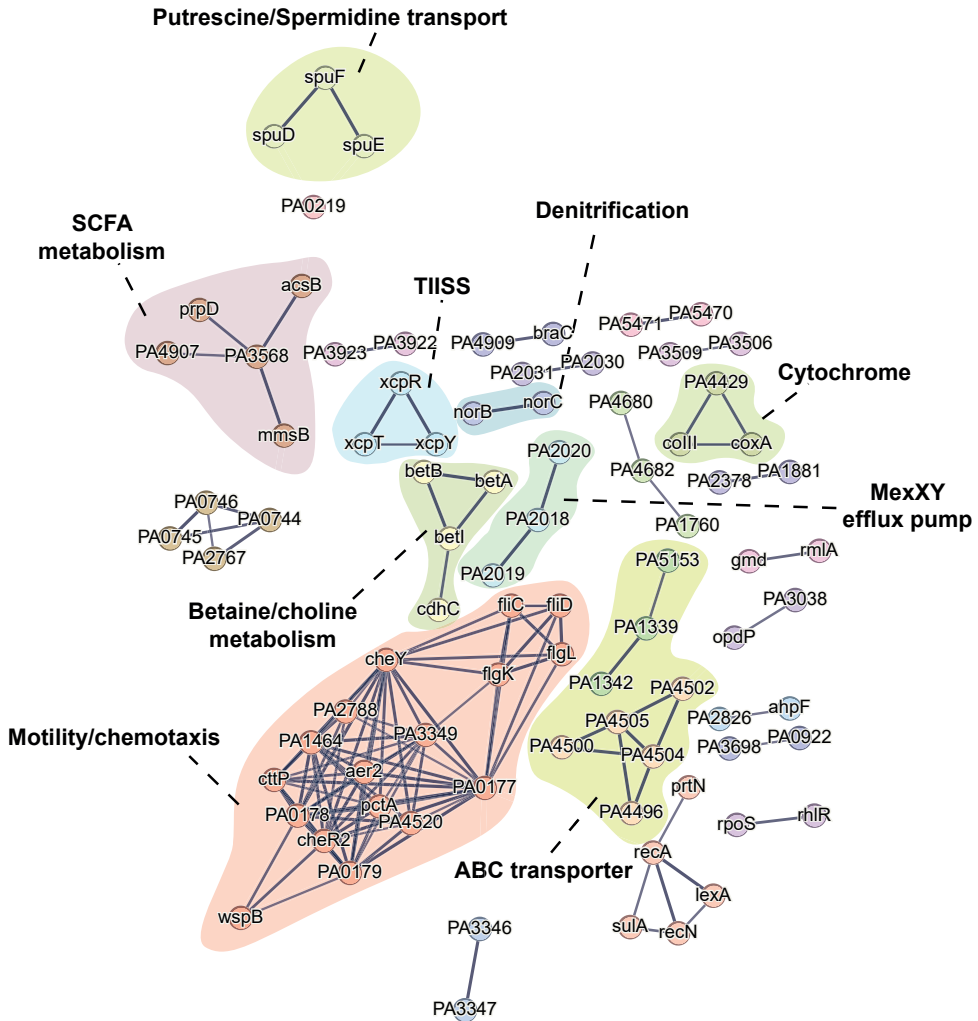
Supplementary figure 3. Extended effects of the epithelium on PAO1 QS regulation. **A)** Volcano plot displaying gene \log_2 fold change and $-\log_{10}$ adjusted p-value when comparing the transcriptomes of WT to $\Delta pqsA$ PAO1 in co-culture. **B)** Volcano plot displaying gene \log_2 fold change and $-\log_{10}$ adjusted p-value when comparing the transcriptomes of WT to $\Delta pqsA$ PAO1 in mono-culture. **C)** Normalized count plots of genes from the anthranilic acid metabolic pathway. **D)** Gene ontology enrichment analysis showing top 10 categories enriched in genes that are specifically downregulated in co-culture in WT and $\Delta pqsA$ PAO1 transcriptomes compared to ΔQS (left) or those that are common to both (right, up and downregulated).



Supplementary figure 4 Cohort integration quality control. A) Log₁₀ of total raw counts per sample before DESeq2

Supplementary Figure 4 legend (continued)

normalization. **B)** Log_{10} of normalized counts per sample after DESeq2 normalization. **C)** Number of genes with more than 1 (red), 5 (green) or 10 (blue) counts per sample. **D)** Gene ontology enrichment analysis showing categories enriched in top common DEGs from co-culture and *in vivo* samples. **E)** Normalized count plots of genes from Figure 6F, performing the analysis only in the samples from our cohort, to exclude bias in the results due to the integration process with the extra datasets.



Supplementary figure 5. Extended protein-protein network results. Protein-protein interaction network of common DEGs (in vivo and co-culture). Each node represents a protein encoded by DEG. Individual gene names are highlighted over the nodes. Edges represent known protein-protein association (either physical or functional) with a confidence level higher than 0.7. Node color represent clusters generated MCL method. Highlighted the pathway to which the cluster proteins belong.

Supplementary Table 1 | Primers used in this study

Primer name	Primer sequence
<i>lasI</i> .UP.Fw	GCCAGTGCCAAGCTTGCATGCGAGGCCAACCGTTTCATG
<i>lasI</i> .UP.Rv	GCTGTTCCACCAGTACGATCATCTTCACTTCCTCCAA
<i>lasI</i> .DN.Fw	GAAGATGATCGTACTGGTGGAAACAGCGACTGG
<i>lasI</i> .DN.Rv	CATGATTACGAATTCGAGCTTTCCTGCCCTGGATAGAAC
<i>lasI</i> .seq.Fw	GCTCGGAAGCCAATGTGAACTT
<i>lasI</i> .seq.Rv	AACTGGAACGCCTCAGCCAG
<i>rhII</i> .UP.Fw	CATGATTACGAATTCGAGCTCGACCAGCAGAACATCTC
<i>rhII</i> .UP.Rv	TGAAGCTAATTCGATCATGCATGAGCTCCAGCGATTACAGAGAGCAA
<i>rhII</i> .DN.Fw	ATCCCAATTCGATCGTCCGGCTACCACCCGGAATGGCT
<i>rhII</i> .DN.Rv	GCCAGTGCCAAGCTTGCATGCCAGGTTGATCGAGATGC
<i>rhII</i> .seq.Fw	ATGTCCTCCGACTGAGAGGG
<i>rhII</i> .seq.Rv	CAGAGAGACTACGCAAGTCGG

Supplementary Table 2 | Plasmids used in this study

Plasmid	Use	Reference
pEX18Gm	Backbone plasmid used for the generation of deletion constructs	Hmelo <i>et al.</i> (2015) ¹⁵⁸
pEX18Gm:: <i>ΔlasI</i>	Plasmid containing <i>lasI</i> deletion construct for use in PAO1	This study
pEX18Gm:: <i>ΔrhII</i>	Plasmid containing <i>rhII</i> deletion construct for use in PAO1	This study



Chapter 5

Pseudomonas aeruginosa quorum sensing related molecules affect the airway epithelial immune response

Wouter A. G. Beenker[#], Cayetano Pleguezuelos-Manzano[#], Hans Clevers, Jeroen den Hertog

[#]Authors contributed equally

Abstract

Bacteria regulate gene expression based upon their cell density, via a process called quorum sensing (QS). The opportunistic Gram-negative bacterium *P. aeruginosa* regulates the production of toxic virulence factors via QS. Various studies have shown that eukaryotic host cells are able to sense QS-induced molecules. In this study, we investigated the effect of *P. aeruginosa* QS-regulated molecules on airway epithelial cells using 2D organoids and RNA-sequencing. We show that QS contributes to the toxicity of PAO1 supernatant and leads to an immunomodulatory response. By testing single QS-regulated compounds, including various phenazines and *Pseudomonas* quinolone signal (PQS), we suggest this response is mostly caused by the effect of 1-phenazinecarboxylic acid and pyocyanin. Treatment with these phenazines led to a significant change in the immunomodulatory response making this an interesting target for future investigations. This explorative research shows the potential of using organoids and bacterial extracts to study the response in human cells.

Keywords: *Pseudomonas aeruginosa*, Airway organoids, Quorum sensing, phenazines, Immune system

Introduction

Cell density regulates bacterial gene expression via a process called quorum sensing (QS). Across Gram-negative bacteria, the QS systems show high similarity: it involves a LuxI-type synthase that produces *N*-acylhomoserine lactones (AHLs), which cross the cell membrane and bind to their cognate LuxR-type receptor. The LuxR-type receptor is a transcription factor that binds to the promoters of QS-regulated genes. This way, when the number of bacterial cells is high, the concentration of AHLs increases and the LuxR receptor is activated, resulting in altered gene expression^{59,106,152}.

In the opportunistic Gram-negative pathogen, *Pseudomonas aeruginosa*, there are three QS pathways, two of which depend on AHLs and one that is unique: the *las*-encoded pathway produces the AHL, 3-oxo-C12-HSL, and the *rhl*-encoded pathway produces the AHL, C4-HSL. The *Pseudomonas* quinolone signal (PQS) pathway is independent of AHLs, and involves the *pqsABCDE* and *pqsH* genes, which mediate production of 4-hydroxy-2-heptylquinoline (HHQ) and PQS, which both bind to the PqsR (also known as MvfR) receptor^{68,69}. Downstream pathways of QS in *P. aeruginosa* involve virulence factor production, including proteases⁷², elastases²⁶⁷, phenazines¹⁰⁹ and rhamnolipids¹¹⁰, which are detrimental to host cells⁶⁰. *P. aeruginosa* strains with reduced or inactive QS systems show reduced tissue damage of the host, increased clearance of bacteria, and improved survival in animal models^{77,85–87,89}.

Besides altering bacterial processes, QS-regulated compounds, including PQS and phenazines, may influence gene regulation in host cells as well^{268–271}. Next to its role in QS, PQS may have a direct effect on the host by inducing oxidative stress and modulating the immune response^{268,272}. Phenazines act downstream of QS and act as major virulence factors during *P. aeruginosa* infections. Toxic effects of phenazines have been demonstrated in various model systems^{183,186–188}. The effects of phenazines on host cells are mostly attributed to their oxidative activity by affecting electron transport, cellular respiration, and energy metabolism. In addition, they also act as pro-inflammatory compounds^{184,186}. Recently, Moura-Alves and colleagues described the aryl hydrocarbon receptor (AhR) to recognize phenazines and subsequently modulate the immune response^{260,261}.

In chapter 4, we described a limited role of QS during infection. However, this limited role could be due to the relatively short time of co-incubation. In addition, the strong host response to lipopolysaccharides (LPS) might have overruled the effects of QS-derived molecules. Testing cell-free extracts of cultured *P. aeruginosa* PAO1 WT and Δ QS bacteria may facilitate to prolong incubation times and study the specific response to QS-regulated metabolites without LPS interference.

In this chapter, we investigated the response of airway epithelium specifically to QS-derived compounds. For this, we used 2D upper airway (nasal) organoids. These airway organoids closely mimic the physiology and cellular composition of the airways, making them a suitable model to study the infection site of *P. aeruginosa*²²⁴. Using RNA-sequencing,

we analyzed the transcriptional response after treatment with PAO1 WT supernatant extract and mutant PAO1 cells lacking QS. We also examined the effect of various phenazines and PQS to learn more about their effect on airway epithelium. Our results reveal a QS-induced effect on the immune response with increased levels of *IL33* and decreased levels of *IL1R1*. This preliminary study provides interesting insights that warrant future studies.

Materials and methods

Supernatant extraction

For this study, we used *P. aeruginosa* PAO1 strain that expresses GFP¹⁹⁴. In addition, we used the PAO1 $\Delta lasI/\Delta rhII$ (ΔQS) strain (as described in chapter 4). PAO1 strains were stored at -80 °C in a 20 % glycerol stock solution. A single colony of PAO1 was plated on Luria agar (LA) plates, before inoculation in Luria broth (LB) at 37 °C O/N. Next day, the cultures were diluted 1000 x in 400 mL LB in plastic Erlenmeyer flasks and grown for 14 h at 37 °C. Erlenmeyer flasks with sterile LB were used as control. Subsequently, the bacteria were pelleted by centrifugation at 11,000 rpm for 10 min before filter-sterilizing using a 0.22 μm Millipore filter (Merck, Amsterdam, The Netherlands). The sterile supernatant and LB control was extracted 2 x with 0.5 volume of acidified ethyl acetate (containing 0.5 % acetic acid (v:v)) and dried using a rotary evaporator with a water bath at 40 °C. The dried pellet was dissolved in DMSO, creating a 500 x concentrated stock. The stock was aliquoted and stored at -80 °C to prevent degradation.

Analysis secondary metabolites

Extracts were analyzed using an analytical HPLC Shimadzu LC-2030C system with PDA detection (190-800 nm) with a Dr. Maisch Reprosil-PUR 120 C18 AQ column (3 μm , 120 \AA , 4.6x100 mm). The mobile phase consisted of 100 % MQ with 0.1 % trifluoroacetic acid (Buffer A) and 100 % acetonitrile with 0.1 % trifluoroacetic acid (Buffer B). Protocol consisted of a linear gradient from 5 % to 95 % buffer B for 10 min, followed by 2.5 min of 95 % buffer B before returning to 5 % buffer B with a constant flow rate of 1 mL/min.

For the quantification of 4-hydroxy-2-heptylquinoline (HHQ) (Sigma-Aldrich, Merck Life Science, Amsterdam, The Netherlands) and 1-phenazinecarboxylic acid (PCA) (Caymen Chemicals), commercially available compounds were used to make calibration curves to quantify the concentrations in supernatant extract.

Organoid culture

Nasal brushing-derived epithelial stem cells were collected and stored with informed consent of all donor and was approved by a specific ethical board for the use of biobanked materials TcBIO (Toetsingscommissie Biobanks), an institutional Medical Research Ethics Committee of the University Medical Center Utrecht (protocol ID: 16/586). Nasal epithelial stem cells were isolated and expanded in 2D cell cultures as previously described²²⁵. After

initial expansion, nasal cells were grown as organoids and cultured as previously described²²⁴. In brief, the organoids were grown in Advanced DMEM F12 expansion medium containing 1X GlutaMax (Life Technologies; 12634-034), 10 mM HEPES (Life Technologies; 15630-056) (AdvDMEMF12++), supplemented with penicillin and streptomycin (10,000 IU/mL each; Life Technologies; 15140-122), 1× B27 supplement (Life Technologies; 17504-044), 1.25 mM N-acetyl-l-cysteine (Sigma-Aldrich; A9165), 10 mM nicotinamide (Sigma-Aldrich; N0636), 500 nM A83-01 (Tocris; 2939), 5 μM Y-27632 (Abmole; Y-27632), 1 μM SB202190 (Sigma-Aldrich; S7067), 100 ng/mL human FGF10 (PeproTech; 100-26), 25 ng/mL FGF7 (PeproTech; 100-19), 1 % (vol/vol) RSP03, and Noggin (produced via the r-PEX protein expression platform at U-Protein Express BV). For passage, the organoids were collected, washed, and resuspended in TrypLE (Gibco), before incubation at 37 °C for 15 min. Next, organoids were disrupted mechanically into single cells and seeded in droplets of Cultrex growth factor reduced BME type 2 (Biotechne | R&D systems 3533-010-02). For the 2D differentiation of the airway organoids, 10⁵ cells were seeded on 24-well polystyrene membranes (Greiner Bio-One). These cells were cultured in expansion medium (both top and bottom compartments) until confluency. Next, the cells were differentiated in air liquid interface, for 1 month, using PneumaCult™-ALI Medium (Stem cell technologies) supplemented with Hydrocortisone stock solution (5 μL/mL; Stem cell technologies #07925) and Heparin solution (2 μL/mL; Stem cell technologies #07980). For the treatment of the organoids, 1.6 x diluted bacterial extract or 50 μM of compound was added to the organoids and incubated for 24 hours. DMSO and LB extracts were used as negative controls. Experiments were done in triplicates.

RNA isolation organoid cultures

After treatment for 24 h, RNA was isolated from organoid cultures using RNeasy kits (Qiagen), following manufacturer's protocol. RNA was dissolved in MQ and stored at -80 °C to prevent degradation until further use. For RNA-sequencing, RNA libraries were validated with the Agilent 2100 bioanalyzer following manufacturer's protocol. Samples were sent for sequencing to the Utrecht Sequencing Facility (Useq). Library preparation was done with TruSeq Stranded mRNA polyA kit. RNAseq was performed using the NextSeq2000 platform.

Organoid viability test

After treatment for 24 h, viability was measured using CellTiter-Glo® 3D Cell Viability Assay (Promega #G9681). In short, the culture was equilibrated at room temperature for 30 min. The supernatant extract was removed and 100 μL of PBS was added. Next, 100 μL of CellTiter-Glo® 3D Reagent was added. The solution was resuspended thoroughly and placed on a shaker for 15 min at room temperature. Thorough resuspension was repeated and samples were incubated extra 15 min in the dark. Luminescence was measured immediately using Tecan spark illuminometer.

RNA isolation bacterial cultures

For RNA isolation, 200 μL of bacterial culture was used, added to 400 μL RNA

stabilizing solution (3.5 M ammonium sulfate, 16.67 mM sodium citrate, 13.3 mM EDTA, in MQ, pH = 5.2) and incubated at room temperature for 5 min. Bacterial cells were pelleted by centrifugation for 2 min at 16,000 rpm at 4 °C, before aspirating the supernatant and snapfreezing the cells.

RNA was isolated using the MasterPure Complete DNA and RNA Purification Kit (Immunosource, Belgium) following manufacturer's protocol. To make sure all gDNA was removed, 2 additional rounds of DNase treatment were performed using TURBO DNase (ThermoFisher Scientific) following manufacturer's protocol. To inactivate the DNase, the RNA was purified again, dissolved in MQ, and stored at -80 °C until further use.

Bacterial growth curves

To compare the growth of the two bacterial strains, the bacteria were grown on LA plates and a single colony was grown overnight in LB medium. The following day, the bacteria were diluted 1000 x in LB medium and 100 µL of bacterial solution was added to a 96-wells plate, covered with Breathe-Easy seal (Sigma-Aldrich, Merck, Life Science, Amsterdam, The Netherlands) to prevent evaporation. Bacterial growth (OD₅₉₅) was measured every 15 min using a Multiskan FC microplate photometer (ThermoFisher Scientific) with incubation temperature at 37 °C.

Quantitative RT-PCR

cDNA was made from similar quantities of RNA using Superscript III reverse transcriptase following manufacturer's protocol (ThermoFisher Scientific). cDNA was added to a mix containing FastStart Universal SYBR Green master mix (Roche, Sigma-Aldrich, Merck Life Science, Amsterdam, The Netherlands) and desired primers (Table 1). The signal was measured using a Biorad CFX RealTime system. Reaction mixtures were incubated for 10 min at 95 °C, followed by 42 cycles of product amplification (58 °C for 30 s, 95 °C for 15 s). For each condition, three samples were used in duplicates. Melting curve analysis was performed to verify specificity of the primers. Relative expression levels were quantified using the 2^{-ΔΔCt} method using *rpoD* as housekeeping gene.

Table 1 | Primers used in this study

Primer name	Primer sequence
<i>lasB</i> .Fw	ACCGTGCGTTCTACCTGTTG
<i>lasB</i> .Rv	CGGTCCAGTAGTAGCGGTTG
<i>rhlA</i> .Fw	CCTGGCCGAACATTCAACG
<i>rhlA</i> .Rv	AGGTGATTGACCTCGAAGCG
<i>pqsA</i> .Fw	TCGACGATTTCTCGCTGGAC
<i>pqsA</i> .Rv	TGGAACCCGAGGTGTATTGC
<i>rpoD</i> .Fw	ACAAGATCCGCAAGGTAAGTGAAG
<i>rpoD</i> .Rv	CGCCAGGTGCGAATC

LPS test

For the quantification of the LPS, the Pierce Chromogenic Endotoxin Quant Kit was used following manufacturer's protocol. Tested extracts were 2x concentrated. The reaction was also performed without enzyme and this background value was subtracted from the signal with enzyme. Three samples were used and reactions were performed in triplicates per sample.

Bioinformatic analysis

Human count tables were analyzed using DESeq2²³⁴. PCA plots were generated using plotPCA function. Volcano plots were generated using EnhancedVolcano package²³⁵. Heatmaps were made using ComplexHeatmap package²⁷³. For the heatmap, we used the GO gene list ("Immune response, GO:006955). We mapped the 60 genes from this list with the strongest fold change when comparing PAO1 WT supernatant extract with LB control treatment.

Results and discussion

Validation of bacterial supernatant

The production and extraction of the supernatant of bacteria is described in the Materials and Methods section and is depicted schematically in Figure 1A. To determine the effect of QS-derived metabolites, we cultured both *P. aeruginosa* PAO1 WT bacteria and a PAO1 QS mutant ($\Delta lasI/\Delta rhII$) strain.

We first confirmed the presence of QS-derived secondary metabolites in the bacterial supernatant extract. To select optimal conditions for the production of metabolites, we measured the expression of QS-regulated genes (*lasB*, *rhIA*, and *pqsA*) at various time points. At 10 hours, the expression of *lasB* and *rhIA* began to increase, peaking at 18 hours before decreasing (Figure 1B-C). The expression of *pqsA* did not show a similar increase as *lasB* and *rhIA* (Figure 1D). However, HHQ, the precursor of PQS, did increase over time (Figure 1E), indicating that the PQS pathway was activated in wild type PAO1 cells. There was a strong increase in the production of HHQ up to a concentration of 3 μ M. As expected, PAO1 Δ QS bacteria did not produce HHQ. In addition, we measured the concentration of 1-phenazinecarboxylic acid (PCA), a precursor of pyocyanin (PYO)¹⁶³, which reached its maximum concentration of approximately 1.3 μ M at 14 hours (Figure 1F). Our findings confirmed that PCA production is QS-dependent, as PAO1 Δ QS did not produce PCA.

In order to maximize the production of QS-regulated metabolites, with minimal levels of non-QS-regulated metabolites, we decided to incubate the PAO1 strains for 14 hours to generate the supernatant extracts. PAO1 Δ QS barely produced any detectable secondary metabolites, which was evident from comparison of the spectrograms of PAO1 Δ QS supernatant extract and LB medium control (Figure 1G). However, WT PAO1 bacteria

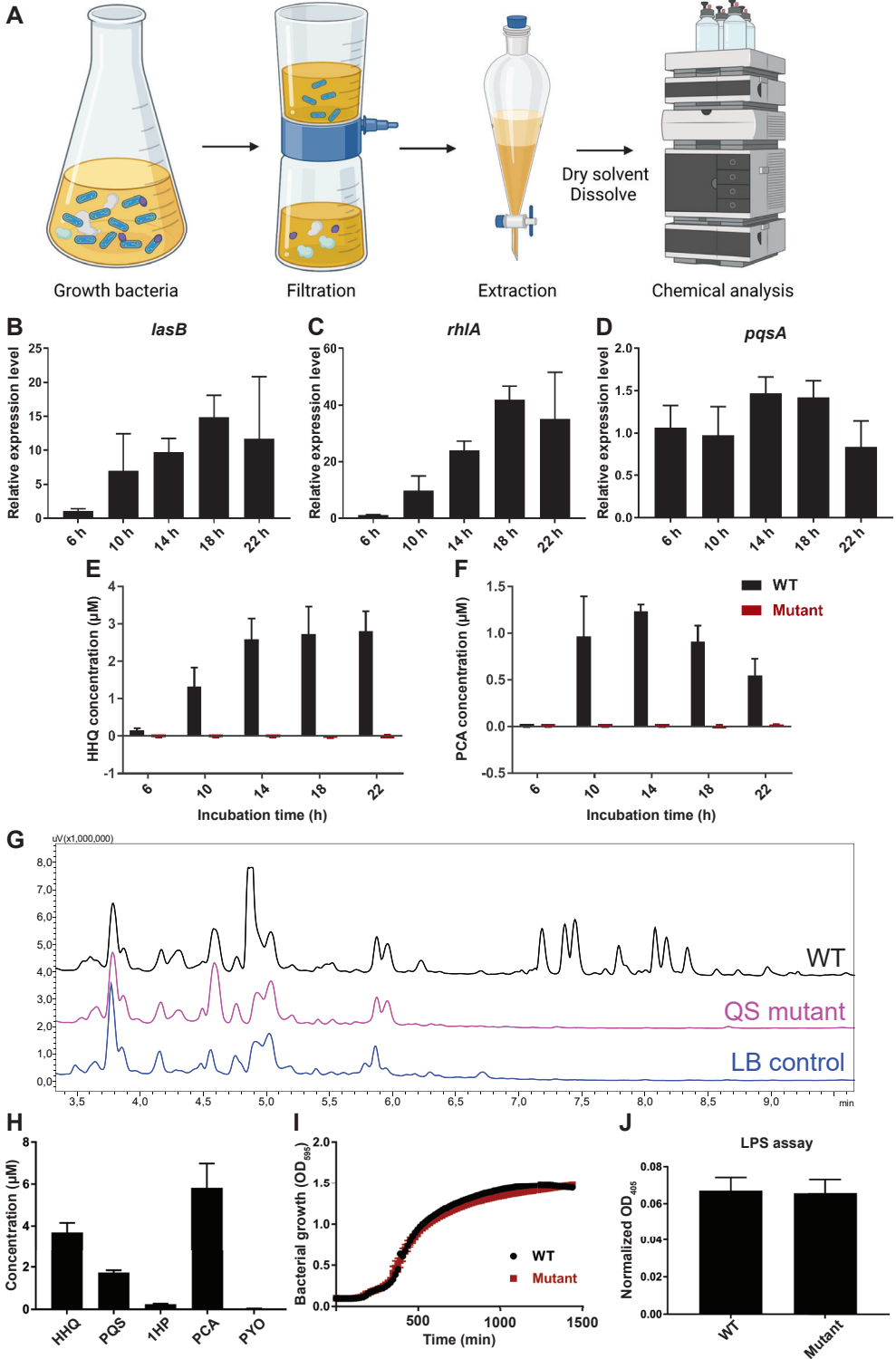


Figure 1. Optimization and validation of bacterial supernatant extract. A) Schematic representation of the preparation and analysis of bacterial supernatant extract. This scheme was created with Biorender.com. Relative expression levels of quorum sensing (QS) regulated genes B) *lasB*, C) *rhlA*, D) *pqsA*, compared to 6 hour time point. Concentration of the QS regulated metabolites E) HHQ, F) PCA. G) Analytical HPLC spectrogram of bacterial supernatant extract after 14 hours of incubation. H) Concentration of various QS-regulated compounds in the working stock solutions. I) Bacterial growth of PAO1 WT and QS mutant bacteria. J) LPS assay comparing the presence of LPS in PAO1 WT and QS mutant bacterial supernatant extract. The means of the triplicates are plotted, error bars represent the standard error of the mean (SEM). Abbreviations: HHQ, 4-hydroxy-2-heptylquinoline; PCA, 1-phenazinecarboxylic acid; PQS, Pseudomonas Quinolone signal; 1HP, 1-Hydroxyphenazine; PYO, Pyocyanin.

did produce a variety of secondary metabolites. For the working stocks, we measured concentrations of various QS-related molecules: 3.69 μM HHQ, 1.73 μM PQS, 0.24 μM 1-hydroxyphenazine (1-HP), 5.83 μM PCA, and 0.04 μM PYO (Figure 1H).

To ensure that any observed effects of supernatant extract treatment were specifically due to QS and not influenced by external factors, we measured several parameters. First, we confirmed that the growth of both strains was similar, eliminating bacterial growth as potential source of differences (Figure 1I). Additionally, we considered the effect of LPS, which can strongly influence the immune response in epithelial cells²⁷⁴. However, the concentrations of LPS were similar in the extract of WT and ΔQS bacteria, excluding the effect of LPS (Figure 1J). Taken together, PAO1 cells and PAO1 ΔQS cells showed similar growth curves and LPS production. PAO1 cells secreted a distinct set of secondary metabolites which were likely attributable to activation of QS.

PAO1 WT supernatant extract is toxic to airway epithelium

To assess potential toxicity on airway epithelium, we tested various concentrations of the supernatant extracts on organoids obtained from various donors: 143 (upper airway from healthy donor), 145 (upper airway from CF patient), N44 (bronchia from healthy donor). Supernatant extract of PAO1 WT bacteria was toxic in all three donors, with 5 x concentrated extract leading to 0 % viability after 5 days of incubation (Figure 2). This toxicity

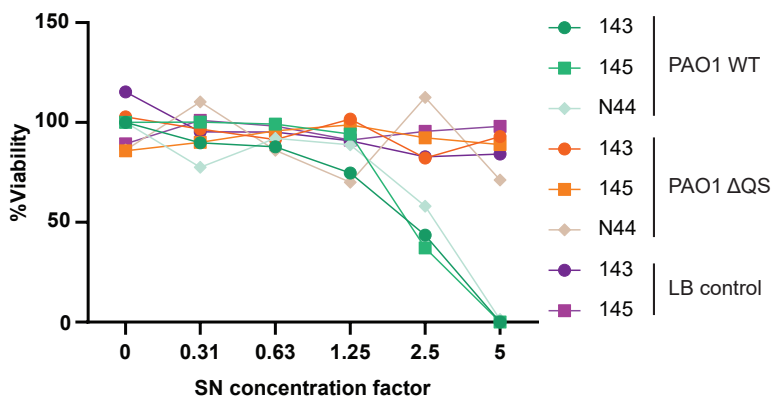


Figure 2. Toxicity of bacterial supernatant extracts. Viability of organoids after treatment with bacterial extracts. Organoids from three donors were used: 143, healthy upper airway organoids; 145, Cystic fibrosis upper airway organoids; N44, bronchial organoids.

was absent at 1.25 x concentrated extract. In contrast, the extract of PAO1 Δ QS supernatant extract did not show toxic effects at any concentration, comparable to medium control. This is in accordance with previous studies showing low virulence effects of QS mutants in infection models⁸⁵.

Bacterial QS response elicits altered gene expression in airway epithelium

To study the effect of QS-regulated compounds on airway epithelium, we incubated the organoid cultures with both PAO1 WT and Δ QS supernatant extract. In addition, we included LB medium extract as control. To test the effect of single QS-induced compounds, we incubated organoids with various structurally related phenazines (1-phenazinecarboxylic acid, PCA; 1-hydroxyphenazine, 1-HP, and pyocyanin, PYO) and PQS (Figure 3A). We selected a concentration of 50 μ M for the single compounds to enable comparison with previous studies^{239,261,268,275–277}, although this concentration exceeds the levels present in the supernatant (*cf.* Figure 1H). After 24 hours of incubation, we isolated the RNA from the samples for subsequent RNA-sequencing.

Analysis of the epithelial transcriptomes after treatment with bacterial supernatant extracts revealed a strong effect of PAO1 WT supernatant extract, compared to the

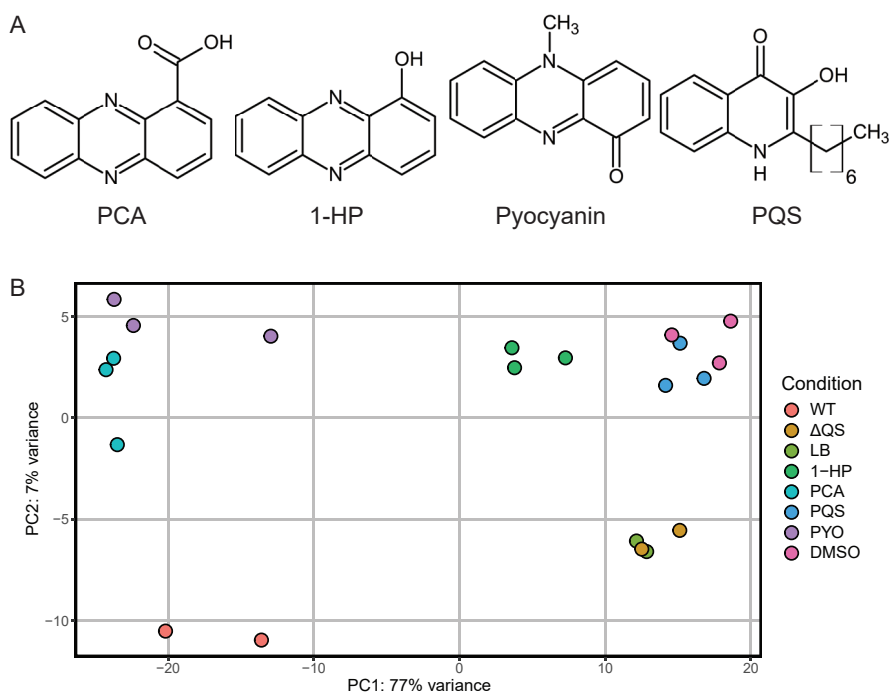


Figure 3. Effect of QS on the transcriptional response of the epithelium. A) Chemical structures of phenazines (PCA, 1-phenazinecarboxylic acid; 1-HP, 1-hydroxyphenazine) and *Pseudomonas* Quinolone signal (PQS) used in this study. **B)** PCA plot of organoid samples after treatment with bacterial supernatant extracts or single QS-regulated molecules (50 μ M).

supernatant extract of PAO1 Δ QS and LB control (Figure 3B). Treatment with PAO1 Δ QS supernatant extract did not lead to a noticeable transcriptional change when compared to LB control. The low production of secondary metabolites by the Δ QS strain was consistent with this lack of effect (*cf.* Figure 1G).

Comparison of the effect of phenazines and PQS on airway epithelium with DMSO control, led to identification of three different clusters (Figure 3B). First, PQS clustered together with DMSO, suggesting a negligible effect of PQS on the airway epithelium. Second, 1-HP had a relatively small transcriptional effect. Third, PCA and PYO both showed a strong effect on the epithelial transcriptome.

WT bacterial supernatant extract induces a small epithelial transcriptional response

The effect of PAO1 Δ QS supernatant extract on gene expression in airway epithelial cells was negligible compared to LB control treated organoids: no genes showed a significantly differential expression between these treatments (Figure 4A). Due to the lack of difference between these two conditions, we decided to combine these data and to compare the combined data with PAO1 WT supernatant extract treatment. Treatment with PAO1 WT supernatant extract induced 519 differentially expressed genes (DEGs) in airway epithelium compared to the control samples (Figure 4B). Of these 519 genes, 246 genes were upregulated and 191 genes were downregulated by more than two-fold, and 82 genes did not show a 2-fold alteration. Unfortunately, GO enrichment analysis of these 246 upregulated genes did not show any over-represented GO terms. Deeper data analysis is needed to study the effect on gene expression after treatment with WT supernatant extract.

PCA and pyocyanin elicit a strong epithelial response

Next, we focused on the effect of the QS-related single molecules on the airway cells. The aforementioned negligible effect of PQS treatment was confirmed by direct

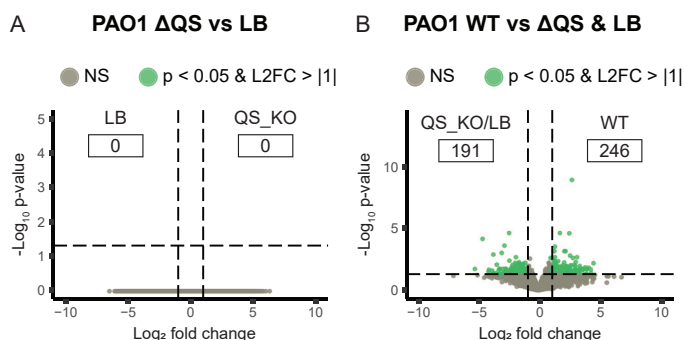


Figure 4. Effect of QS on the transcriptome of the epithelium. A) Volcano plot showing the \log_2 fold change and $-\log_{10}$ adjusted p-value of all genes, when comparing the transcriptome of 2D organoids exposed to PAO1 Δ QS supernatant extract compared to LB control. **B)** Volcano plot comparing the transcriptome of 2D organoids exposed to PAO1 WT supernatant extract compared to PAO1 Δ QS supernatant extract and LB control combined. Green indicates differentially expressed genes (DEGs) (\log_2 fold change > 1 and adjusted p value < 0.05).

comparison of PQS and DMSO treatment (Figure 5A). Second, treatment with 1-HP caused a minor effect on the epithelium compared to DMSO control, with 7 DEGs in total (Figure 5B). Third, PCA and PYO treatment produced a strong transcriptional response in airway epithelial cells compared to DMSO control with 5025 and 3029 DEGs respectively (Figure 5C-D). Although the epithelial transcriptomes after PCA and PYO treatment clustered

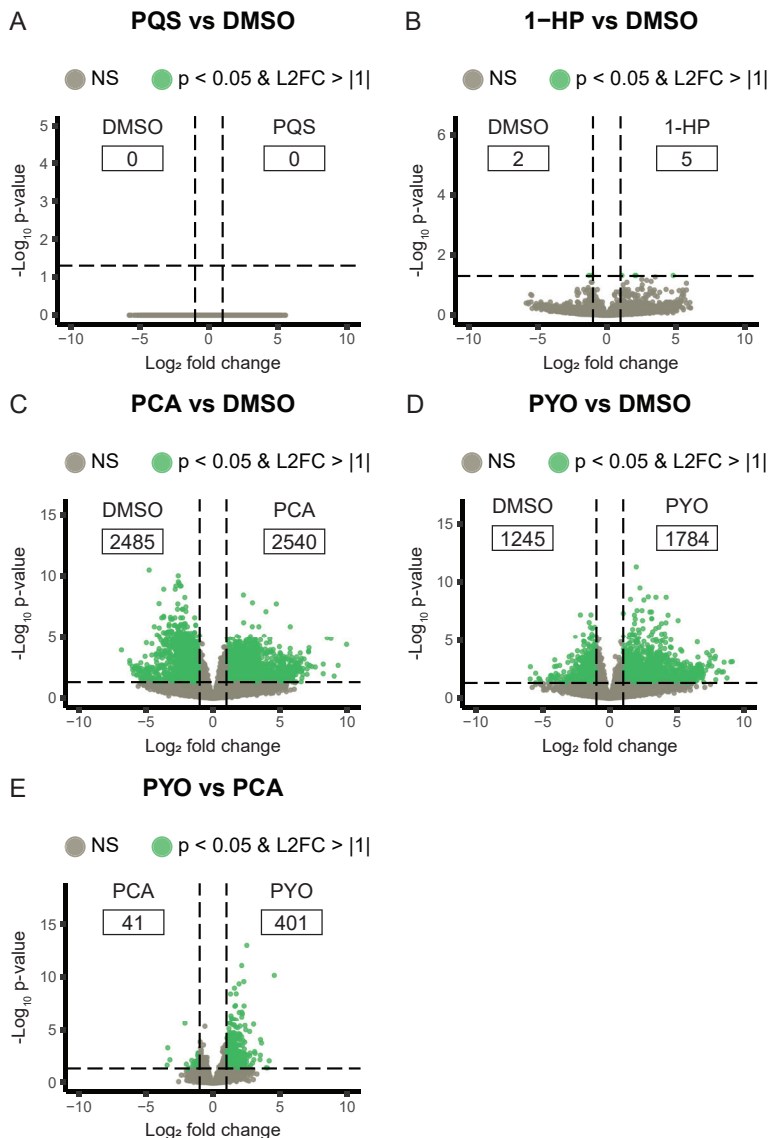


Figure 5. Effect of single QS-regulated compounds on the transcriptome of the epithelium. Volcano plots showing the \log_2 fold change and $-\log_{10}$ adjusted p-value of all genes, when comparing the transcriptome of 2D organoids exposed to **A**) *Pseudomonas* Quinolone Signal (PQS, 50 μ M), **B**) 1-hydroxyphenazine (1-HP, 50 μ M), **C**) 1-phenazinecarboxylic acid (PCA, 50 μ M), **D**) Pyocyanin (PYO, 50 μ M), compared to DMSO control (1%). **E**) Volcano plot comparing the transcriptome of 2D organoids exposed to PYO compared to PCA. Green indicates differentially expressed genes (DEGs) (\log_2 fold change > 1 and adjusted p value < 0.05).

together, these two compounds induced different epithelial responses with 401 genes being differentially expressed (Figure 5E). Taken together, whereas phenazines show high structural similarity, they induced major differences in gene expression in upper airway organoids. However, PQS treatment did not affect the epithelial cells, which is in contrast with previous studies^{268,272}.

Immunomodulatory effect of QS

Various studies indicate an immunomodulatory role of phenazines and QS related metabolites^{184,186,268,272}. Both an increase as well as a decrease of the immune response have been reported due to *P. aeruginosa* QS-regulated molecules. For example, pulmonary mouse infections with *P. aeruginosa* QS mutants caused a stronger and faster inflammatory response, suggesting inhibition of the immune response by the QS system⁶³. The *P. aeruginosa* AHL, 3-oxo-C12-HSL, induces expression of the murine IL-6 and IL-8 homologue KC, despite inhibiting the secretion of these pro-inflammatory cytokines²⁶⁸. To learn more about the immunomodulatory role of QS molecules, we focused on the immune response in our samples.

We observed an immunomodulatory effect of PAO1 WT supernatant extract (Figure 6A) with upregulation (e.g. *TNFSF*, *TLR1*, *IL33*, and *IL1B*) and downregulation (e.g. *IL4R*, *IL1R1*, and *CXCR6*) of pro-inflammatory genes. To investigate if phenazines are responsible for this immunomodulatory effect, we compared the effect of phenazines and PQS treatment on the same list of genes (Figure 6B). Both PYO and PCA showed a similar response as WT supernatant extract, suggesting these phenazines play an important role in the immunomodulatory role of QS-regulated molecules.

Some of these 60 genes were expressed at a low level in airway epithelial cells. Therefore, we decided to focus on the constitutively expressed genes *IL33* and *IL1R1*. *IL-33* is a pro-inflammatory cytokine belonging to the IL-1 family, and plays a key role in both the innate and adaptive immune response. *IL-33* is localized in the nucleus of various cell types, including airway epithelium, and is generally released upon cell damage, activating various immune cells, such as T_H2 cells, mast cells, group 2 innate lymphoid cells (ILC2s), T_{reg} cells, T_H1 cells, CD8⁺ T cells and NK cells²⁷⁸. Previous studies have demonstrated that treatment with *IL-33* leads to improved outcomes in mice after corneal infection by *P. aeruginosa* and after lung infection by *Klebsiella pneumoniae*^{279,280}, indicating that *IL-33* cytokine expression may play an important role during bacterial infection. Interestingly, we measured a clear increase in *IL33* expression after treatment with PAO1 WT supernatant extract, compared to PAO1 Δ QS or LB control (Figure 6C). Treatment with PCA and PYO induced a similar increase of *IL33* expression. This suggest that QS-regulated molecules, and in particular PCA and PYO induce a pro-inflammatory response via upregulation of *IL33*.

In contrast, PAO1 WT supernatant extract, PYO, and PCA treatment caused a decrease in *IL1R1* expression compared to the controls. *IL-1R1* is an important immune receptor mediating a pro-inflammatory response after binding of the interleukins IL-1 α and

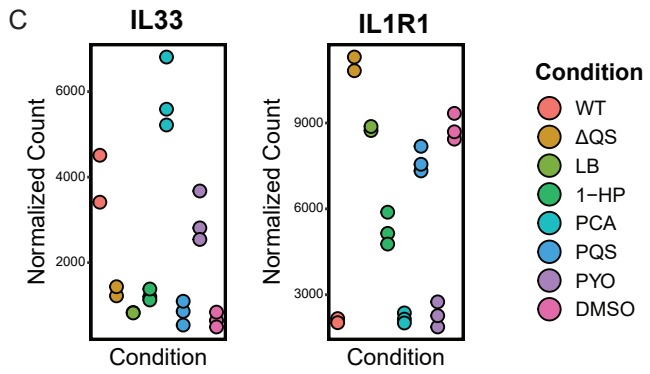
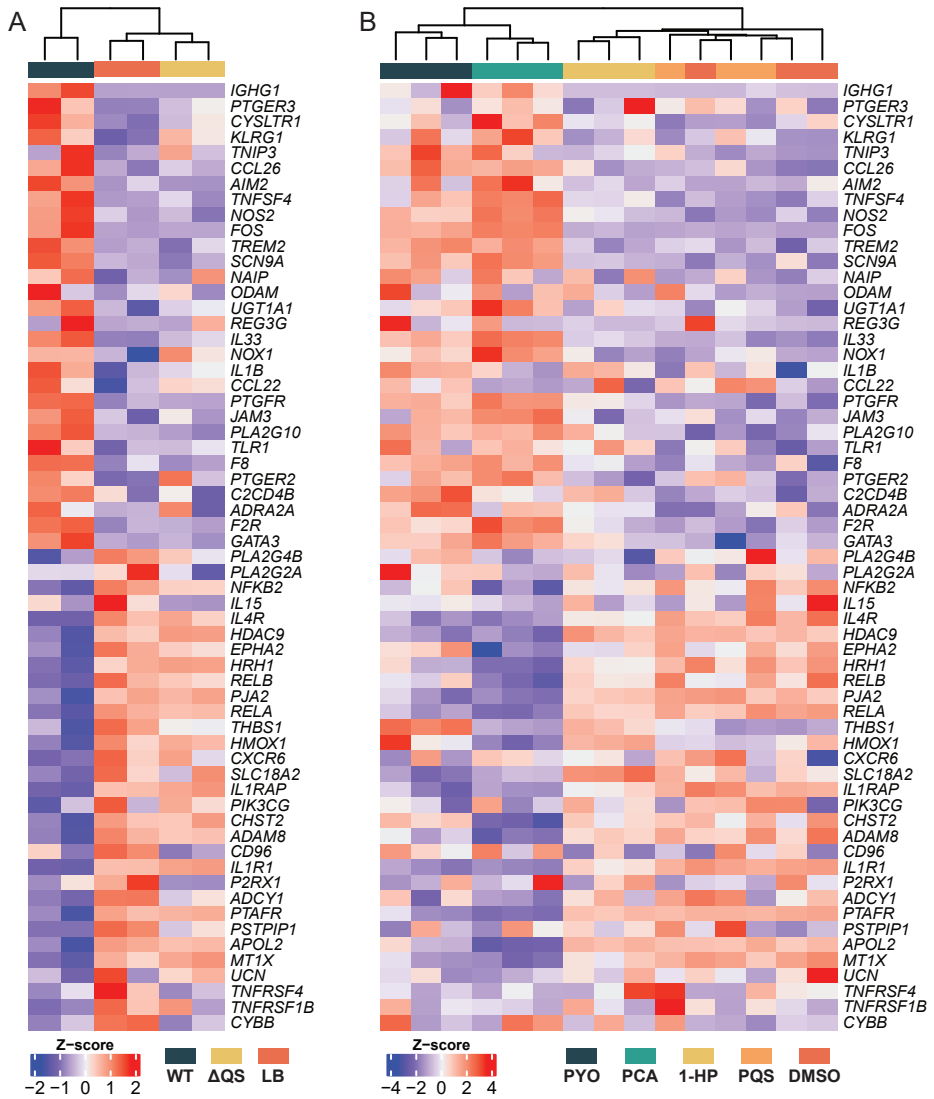


Figure 6. Immunomodulatory response of QS. A) Gene expression heat map of top DEGs (when comparing PAO1 WT supernatant extract treatment compared to LB control) from “Immune response” (GO:0006955), including supernatant extract samples. **B)** Gene expression heat map of the same genes as in (A), after treatment with single molecules (PYO, PCA, 1-HP, PQS, all 50 μ M) and DMSO control (1 %). **C)** Normalized counts of *IL33* and *IL1R1* across different conditions in the cohort.

IL-1 β ^{281,282}. Just like IL-33, IL-1 α functions as an alarmin and is released upon cell death. IL-1 β plays an important role during bacterial infection, and shows a strong activation after LPS stimulation²⁸³. This suggests that QS inhibits the inflammatory response via inhibition of the expression of *IL1R1*.

In conclusion, although the role of IL-33 during *P. aeruginosa* lung infection remains relatively underexplored, it holds promise as a target for future studies. Particularly the phenazines PCA and PYO appear to play a role in the induction of this cytokine. However, it needs to be stressed that the host immune response is not only mediated by QS-induced molecules, and is not limited to airway epithelial cells. LPS, expressed on the outer membrane of Gram-negative bacteria, induces a strong immune response, which may overrule the effect of QS molecules. It is noteworthy that, comparing the immune response after treatment with PAO1 WT and PAO1 Δ QS bacteria, instead of using supernatant, did not reveal an immunomodulatory effect (as discussed in Chapter 4). Therefore, QS-regulated compounds may only reflect a minor modification in the immune response compared to LPS. Moreover, our model lacks immune cells, making it impossible to study the immune response outside of the epithelial barrier. Nevertheless, investigating the immunomodulatory effects of QS molecules and phenazines in airway epithelial cells is of great interest to learn more about the impact of *P. aeruginosa* infections.

Conclusion and future perspective

Organoid technology makes it possible to study the epithelial response to certain bacterial molecules. In this study, we studied the transcriptional response of airway epithelial organoids to QS-regulated molecules, using cell-free bacterial extracts and single QS-derived molecules. We measured the effect of PAO1 WT supernatant extract treatment compared to PAO1 Δ QS and LB control. Unfortunately, the response was too small to find overrepresented GO terms. In addition, we report strong differences in epithelial response after treatment with various phenazines, despite their high structural resemblance. Last, we focused on the immunomodulatory role of QS. We saw both an activation (IL-33) and inhibition (IL-1R1) of immune factors. This suggests that IL-33, although being underexplored, plays a role during *P. aeruginosa* airway infection. Deeper analysis of the data should explain more about the effect of QS on airway epithelial cells, both on the immune response as well as on other epithelial responses. Moreover, by using organoids, this model makes it possible to study the effect of QS molecules in single cells. In conclusion, although the data is limited, this explorative research hopefully sparks ideas for future research, using bacterial extracts and organoids to study the effect of bacterial processes on human cells.



Chapter 6

General Discussion

As discussed in **Chapter 1**, antibiotic resistance is a growing problem worldwide. Without action, antibiotics will lose efficacy and infectious diseases may become deadly again^{13,15,284}. Due to its high intrinsic resistance, *Pseudomonas aeruginosa* bacteria are among the most critical bacteria that pose a threat to human health^{19,26}. To be able to treat *P. aeruginosa* infections in the future, alternative targets are needed. In this thesis, we focused on the potential of targeting quorum sensing (QS).

The promises of QS as an alternative antimicrobial target have been shown by improved outcomes in animal models after infection with QS mutants compared to infection with WT bacteria^{85–87}. Similarly, inhibition of QS by small molecule inhibitors showed promising effects^{77,88,89}. Due to these promising results, we started the search for novel QS inhibitors using a unique library of 10,207 fungal filtrates (**Chapter 2**).

The search for novel quorum sensing inhibitors

QS inhibitors have been purified from various natural sources including oak, garlic and algae^{81,82,112}. The richness of natural sources of QS inhibitors is not surprising, since they might have co-evolved with bacteria to limit toxic virulence factor synthesis. Still, fungi remain an underexplored niche¹¹⁵. To screen our library, we used the reporter bacterium *Chromobacterium violaceum*. Of the 10,207 samples, 79 fungal filtrates showed inhibition of QS while not affecting the viability. Among the active compounds, we found two previously described QS inhibitors: penicillic acid and patulin. Penicillic acid and patulin showed inhibition of QS in concentrations that were ~6-fold and ~2-fold lower than the toxic concentrations, respectively.

This screening also led to the identification of multiple compounds that were not known as QS inhibitor before. The newly identified QS inhibitors showed a higher fold difference between QS inhibition and toxic concentrations in *C. violaceum* than penicillic acid and patulin. Among these compounds, desmethyl-gregatin A showed the most promising results in *C. violaceum* with a 74-fold difference between the QS inhibitory concentration and the toxic concentration. Unfortunately, the inhibitory effect of the novel QS inhibitors on *P. aeruginosa* QS and downstream processes was minor.

This raised the question if *C. violaceum* is a good reporter to search for novel QS inhibitors. *C. violaceum* bacteria do not have high clinical relevance with only a very small number of human infections over the years²⁸⁵. In addition, although *C. violaceum* and *P. aeruginosa* both possess LuxI/R-type QS systems, their QS systems do show differences as well. Nevertheless, violacein production by *C. violaceum* is easily quantifiable. Therefore, we were able to screen a large number of filtrates. Screening the entire library using the PAO1 QS reporters that were mentioned in **Chapter 2 and 3** is not feasible. With a throughput of one 96-well plate per day, it would take months to screen the entire library. Genetic modification of *P. aeruginosa* might facilitate high-throughput screens to overcome this problem. For example, deriving strains in which activation of QS pathways is lethal, would lead to bacteria

that only grow when QS is inhibited, that is when *P. aeruginosa*-specific QS inhibitors are present¹⁴⁰. Whether these molecules are active in other Gram-negative bacteria remains to be determined. Therefore, it is important to keep the available resources and bacterial strain of choice in mind when choosing the appropriate reporter bacterium when screening for QS inhibitors.

QS inhibitor concentrations needed to inhibit QS in *P. aeruginosa* were often higher than in *C. violaceum*. This is due to the highly impermeable membrane of *P. aeruginosa* in comparison to other Gram-negative bacteria. These high concentrations of QS inhibitors may result in concentrations that are toxic to human cells. For this reason, it might be interesting to inhibit the QS response by targeting the QS signal molecules, which are present in the extracellular milieu. Enzymatic degradation of these molecules would lead to inhibition of QS without the need for QS inhibitors to cross the bacterial membrane²⁸⁶.

The potential of fungi as producers of QS inhibitors

Since the discovery of penicillin in fungi in 1928, fungi became a popular source to search for antimicrobials. Since then, many labs focused on the search for bioactive antimicrobial secondary metabolites in fungi¹¹⁴. Dereplication is a problem nowadays, in that the same active compounds are repeatedly found in screens. To be able to find novel promising leads from fungal metabolites, innovative research is needed. First, new tools to activate secondary metabolite gene clusters make it possible to express novel secondary metabolites to target bacteria⁵¹. Second, targeting alternative bacterial processes make it possible to find novel mechanisms of known compounds. In **Chapter 2**, we used the latter approach, showing that fungi, after 100 years of extensive studies, still hold the promise for future medicine when alternative targets are studied.

Antibiotics are often regarded as molecules that evolved due to the competition between microbes for limited resources and nutrients. Similarly, fungal molecules that interfere with QS could have evolved as weaponry to limit the virulence of the bacteria during competition. Nevertheless, it is unknown if the compounds found in **Chapter 2 and 3** are truly QS inhibitors in natural environments. It is likely that the concentrations needed for QS inhibition are higher than the concentrations found in complex, multispecies, natural environments. Therefore, the identified hits might play a different role in the fungal-microbial interaction in natural environments than to affect bacterial communication.

Due to its size, our library contained a large variety of organic compounds in various concentrations. For that reason, it was possible to identify and describe the low-hanging fruits of QS inhibitors. These compounds were often relatively easy to extract, purify and reach concentrations high enough to elucidate their structures. It is likely that many more fungal QS inhibitors are still to be found.

Using our approach, we might have missed many fungal QS inhibitors. First, the

concentration of the QS inhibitor is important. Many fungal filtrates might contain too low concentrations of the bioactive molecule to measure an effect. In contrast, the concentration in some fungal filtrates might have been too high, leading to exclusion for further analysis due to toxic effects in the bacteria. Second, the filtrates and extracts contained a variety of secondary metabolites. Therefore, the presence of additional toxic compounds or known QS inhibitors might have led to the exclusion of interesting samples. Third, it was not always possible to find the active molecule in an active filtrate. For example, our extraction and fractionation method is less optimal for water-soluble compounds. Last, it was not always possible to purify the active compound using our methods or to elucidate the structure of the compound in a pure bioactive fraction. Therefore, optimization of analytical chemical methods could lead to the discovery of other, still unknown, QS inhibitors.

Optimization of fungal growth conditions might also increase the concentration or number of compounds. Both the concentration and variety of secondary metabolites may be increased when the fungus is grown in other environmental conditions (e.g. temperature, pH, and nutrients). An interesting example is activating silent gene clusters by opening the chromatin of fungi with the HDAC inhibitor suberoylanilide hydroxamic acid (SAHA)²⁸⁷. Preliminary research from our lab showed that the addition of SAHA led to an increase of secondary metabolites. A screen, performed by Helen Buttstedt (student in our lab), using filtrates from fungi grown in the presence of SAHA, led to active fractions that were not found in the initial screen described in **Chapter 2**. This shows that by altering the fungal growth, distinct interesting compounds may be found.

The discovery of paecilomycone

Optimization of the chemical purification methods led to the discovery of paecilomycone as described in **Chapter 3**. In contrast to the QS inhibitors found in **Chapter 2**, treatment with paecilomycone showed promising results in *P. aeruginosa*. Paecilomycone treatment led to a decrease in biofilm formation and a decrease in the production of phenazines, while not being toxic to human cells. As mentioned in **Chapter 3**, the exact target is still unknown. Therefore, more research is needed to learn more about its exact target molecule and its corresponding mechanism of action.

We believe one of the targets of paecilomycone is the PqsBC complex due to the inhibition of HHQ and PQS while not affecting 2'-aminoacetophenone. However, inhibition of only the PqsBC complex does not explain the strong inhibition of phenazines. Moreover, in a *pqsBC* mutant, paecilomycone treatment still showed inhibition of pyocyanin production. Therefore, paecilomycone might target more upstream or general processes. In this respect, it is interesting to mention pyrogallol, which is a trihydroxybenzene. Paecilomycone contains a similar trihydroxybenzene, while funalenone does not (Figure 1). The QS inhibitory activity of pyrogallol in *Vibrio harveyi* is due to the peroxide-generating side effect of this compound instead of directly targeting QS. Treatment with catalase, which quenches hydrogen peroxide,

neutralizes the effect of pyrogallol²⁸⁸. Whether paecilomycone also acts via production of peroxide next to acting via the PqsBC complex remains to be determined.

Comparing the activity of paecilomycone with funalenone, a compound with high structural resemblance, shows the promise of optimization of the structure. Although funalenone and paecilomycone only differ in the position of the methoxy group, only paecilomycone showed QS inhibitory activity. Therefore, further optimization of the structure may lead to increased activity and reduced toxicity making it more interesting to develop into the clinic²⁸⁹.

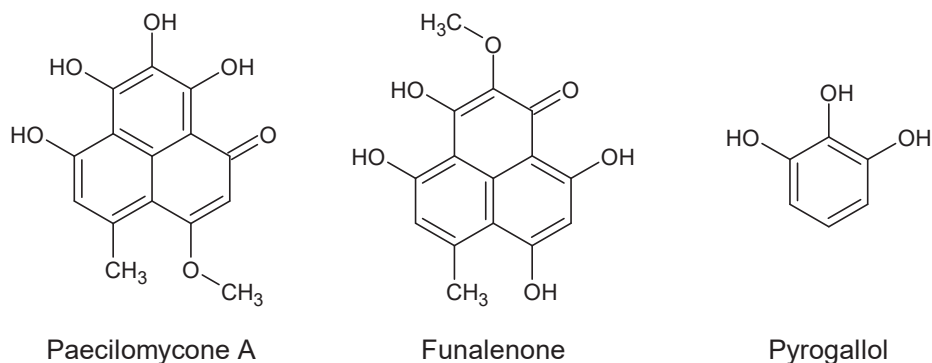


Figure 1: Chemical structures of Paecilomycone A, Funalenone, and Pyrogallol

The role of QS during infection

The potential of QS inhibitors as treatment against bacterial infections is still unknown. To learn more about the potential of QS inhibitors, it is important to learn more about the role of QS during human infection. This area of research is still underexplored and optimization of infection models is necessary. To learn more about the role of QS during infection, we made use of organoids as described in **Chapter 4 and 5**.

Stem-cell derived organoids closely resemble the cell types present in organs. This gives a platform to study human epithelial cell responses in settings that represent physiological conditions, making it an interesting alternative for animal studies. Contrary to animal studies, organoids allow clonal expansion, analysis of human-specific systems, and genetic modification²²⁶. Experiments may be conducted in a culture dish, without harming laboratory animals, providing an appealing alternative for animal studies. Lately, co-cultures of bacteria and organoids have shown that organoids may also be used to study infections and host-microbe interactions^{159,226,290,291}.

Due to the great transcriptomic differences between bacteria and eukaryotes, the use of dual RNA-sequencing was still only a thought experiment ten years ago. Until then, RNA-seq experiments were only one-sided making it impossible to study gene expression in parallel²⁹². Due to optimization of sequencing methods and the ability to deplete rRNA,

it became possible to actually perform dual-RNAseq²⁹³. Since then, various bacterial strains and host platforms have been used to gain more biological insight into bacterium-host crosstalk^{230,293}. We used this approach in **Chapter 4** to study *P. aeruginosa* during CF infection using organoid technology. In addition, by using *P. aeruginosa* mutant strains, we were able to study the role of *P. aeruginosa* QS during CF infection.

Similar as described previously^{97–99}, our model showed that QS is less active during infection than *in vitro*. Interestingly, the QS mutant did not lead to altered gene expression in organoid epithelial cells compared to WT bacteria. This is in contrast with other studies, that suggest that QS molecules or QS downstream effectors affect host cells^{240,241,260,271}. The effect of QS molecules on host cells is dependent on the concentration and exposure time. It is likely that the concentration of QS effectors was lower than 50 μ M which is used in other studies²⁶⁰. Although concentrations of QS related molecules may be high in *in vitro* biofilm models²⁹⁴, concentrations of QS molecules in the sputum of CF patients was in the range of nanomolar instead of micromolar^{295–297}. Besides the concentration of QS molecules, the incubation time of the co-culture might prevent effects in eukaryotic cells. It takes time for bacteria to proliferate and to produce AHLs to a concentration that QS becomes detectable. Subsequently, the eukaryotic response will take some time as well. Therefore, it might take longer than 14 hours of co-culture to measure transcriptomic alterations in organoids. In addition, the eukaryotic response to QS molecules might be cell type specific²⁶³. This response would be missed using bulk RNA-seq. Still, the results from **Chapter 4** do suggest that QS might play less of a role than previously suggested.

To resemble the physiological conditions of infection more closely an interesting improvement of our co-culture would be to add immune cells. Immune cells play a pivotal role during infection by predated pathogenic bacteria, producing reactive oxygen species, and altering available nutrients in the environment²⁹⁸. This would lead to major differences in the interaction between host and co-cultured bacteria. However, due to the interaction between two complex cell populations, small differences might lead to large outcomes. Finding a viable balance between *P. aeruginosa* and organoid epithelial cells was already challenging. Adding immune cells will disturb this balance. Therefore, it will take time to optimize the model, so bacteria can thrive, without destroying the epithelial cell layer.

It might also be possible to improve the model, without adding complex cell populations. Combining the co-culture with other innovative techniques could help to learn more about *P. aeruginosa* CF infection. During infection, bacterial cells show genetic and phenotypic heterogeneity²⁹⁹. In addition, as mentioned before, the response to QS might be cell type specific²⁶³. To learn more about this diverse response, studying the transcriptome on single cells would be interesting. Although still in its infancy, Avital and colleagues already reported a protocol for dual single-cell sequencing³⁰⁰. The downside of these single cell RNA-sequencing approaches is the lack of spatial information. Fluorescence *in situ* hybridization (FISH) overcomes this problem by fluorescently labeling RNA molecules upon expression. With the use of the recently developed par-seqFISH, it is possible to study the expression

of hundreds of genes in a spatiotemporal context at single-cell resolution²⁶⁵. A combination of par-seqFISH with our 2D organoid co-culture infection model may provide interesting insights into the heterogeneous landscape of *P. aeruginosa* during CF infection.

Nevertheless, QS signal molecules are detectable in CF patients with *P. aeruginosa* infection, showing that QS is active during infection²⁹⁵. In addition, toxic virulence factors harm tissues, and *P. aeruginosa* strains that are isolated from CF patients are still able to produce these toxic virulence factors¹⁸⁴. Moreover, overproduction of virulence factors by these clinical strains has been reported⁶⁰. However, more studies are needed to learn more about the concentrations and role of these virulence factors during infection⁶⁰. To be able to study higher concentrations of QS related compounds at longer incubation times, we also used organoids to study the supernatant of WT and QS mutant bacteria as described in **Chapter 5**. This model allowed analysis of the effect of single metabolites on the epithelial transcriptome at later time points, which was more robust than the co-culture model.

As **Chapter 5** showed, supernatant of *P. aeruginosa* WT bacteria is more toxic to organoids than supernatant of QS mutant bacteria. In addition, QS-derived molecules influence gene expression of epithelial cells. Especially phenazine-1-carboxylic acid and pyocyanin treatment caused a strong epithelial response. When specifically studying the immune response, we observed a QS-dependent immunomodulatory effect with an increase in *IL33* expression and a decrease in *IL1R1* expression. The difference in QS-induced epithelial response between **Chapter 4 and 5** may be explained by a strong LPS-induced inflammation response in the bacterial co-cultures^{301,302}. Without LPS present in bacterial supernatant, small effects might become detectable. In addition, the strong effect of phenazine-1-carboxylic acid and pyocyanin treatment might be caused by the high concentrations, which were considerably higher than the concentrations present in the extract.

In conclusion, although QS is active during infection and QS regulated virulence factors may harm tissues, QS might play less of a role than previously expected. To study the role of QS during human infection is challenging and therefore model systems are needed. Organoid technology provides an interesting platform, because it allows the study of early infection in systems that closely resemble physiological human conditions. Further optimization (e.g. co-culture of immune cells) may help to resemble infections even more closely.

What is the potential of quorum sensing inhibitors in the clinic?

For the discussion of QS inhibitors in the clinic, we assume that QS does play a role during infection and is a good target to limit virulence factors and biofilm formation. As **Chapter 2 and 3** show, many promising QS inhibitors are still to be found. However, these chapters also showed that the concentration range for QS inhibition may be relatively small. For example, patulin treatment only showed a 2-fold difference between the QS inhibitor and lethal concentrations. While low concentrations might not show any activity, high

concentrations can sometimes even lead to activation of certain virulence factors as shown with gregatin A and gregatin D. In addition, high concentrations might become toxic to tissues. In patients, homeostasis and degradation of QS inhibitors will take place. Therefore, it will become a challenge to reach the correct concentration of QS inhibitors in complex environments like host tissues.

QS inhibition does not affect viability of the bacteria in rich medium. Without this selective pressure, researchers argued that it is unlikely for bacteria to become resistant to QS inhibitors. However, studies have shown that resistance can also occur against QS inhibitors by increased expression of efflux pumps or degradation of the QS inhibitors. These resistance mechanisms may be similar to resistance mechanisms against antibiotics used in the clinic (e.g. overexpression of efflux pumps)³⁰³. Therefore, antimicrobial resistant clinical strains might be less susceptible to QS inhibitors. It is good to consider that just like with the introduction of novel antibiotics, resistance might occur quickly after introduction of QS inhibitors to the clinic.

However, QS inhibitors might hold potential besides treating infections within the human body. QS inhibitors might be of interest in other types of infections, like skin infections where the QS inhibitors can be applied locally. Besides medicine, QS inhibitors might have potential in other fields where bacterial contamination is a problem, like biofouling, agriculture, or medical equipment.

Future of antibiotics

Although pharmaceutical companies mostly left antibiotic research due to difficulties finding new antibiotics and low profits, renewed interest in antibiotic research in academia led to lots of innovative, alternative ideas to treat bacterial infections. For the future, antibiotics will remain necessary. To find novel conventional antibiotics -small molecules that target essential bacterial processes- we need alternative strategies (e.g. genome mining, novel culturing techniques, synthetic biology, or computational approaches). In addition, other ways to kill bacteria will become more prominent in the antimicrobial field. Examples are the use of antibodies³⁰⁴, nanoparticles³⁰⁵, bacteriophages³⁰⁶, or prophylactic treatment by vaccination³⁰⁷. However, targeting essential processes will cause selective pressure. This will eventually lead to antimicrobial resistance, requiring continuous innovation or optimization. Therefore, combination therapies might become of great interest.

Combination therapies make use of an antibiotic, together with a conjugate that inhibits bacterial resistance. A common example is the combination of β -lactam antibiotics with β -lactamase inhibitors (that inhibit β -lactam degrading enzymes)³⁰⁸. Other ways to reduce bacterial resistance are also under investigation. This includes inhibition of efflux pumps to increase the accumulation of antibiotics in the bacteria³⁰⁹, silencing drug resistance genes via CRISPR-Cas or synthetic oligomers³¹⁰, or anti-biofilm molecules³¹¹. By inhibiting antimicrobial resistance, resistant bacteria may become susceptible to antibiotics again.

Antibiotic adjuvants may also be used to potentiate the antibiotic action by altering the immune system. A recent example showed promise of an antibiotic-antibody combination that enhances the intracellular killing of *P. aeruginosa* in macrophages by releasing antibiotics within this immune cell³¹². In addition, existing, marketed drugs could be repurposed as antibiotic adjuvant for its immune regulatory actions³¹³. With the help of the immune system, antibiotics might become more powerful in eradicating bacterial infection.

Tissue damage may be prevented by reducing the toxicity of the bacteria, leading to a decrease in symptoms. Reduction of toxicity is possible via inhibition of virulence factor synthesis, disruption of virulence factor secretion, or neutralization of virulence factors³¹⁰. Neutralization of virulence factors will be very specific. Inhibition of QS allows inhibition of a wider arsenal of virulence factors. While anti-virulence therapies could alleviate the symptoms, antibiotics are still needed to eliminate the bacteria.

These examples of potential antibiotics and adjuvants are narrow-spectrum, in other words, they target specific bacterial species. This has the advantage that resistance mechanisms will be less common within bacterial populations and they will do less harm to the human microbiota during antibiotic therapies. The disadvantage is that it will take longer before the treatment can start since it requires identification of the bacterial species causing the infection. Therefore, conventional, wide-spectrum antibiotics will remain important in the future for acute infections or prophylactic treatments. For hard-to-eradicate, chronic infections, innovative treatments hold great potential.

Conclusion

The aim of this thesis was to learn more about the potential of QS inhibition as alternative treatment against bacterial infection. For this, we mostly used *P. aeruginosa* as model bacterium. Natural compounds still hold great promise to find novel QS inhibitors (**Chapter 2**), and these QS inhibitors show promising effects in *P. aeruginosa* by limiting production of virulence factors (**Chapter 3**). However, more research and optimized platforms are needed, like organoid technology (**Chapter 4 and 5**), to learn more about the role of QS during infection before QS inhibitors may enter the field of antibiotics.



References

References

1. Fleming, A. On the Antibacterial Action of Cultures of a *Penicillium*, with Special Reference to their Use in the Isolation of *B. influenzae*. *The British Journal of Experimental Pathology* **10**, 226–236 (1929).
2. Duckett, S. Ernest Duchesne and the concept of fungal antibiotic therapy. *Lancet* **354**, 2068–2071 (1999).
3. Mohr, K. I. History of Antibiotics Research. *Curr. Top. Microbiol. Immunol.* **398**, 237–272 (2016).
4. Gould, K. Antibiotics: From prehistory to the present day. *J. Antimicrob. Chemother.* **71**, 572–575 (2016).
5. Gaynes, R. The Discovery of Penicillin - New Insights After More Than 75 years of Clinical Use. *Emerg. Infect. Dis.* **23**, (2017).
6. Hutchings, M., Truman, A. & Wilkinson, B. Antibiotics: past, present and future. *Curr. Opin. Microbiol.* **51**, 72–80 (2019).
7. Velkov, T. *et al.* Teaching ‘old’ polymyxins new tricks: New-generation lipopeptides targeting Gram-negative ‘superbugs’. *ACS Chem. Biol.* **9**, 1172–1177 (2014).
8. Coates, A., Hu, Y., Bax, R. & Page, C. The Future Challenges Facing the Development of New Antimicrobial Drugs. *Nat. Rev. Drug Discov.* **1**, 895–910 (2002).
9. D’Costa, V. M. *et al.* Antibiotic resistance is ancient. *Nature* **477**, 457–461 (2011).
10. Bhullar, K. *et al.* Antibiotic Resistance Is Prevalent in an Isolated Cave Microbiome. *PLoS One* **7**, 1–11 (2012).
11. Holmes, A. H. *et al.* Understanding the mechanisms and drivers of antimicrobial resistance. *Lancet* **387**, 176–187 (2016).
12. Blair, J. M. A., Webber, M. A., Baylay, A. J., Ogbolu, D. O. & Piddock, L. J. V. Molecular mechanisms of antibiotic resistance. *Nat. Rev. Microbiol.* **13**, 42–51 (2015).
13. Nathan, C. Resisting antimicrobial resistance. *Nat. Rev. Microbiol.* **18**, 259–260 (2020).
14. Falagas, M. E. & Bliziotis, I. A. Pandrug-resistant Gram-negative bacteria: the dawn of the post-antibiotic era? *Int. J. Antimicrob. Agents* **29**, 630–636 (2007).
15. Antimicrobial Resistance Collaborators. Global burden of bacterial antimicrobial resistance in 2019: a systematic analysis. *Lancet* **399**, 629–655 (2022).
16. Rice, L. B. Federal Funding for the Study of Antimicrobial Resistance in Nosocomial Pathogens: No ESKAPE. *J. Infect. Dis.* **197**, 1079–1081 (2008).
17. Mulani, M. S., Kamble, E. E., Kumkar, S. N. & Tawre, M. S. Emerging Strategies to Combat ESKAPE Pathogens in the Era of Antimicrobial Resistance: A Review. *Front. Microbiol.* **10**, (2019).
18. Founou, R. C., Founou, L. L. & Essack, S. Y. Clinical and economic impact of antibiotic resistance in developing countries: A systematic review and meta-analysis. *PLoS One* **12**, 1–18 (2017).
19. World Health Organization. WHO publishes list of bacteria for which new antibiotics are urgently needed. Available online: <https://www.who.int/news/item/27-02-2017-who-publishes-list-of-bacteria-for-which-new-antibiotics-are-urgently-needed> (Accessed on 11 October 2022).
20. Poulsen, B. E. *et al.* Defining the core essential genome of *Pseudomonas aeruginosa*. *Proc. Natl. Acad. Sci. U. S. A.* **116**, 10072–10080 (2019).
21. Ozer, E. A., Allen, J. P. & Hauser, A. R. Characterization of the core and accessory genomes of *Pseudomonas aeruginosa* using bioinformatic tools Spine and AGEnt. *BMC Genomics* **15**, 1–17 (2014).
22. Stover, C. K. *et al.* Complete genome sequence of *Pseudomonas aeruginosa* PAO1, an opportunistic pathogen. *Nature* **406**, 959–964 (2000).
23. Gross, J. & Welch, M. Why is *Pseudomonas aeruginosa* a common cause of infection in individuals with cystic fibrosis? *Future Microbiol.* **8**, 697–699 (2013).
24. Stratton, C. W. *Pseudomonas aeruginosa*. *Infect. Control* **4**, 36–40 (1983).
25. Moore, N. M. & Flaws, M. Introduction: *Pseudomonas aeruginosa*. *Clin. Lab. Sci.* **24**, 41–42 (2011).
26. Botelho, J., Grosso, F. & Peixe, L. Antibiotic resistance in *Pseudomonas aeruginosa* – Mechanisms, epidemiology and evolution. *Drug Resist. Updat.* **44** (2019).
27. LiPuma, J. J. The changing microbial epidemiology in cystic fibrosis. *Clin. Microbiol. Rev.* **23**, 299–323 (2010).

28. Fischer, A. J. *et al.* Sustained Coinfections with *Staphylococcus aureus* and *Pseudomonas aeruginosa* in Cystic Fibrosis. *Am. J. Respir. Crit. Care Med.* **203**, 328–338 (2021).
29. Cystic Fibrosis Foundation. Cystic Fibrosis Foundation Patient Registry, 2019 Annual Data Report. *Cyst. Fibros. Found.* 1–26 (2020).
30. Parkins, M. D., Somayaji, R. & Waters, V. J. Epidemiology, biology, and impact of clonal *Pseudomonas aeruginosa* infections in cystic fibrosis. *Clin. Microbiol. Rev.* **31** (2018).
31. Zgurskaya, H. I., López, C. A. & Gnanakaran, S. Permeability Barrier of Gram-Negative Cell Envelopes and Approaches To Bypass it. *ACS Infect. Dis.* **1**, 512–522 (2015).
32. Hancock, R. E. W. Resistance Mechanisms in *Pseudomonas aeruginosa* and Other Nonfermentative Gram-Negative Bacteria. *Clin. Infect. Dis.* **27**, 93–99 (1998).
33. Tamber, S. & Hancock, R. E. The outer membranes of *Pseudomonads*. In: Ramos, J-L., (eds) *Pseudomonas*. Springer, Boston, MA. 575–601 (2004).
34. Chevalier, S. *et al.* Structure , function and regulation of *Pseudomonas aeruginosa* porins. *FEMS Microbiol. Rev.* **41**, 698–722 (2017).
35. Pagès, J. M., James, C. E. & Winterhalter, M. The porin and the permeating antibiotic: A selective diffusion barrier in Gram-negative bacteria. *Nat. Rev. Microbiol.* **6**, 893–903 (2008).
36. Vergalli, J. *et al.* Porins and small-molecule translocation across the outer membrane of Gram-negative bacteria. *Nat. Rev. Microbiol.* **18**, 164-176 (2019).
37. Li, X.-Z. & Nikaido, H. Efflux-Mediated Drug Resistance in Bacteria An Update. *Drugs* **69**, 1555–1623 (2009).
38. Huang, L. *et al.* Bacterial Multidrug Efflux Pumps at the Frontline of Antimicrobial Resistance: An Overview. *Antibiotics* **11** (2022).
39. Ciofu, O. & Tolker-Nielsen, T. Tolerance and resistance of *Pseudomonas aeruginosa* biofilms to antimicrobial agents- how *P. aeruginosa* can escape antibiotics. *Front. Microbiol.* **10** (2019).
40. Sindeldecker, D. & Stoodley, P. The many antibiotic resistance and tolerance strategies of *Pseudomonas aeruginosa*. *Biofilm* **3** (2021).
41. Katz, L. & Baltz, R. H. Natural product discovery: past, present, and future. *J. Ind. Microbiol. Biotechnol.* **43**, 155–176 (2016).
42. Berdy, J. Thoughts and facts about antibiotics: Where we are now and where we are heading. *J. Antibiot. (Tokyo)*. **65**, 385–395 (2012).
43. Chan, P. F., Holmes, D. J. & Payne, D. J. Finding the gems using genomic discovery: antibacterial drug discovery strategies – the successes and the challenges. *Drug Discov. Today Ther. Strateg.* **1**, 519–527 (2004).
44. Tommasi, R., Brown, D. G., Walkup, G. K., Manchester, J. I. & Miller, A. A. ESKAPEing the labyrinth of antibacterial discovery. *Nat. Rev. Drug Discov.* **14**, 529–542 (2015).
45. Payne, D. J., Gwynn, M. N., Holmes, D. J. & Pompliano, D. L. Drugs for bad bugs: Confronting the challenges of antibacterial discovery. *Nat. Rev. Drug Discov.* **6**, 29–40 (2007).
46. Brown, E. D. & Wright, G. D. Antibacterial drug discovery in the resistance era. *Nature* **529**, 336–343 (2016).
47. Imai, Y. *et al.* A new antibiotic selectively kills Gram-negative pathogens. *Nature* **576**, (2019).
48. Ling, L. L. *et al.* A new antibiotic kills pathogens without detectable resistance. *Nature* **517**, 455–459 (2015).
49. Crits-christoph, A., Diamond, S., Butterfield, C. N., Thomas, B. C. & Banfield, J. F. Novel soil bacteria possess diverse genes for secondary metabolite biosynthesis. *Nature* **558**, 440–444 (2018).
50. Ochi, K. & Hosaka, T. New strategies for drug discovery: Activation of silent or weakly expressed microbial gene clusters. *Appl. Microbiol. Biotechnol.* **97**, 87–98 (2013).
51. Rutledge, P. J. & Challis, G. L. Discovery of microbial natural products by activation of silent biosynthetic gene clusters. *Nat. Rev. Microbiol.* **13**, 509–523 (2015).
52. Wang, B., Guo, F., Dong, S.-H. & Zhao, H. Activation of silent biosynthetic gene clusters using transcription factors decoys. *Nat. Chem. Biol.* **15**, 111–114 (2019).

References

53. Liu, R. *et al.* A Synthetic Dual Drug Sideromycin Induces Gram-Negative Bacteria to Commit Suicide with a Gram-Positive Antibiotic. *J. Med. Chem.* **61**, 3845–3854 (2018).
54. Ong'uti, S., Czech, M., Robilotti, E. & Holubar, M. Cefiderocol : A New Cephalosporin Stratagem Against Multidrug-Resistant Gram-Negative Bacteria. *Rev. Anti-Infective Agents* **74**, 1303–1312 (2022).
55. Wright, G. D. Opportunities for natural products in 21st century antibiotic discovery. *Nat. Prod. Rep.* **34**, 694–701 (2017).
56. Newman, D. J. & Cragg, G. M. Natural Products as Sources of New Drugs over the Nearly Four Decades from 01/1981 to 09/2019. *J. Nat. Prod.* **83**, 770–803 (2020).
57. Demain, A. L. Importance of microbial natural products and the need to revitalize their discovery. *J. Ind. Microbiol. Biotechnol.* **41**, 185–201 (2014).
58. Fetzner, S. Quorum quenching enzymes. *J. Biotechnol.* **201**, 2–14 (2015).
59. Defoirdt, T. Quorum-Sensing Systems as Targets for Antivirulence Therapy. *Trends Microbiol.* **26**, 313–328 (2018).
60. Vilaplana, L. & Marco, M. P. Phenazines as potential biomarkers of *Pseudomonas aeruginosa* infections: synthesis regulation, pathogenesis and analytical methods for their detection. *Anal. BioAnal. Chem.* **412**, 5897–5912 (2020).
61. Anwar, H. & Costerton, J. W. Enhanced activity of combination of tobramycin and piperacillin for eradication of sessile biofilm cells of *Pseudomonas aeruginosa*. *Antimicrob. Agents Chemother.* **34**, 1666–1671 (1990).
62. Moskowitz, S. M., Foster, J. M., Emerson, J. & Burns, J. L. Clinically Feasible Biofilm Susceptibility Assay for Isolates of *Pseudomonas aeruginosa* from Patients with Cystic Fibrosis. *J. Clin. Microbiol.* **42**, 1915–1922 (2004).
63. Bjarnsholt, T. *et al.* *Pseudomonas aeruginosa* tolerance to tobramycin, hydrogen peroxide and polymorphonuclear leukocytes is quorum-sensing dependent. *Microbiology* **151**, 373–383 (2005).
64. Hall, C. W. & Mah, T. F. Molecular mechanisms of biofilm-based antibiotic resistance and tolerance in pathogenic bacteria. *FEMS Microbiol. Rev.* **41**, 276–301 (2017).
65. Engebrecht, J. & Silverman, M. Identification of genes and gene products necessary for bacterial bioluminescence. *Proc. Natl. Acad. Sci. U. S. A.* **81**, 4154–4158 (1984).
66. Eberhard, A. *et al.* Structural Identification of Autoinducer of *Photobacterium fischeri* Luciferase. *Biochemistry* **20**, 2444–2449 (1981).
67. Galloway, W. R. J. D., Hodgkinson, J. T., Bowden, S. D., Welch, M. & Spring, D. R. Quorum sensing in Gram-negative bacteria: Small-molecule modulation of AHL and AI-2 quorum sensing pathways. *Chem. Rev.* **111**, 28–67 (2011).
68. Lee, J. & Zhang, L. The hierarchy quorum sensing network in *Pseudomonas aeruginosa*. *Protein Cell* **6**, 26–41 (2014).
69. García-Reyes, S., Soberón-Chávez, G. & Cocotl-Yanez, M. The third quorum-sensing system of *Pseudomonas aeruginosa*: *Pseudomonas* quinolone signal and the enigmatic PqsE protein. *J. Med. Microbiol.* **69**, 25–34 (2020).
70. Schuster, M. & Greenberg, E. P. A network of networks: Quorum-sensing gene regulation in *Pseudomonas aeruginosa*. *Int. J. Med. Microbiol.* **296**, 73–81 (2006).
71. Passador, L., Cook, J. M., Gambello, M. J., Rust, L. & Iglewski, B. H. Expression of *Pseudomonas aeruginosa* virulence genes requires cell-to-cell communication. *Science* **260**, 1127–1130 (1993).
72. Gambello, M. J., Kaye, S. & Iglewski, B. H. LasR of *Pseudomonas aeruginosa* is a transcriptional activator of the alkaline protease gene (*apr*) and an enhancer of exotoxin A expression. *Infect. Immun.* **61**, 1180–1184 (1993).
73. Everett, M. J. & Davies, D. T. *Pseudomonas aeruginosa* elastase (LasB) as a therapeutic target. *Drug Discov. Today* **26**, 2108–2123 (2021).
74. Cruz, R. L. *et al.* RhlR-Regulated Acyl-Homoserine Lactone Quorum Sensing in a Cystic Fibrosis Isolate of

-
- Pseudomonas aeruginosa*. *mBio* **11**, 1–14 (2020).
75. Jakobsen, T. H., Tolker-Nielsen, T. & Givskov, M. Bacterial biofilm control by perturbation of bacterial signaling processes. *Int. J. Mol. Sci.* **18**, (2017).
 76. Jakobsen, T. H., Bjarnsholt, T., Jensen, P. Ø., Givskov, M. & Høiby, N. Targeting quorum sensing in *Pseudomonas aeruginosa* biofilms: current and emerging inhibitors. *Future Microbiol.* **8**, 901–921 (2013).
 77. Hentzer, M. *et al.* Attenuation of *Pseudomonas aeruginosa* virulence by quorum sensing inhibitors. *EMBO J.* **22**, 3803–3815 (2003).
 78. Duplantier, M., Lohou, E. & Sonnet, P. Quorum Sensing Inhibitors to Quench *P. aeruginosa* Pathogenicity. *Pharmaceuticals* **14** (2021).
 79. O’Loughlin, C. T. *et al.* A quorum-sensing inhibitor blocks *Pseudomonas aeruginosa* virulence and biofilm formation. *Proc. Natl. Acad. Sci. U. S. A.* **110**, 17981–17986 (2013).
 80. Manefield, M. *et al.* Halogenated furanones inhibit quorum sensing through accelerated LuxR turnover. *Microbiology* **148**, 1119–1127 (2002).
 81. Jakobsen, T. H. *et al.* Ajoene, a Sulfur-Rich Molecule from Garlic, Inhibits Genes Controlled by Quorum Sensing. *Antimicrob. Agents Chemother.* **56**, 2314–2325 (2012).
 82. Gopu, V., Meena, C. K. & Shetty, P. H. Quercetin Influences Quorum Sensing in Food Borne Bacteria: *In-Vitro* and *In-Silico* Evidence. *PLoS One* **10**, 1–17 (2015).
 83. Rasmussen, T. B. *et al.* Identity and effects of quorum-sensing inhibitors produced by *Penicillium* species. *Microbiology* **151**, 1325–1340 (2005).
 84. Skogman, M. E., Kanerva, S., Manner, S., Vuorela, P. M. & Fallarero, A. Flavones as quorum sensing inhibitors identified by a newly optimized screening platform using *Chromobacterium violaceum* as reporter bacteria. *Molecules* **21** (2016).
 85. Pearson, J. P., Feldman, M., Iglewski, B. H. & Prince, A. *Pseudomonas aeruginosa* cell-to-cell signaling is required for virulence in a model of acute pulmonary infection. *Infect. Immun.* **68**, 4331–4334 (2000).
 86. Rumbaugh, K. P., Griswold, J. A. & Iglewski, B. H. Contribution of Quorum Sensing to the Virulence of *Pseudomonas aeruginosa* in Burn Wound Infections. *Infect. Immun.* **67**, 5854–5862 (1999).
 87. Tang, H. B. *et al.* Contribution of Specific *Pseudomonas aeruginosa* Virulence Factors to Pathogenesis of Pneumonia in a Neonatal Mouse Model of Infection. *Infect. Immun.* **64**, 37–43 (1996).
 88. Tang, H. *et al.* Epigallocatechin-3-Gallate Ameliorates Acute Lung Damage by Inhibiting Quorum-Sensing-Related Virulence Factors of *Pseudomonas aeruginosa*. *Front. Microbiol.* **13**, (2022).
 89. Singh, V. K. *et al.* Tackling recalcitrant *Pseudomonas aeruginosa* infections in critical illness via anti-virulence monotherapy. *Nat. Commun.* **13**, (2022).
 90. Azimi, S., Klementiev, A. D., Whiteley, M. & Diggle, S. P. Bacterial Quorum Sensing During Infection. *Annu. Rev. Microbiol.* **74**, 201–219 (2020).
 91. Feltner, J. B. *et al.* LasR Variant Cystic Fibrosis Isolates Reveal an Adaptable Quorum-Sensing Hierarchy in *Pseudomonas aeruginosa*. *mBio* **7** (2016).
 92. Kostylev, M. *et al.* Evolution of the *Pseudomonas aeruginosa* quorum-sensing hierarchy. *Proc. Natl. Acad. Sci. U. S. A.* **116**, 7027–7032 (2019).
 93. Middleton, B. *et al.* Direct detection of N-acylhomoserine lactones in cystic fibrosis sputum. *FEMS Microbiol. Lett.* **207**, 1–7 (2002).
 94. Singh, P. K. *et al.* Quorum-sensing signals indicate that cystic fibrosis lungs are infected with bacterial biofilms. *Nature* **407**, 762–764 (2000).
 95. Erickson, D. L. *et al.* *Pseudomonas aeruginosa* quorum-sensing systems may control virulence factor expression in the lungs of patients with cystic fibrosis. *Infect. Immun.* **70**, 1783–1790 (2002).
 96. Collier, D. N. *et al.* A bacterial cell to cell signal in the lungs of cystic fibrosis patients. *FEMS Microbiol. Lett.* **215**, 1–6 (2002).

References

97. Cornforth, D. M. *et al.* *Pseudomonas aeruginosa* transcriptome during human infection. *Proc. Natl. Acad. Sci. U. S. A.* **115** (2018).
98. Gifford, A. H. *et al.* Use of a multiplex transcript method for analysis of *Pseudomonas aeruginosa* gene expression profiles in the cystic fibrosis lung. *Infect. Immun.* **84**, 2995–3006 (2016).
99. Rossi, E., Falcone, M., Molin, S. & Johansen, H. K. High-resolution *in situ* transcriptomics of *Pseudomonas aeruginosa* unveils genotype independent patho-phenotypes in cystic fibrosis lungs. *Nat. Commun.* **9**, 1–13 (2018).
100. Laxminarayan, R. *et al.* Access to effective antimicrobials: A worldwide challenge. *Lancet* **387**, 168–175 (2016).
101. Ventola, C. L. The Antibiotic Resistance Crisis. *Pharm. Ther.* **40**, 561–564 (2019).
102. Cassini, A. *et al.* Attributable deaths and disability-adjusted life-years caused by infections with antibiotic-resistant bacteria in the EU and the European Economic Area in 2015: a population-level modelling analysis. *Lancet Infect. Dis.* **19**, 56–66 (2019).
103. Masi, M., Réfregiers, M., Pos, K. M. & Pagès, J. M. Mechanisms of envelope permeability and antibiotic influx and efflux in Gram-negative bacteria. *Nat. Microbiol.* **2** (2017).
104. Richter, M. F. & Hergenrother, P. J. The challenge of converting Gram-positive-only compounds into broad-spectrum antibiotics. *Ann. N. Y. Acad. Sci.* **1435**, 1–21 (2018).
105. Fischbach, M. A. & Walsh, C. T. Antibiotics For Emerging Pathogens. *Science* **325**, 1089–1093 (2009).
106. Bassler, B. L. & Losick, R. Bacterially Speaking. *Cell* **125**, 237–246 (2006).
107. Mukherjee, S. *et al.* The PqsE and RhIR proteins are an autoinducer synthase–receptor pair that control virulence and biofilm development in *Pseudomonas aeruginosa*. *Proc. Natl. Acad. Sci. U. S. A.* **115** (2018).
108. Cornelis, P. Putting an end to the *Pseudomonas aeruginosa* IQS controversy. *Microbiologyopen* **9**, 2019–2020 (2020).
109. Brint, J. M. & Ohman, D. E. Synthesis of multiple exoproducts in *Pseudomonas aeruginosa* is under the control of RhIR-RhII, another set of regulators in strain PAO1 with homology to the autoinducer-responsive LuxR-LuxI family. *J. Bacteriol.* **177**, 7155–7163 (1995).
110. Ochsner, U. A. & Reiser, J. Autoinducer-mediated regulation of rhamnolipid biosurfactant synthesis in *Pseudomonas aeruginosa*. *Proc. Natl. Acad. Sci. U. S. A.* **92**, 6424–6428 (1995).
111. Allesen-Holm, M. *et al.* A characterization of DNA release in *Pseudomonas aeruginosa* cultures and biofilms. *Mol. Microbiol.* **59**, 1114–1128 (2006).
112. Givskov, M. *et al.* Eukaryotic interference with homoserine lactone-mediated prokaryotic signalling. *J. Bacteriol.* **178**, 6618–6622 (1996).
113. Brakhage, A. A. Regulation of fungal secondary metabolism. *Nat. Rev. Microbiol.* **11**, 21–32 (2013).
114. Keller, N. P. Fungal secondary metabolism: regulation, function and drug discovery. *Nat. Rev. Microbiol.* **17**, 167–180 (2018).
115. Kalia, V. C. Quorum sensing inhibitors: An overview. *Biotechnol. Adv.* **31**, 224–245 (2013).
116. Hoeksma, J. *et al.* A new perspective on fungal metabolites: identification of bioactive compounds from fungi using zebrafish embryogenesis as read-out. *Sci. Rep.* **9**, 1–16 (2019).
117. Manner, S. & Fallarero, A. Screening of natural product derivatives identifies two structurally related flavonoids as potent quorum sensing inhibitors against Gram-negative bacteria. *Int. J. Mol. Sci.* **19** (2018).
118. Jakobsen, T. H., Alhede, M., Hultqvist, L. D., Bjarnsholt, T. & Givskov, M. Qualitative and Quantitative Determination of Quorum Sensing Inhibition *In Vitro*. *Quor. Sens. Methods Protoc.* **1673**, 275–285 (2010).
119. Essar, D. W., Eberly, L., Hadero, A. & Crawford, I. P. Identification and characterization of genes for a second anthranilate synthase in *Pseudomonas aeruginosa*: Interchangeability of the two anthranilate synthase and evolutionary implications. *J. Bacteriol.* **172**, 884–900 (1990).
120. Zhou, S., Zhang, A. & Chu, W. Phillyrin is an effective inhibitor of quorum sensing with potential as an anti-

-
- Pseudomonas aeruginosa* infection therapy. *J. Vet. Med. Sci.* **81**, 473–479 (2019).
121. Guerin, T. F., Mondido, M., McClenn, B. & Peasley, B. Application of resazurin for estimating abundance of contaminant-degrading micro-organisms. *Lett. Appl. Microbiol.* **32**, 340–345 (2001).
 122. Rampersad, S. N. Multiple applications of alamar blue as an indicator of metabolic function and cellular health in cell viability bioassays. *Sensors* **12**, 12347–12360 (2012).
 123. Rasmussen, T. B. *et al.* Screening for Quorum-Sensing Inhibitors (QSI) by Use of a Novel Genetic System, the QSI Selector. *J. Bacteriol.* **187**, 1799–1814 (2005).
 124. Ahmed, S. A. K. S. *et al.* Natural quorum sensing inhibitors effectively downregulate gene expression of *Pseudomonas aeruginosa* virulence factors. *Appl. Microbiol. Biotechnol.* **103**, 3521–3535 (2019).
 125. Yang, L. *et al.* Computer-aided identification of recognized drugs as *Pseudomonas aeruginosa* quorum-sensing inhibitors. *Antimicrob. Agents Chemother.* **53**, 2432–2443 (2009).
 126. Biswas, N. N. *et al.* Indole-based novel small molecules for the modulation of bacterial signalling pathways. *Org. Biomol. Chem.* **13**, 925–937 (2015).
 127. Hidalgo-Romano, B. *et al.* Indole inhibition of N-acylated homoserine lactone-mediated quorum signalling is widespread in Gram-negative bacteria. *Microbiology* **160**, 2464–2473 (2014).
 128. Lee, J., Attila, C., Cirillo, S. L. G., Cirillo, J. D. & Wood, T. K. Indole and 7-hydroxyindole diminish *Pseudomonas aeruginosa* virulence. *Microb. Biotechnol.* **2**, 75–90 (2009).
 129. Monte, J., Abreu, A. C., Borges, A., Simões, L. C. & Simões, M. Antimicrobial activity of selected phytochemicals against *Escherichia coli* and *Staphylococcus aureus* and their biofilms. *Pathogens* **3**, 473–498 (2014).
 130. Tan, S. Y. Y. *et al.* Identification of five structurally unrelated quorum-sensing inhibitors of *Pseudomonas aeruginosa* from a natural-derivative database. *Antimicrob. Agents Chemother.* **57**, 5629–5641 (2013).
 131. Anke, H., Schwab, H. & Achenbach, H. Tetrionic Acid Derivatives From *Aspergillus Panamensis*. *J. Antibiot.* **33**, 6–11 (1980).
 132. Burghart-Stoll, H. & Brückner, R. Total syntheses of the gregatins A-D and aspertetronin A: Structure revisions of these compounds and of aspertetronin B, together with plausible structure revisions of gregatin E, cyclogregatin, graminin A, the penicillols A and B, and the huaspenones A. *European J. Org. Chem.* 3978–4017 (2012)
 133. Proctor, C. R., McCarron, P. A. & Ternan, N. G. Furanone quorum-sensing inhibitors with potential as novel therapeutics against *Pseudomonas aeruginosa*. *J. Med. Microbiol.* **69**, 195–206 (2020).
 134. Altschul, S. F. *et al.* Gapped BLAST and PSI-BLAST: a new generation of protein database search programs. *Nucleic Acids Res.* **25**, 3389–3402 (1997).
 135. Altschul, S. F. *et al.* Protein Database Searches Using Compositionally Adjusted Substitution Matrices. *FEBS J.* **272**, 5101–5109 (2005).
 136. Stauff, D. L., Bassler, B. L., Hughes, H. & Chase, C. Quorum Sensing in *Chromobacterium violaceum*: DNA Recognition and Gene Regulation by the CviR Receptor. *J. Bacteriol.* **193**, 3871–3878 (2011).
 137. Dreier, J. & Ruggerone, P. Interaction of antibacterial compounds with RND efflux pumps in *Pseudomonas aeruginosa*. *Front. Microbiol.* **6**, 1–21 (2015).
 138. Williams, P. & Cámara, M. Quorum sensing and environmental adaptation in *Pseudomonas aeruginosa*: a tale of regulatory networks and multifunctional signal molecules. *Curr. Opin. Microbiol.* **12**, 182–191 (2009).
 139. Kang, D., Zhang, L. & Kirienko, N. V. High-Throughput Approaches for the Identification of *Pseudomonas aeruginosa* Antivirulents. *mBio* **12**, 1–16 (2021).
 140. Starkey, M. *et al.* Identification of Anti-virulence Compounds That Disrupt Quorum-Sensing Regulated Acute and Persistent Pathogenicity. *PLoS Pathog.* **10** (2014).
 141. Müh, U. *et al.* Novel *Pseudomonas aeruginosa* quorum-sensing inhibitors identified in an ultra-high-throughput screen. *Antimicrob. Agents Chemother.* **50**, 3674–3679 (2006).
 142. Welsh, M. A., Eibergen, N. R., Moore, J. D. & Blackwell, H. E. Small Molecule Disruption of Quorum Sensing Cross-Regulation in *Pseudomonas aeruginosa* Causes Major and Unexpected Alterations to Virulence

References

- Phenotypes. *J. Am. Chem. Soc.* **137**, 1510–1519 (2015).
143. Welsh, M. A. & Blackwell, H. E. Chemical Genetics Reveals Environment-Specific Roles for Quorum Sensing Circuits in *Pseudomonas aeruginosa*. *Cell Chem. Biol.* **23**, 361–369 (2016).
144. Smith, K. M., Bu, Y. & Suga, H. Library Screening for Synthetic Agonists and antagonists of a *Pseudomonas aeruginosa* Autoinducer. *Chem. Biol.* **10**, 563–571 (2003).
145. Smith, K. M., Bu, Y. & Suga, H. Induction and Inhibition of *Pseudomonas aeruginosa* Quorum Sensing by Synthetic Autoinducer Analogs. *Chem. Biol.* **10**, 81–89 (2003).
146. Huang, H. *et al.* An integrated genomic regulatory network of virulence-related transcriptional factors in *Pseudomonas aeruginosa*. *Nat. Commun.* **10**, (2019).
147. Perinbam, K., Chacko, J. V., Kannan, A., Digman, M. A. & Siryaporn, A. A shift in Central metabolism accompanies virulence activation in *Pseudomonas aeruginosa*. *mBio* **11**, 1–16 (2020).
148. Bartell, J. A. *et al.* Reconstruction of the metabolic network of *Pseudomonas aeruginosa* to interrogate virulence factor synthesis. *Nat. Commun.* **8** (2017).
149. Bode, H. B., Bethe, B., Höfs, R. & Zeeck, A. Big effects from small changes: possible ways to explore nature's chemical diversity. *ChemBiochem* **3**, 619–627 (2002).
150. Burrows, L. L. The Therapeutic Pipeline for *Pseudomonas aeruginosa* Infections. *ACS Infect. Dis.* **4**, 1041–1047 (2018).
151. Williams, H. D. & Davies, J. C. Basic science for the chest physician: *Pseudomonas aeruginosa* and the cystic fibrosis airway. *Thorax* **67**, 465–467 (2012).
152. Whitehead, N. A., Barnard, A. M. L., Slater, H., Simpson, N. J. L. & Salmond, G. P. C. Quorum-sensing in Gram-negative bacteria. *FEMS Microbiol. Lett.* **25**, 365–404 (2001).
153. Soto-Aceves, M. P., González-Valdez, A., Cocotl-Yañez, M. & Soberón-Chávez, G. *Pseudomonas aeruginosa* LasR overexpression leads to a RsaL-independent pyocyanin production inhibition in a low phosphate condition. *Microbiology* **168**, 1–8 (2022).
154. Soukarieh, F., Williams, P., Stocks, M. J. & Cámara, M. *Pseudomonas aeruginosa* Quorum Sensing Systems as Drug Discovery Targets: Current Position and Future Perspectives. *J. Med. Chem.* **61**, 10385–10402 (2018).
155. Schütz, C. & Empting, M. Targeting the *Pseudomonas* quinolone signal quorum sensing system for the discovery of novel anti-infective pathoblockers. *Beilstein J. Org. Chem.* **14**, 2627–2645 (2018).
156. D'Angelo, F. *et al.* Identification of FDA-approved drugs as antivirulence agents targeting the PQS Quorum-Sensing system of *Pseudomonas aeruginosa*. *Antimicrob. Agents Chemother.* **62**, 1–20 (2018).
157. Beenker, W. A. G., Hoeksma, J. & den Hertog, J. Gregatins, a Group of Related Fungal Secondary Metabolites, Inhibit Aspects of Quorum Sensing in Gram-Negative Bacteria. *Front. Microbiol.* **13** (2022).
158. Hmelo, L. R. *et al.* Precision-engineering the *Pseudomonas aeruginosa* genome with two-step allelic exchange. *Nat. Protoc.* **10**, 1820–1841 (2015).
159. Pleguezuelos-Manzano, C. *et al.* Establishment and Culture of Human Intestinal Organoids Derived from Adult Stem Cells. *Curr. Protoc. Immunol.* **130** (2020).
160. Driehuis, E., Kretzschmar, K. & Clevers, H. Establishment of patient-derived cancer organoids for drug-screening applications. *Nat. Protoc.* **15**, 3380–3409 (2020).
161. Aleström, P. *et al.* Zebrafish: Housing and husbandry recommendations. *Lab. Anim.* **54**, 213–224 (2020).
162. Lu, R. *et al.* New tyrosinase inhibitors from *Paecilomyces gunnii*. *J. Agric. Food Chem.* **62**, 11917–11923 (2014).
163. Nadal Jimenez, P. *et al.* The Multiple Signaling Systems Regulating Virulence in *Pseudomonas aeruginosa*. *Microbiol. Mol. Biol. Rev.* **76**, 46–65 (2012).
164. Calfee, M. W., Coleman, J. P. & Pesci, E. C. Interference with *Pseudomonas* quinolone signal synthesis inhibits virulence factor expression by *Pseudomonas aeruginosa*. *Proc. Natl. Acad. Sci. U. S. A.* **98**, 11633–11637 (2001).

165. Déziel, E. *et al.* Analysis of *Pseudomonas aeruginosa* 4-hydroxy-2-alkylquinolines (HAQs) reveals a role for 4-hydroxy-2-heptylquinoline in cell-to-cell communication. *Proc. Natl. Acad. Sci. U. S. A.* **101**, 1339–1344 (2004).
166. Coleman, J. P. *et al.* *Pseudomonas aeruginosa* PqsA is an anthranilate-coenzyme A ligase. *J. Bacteriol.* **190**, 1247–1255 (2008).
167. Dulcey, C. E. *et al.* The end of a long-standing hypothesis: the *Pseudomonas* signalling molecules 4-hydroxy-2-alkylquinolines are derived from fatty acids, not 3-ketofatty acids. *Chem. Biol.* **20** (2013).
168. Zhang, Y. M., Frank, M. W., Zhu, K., Mayasundari, A. & Rock, C. O. PqsD is responsible for the synthesis of 2,4-dihydroxyquinoline, an extracellular metabolite produced by *Pseudomonas aeruginosa*. *J. Biol. Chem.* **283**, 28788–28794 (2008).
169. Drees, S. L. & Fetzner, S. PqsE of *Pseudomonas aeruginosa* acts as pathway-specific thioesterase in the biosynthesis of alkylquinolone signaling molecules. *Chem. Biol.* **22**, 611–618 (2015).
170. Schertzer, J. W., Brown, S. A. & Whiteley, M. Oxygen Levels Rapidly Modulate *Pseudomonas aeruginosa* Social Behaviors via Substrate Limitation of PqsH. *Mol. Microbiol.* **77**, 1527–1538 (2010).
171. Drees, S. L. *et al.* PqsL uses reduced flavin to produce 2-hydroxylaminobenzoylacetate, a preferred PqsBC substrate in alkyl quinolone biosynthesis in *Pseudomonas aeruginosa*. *J. Biol. Chem.* **293**, 9345–9357 (2018).
172. Allegretta, G. *et al.* In-depth profiling of MvfR-regulated small molecules in *Pseudomonas aeruginosa* after Quorum Sensing inhibitor treatment. *Front. Microbiol.* **8**, 1–12 (2017).
173. Maura, D. *et al.* Polypharmacology Approaches against the *Pseudomonas aeruginosa* MvfR Regulon and Their Application in Blocking Virulence and Antibiotic Tolerance. *ACS Chem. Biol.* **12**, 1435–1443 (2017).
174. Witzgall, F. *et al.* The alkylquinolone repertoire of *Pseudomonas aeruginosa* is linked to structural flexibility of the Fabh-like 2-heptyl-3-hydroxy-4(1h)-quinolone (PQS) biosynthesis enzyme PqsBC. *ChemBiochem* **19**, 1531–1544 (2018).
175. Drees, S. L. *et al.* PqsBC, a condensing enzyme in the biosynthesis of the *Pseudomonas aeruginosa* quinolone signal: Crystal structure, inhibition, and reaction mechanism. *J. Biol. Chem.* **291**, 6610–6624 (2016).
176. Maura, D., Hazan, R., Kitao, T., Ballok, A. E. & Rahme, L. G. Evidence for direct control of virulence and defense gene circuits by the *Pseudomonas aeruginosa* quorum sensing regulator, MvfR. *Sci. Rep.* **6**, 1–14 (2016).
177. Rampioni, G. *et al.* Unravelling the Genome-Wide Contributions of Specific 2-Alkyl-4-Quinolones and PqsE to Quorum Sensing in *Pseudomonas aeruginosa*. *PLoS Pathog.* **12**, 1–25 (2016).
178. Déziel, E. *et al.* The contribution of MvfR to *Pseudomonas aeruginosa* pathogenesis and quorum sensing circuitry regulation: Multiple quorum sensing-regulated genes are modulated without affecting *lasRI*, *rhlRI* or the production of N-acyl-L-homoserine lactones. *Mol. Microbiol.* **55**, 998–1014 (2005).
179. Farrow, J. M. *et al.* PqsE functions independently of PqsR-*Pseudomonas* quinolone signal and enhances the *rhl* quorum-sensing system. *J. Bacteriol.* **190**, 7043–7051 (2008).
180. Hazan, R. *et al.* Homeostatic interplay between bacterial cell-cell signaling and iron in virulence. *PLoS Pathog.* **6** (2010).
181. Simanek, K. A., Taylor, I. R., Richael, E. K. & Lasek-nesselquist, E. The PqsE-RhIR Interaction Regulates RhIR DNA Binding to Control Virulence Factor Production in *Pseudomonas aeruginosa*. *Microbiol. Spectr.* **10** (2022).
182. Borgert, S. R. *et al.* Moonlighting chaperone activity of the enzyme PqsE contributes to RhIR-controlled virulence of *Pseudomonas aeruginosa*. *Nat. Commun.* **13** (2022).
183. Lau, G. W., Hassett, D. J., Ran, H. & Kong, F. The role of pyocyanin in *Pseudomonas aeruginosa* infection. *Trends Mol. Med.* **10**, 599–606 (2004).
184. Price-Whelan, A., Dietrich, L. E. P. & Newman, D. K. Rethinking ‘secondary’ metabolism: Physiological roles for phenazine antibiotics. *Nat. Chem. Biol.* **2**, 71–78 (2006).
185. Hall, S. *et al.* Cellular effects of pyocyanin, a secreted virulence factor of *Pseudomonas aeruginosa*. *Toxins* **8**, 1–14 (2016).

References

186. Rada, B. & Leto, T. L. Pyocyanin effects on respiratory epithelium: Relevance in *Pseudomonas aeruginosa* airway infections. *Trends Microbiol.* **21**, 73–81 (2013).
187. Mahajan-Miklos, S., Tan, M. W., Rahme, L. G. & Ausubel, F. M. Molecular mechanisms of bacterial virulence elucidated using a *Pseudomonas aeruginosa*-*Caenorhabditis elegans* pathogenesis model. *Cell* **96**, 47–56 (1999).
188. Lau, G. W. *et al.* The *Drosophila melanogaster* toll pathway participates in resistance to infection by the Gram-negative human pathogen *Pseudomonas aeruginosa*. *Infect. Immun.* **71**, 4059–4066 (2003).
189. Lau, G. W., Ran, H., Kong, F., Hassett, D. J. & Mavrodi, D. *Pseudomonas aeruginosa* pyocyanin is critical for lung infection in mice. *Infect. Immun.* **72**, 4275–4278 (2004).
190. Wilson, R. *et al.* Measurement of *Pseudomonas aeruginosa* phenazine pigments in sputum and assessment of their contribution to sputum sol toxicity for respiratory epithelium. *Infect. Immun.* **56**, 2515–2517 (1988).
191. Ramos, I., Dietrich, L. E. P., Price-Whelan, A. & Newman, D. K. Phenazines affect biofilm formation by *Pseudomonas aeruginosa* in similar ways at various scales. *Res. Microbiol.* **161**, 187–191 (2010).
192. Cox, C. D. Role of pyocyanin in the acquisition of iron from transferrin. *Infect. Immun.* **52**, 263–270 (1986).
193. Hentzer, M. & Givskov, M. Pharmacological inhibition of quorum sensing for the treatment of chronic bacterial infections. *J. Clin. Invest.* **112**, 1300–1307 (2003).
194. Yang, L. *et al.* Effects of iron on DNA release and biofilm development by *Pseudomonas aeruginosa*. *Microbiology* **153**, 1318–1328 (2007).
195. Hentzer, M. *et al.* Inhibition of quorum sensing in *Pseudomonas aeruginosa* biofilm bacteria by a halogenated furanone compound. *Microbiology* **148**, 87–102 (2002).
196. Fong, J. *et al.* Disulfide Bond-Containing Ajoene Analogues As Novel Quorum Sensing Inhibitors of *Pseudomonas aeruginosa*. *J. Med. Chem.* **60**, 215–227 (2017).
197. Malhotra, S., Hayes, D. & Wozniak, D. J. Cystic fibrosis and *Pseudomonas aeruginosa*: The host-microbe interface. *Clin. Microbiol. Rev.* **32**, 1–46 (2019).
198. Quinton, P. M. Cystic fibrosis: impaired bicarbonate secretion and mucoviscidosis. *Lancet* **372**, 415–417 (2008).
199. Kunzelmann, K., Schreiber, R. & Hadorn, H. B. Bicarbonate in cystic fibrosis. *J. Cyst. Fibros.* **16**, 653–662 (2017).
200. Forbes, E. & Abu-Sbaih, R. Cystic fibrosis. *Nat. Rev. Dis. Prim.* (2015)
201. De Boeck, K. Cystic fibrosis in the year 2020: A disease with a new face. *Acta Paediatr. Int. J. Paediatr.* **109**, 893–899 (2020).
202. Rossi, E. *et al.* *Pseudomonas aeruginosa* adaptation and evolution in patients with cystic fibrosis. *Nat. Rev. Microbiol.* **19** (2021).
203. Foundation, C. F. Cystic Fibrosis Foundation Patient Registry, 2021 Annual Data Report. *Cyst. Fibros. Found. Publ.* (2022).
204. SINGH, V. K. *et al.* Tackling Recalcitrant *Pseudomonas aeruginosa* Infections In Critical Illness via Anti-virulence Monotherapy. *Nat. Commun.* **13** (2022).
205. Marvig, R. L., Sommer, L. M., Molin, S. & Johansen, H. K. Convergent evolution and adaptation of *Pseudomonas aeruginosa* within patients with cystic fibrosis. *Nat. Genet.* **47**, 57–64 (2015).
206. Smith, E. E. *et al.* Genetic adaptation by *Pseudomonas aeruginosa* to the airways of cystic fibrosis patients. *Proc. Natl. Acad. Sci. U. S. A.* **103**, 8487–8492 (2006).
207. Turner, K. H., Wessel, A. K., Palmer, G. C., Murray, J. L. & Whiteley, M. Essential genome of *Pseudomonas aeruginosa* in cystic fibrosis sputum. *Proc. Natl. Acad. Sci. U. S. A.* **112**, 4110–4115 (2015).
208. Gannon, A. D. & Darch, S. E. Tools for the Real-Time Assessment of a *Pseudomonas aeruginosa* Infection Model. *J. Vis. Exp.* 1–17 (2021)
209. Tata, M. *et al.* RNAseq based transcriptional profiling of *Pseudomonas aeruginosa* PA14 after shortand long-

-
- term anoxic cultivation in synthetic cystic fibrosis sputum medium. *PLoS One* **11**, 1–18 (2016).
210. Palmer, K. L., Aye, L. M. & Whiteley, M. Nutritional cues control *Pseudomonas aeruginosa* multicellular behavior in cystic fibrosis sputum. *J. Bacteriol.* **189**, 8079–8087 (2007).
211. Fung, C. *et al.* Gene expression of *Pseudomonas aeruginosa* in a mucin-containing synthetic growth medium mimicking cystic fibrosis lung sputum. *J. Med. Microbiol.* **59**, 1089–1100 (2010).
212. Rosen, B. H. *et al.* Animal and Model Systems for Studying Cystic Fibrosis. *J. Cyst. Fibros.* **17**, S28–S34 (2018).
213. O’Toole, G. A. *et al.* Model Systems to Study the Chronic, Polymicrobial Infections in Cystic Fibrosis: Current Approaches and Exploring Future Directions. *mBio* **12**, 1–8 (2021).
214. McCarron, A., Donnelley, M. & Parsons, D. Airway disease phenotypes in animal models of cystic fibrosis. *Respir. Res.* **19**, 1–12 (2018).
215. Harrington, N. E. *et al.* Antibiotic efficacy testing in an *Ex vivo* model of *Pseudomonas aeruginosa* and *Staphylococcus aureus* biofilms in the cystic fibrosis lung. *J. Vis. Exp.* 1–16 (2021).
216. Harrington, N. E., Littler, J. L. & Harrison, F. Transcriptome Analysis of *Pseudomonas aeruginosa* Biofilm Infection in an *Ex Vivo* Pig Model of the Cystic Fibrosis Lung. *Appl. Environ. Microbiol.* **88** (2022).
217. Joseph, T., Look, D. & Ferkol, T. NF- κ B activation and sustained IL-8 gene expression in primary cultures of cystic fibrosis airway epithelial cells stimulated with *Pseudomonas aeruginosa*. *Am. J. Physiol. - Lung Cell. Mol. Physiol.* **288**, 471–479 (2005).
218. Balloy, V. *et al.* Bronchial epithelial cells from cystic fibrosis patients express a specific long non-coding RNA signature upon *Pseudomonas aeruginosa* infection. *Front. Cell. Infect. Microbiol.* **7**, 1–9 (2017).
219. Tang, M. *et al.* Evaluating Bacterial Pathogenesis Using a Model of Human Airway Organoids Infected with *Pseudomonas aeruginosa* Biofilms. *Microbiol. Spectr.* **10** (2022).
220. Frisk, A. *et al.* Transcriptome analysis of *Pseudomonas aeruginosa* after interaction with human airway epithelial cells. *Infect. Immun.* **72**, 5433–5438 (2004).
221. Zulianello, L. *et al.* Rhamnolipids are virulence factors that promote early infiltration of primary human airway epithelia by *Pseudomonas aeruginosa*. *Infect. Immun.* **74**, 3134–3147 (2006).
222. Tseng, J., Do, J., Widdicombe, J. H. & Machen, T. E. Innate immune responses of human tracheal epithelium to *Pseudomonas aeruginosa* flagellin, TNF- α , and IL-1 β . *Am. J. Physiol. - Cell Physiol.* **290**, 678–690 (2006).
223. Laucirica, D. R., Garratt, L. W. & Kicic, A. Progress in Model Systems of Cystic Fibrosis Mucosal Inflammation to Understand Aberrant Neutrophil Activity. *Front. Immunol.* **11**, 1–12 (2020).
224. Sachs, N. *et al.* Long-term expanding human airway organoids for disease modeling. *EMBO J.* **38**, 1–20 (2019).
225. Dekkers, J. F. *et al.* A functional CFTR assay using primary cystic fibrosis intestinal organoids. *Nat. Med.* **19**, 939–945 (2013).
226. Puschhof, J. *et al.* Intestinal organoid cocultures with microbes. *Nat. Protoc.* **16**, 4633–4649 (2021).
227. Westermann, A. J. & Vogel, J. Host-pathogen transcriptomics by dual RNA-seq. *Methods Mol. Biol.* **1737**, 59–75 (2018).
228. Beenker, W. A. G., Hoeksma, J., Bannier-Hélaouët, M., Clevers, H. & den Hertog, J. Paecilomycone inhibits quorum sensing in Gram-negative bacteria. *Microbiol. Spectr.* **11** (2023).
229. Amatngalim, G. D. *et al.* Measuring cystic fibrosis drug responses in organoids derived from 2D differentiated nasal epithelia. *Life Sci. Alliance* **5**, 1–14 (2022).
230. Aprianto, R., Slager, J., Holsappel, S. & Veening, J. W. Time-resolved dual RNA-seq reveals extensive rewiring of lung epithelial and *Pneumococcal* transcriptomes during early infection. *Genome Biol.* **17**, 1–16 (2016).
231. Dobin, A. *et al.* STAR: Ultrafast universal RNA-seq aligner. *Bioinformatics* **29**, 15–21 (2013).
232. Liao, Y., Smyth, G. K. & Shi, W. FeatureCounts: An efficient general purpose program for assigning sequence reads to genomic features. *Bioinformatics* **30**, 923–930 (2014).
233. Schoch, C. L. *et al.* NCBI Taxonomy: A comprehensive update on curation, resources and tools. *Database*, 1–21 (2020).

References

234. Love, M. I., Huber, W. & Anders, S. Moderated estimation of fold change and dispersion for RNA-seq data with DESeq2. *Genome Biol.* **15**, 1–21 (2014).
235. Blighe, K., Rana, S. & Lewis, M. EnhancedVolcano: Publication-ready volcano plots with enhanced colouring and labeling. <https://github.com/kevinblighe/EnhancedVolcano> (2018).
236. Yu, G., Wang, L. G., Han, Y. & He, Q. Y. ClusterProfiler: An R package for comparing biological themes among gene clusters. *Omi. A J. Integr. Biol.* **16**, 284–287 (2012).
237. Winsor, G. L. *et al.* Enhanced annotations and features for comparing thousands of *Pseudomonas* genomes in the *Pseudomonas* genome database. *Nucleic Acids Res.* **44**, 646–653 (2016).
238. Szklarczyk, D. *et al.* STRING v11: Protein-protein association networks with increased coverage, supporting functional discovery in genome-wide experimental datasets. *Nucleic Acids Res.* **47**, D607–D613 (2019).
239. Moura-Alves, P. *et al.* Host monitoring of quorum sensing during *Pseudomonas aeruginosa* infection. *Science* **366** (2019).
240. Hughes, D. T. & Sperandio, V. Inter-kingdom signalling: communication between bacteria and their hosts. *Nat. Rev. Microbiol.* **6**, 111–120 (2008).
241. Kendall, M. M. & Sperandio, V. What a dinner party! Mechanisms and functions of interkingdom signaling in host-pathogen associations. *mBio* **7**, 1–14 (2016).
242. Vasil, M. L. & Ochsner, U. A. The response of *Pseudomonas aeruginosa* to iron: genetics, biochemistry and virulence. *Mol. Microbiol.* **34**, 399–413 (1999).
243. Bharwad, K. & Rajkumar, S. Rewiring the functional complexity between Crc, Hfq and sRNAs to regulate carbon catabolite repression in *Pseudomonas*. *World J. Microbiol. Biotechnol.* **35**, 1–12 (2019).
244. Rojo, F. Carbon catabolite repression in *Pseudomonas*: Optimizing metabolic versatility and interactions with the environment. *FEMS Microbiol. Rev.* **34**, 658–684 (2010).
245. Line, L. *et al.* Physiological levels of nitrate support anoxic growth by denitrification of *Pseudomonas aeruginosa* at growth rates reported in cystic fibrosis lungs and sputum. *Front. Microbiol.* **5**, 1–11 (2014).
246. Palmer, K. L., Brown, S. A. & Whiteley, M. Membrane-bound nitrate reductase is required for anaerobic growth in cystic fibrosis sputum. *J. Bacteriol.* **189**, 4449–4455 (2007).
247. Hauser, A. R. The Type III Secretion System of *Pseudomonas aeruginosa*: Infection by Injection. *Nat. Rev. Microbiol.* **7**, 654–665 (2009).
248. Hernandez, R. E., Gallegos-Monterrosa, R. & Coulthurst, S. J. Type VI secretion system effector proteins: Effective weapons for bacterial competitiveness. *Cell. Microbiol.* **22**, 1–9 (2020).
249. Chen, L., Zou, Y., She, P. & Wu, Y. Composition, function, and regulation of T6SS in *Pseudomonas aeruginosa*. *Microbiol. Res.* **172**, 19–25 (2015).
250. Sana, T. G., Berni, B. & Bleves, S. The T6SSs of *Pseudomonas aeruginosa* strain PAO1 and their effectors: Beyond bacterial-cell targeting. *Front. Cell. Infect. Microbiol.* **6** (2016).
251. Sana, T. G. *et al.* The second type VI secretion system of *Pseudomonas aeruginosa* strain PAO1 is regulated by quorum sensing and Fur and modulates internalization in epithelial cells. *J. Biol. Chem.* **287**, 27095–27105 (2012).
252. Bundy, B. M., Campbell, A. L. & Neidle, E. L. Similarities between the *antABC*-encoded anthranilate dioxygenase and the *benABC*-encoded benzoate dioxygenase of *Acinetobacter* sp. strain ADP1. *J. Bacteriol.* **180**, 4466–4474 (1998).
253. Thomas, S. R., Anjana, R., Hodson, M. E. & Pitt, T. L. Increased sputum amino acid concentrations and auxotrophy of *Pseudomonas aeruginosa* in severe cystic fibrosis lung disease. *Thorax* **55**, 795–797 (2000).
254. Wilton, M., Halverson, T. W. R., Charron-Mazenod, L., Parkins, M. D. & Lewenza, S. Secreted phosphatase and deoxyribonuclease are required by *Pseudomonas aeruginosa* to defend against neutrophil extracellular traps. *Infect. Immun.* **86**, 1–12 (2018).
255. Kordes, A. *et al.* Genetically diverse *Pseudomonas aeruginosa* populations display similar transcriptomic profiles in a cystic fibrosis explanted lung. *Nat. Commun.* **10** (2019).

256. Wargo, M. J. Choline Catabolism to Glycine Betaine Contributes to *Pseudomonas aeruginosa* Survival during Murine Lung Infection. *PLoS One* **8**, 1–7 (2013).
257. Randell, S. H., Fulcher, M. L., O’Neal, W. & Olsen, J. C. Primary epithelial cell models for cystic fibrosis research. *Methods Mol. Biol.* **742**, 285–310 (2011).
258. Liu, Y. C. *et al.* Contribution of the Alkylquinolone Quorum-Sensing System to the Interaction of *Pseudomonas aeruginosa* With Bronchial Epithelial Cells. *Front. Microbiol.* **9** (2018).
259. Geurts, M. H. & Clevers, H. CRISPR engineering in organoids for gene repair and disease modelling. *Nat. Rev. Bioeng.* **1**, 32–45 (2023).
260. Moura-Alves, P. *et al.* Host monitoring of quorum sensing during *Pseudomonas aeruginosa* infection. *Science* **366** (2019).
261. Moura-Alves, P. *et al.* AhR sensing of bacterial pigments regulates antibacterial defence. *Nature* **512**, 387–392 (2014).
262. Nadsombati, M. S. *et al.* Detection of Succinate by Intestinal Tuft Cells Triggers a Type 2 Innate Immune Circuit. *Immunity* **49**, 33–41 (2018).
263. Tizzano, M. *et al.* Nasal chemosensory cells use bitter taste signaling to detect irritants and bacterial signals. *Proc. Natl. Acad. Sci. U. S. A.* **107**, 3210–3215 (2010).
264. Rossy, T. *et al.* *Pseudomonas aeruginosa* contracts mucus to rapidly form biofilms in tissue-engineered human airways. *bioRxiv* **2** (2022).
265. Dar, D., Dar, N., Cai, L. & Newman, D. K. Spatial transcriptomics of planktonic and sessile bacterial populations at single-cell resolution. *Science* **373** (2021).
266. Shi, H. *et al.* Highly multiplexed spatial mapping of microbial communities. *Nature* **588**, 676–681 (2020).
267. Passador, L. *et al.* Expression of *Pseudomonas aeruginosa* Virulence Genes Requires Cell-to-Cell Communication. *Science* **260**, 1127–1130 (1993).
268. Liu, Y. C., Chan, K. G. & Chang, C. Y. Modulation of host biology by *Pseudomonas aeruginosa* quorum sensing signal molecules: Messengers or traitors. *Front. Microbiol.* **6** (2015).
269. Hartmann, A. & Schikora, A. Quorum Sensing of Bacteria and Trans-Kingdom Interactions of N-Acyl Homoserine Lactones with Eukaryotes. *J. Chem. Ecol.* **38**, 704–713 (2012).
270. Neely, A. M. *et al.* N-(3-oxo-acyl)-homoserine lactone induces apoptosis primarily through a mitochondrial pathway in fibroblasts. *Cell Microbiol.* **20** (2018).
271. Xiao, Y. *et al.* Impact of quorum sensing signaling molecules in Gram-negative bacteria on host cells: current understanding and future perspectives. *Gut Microbes* **14**, 1–19 (2022).
272. Lin, J., Cheng, J., Wang, Y. & Shen, X. The *Pseudomonas* quinolone signal (PQS): Not just for quorum sensing anymore. *Front. Cell. Infect. Microbiol.* **8**, 1–9 (2018).
273. Gu, Z., Eils, R. & Schlesner, M. Complex heatmaps reveal patterns and correlations in multidimensional genomic data. *Bioinformatics* **32**, 2847–2849 (2016).
274. McIntyre, B. A. S. *et al.* Innate immune response of human pluripotent stem cell-derived airway epithelium. *Innate Immun.* **21**, 504–511 (2015).
275. Britigan, B. E., Railsback, M. A. & Cox, C. D. The *Pseudomonas aeruginosa* secretory product pyocyanin inactivates $\alpha 1$ protease inhibitor: Implications for the pathogenesis of cystic fibrosis lung disease. *Infect. Immun.* **67**, 1207–1212 (1999).
276. O’Malley, Y. Q. *et al.* The *Pseudomonas* secretory product pyocyanin inhibits catalase activity in human lung epithelial cells. *Am. J. Physiol. - Lung Cell. Mol. Physiol.* **285** (2003).
277. Rada, B., Lekstrom, K., Damian, S., Dupuy, C. & Leto, T. L. The *Pseudomonas* toxin pyocyanin inhibits the Dual oxidase-based antimicrobial system as it imposes oxidative stress on airway epithelial cells. *J. Immunology* **181**, 4883–4893 (2008).
278. Liew, F. Y., Girard, J. P. & Turnquist, H. R. Interleukin-33 in health and disease. *Nat. Rev. Immunol.* **16**, 676–689 (2016).

References

279. Ramirez-Moral, I. *et al.* Interleukin-33 improves local immunity during Gram-negative pneumonia by a combined effect on neutrophils and inflammatory monocytes. *J. Pathol.* **253**, 374–383 (2021).
280. Hazlett, L. D. *et al.* IL-33 shifts macrophage polarization, promoting resistance against *Pseudomonas aeruginosa* keratitis. *Investig. Ophthalmol. Vis. Sci.* **51**, 1524–1532 (2010).
281. Pinteaux, E. *et al.* Cell-specific conditional deletion of interleukin-1 (IL-1) ligands and its receptors: a new toolbox to study the role of IL-1 in health and disease. *J. Mol. Med.* **98**, 923–930 (2020).
282. Boraschi, D., Italiani, P., Weil, S. & Martin, M. U. The family of the interleukin-1 receptors. *Immunol. Rev.* **281**, 197–232 (2018).
283. Dinarello, C. A. Overview of the IL-1 family in innate inflammation and acquired immunity. *Immunol. Rev.* **281**, 8–27 (2018).
284. World Health Organization. Antimicrobial resistance. Available online : <https://www.who.int/news-room/fact-sheets/detail/antimicrobial-resistance>. (Accessed on 9 December 2022)
285. Alisjahbana, B., Debora, J., Susandi, E. & Darmawan, G. *Chromobacterium violaceum*: A review of an unexpected scourge. *Int. J. Gen. Med.* **14**, 3259–3270 (2021).
286. Grandclément, C., Tannières, M., Moréra, S., Dessaux, Y. & Faure, D. Quorum quenching: Role in nature and applied developments. *FEMS Microbiol. Rev.* **40**, 86–116 (2015).
287. Williams, R. B., Henrikson, J. C., Hoover, A. R., Lee, A. E. & Cichewicz, R. H. Epigenetic remodeling of the fungal secondary metabolome. *Org. Biomol. Chem.* **6** (2008).
288. Defoirdt, T., Pande, G. S. J., Baruah, K. & Bossier, P. The apparent quorum-sensing inhibitory activity of pyrogallol is a side effect of peroxide production. *Antimicrob. Agents Chemother.* **57**, 2870–2873 (2013).
289. Majik, M. S., Gawas, U. B. & Mandrekar, V. K. Next generation quorum sensing inhibitors: Accounts on structure activity relationship studies and biological activities. *Bioorganic Med. Chem.* **28** (2020).
290. Dutta, D. & Clevers, H. Organoid culture systems to study host–pathogen interactions. *Curr. Opin. Immunol.* **48**, 15–22 (2017).
291. Puschhof, J., Pleguezuelos-Manzano, C. & Clevers, H. Organoids and organs-on-chips: Insights into human gut-microbe interactions. *Cell Host Microbe* **29**, 867–878 (2021).
292. Westermann, A. J., Gorski, S. A. & Vogel, J. Dual RNA-seq of pathogen and host. *Nat. Rev. Microbiol.* **10**, 618–630 (2012).
293. Westermann, A. J., Barquist, L. & Vogel, J. Resolving host–pathogen interactions by dual RNA-seq. *PLoS Pathog.* **13**, 1–19 (2017).
294. Charlton, T. S. *et al.* A novel and sensitive method for the quantification of N-3-oxoacyl homoserine lactones using gas chromatography-mass spectrometry: Application to a model bacterial biofilm. *Environ. Microbiol.* **2**, 530–541 (2000).
295. Barr, H. L. *et al.* *Pseudomonas aeruginosa* quorum sensing molecules correlate with clinical status in cystic fibrosis. *Eur. Respir. J.* **46**, 1046–1054 (2015).
296. Wen, K. Y. *et al.* A Cell-Free Biosensor for Detecting Quorum Sensing Molecules in *P. aeruginosa*-Infected Respiratory Samples. *ACS Synth. Biol.* **6**, 2293–2301 (2017).
297. Struss, A. K. *et al.* Towards implementation of Quorum Sensing Autoinducers as Biomarkers for Infectious Disease States. *Anal. Chem.* **85**, 3355–3362 (2013).
298. Riquelme, S. A., Wong, T., Lung, F. & Prince, A. Pulmonary Pathogens Adapt to Immune Signaling Metabolites in the Airway. *Front. Immunol.* **11**, 1–14 (2020).
299. Mukherjee, S. & Bassler, B. L. Bacterial quorum sensing in complex and dynamically changing environments. *Nat. Rev. Microbiol.* **17**, 371–382 (2019).
300. Avital, G. *et al.* scDual-Seq: Mapping the gene regulatory program of *Salmonella* infection by host and pathogen single-cell RNA-sequencing. *Genome Biol.* **18**, 1–8 (2017).
301. Rosadini, C. V. & Kagan, J. C. Early innate immune responses to bacterial LPS. *Curr. Opin. Immunol.* **44**, 14–19 (2017).

-
302. Montminy, S. W. *et al.* Virulence factors of *Yersinia pestis* are overcome by a strong lipopolysaccharide response. *Nat. Immunol.* **7**, 1066–1073 (2006).
 303. García-Contreras, R., Maeda, T. & Wood, T. K. Resistance to quorum-quenching compounds. *Appl. Environ. Microbiol.* **79**, 6840–6846 (2013).
 304. Cook, M. A. & Wright, G. D. The past, present, and future of antibiotics. *Sci. Transl. Med.* **14**, (2022).
 305. Baptista, P. V. *et al.* Nano-strategies to fight multidrug resistant bacteria—"A Battle of the Titans". *Front. Microbiol.* **9**, 1–26 (2018).
 306. Holger, D. *et al.* Clinical pharmacology of bacteriophage therapy: A focus on multidrug-resistant *Pseudomonas aeruginosa* infections. *Antibiotics* **10**, 1–21 (2021).
 307. Gonzaga, Z. J. C., Merakou, C., Digiandomenico, A., Priebe, G. P. & Rehm, B. H. A. A *Pseudomonas aeruginosa*-derived particulate vaccine protects against *P. aeruginosa* infection. *Vaccines* **9**, 1–20 (2021).
 308. Docquier, J. D. & Mangani, S. An update on β -lactamase inhibitor discovery and development. *Drug Resist. Updat.* **36**, 13–29 (2018).
 309. Sun, J., Deng, Z. & Yan, A. Bacterial multidrug efflux pumps: Mechanisms, physiology and pharmacological exploitations. *Biochem. Biophys. Res. Commun.* **453**, 254–267 (2014).
 310. Theuretzbacher, U. & Piddock, L. J. V. Non-traditional Antibacterial Therapeutic Options and Challenges. *Cell Host Microbe* **26**, 61–72 (2019).
 311. Shrestha, L., Fan, H.-M., Tao, H.-R. & Huang, J.-D. Recent Strategies to Combat Biofilms Using Antimicrobial Agents and Therapeutic Approaches. *Pathogens* **11**, 292 (2022).
 312. Kajihara, K. K. *et al.* Potent killing of *Pseudomonas aeruginosa* by an antibody-antibiotic conjugate. *mBio* **12**, 1–14 (2021).
 313. Brown, D. Antibiotic resistance breakers: Can repurposed drugs fill the antibiotic discovery void? *Nat. Rev. Drug Discov.* **14**, 821–832 (2015).



Addendum

Dutch summary | Nederlandse Samenvatting

Curriculum vitae

List of publications

Acknowledgements | Dankwoord

Nederlandse Samenvatting

Bacteriën zijn wijdverspreid in onze omgeving en lichaam en zijn cruciaal voor ons bestaan. Ze helpen bij de vertering van voedsel, de afgifte van voedingsstoffen en beschermen ons tegen ziekmakende bacteriën en virussen. Echter, een verkeerde bacterie op de verkeerde plek kan ernstige problemen veroorzaken. Voordat antibiotica werden ontdekt waren dergelijke infecties vaak fataal en de geschiedenis biedt verschillende voorbeelden van epidemieën die door bacteriën werden veroorzaakt, waarvan de pest (veroorzaakt door de bacterie *Yersinia pestis*) de meest beruchte is.

In 1928 ontdekte Alexander Fleming dat een schimmel op een agarplaat een stof produceerde die de groei van bacteriën remde of zelfs de bacterie doodmaakte. Dit stofje bleek later penicilline te zijn en werd in 1945 beschikbaar gesteld voor het publiek. Na de komst van penicilline werden veel verschillende soorten antibiotica ontdekt met verschillend werkingsmechanisme. Echter, tegen elk type antibiotica zijn snel na de introductie in de kliniek bacteriën gevonden die er resistent tegen zijn.

Bacteriën kunnen zich razendsnel vermenigvuldigen, wat zorgt voor snelle evolutie. Als een bacterie toevallig resistent wordt tegen een antibioticum tijdens een behandeling, kan deze zich blijvend vermenigvuldigen en meer bacteriën maken die resistent zijn. Dit is de paradox van antibiotica: hoe meer het wordt gebruikt, hoe inefficiënter het wordt. Dit kan in de toekomst leiden tot een stijging van onbehandelbare infecties.

De Wereldgezondheidsorganisatie (WHO) heeft een lijst opgesteld met 12 soorten bacteriën die de grootste bedreiging vormen voor de volksgezondheid. Vanwege hun vermogen om dodelijke infecties te veroorzaken behoren *Pseudomonas*, *Acinetobacter* en verschillende *Enterobacteriaceae* tot de meest kritieke soorten. Dit proefschrift richt zich voornamelijk op een van deze bacteriën, de *Pseudomonas aeruginosa*.

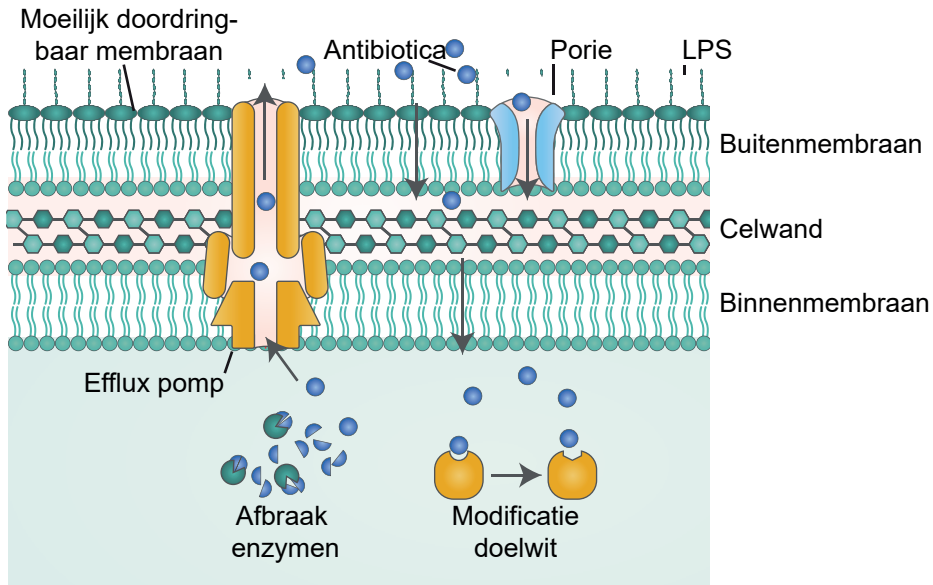
Pseudomonas aeruginosa

P. aeruginosa staat bekend als ziekenhuisbacterie die infecties kan veroorzaken bij mensen met verlaagde weerstand. Vooral bij individuen met taaislijmziekte zorgen deze infecties vaak voor ernstige symptomen en uiteindelijk sterfte door longfalen.

De behandeling van *P. aeruginosa* infecties is erg lastig. Om te beginnen is *P. aeruginosa* een Gram-negatieve bacterie. Gram-negatieve bacteriën hebben echter een extra membraan rondom hun celwand, dat de diffusie van moleculen bemoeilijkt. Daardoor dringen moleculen vaak binnen via de poriën. De poriën van *P. aeruginosa* zijn echter erg specifiek en laten slechts een beperkte variatie aan moleculen door. De moleculen die er toch in slagen om binnen te dringen worden er vaak weer uitgestoten door pompen. Dit maakt het erg lastig voor antibiotica om een hoge concentratie te bereiken en de bacterie te doden.

Daarbovenop kan een bacterie minder gevoelig, of zelfs resistent, worden tegen

antibiotica (Figuur 1). Zo kan een bacterie minder poriën tot expressie brengen die de antibiotica doorlaten. Ook kan de bacterie enzymen produceren die de antibiotica afbreken of de doelwitten van antibiotica veranderen, zodat deze niet meer werkzaam zijn. Daardoor zijn *P. aeruginosa* infecties moeilijk te behandelen en daarom is meer onderzoek noodzakelijk om ervoor te zorgen dat de behandelingen ook in de toekomst effectief blijven.



Figuur 1: Verschillende factoren betrokken bij de resistentie van *P. aeruginosa*. *P. aeruginosa* bacteriën hebben een hoge tolerantie tegen antibiotica via verschillende mechanismes. Ten eerste maakt het moeilijk doordringbare buitenste membraan het lastig voor antibiotica om de cel binnen te dringen. De antibiotica komen vaak binnen via de poriën. Wanneer ze in de cel zijn, worden ze er weer vaak uitgepompt wat het lastig maakt om een hoge concentratie te bereiken. Daarnaast kan *P. aeruginosa* verschillende enzymen tot expressie brengen die de antibiotica afbreken of het doelwit veranderen zodat de antibiotica er niet meer aan kunnen binden.

Inhibitie van Quorum sensing als alternatief voor antibiotica

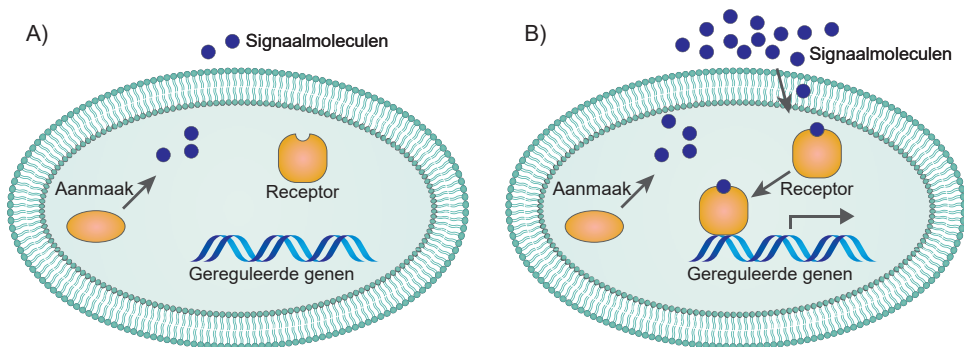
Gram-negatieve bacteriën zijn zoals eerder benoemd lastig te behandelen. Het is dan ook geruime geruime tijd geleden dat er een nieuwe klasse van antibiotica op de markt is gebracht die effectief is tegen deze groep bacteriën. Daardoor is het noodzakelijk om alternatieven te verkennen. De inhibitie van quorum sensing is zo een alternatief.

Quorum sensing (QS) is de 'communicatie' tussen bacteriën waarbij genen worden gereguleerd op basis van populatiedichtheid. Het proces omvat de aanmaak, uitstoot en detectie van signaalmoleculen (Figuur 2). Deze signaalmoleculen kunnen membranen passeren en binden aan receptoren in cellen die genexpressie reguleren. Wanneer er veel bacteriën zijn, is de concentratie van signaalmoleculen hoog, wat ervoor zorgt dat er andere genen actief zijn dan wanneer er weinig bacteriën zijn. Dit maakt samenwerking tussen bacteriën mogelijk.

De genen die door QS worden gereguleerd omvatten onder andere virulentiefactoren

en factoren die betrokken zijn bij de vorming van een biofilm. Virulentiefactoren bevatten onder andere enzymen die schade kunnen veroorzaken aan menselijk weefsel, waardoor de symptomen van de infectie verergeren. Een biofilm is een samenklontering van bacteriën. Bacteriën in een biofilm zijn minder gevoelig voor antibiotica. Hierdoor zou het remmen van QS leiden tot minder weefschade en een verhoogde gevoeligheid voor antibiotica. Dit maakt QS een interessant doelwit voor het bestrijden van bacteriële infecties.

In dit proefschrift zijn we opzoek gegaan naar nieuwe QS-remmers die effectief zijn tegen *P. aeruginosa*. Daarnaast hebben we meer inzicht proberen te krijgen in de rol die QS speelt tijdens infecties.



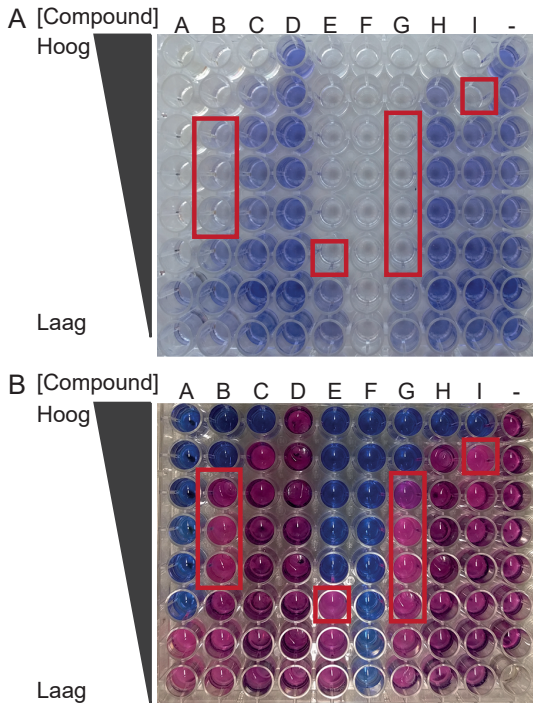
Figuur 2: Gesimplificeerde weergave van quorum sensing in Gram-negatieve bacteriën. Het concept van quorum sensing is hetzelfde onder Gram-negatieve bacteriën. Synthase eiwitten produceren kleine signaalmoleculen die het membraan kunnen passeren. **A)** Wanneer het aantal bacteriën laag is, zal de concentratie signaalmoleculen laag zijn. **B)** Wanneer het aantal bacteriën hoog is, zal de concentratie signaalmoleculen toenemen. De signaalmoleculen passeren het membraan de cel in en binden aan receptoren. Deze receptoren binden dan aan het DNA en veranderen de genexpressie.

Screening voor nieuwe QS-remmers

Antibiotica worden vaak beschouwd als moleculen die zijn geëvolueerd in de strijd tussen microben voor competitie om voedsel en ruimte. Op dezelfde manier kunnen moleculen die QS remmen zijn geëvolueerd als wapens om de toxiciteit van de bacteriën te limiteren. In **hoofdstuk 2** beschrijven we een uitgebreide screening die we hebben uitgevoerd om nieuwe QS-remmers te identificeren. Hiervoor hebben we een grote databank gebruikt die filtraten bevat van 10,207 schimmelsoorten. Om snel veel samples gebruikten we de bacterie *Chromobacterium violaceum* als indicator. Deze bacterie produceert namelijk een paarse stof wanneer QS actief is, waardoor we gemakkelijk konden bepalen of QS actief was. Een extra test bevestigde of de remming van QS te wijten was aan een dode bacterie (een dode bacterie kan immers niet communiceren) of dat de stof daardwerkelijk specifiek was voor QS (Figuur 3).

Deze screening identificeerde bekende QS-remmers (patuline en penicillinezuur) en veelbelovende stoffen die nog niet bekend waren als QS-remmers. De meest belovende

stoffen waren verschillende gregatines die veel overlap hebben qua structuur. Helaas is het QS-remmende effect van deze stoffen in de klinisch relevante bacterie *P. aeruginosa* minimaal.



Figuur 3: Screening met behulp van *Chromobacterium violaceum*. A) *C. violaceum* produceert een paarse stof wanneer QS actief is. Veel verschillende moleculen of schimmelfiltraten kunnen zo tegelijk getest worden. Wanneer de paarse stof niet geproduceerd wordt betekent dit dat er geen communicatie heeft plaatsgevonden. B) Een tweede plaat met dezelfde moleculen in dezelfde concentraties wordt tegelijkertijd gemeten om de viabiliteit van de bacteriën te bestuderen. Blauw betekent dat de bacterie dood is, roze betekent dat de bacterie leeft. De rode vierkanten laten de QS-remmende concentraties zien: Geen communicatie maar wel levende bacteriën.

De ontdekking van paecilomycone

Na optimalisatie van de chemische purificatietechnieken ontdekten we paecilomycone, beschreven in **hoofdstuk 3**. In tegenstelling tot de moleculen beschreven in **hoofdstuk 2**, is paecilomycone ook effectief tegen *P. aeruginosa*. Paecilomycone vermindert biofilm formatie en productie van toxische stoffen in *P. aeruginosa*. De werkzame concentraties zijn niet toxisch voor humane cellen. Dit maakt paecilomycone interessant voor klinische toepassingen. Daarnaast beschrijven we in **hoofdstuk 3** de zoektocht naar de target van paecilomycone. Ondanks verschillende suggesties, blijft de target onbekend en er is meer onderzoek nodig naar de werking van paecilomycone.

De rol van Quorum sensing tijdens humane infecties

Lab-experimenten tonen aan dat het remmen van QS effectief kan zijn. Zo leidt het remmen van QS in proefdieren tot een vermindering van de toxiciteit van de bacteriën, een langere levensduur van de dieren en een effectievere afweerreactie. Hoewel deze resultaten veelbelovend zijn, zijn er momenteel nog geen QS-remmers in de kliniek beschikbaar en is de rol van QS tijdens humane infecties nog relatief onbekend vanwege verschillende

redenen die onderzoek naar bacteriële infecties in mensen bemoeilijken.

In **Hoofdstuk 4** beschrijven we een nieuw infectiemodel om de interactie tussen humane cellen en bacteriën te bestuderen met het gebruik van organoids. Organoids zijn miniatuurorganen die gekweekt kunnen worden in een lab. Organoids vertonen veel overeenkomsten met de celtypes die voorkomen in onze organen, waardoor ze geschikt zijn om de reactie van menselijke cellen te bestuderen in fysiologisch relevante omstandigheden zonder het gebruik van dieren.

Hoofdstuk 4 toont aan dat dit model verschillende kenmerken van een infectie vertoont. Zo is er een sterke immuunreactie in de organoids en zorgen de organoids voor een activatie van verschillende infectie-gerelateerde processen in *P. aeruginosa*. Interessant is dat QS in *P. aeruginosa* minder actief is in co-culture dan wanneer de bacterie wordt opgegroeid zonder organoid. Daarnaast hebben *P. aeruginosa* bacteriën zonder actief QS systeem geen afwijkend effect op de organoids in vergelijking met normale *P. aeruginosa* bacteriën. Dit staat in contrast met andere studies waaruit blijkt dat QS-gereguleerde moleculen effect hebben op menselijke cellen. Dit kan verschillend redenen hebben, waaronder hogere concentraties in die studies en de afweerrespons van organoids veroorzaakt door lipopolysachariden (LPS, toxines in de buitenmembraan van Gram-negatieve bacteriën).

Om hogere concentraties van QS gereguleerde moleculen te kunnen testen zonder invloed van LPS, behandelden we in **hoofdstuk 5** organoids met steriel supernatant van *P. aeruginosa*. Na het kweken van wildtype en QS mutanten in medium, werd het medium gefilterd om het effect van de uitgestoten moleculen te kunnen testen zonder invloed van levende bacteriën. Daarnaast maakt dit model het mogelijk om het effect van individuele moleculen te onderzoeken

Hoofdstuk 5 toont aan dat het supernatant van wildtype bacteriën schadelijker is voor de organoids dan dat van QS mutanten. Bovendien hebben QS-gereguleerde moleculen effect op genexpressie van de organoids. Wanneer we specifiek de immuunresponse bestuderen zien we dat QS-gereguleerde moleculen zowel een stimulerend als remmend effect kunnen hebben. Het verschil tussen de bevindingen in **hoofdstuk 4** en **hoofdstuk 5** kan verklaard worden door de sterke immuunrespons veroorzaakt door LPS. Zonder LPS kunnen kleine effecten gedetecteerd worden.

Samenvattend, hoewel QS actief is tijdens infectie en QS-gereguleerde factoren weefsel kunnen beschadigen, suggereert dit onderzoek dat QS minder invloed heeft tijdens een infectie dan vooraf gedacht. Studies naar de rol van QS tijdens infectie zijn echter lastig, maar organoid technologie kan een interessant platform zijn om dit te bestuderen.

De potentie van QS-remmers in de kliniek

In **hoofdstuk 6** geef ik mijn visie over de potentie van QS-remmers in de kliniek. QS-remmers zijn erg interessant omdat ze de toxiciteit van de bacteriën verminderen, wat zal leiden tot een vermindering van de symptomen, en biofilm formatie verminderen, waardoor

bacteriën gevoeliger zijn voor antibiotica. Echter, aannemende dat QS een belangrijke rol speelt tijdens humane infecties, zal het alsnog lastig zijn om QS-remmers als medicatie toe te passen. De concentratie van QS-remmers speelt een belangrijke rol: te hoge concentraties doden de bacteriën of zorgen voor ongewenste effecten, terwijl te lage concentraties geen effect hebben. Het bepalen van de juiste concentratie voor een individuele patiënt, waar homeostase en afbraak van moleculen een rol spelen, is daarom een uitdaging.

Er zijn echter andere toepassingen van QS-remmers buiten het lichaam die meer potentie bieden. Zo zou de concentratie beter gereguleerd kunnen worden tijdens infecties van de huid. Daarnaast zijn er mogelijk interessante toepassingen buiten de geneeskunde, zoals biologische vervuiling, de landbouw, of het reinigen van medische apparatuur. Deze alternatieve toepassingen kunnen een veelbelovende optie bieden voor de ontwikkeling en gebruik van QS-remmers.

De toekomst van antibiotica

Om in de toekomst infecties effectief te blijven behandelen, is het van groot belang dat we beschikken over meer soorten antibiotica. De antibiotica die we momenteel gebruiken zijn vaak breedspectrum, wat betekent dat ze veel verschillende soorten bacteriën kunnen bestrijden. Dit is essentieel wanneer de bacterie die de infectie veroorzaakt nog niet bekend is of wanneer de antibiotica profylactisch wordt toegediend, zoals bij operaties. In de toekomst zal er een grotere rol zijn voor smalspectrum antibiotica, die slechts effectief zijn tegen een enkele soort bacterie. Mogelijke oplossingen hiervoor zijn vaccinatie, bacteriofagen of antilichamen. Ondanks deze ontwikkelingen zullen bacteriën resistentie blijven ontwikkelen, waardoor we ons voortdurend zullen moeten blijven ontwikkelen om infecties effectief te blijven bestrijden.

Conclusie

Het doel van dit proefschrift was om meer te leren over de potentie van QS-remmers als alternatief voor antibiotica tegen bacteriële infecties. Hiervoor hebben we voornamelijk *P. aeruginosa* bestudeerd. We hebben gezien dat natuurlijke stoffen, geproduceerd door schimmels, nog steeds veel rijkdommen bevatten voor het ontdekken van nieuwe QS-remmers (**hoofdstuk 2**) en dat paecilomycone ook een veelbelovende effect heeft op *P. aeruginosa* door het remmen van virulentiefactoren (**hoofdstuk 3**). Echter is er meer onderzoek nodig en betere modellen, zoals organoid technologie (**hoofdstuk 4 en 5**) om meer te leren over de rol van QS tijdens infectie. Of QS-remmers ooit in de kliniek gebruikt zullen worden, de toekomst zal het ons leren.

Curriculum vitae

Wouter Beenker was born on the 22th of June 1993 in Best. In 2015 he finished his Bachelor's degree in Biomedical Sciences after doing an internship for 3 months at the University of New South Wales in the group of Prof. dr. McNally in Sydney. During this internship he studied the role of a neural circuit in feeding behavior. He continued his academic career with a Master's in Neuroscience and Cognition at Utrecht University. As part of this Master's degree, Wouter did a research internship of 9 months in the group of Prof. dr. Pasterkamp at the UMC Utrecht where he studied the role of axon guidance molecules during brain development. Later, he did a research internship of 6 months in the group of Prof. dr. Castelo-Branco at the Karolinska Institute in Stockholm where he studied the role of epigenetics in multiple sclerosis. After obtaining his Master's Degree, Wouter decided it was time for a switch in research fields, from Neuroscience to Microbiology. He started his PhD at the Hubrecht Institute in Utrecht in the group of Prof. dr. Jeroen den Hertog, studying alternatives for antibiotics. The results obtained during this research are published in this thesis.

List of publications

Published articles

Beenker, W. A. G., Hoeksma, J., Bannier-Hélaouët, M., Clevers, H. & den Hertog, J. Paecilomycone inhibits quorum sensing in Gram- negative bacteria. *Microbiol. Spectr.* **11** (2023).

Beenker, W. A. G., Hoeksma, J. & den Hertog, J. Gregatins, a Group of Related Fungal Secondary Metabolites, Inhibit Aspects of Quorum Sensing in Gram-Negative Bacteria. *Front. Microbiol.* **13** (2022).

Ouyang, X., Hoeksma, J., van der Velden, G., **Beenker, W.A.G.**, van Triest, M.H., Burgering, B.M.T. & den Hertog J. Berkchaetoazaphilone B has antimicrobial activity and affects energy metabolism. *Sci. Rep.* **11** (2021).

Manuscript submitted

Pleguezuelos-Manzano, C.#, **Beenker, W.A.G.**#, van Son, G.J.F., Harry Begthel, H., Amatngalim, G.D., Beekman J.M., Clevers, H., & den Hertog J. Establishment and characterization of a new *Pseudomonas aeruginosa* infection model using 2D airway organoids and dual RNA sequencing

#Authors contributed equally

Acknowledgements

Zojuist is het manuscript opgestuurd, Sean Paul speelt op de achtergrond, een perfect moment om terug te kijken op mijn jaren als PhD student aan het Hubrecht Instituut. Het was een avontuur wat ik niet alleen beleefd zou kunnen én willen hebben. Met dank aan veel mensen is een proefschrift tot stand gekomen waar ik enorm trots op ben.

Ik wil beginnen bij **Jeroen den Hertog**. Solliciteren op iets waar ik helemaal geen verstand van heb, dat kan geen succes worden. Al helemaal niet wanneer de uitnodiging voor de sollicitatie in mijn spambox beland en ik na de eerste vraag meteen onbeschaamd opmerk dat jullie ook geen verstand van het onderwerp zouden hebben. Desondanks besloot je mij toch een kans te geven en daar ben ik enorm dankbaar voor. Het was een geweldig project om aan te werken en ik heb er veel van geleerd. Bedankt voor het vertrouwen bij het veranderen van onderwerp naar quorum sensing inhibitors, de gezellige BBQ's en de algehele begeleiding de afgelopen jaren! Ik hoop dat ik je positief heb kunnen verrassen!

Alexander van Oudenaarden en **Jerome Collemare**, thanks for your advice in my PhD committee. It really helped to structure and push my project further.

Jelmer en **Bart**, de paranimfen. Iemand die centraal stond bij het onderzoek, en iemand die centraal stond in mijn leven buiten werk. Jelmer, zonder jou was dit boekje er niet geweest. Jij hebt mij wegwijs gemaakt in het Hubrecht Instituut, het Westerdijk Instituut, de wetenschappelijke wereld en Alva Noto. Jij was altijd geduldig als ik je weer stoorde met een nieuwe vraag. Naast alle hulp die je mij hebt gegeven waardeer ik ook enorm je positieve houding en alle gezellige praatjes! Bart, wij gaan ondertussen alweer vele jaren terug, tot de eerste klas middelbare school. Daarna kon het niet meer op. Eerste biertje, eerste meerdaagse festival, eerste vakantie zonder ouders, jij was erbij. Jij was er op de mooie momenten, maar gelukkig ook op de momenten dat het minder ging. Daarom ben ik enorm blij dat jij er ook bij bent, en naast mij staat tijdens mijn PhD defense!

Het den Hertog lab, bedankt voor de afgelopen jaren: voor alle hulp maar ook alle gezelligheid! **John**, ook al was je niet meer bij de labmeetings, ik beschouw jou natuurlijk nog steeds als onderdeel van het lab. Al is het maar voor de praatjes bij het handen wassen, of alle jerrycans die nog steeds in het labhok staan. Maar natuurlijk ook veel dank voor alle hulp wanneer incubatoren raar deden of wanneer ik weer een pipet kapot had gemaakt.

De Funguys/girls/galls, een groep die vele leden heeft gekend maar waar helaas nog weinig van over is. **Ouyang**, you were already there when I started and was so kind to help me out with everything I needed to know about antibiotics and bacteria. I was impressed by your enthusiasm and dedication for science! Thanks for all the interesting discussions, the delicious food and interesting candy. I hope everything is good and well back in China! **Samantha**, enorm bedankt voor alle hulp, waaronder ons te introduceren in het grote lab in het UMC! **Marieke**, jouw gezelligheid was een goede toevoeging aan het team. Je kon goed lachen om grappen, maar het hardst lachte je nog om je eigen fouten.

Ronnie, toen jij begon kregen we eindelijk iemand in het team met verstand van schimmels en goede connecties in het Westerdijk. Maar jij stond ook altijd klaar om mee te helpen met andermans taken (zoals het opruimen van mijn gigantische voorraad schimmelpotjes) en was flexibel wanneer ik ook de spectrofotometer wilde gebruiken. Enorm bedankt! **Helen**, over de jaren heb ik gezien dat je geluk en pech kunt hebben met een student. Gelukkig had ik geluk. Ik was onder de indruk van je kwaliteiten en wil je dan ook enorm bedanken voor je inzet!

Dan over naar de andere helft van het lab, de zebravis kant. **Sasja**, vele woorden zijn er al over gezegd en we hebben er nog vaak over gelachen, maar de eerste ontmoeting verliep niet soepel. Gelukkig is dat later helemaal goed gekomen en bleek dat we het juist heel goed kunnen vinden samen. We hebben in, maar ook buiten het kantoor, veel gezelligheid gekend. Ik kon de directheid en openheid enorm waarderen in je. **Maaïke**, jij was iets voor mij begonnen maar over het algemeen liep het traject van onze PhD gelijk op. Ik was onder de indruk hoe kalm je bleef en de balans die je vond in je werk en privé. Daarnaast was het soms ook heel fijn om over de frustrerende dingen te praten. Ik hoop dat ik snel de uitnodiging krijg voor jouw defense! **Petra**, ondertussen alweer een tijdje geleden, maar daardoor mag je niet ontbreken. Bedankt voor alle scherpe opmerkingen, ongezouten mening en waardevolle adviezen! **Maja**, I am sorry I am still not familiar with the Kelly family. However, we were often on the same page and shared similar opinions on a lot of subjects, some of which were a “Total disaster”. I really enjoyed my time with you in the lab! **Danielle**, we hadden al een voorproefje gekregen van jou als student, maar het werd pas echt gezellig toen je begon als PhD student en erbij kwam in het kantoor. Jouw duidelijke mening, jouw Rotterdamse vocabulaire en jouw enthousiasme voor de natuur waardeerde ik enorm! **Jisca**, met jou kwam ook een nieuwe lading gezelligheid het lab binnen. Iemand die meeging naar de vrijdagmiddagborrels! Regelmatig waren we zelfs de enige die aanwezig waren in het lab op de vrijdagen, gelukkig mocht dat de pret niet drukken! **Pakize**, last but not least. Bedankt voor alle goede gesprekken en oprechtheid. Ik vond het altijd erg leuk om met je te praten en kon goed met je lachen. Veel succes met jouw nieuwe baan!

Besides our own lab, there are of course many people within the institute to thank for making the Hubrecht such a nice place to work. The people you run into the most, are the people you share the coffee machine with. The **Bakkers lab (Dennis, Federico, Henriëtte, Hessel, Jeroen, Lotte, Melanie, Phong, and Sven)**, our neighbors. With a special thanks to **Hessel, Melanie, and Sven**. Melanie and Sven, toen ik met mijn PhD begon deelden wij nog ons kantoor met jullie groep en daar was ik erg blij mee. Bedankt voor alle gezelligheid en de opvulling van mijn plankjes boven mijn bureau (Melanie, kom jij je spullen nog een keer ophalen?). Hessel, mijn kamergenoot van de masterclass. Ondanks verwoede pogingen lukte het je helaas niet om als laatste naar bed te gaan. Maar ik zal voor je duimen dat Feyenoord kampioen wordt dit jaar! Wanneer we het over Feyenoord hebben is het bruggetje gemakkelijk gemaakt naar **Wessel**. Kijkende naar de hoeveelheden koffie die jij dronk was ik verbaasd dat je nog fatsoenlijk kon pipetteren. Maar ik mag niet klagen, aangezien de praatjes me altijd goed deden! **Rianne**, vele uren hebben we samen

doorgebracht in de celweek, dit maakte het werk een stuk leuker!

If I wasn't on our own floor, chances were big I was wandering around a level below at the Clevers lab. **Cayetano**, without you my PhD would have had way less flare. It started off with a good question at the PhD retreat and it ended up in a great collaboration, which taught me a lot. The day after the first injection of bacteria into the organoids is my highlight of my research career at the Hubrecht. Seeing the bacteria swim around within the organoid was great. Your enthusiasm and response to this made it even better! The enthusiasm never faded and really kept the project going, even when it got tough. I am super grateful for this awesome collaboration and I hope the project will be published soon! To all the **office members of Cayetano**, thank you for all your help finding Cayetano. **Amanda**, thank you for your help with the Bioanalyzer and RNA-sequencing! Hope we both never have bike accidents again. Besides this office: **Marie**, merci with your help finding the toxicity of paecilomycone on organoids. It was not only helpful, but also real fun collaborating with you! **Gijs**, thank you for all your help with mapping the raw datasets.

If you want to work with interesting bacteria, you most probably need a ML2 laboratory. Luckily, there were a couple of square meters within the institute that had room for it. To make it work smoothly, I want to thank all the **ML2 buddies**. Thanks for all the flexibility when experiments were delayed, the suspicions when your organoids were infected with *P. aeruginosa* (it wasn't me), and all the great GIFs. I am fairly sure, this small lab was the lab with the largest output per square meter!

I could go on a long time to thank all the people for the help and fun times at the Hubrecht institute. But before I move on to people outside the institute, I want to thank a special group of people: the people of the PV committee. **Wouter, Anne, Roxanne, Clément, Joris, Jorik, and Reinier**, thank you for all the amazing times! I really enjoyed organizing all the borrels and activities with you. I am happy we still hang out and I can't wait for the next party!

Naast ons eigen instituut was ik ook regelmatig te vinden in het Westerdijk Instituut voor al het schimmelwerk. Om ervoor te zorgen dat ik genoeg paecilomycone en andere stoffen had voor alle experimenten zijn er honderden liters medium doorheen gegaan. Gelukkig hoefde ik voor de bereiding bijna niks te doen. Hiervoor ben ik de mensen van de **Mediakeuken** enorm dankbaar! **Ronald, Ralph, Remco, Sander en anderen**, bedankt voor al jullie hulp en moeite!

Binnen het Westerdijk instituut wil ik verder nog een aantal personen bedanken. **Arien**, voor corona hebben we vele uren naast elkaar gezeten in het lab. Bedankt voor de gezelligheid en jouw welgemeende interesse! **Michel**, ik kwam je regelmatig in de gangen tegen, maar je stond ook altijd klaar voor hulp als er iets misging, dank daarvoor! **Olga**, unfortunately the collaborations between our groups didn't go as planned. Nevertheless, it was always fun having you around!

Daarnaast wil ik ook mensen van het UMC bedanken, zowel van de **afdeling Kaakchirurgie** als van de **afdeling Medische Microbiologie**. De eerste bedankt voor alle goede zorgen en het feit dat ik mét tanden kan verdedigen. De laatste bedankt dat ik vele experimenten bij jullie kon uitvoeren. Ik wil hiervan een aantal mensen in het bijzonder bedanken. **Bart**, bedankt dat je mij zo enorm hebt geholpen met het maken van *P. aeruginosa* mutanten. Je stond altijd klaar voor extra uitleg en hebt mij verschillende protocollen, plasmides, en bacteriestammen gegeven zodat ik verder kon met mijn onderzoek. **Lisanne**, jouw tegenkomen in het lab was altijd feest! Bedankt voor de uitleg over biofilms, maar ook de vele koffietjes in het UMC. **Piet**, je had mij meteen in de gaten toen ik voor het eerst op jullie lab rondhing, niks vergaat jou onopgemerkt. Bedankt dat je mij welkom heette met warme Brabantse gezelligheid! **Julia**, we did our best to start and finish a project as efficiently as possible. In an ideal scenario we would have a paper ready within no-time. Unfortunately, it didn't work out that way and we aborted the project soon. However, I still enjoyed the process and collaborating with you!

Gelukkig bestond mijn leven de afgelopen jaren niet alleen uit werk. Ik wil daarom ook alle lieve en leuke mensen om mij heen bedanken voor de mooie jaren, de steun en de afleiding. Bedankt voor de vele avonden samen in de klimhal; de spelletjesavonden; de hulp met het programmeren; de hulp met het ontwerp van dit boekje; de vakanties; de weekendjes weg; de wandelingen; hét schaaktoernooi; de leuke feestjes; de slechte feestjes; de biertjes in de kroeg; de biertjes buiten de kroeg; het basketballen; het flunkyballen; al die keren dat er voor mij heerlijk gekookt is; de goede gesprekken; het slappe gewouwel; de ritjes op de racefiets; de game nights; de dj nights; de escalerende avonden; de alcoholvrije avonden; de tranen; het vele lachen; jullie vriendschap, ik waardeer het enorm.

Lieve **Annerie** en **Martijn**, de afgelopen jaren waren niet altijd gemakkelijk. Maar dankzij jullie liefde en steun is dit toch een stuk gemakkelijker geworden. Jullie zijn mijn grote voorbeeld en mede dankzij jullie heb ik de keuzes gemaakt die ervoor hebben gezorgd dat ik hier nu sta. Ik kan mij niet een lievere én leukere broer en zus voorstellen.

Lieve **Laura** en **Vincent**, wat zijn jullie een fijne aanvulling op de familie. De een loopt al langer mee dan de ander, maar het voelt altijd enorm vertrouwd en fijn om bij jullie te zijn!

Lieve **Eddie** en **Lucas**, helaas zijn jullie nog te jong om de verdediging mee te maken. Maar ik geniet altijd van jullie aanwezigheid en lach. Ik vind het een voorrecht jullie te zien opgroeien en ik ben dan ook een enorm trotse oom!

Lieve **Papa** en **Mama**, bedankt voor de onvoorwaardelijke liefde de afgelopen jaren. Jullie interesse in mijn werk en onderzoek deed mij altijd erg goed. Ik zal proberen jullie de komende jaren wat minder te laten schrikken en wat beter op mijn fiets te blijven zitten. Maar dankzij jullie steun was het een stuk gemakkelijker om door deze tegenslagen heen te komen. Bedankt daarvoor!

